Involvement of ICE-like protease(s) in TGF-β_1 induced apoptosis in hepatocytes

Thesis submitted for the degree of

Doctor of Philosophy

at the University of Leicester

by

Salmaan H. Inayat-Hussain B.Sc (UKM)

Biochemical Toxicology Section

MRC Toxicology Unit

March 1997

UMI Number: U528825

All rights reserved

INFORMATION TO ALL USERS
The quality of this reproduction is dependent upon the quality of the copy submitted.

In the unlikely event that the author did not send a complete manuscript
and there are missing pages, these will be noted. Also, if material had to be removed,
a note will indicate the deletion.

UMI U528825
Published by ProQuest LLC 2013. Copyright in the Dissertation held by the Author.
Microform Edition © ProQuest LLC.
All rights reserved. This work is protected against
unauthorized copying under Title 17, United States Code.

ProQuest LLC
789 East Eisenhower Parkway
P.O. Box 1346
Ann Arbor, MI 48106-1346

INVOLVEMENT OF ICE-LIKE PROTEASE(S) IN TGF-$ß_1$ INDUCED APOPTOSIS IN HEPATOCYTES

Salmaan H. Inayat-Hussain, Biochemical Toxicology Section, MRC Toxicology Unit, Hodgkin Building, University of Leicester, Leicester LE1 9HN.

Abstract

Apoptosis has been implicated as a mode of cell death in many mammalian organs including liver. Internucleosomal DNA cleavage is often regarded as the biochemical hallmark of apoptosis and can be reproduced *in vitro* in rat liver nuclei. This chromatin cleavage in rat liver nuclei was further characterised and studies described in this thesis showed that the DNA was initially cleaved into ≥700kbp, 200-250kbp and 30-50kbp fragments via a Mg^{2+} dependent process which was potentiated by Ca^{2+}. The subsequent internucleosomal cleavage required both Ca^{2+} and Mg^{2+}. Furthermore, Mn^{2+} alone was able to substitute for Mg^{2+} and Ca^{2+}, thereby activating this multi-step DNA cleavage. DNA cleavage induced by either Mn^{2+}, Mg^{2+} or Ca^{2+}/Mg^{2+} was equally susceptible to inhibition by Zn^{2+}, N-ethylmaleimide and 3,4-dichloroisocoumarin and as these compounds react with sulphydryl groups, it is proposed that a critical thiol(s) is involved in multi-step DNA cleavage in rat liver nuclei. Further investigations of the DNA cleavage processes were carried out in primary hepatocytes using TGF-$ß_1$ to induce apoptosis. The studies showed for the first time that treatment of hepatocytes with TGF-$ß_1$ resulted in multi-step DNA cleavage as seen in rat liver nuclei. Cycloheximide and an interleukin-1ß-converting enzyme (ICE)-like inhibitor, benzyloxycarbonyl-Val-Ala-Asp-(OMe) fluoromethyl ketone (Z-VAD.FMK) and Z-Asp-Glu-Val-Asp-(OMe) fluoromethyl ketone (Z-DEVD.FMK), a potent inhibitor of CPP32, blocked DNA cleavage and apoptosis. During apoptosis there was a time dependent increase in CPP32-like proteolytic activity in lysates isolated from TGF-$ß_1$ treated hepatocytes, which was detected with the fluorogenic assay using Z-DEVD-amino-trifluoromethyl-coumarin (Z-DEVD.AFC). This activity was abolished when hepatocytes were pre-treated with either Z-VAD.FMK, Z-DEVD.FMK or cycloheximide. Unlike cycloheximide, Z-VAD.FMK and Z-DEVD.FMK were potent inhibitors of activated lysate from TGF-$ß_1$ treated hepatocytes. Immunoblotting showed the processing of pro-CPP32 to its active form. In conclusion, this study shows for the first time that TGF-$ß_1$ mediated apoptosis involves the activation of ICE-like proteases and that cycloheximide inhibits apoptosis by blocking upstream of this ICE-like activity.

Acknowledgements

I would like to dedicate this thesis to my wife for her patience, support and understanding. This thesis could not have been completed without her persistent encouragement and help. Thanks for being there when I needed you.

I am deeply indebted to Prof. Gerald M. Cohen who kindly offered me a place in this group. I would also like to thank Dr. Kelvin Cain who supervised, guided and advised me in both the scientific and non-scientific matters. He has taught me the discipline of research and I have truly enjoyed collaborating with him. I have benefited immeasurably from both Kelvin and Gerry in their meticulous analyses and detailed critiques, and a heartfelt thanks to both of you.

I am also indebted to Drs. Ludmilla Kokileva, Franziska Oberhammer and Carole Couet who have been involved either directly or indirectly in some of the work in this thesis. I would also like to thank Dr. V Cunningham at the MRC Cyclotron Unit, London for his invaluable advice on enzyme kinetics, and Andy Hubbard for confocal microscopy.

I would also like to thank Carole, Marion, Roger, Dave, John, Jack, James, Gareth, Xiao-Ming, Huijun, Sek, Howard, Liz, Julia, Siobhan, Tim, Jerry, Katherine, Joan, Fang and Darren for their company and friendship during my stay here. Thank you to Aamer who helped me a lot during my stay in Leicester and has become a great friend.

I am grateful to Aishah Adam for introducing me to Biochemical Toxicology and also to Universiti Kebangsaan Malaysia for the financial assistance.

To Jawaid, thanks for being a great brother and always encouraging me to obtain the highest education possible.

Finally I am truly indebted to my mother who brought me up through difficult times and has been a constant support and inspiration.

Contents

CHAPTER 1. Introduction 1

1.1 Modes of cell death 1

1.2 Apoptosis in the liver 2

1.2.1 Apoptosis and hepatocarcinogenesis 3

1.2.2 Toxin and drug induced liver apoptosis 5

1.2.3 Viral and immune mediated apoptosis in the liver 7

1.2.4 Receptor mediated signalling in liver apoptosis 8

1.2.4.1 Transforming growth factor-beta1 (TGF-$ß_1$) 8

1.2.4.1.a Structure of TGF-$ß_1$ 9

1.2.4.1.b Receptors of TGF-$ß_1$ 10

1.2.4.1c Growth inhibition by TGF-$ß_1$ 13

1.2.4.1.d Apoptosis induced by TGF-$ß_1$ 15

1.2.4.2 Fas/APO-1/CD95 and tumour necrosis factor (TNF) 17

1.3 Biochemical mechanisms of apoptosis 19

1.3.1 DNA cleavage during apoptosis 19

1.3.2 Proteolysis in apoptosis 21

1.3.2.1 ICE/CED-3 related proteases in apoptosis 24

1.3.2.2 Substrates of ICE-like proteases 26

1.3.2.2a Cytoplasmic and nuclear proteins 27

1.3.2.2.b Auto-processing or cleavage of members of ICE family 30

1.3.2.2.c Peptide based inhibitors 31

1.4 Aims of study 33

CHAPTER 2. Materials and Methods 34

2.1 Materials 34

2.2 Methods 34

2.2.1 Isolation of nuclei in magnesium buffers 34

2.2.2 Isolation of nuclei in spermidine/spermine buffers (SP-buffers) 35

2.2.3 Autodigestion of isolated nuclei 35

2.2.4 Isolation of hepatocytes 35

2.2.5 Culturing of hepatocytes 36

2.2.6 Isolation of nuclei from hepatocytes monolayer (enucleation method) 36

2.2.7 Preparation of hepatocyte lysates 37
2.2.8 Gel electrophoresis 37
2.2.8.a Conventional agarose gel electrophoresis (CAGE) 37
2.2.8.b Field inversion gel electrophoresis (FIGE) 37
2.2.9 In situ end labelling (ISEL) and Flow Cytometry 38
2.2.9.a ISEL on isolated rat liver nuclei 38
2.2.9.b ISEL on hepatocyte nuclei 39
2.2.9.c Flow cytometry 39
2.2.10 Morphological assessment of apoptosis in hepatocytes culture 39
2.2.11 Confocal Microscopy 40
2.2.12 Fluorimetric assay of proteolytic activity 40
2.2.13 Kinetic studies of the proteolytic activity 41
2.2.14 Determination of protein concentration 41
2.2.15 Coulter Counting 42
2.2.15.a Rat liver nuclei 42
2.2.15.b Hepatocyte nuclei 42
2.2.16 Collagen coating of coverslips and petri dishes 42
2.2.17 SDS-PAGE gel electrophoresis and Western blotting 42

CHAPTER 3. Formation of large DNA fragments in rat liver nuclei is a Mg^{2+} and/or Ca^{2+}/Mg^{2+} dependent process 44
3.1 Introduction 44
3.2 Results 46
3.2.1 Isolation and autodigestion assays of rat liver nuclei in spermine/spermidine-containing buffers 46
3.2.2 Effects of Mg^{2+} and Ca^{2+}/Mg^{2+} on DNA fragmentation in rat liver nuclei 50
3.2.3 Size distribution of DNA fragments after Mg^{2+} dependent degradation 50
3.2.4 In situ end labelling (ISEL) and flow cytometry as a semi quantitative measure of DNA strand breakage in rat liver nuclei 52
3.2.5 The effect of Mg^{2+} and Ca^{2+} on ISEL in rat liver nuclei 53
3.2.6 Time dependence of Mg^{2+} dependent DNA cleavage 54
3.3. Discussion 56
3.4 Summary 59

CHAPTER 4. Multi-step DNA cleavage in rat liver nuclei is inhibited by thiol reactive agents 60
4.1 Introduction 60
4.2 Results Section I 62
4.2.1 Inhibition of Mg^{2+} and Ca^{2+}/Mg^{2+} induced DNA cleavage in isolated rat liver nuclei by Hg^{2+} and Cd^{2+} 62
4.2.2 Inhibition of Ca^{2+}/Mg^{2+} induced DNA fragmentation in isolated rat liver nuclei by protease inhibitors 66
4.2.3 Inhibition of Mg^{2+} dependent degradation of DNA into 'large fragments' by protease inhibitors and N-ethylmaleimide 69
4.2.4. Effect of dithiothreitol on DCI and NEM inhibition of DNA cleavage 71
4.3 Discussion 73
4.4 Results Section II 76
4.4.1 Mn^{2+} activates 'large fragment' formation and internucleosomal DNA cleavage in rat liver nuclei 76
4.4.2 Time course of Mn^{2+} dependent DNA cleavage 78
4.4.3 Mn^{2+} activated cleavage of DNA into 'large fragments' and mono-oligonucleosomes is inhibited by Zn^{2+} 81
4.4.4 DCI and NEM inhibit multi-step DNA cleavage induced by Mn^{2+} 84
4.4.5 Mn^{2+} induces high levels of ISEL in rat liver nuclei 86
4.5 Discussion 87
4.6 Summary 90

CHAPTER 5. Characterisation of TGF-$ß_1$ induced apoptosis in primary hepatocytes culture 92
5.1 Introduction 92
5.2 Results 94
5.2.1 TGF-$ß_1$ induced apoptosis in primary hepatocytes 94
5.2.2 Isolation of nuclei from hepatocyte monolayers 96
5.2.3 ISEL of DNA strand breaks in nuclei isolated from hepatocyte monolayers treated with TGF-$ß_1$ 98
5.2.4 TGF-$ß_1$ induced apoptosis in hepatocytes is associated with multi-step DNA cleavage 101
5.2.5 Comparison of morphological and ISEL methods for assessing apoptosis 103

5.2.6 Confocal Microscopy of end-labelled nuclei 104
5.2.7 Effects of cycloheximide and Zn^{2+} on TGF-$ß_1$ induced apoptosis 108
5.3 Discussion 111
5.4 Summary 116

CHAPTER 6. ICE-like proteases are involved in TGF-$ß_1$ treated hepatocytes 117
6.1 Introduction 117
6.2 Results 120
6.2.1 A serine protease(s) is not involved during apoptosis in TGF-$ß_1$ treated hepatocytes 120
6.2.2 ICE-like protease inhibitors blocks chromatin condensation in apoptotic hepatocytes 121
6.2.3 Z-VAD.FMK blocks ISEL in apoptotic hepatocytes 126
6.2.4 Z-VAD.FMK abolishes internucleosomal cleavage and large fragment formation 126
6.2.5 TGF-$ß_1$ induces a CPP32/Mch3α like protease activity in hepatocytes 126
6.2.6 Kinetic and inhibitor characteristics of Z-DEVD.AFC activity in hepatocyte lysates 131
6.2.7 Identification of ICE-like proteases in activated hepatocyte lysates 136
6.2.8 PARP cleavage is not detected in apoptotic hepatocyte cultures 136
6.2.9 Cycloheximide blocks TGF-$ß_1$ induced apoptosis and activation of Z-DEVD.AFC cleavage but is not an inhibitor of CPP32/ Mch3α-like proteases. 138
6.3 Discussion 139
6.4 Summary 144

CHAPTER 7. General discussion 145

References 157

List of Figures

Figure 1.1 Schematic illustration of liver apoptosis induced by various physiological and toxicological stimuli. 3

Figure 1.2 Schematic representation of the effects of tumour promoters on proliferation and apoptosis. 4

Figure 1.3 The members of TGF-ß superfamily 8

Figure 1.4 Schematic illustration of precursor, latent and bioactive forms of TGF-$ß_1$ 10

Figure 1.5 Activation of the heteromeric TGF-$ß_1$ receptor complex 11

Figure 1.6 Targets of TGF-$ß_1$ in G_1 phase progression 14

Figure 1.7 Substrates of ICE-like proteases during apoptosis 27

Figure 1.8 Processing of ICE family members 30

Figure 3.1 CAGE analysis of DNA cleavage in rat liver nuclei stimulated with Ca^{2+} 47

Figure 3.2. CAGE and FIGE of rat liver nuclei after Mg^{2+} and Mg^{2+} plus Ca^{2+} activation 49

Figure 3.3. CAGE and FIGE of Mg^{2+} induced DNA fragmentation in rat liver nuclei 51

Figure 3.4 Flow cytometric detection of DNA fragmentation in isolated rat liver nuclei using ISEL 53

Figure 3.5 Effects of Ca^{2+} on Mg^{2+} induced ISEL cleavage in rat liver nuclei 54

Figure 3.6 Time course for Mg^{2+} induced DNA cleavage in rat liver nuclei 55

Figure 3.7 Time course of Mg^{2+} induced DNA cleavage as measured by ISEL 56

Figure 4.1 Cd^{2+} inhibition of Ca^{2+}/Mg^{2+}-activated DNA cleavage in rat liver nuclei 63

Figure 4.2 Cd^{2+} and Hg^{2+} inhibition of DNA cleavage in rat liver nuclei 65

Figure 4.3 Effects of NEM and protease inhibitors on DNA cleavage in rat liver nuclei 67

Figure 4.4 The effect of TLCK on Ca^{2+}/Mg^{2+}-activated DNA cleavage in rat liver nuclei 68

Figure 4.5 The effect of NEM and protease inhibitors on Mg^{2+}-activated DNA cleavage 70

Figure 4.6 The effect of TLCK on Mg^{2+}-dependent DNA cleavage 71

Figure 4.7 The effect of DTT on the inhibition of DNA cleavage by NEM and DCI 72

Figure 4.8 Mn^{2+} dependent DNA cleavage in rat liver nuclei 77

Figure 4.9 Time course of DNA cleavage in rat liver nuclei activated with 100µM and 200µM Mn^{2+} 79

Figure 4.10 Time course of DNA cleavage in rat liver nuclei activated with 400µM Mn^{2+} 80

Figure 4.11 Inhibition of Mg^{2+} and Ca^{2+}/Mg^{2+} dependent DNA cleavage by Zn^{2+} 82

Figure 4.12 Zn^{2+} inhibition of Mn^{2+}-activated DNA cleavage 83

Figure 4.13 Inhibition of Mn^{2+}-activated DNA cleavage by DCI and NEM 85

Figure 4.14 Flow cytometric detection of DNA fragmentation in isolated rat liver nuclei using *in situ* end labelling (ISEL) 86
Figure 4.15 Scheme for DNA cleavage in isolated liver nuclei 89
Figure 5.1 TGF-$ß_1$ induced apoptosis in primary culture hepatocytes 95
Figure 5.2 Effects of TGF-$ß_1$ on the mode of cell death in primary hepatocytes 96
Figure 5.3 Size profile of nuclei isolated from monolayer hepatocytes 97
Figure 5.4 ISEL of DNA strand breaks in nuclei isolated from hepatocyte monolayers treated with TGF-$ß_1$ 99
Figure 5.5 Concentration response curve of TGF-$ß_1$ treated hepatocytes as assessed by ISEL 101
Figure 5.6 TGF-$ß_1$ treated hepatocytes induced multi-step DNA cleavage 102
Figure 5.7 Comparison of the time course of apoptosis as assessed by morphology and ISEL 104
Figure 5.8 Confocal microscopy of end-labelled nuclei isolated from untreated hepatocytes 105
Figure 5.9 Confocal microscopy of end-labelled nuclei from TGF-$ß_1$ treated hepatocytes 107
Figure 5.10 Cycloheximide inhibition of TGF-$ß_1$ induced apoptosis 108
Figure 5.11 Cycloheximide inhibition of TGF-$ß_1$ induced DNA fragmentation 109
Figure 5.12 Effects of Zn^{2+} on TGF-$ß_1$ mediated apoptosis in hepatocytes as assessed by H33258 110
Figure 5.13 Effect of Zn^{2+} on ISEL of nuclei extracted from TGF-$ß_1$ treated hepatocytes 111
Figure 5.14 Effect of Zn^{2+} on TGF-$ß_1$ mediated apoptosis as analysed by gel electrophoresis 112
Figure 6.1 Effect of TLCK on TGF-$ß_1$ treated hepatocytes as assessed by ISEL 121
Figure 6.2 Effect of Z-VAD.FMK on TGF-$ß_1$ induced apoptosis in hepatocytes 122
Figure 6.3 Effect of Z-VAD.CMK and Z-AAD.CMK on TGF-$ß_1$ induced apoptosis in hepatocytes 123
Figure 6.4 Effect of Ac-YVAD.CMK and Ac-YVAD.CHO on TGF-$ß_1$ induced apoptosis in hepatocytes 124
Figure 6.5 Effect of Z-VAD.FMK on ISEL of nuclei extracted from hepatocytes treated with TGF-$ß_1$ 125

Figure 6.6 FIGE and CAGE of nuclei from hepatocytes treated with TGF-$ß_1$ with and without Z-VAD.FMK 127
Figure 6.7 Time dependent increase in Z-DEVD.AFC cleavage in lysates isolated from hepatocytes treated with TGF-$ß_1$ 128
Figure 6.8 Inhibition of TGF-$ß_1$ induced apoptosis by Ac-DEVD.CHO and Z-DEVD.FMK 130
Figure 6.9 Inhibition of TGF-$ß_1$ induced Z-DEVD.AFC cleavage by Z-DEVD.FMK 131
Figure 6.10 Progressive inhibition curves of Z-DEVD.AFC cleavage in activated cell lysate by ICE-like protease inhibitors 132
Figure 6.11 Limited processing/activation of CPP32 in hepatocytes 135
Figure 6.12 PARP cleavage is not detected in hepatocyte nuclei and cell lysates 137
Figure 6.13 Cycloheximide inhibition of TGF-$ß_1$ induced Z-DEVD.AFC cleavage activity 138
Figure 7.1 Involvement of ICE-like proteases in TGF-$ß_1$ mediated hepatocyte apoptosis 155

List of Tables

Table 1.1 List of toxic compounds known to induce liver apoptosis 5

Table 1.2 Biological properties of TGF-ß 12

Table 1.3 Cleavage of proteins during apoptosis 22

Table 1.4 Subfamilies of ICE related protease 25

Table 3.1. The effect of spermine and spermidine on ISEL in rat liver nuclei 48

Table 5.1 Effects of TGF-$ß_1$ on size and number of nuclei containing DNA strand breaks 100

Table 6.1. Properties of various tetra/tripeptide inhibitors 119

Table 6.2 Inhibitor characterisation of Z-DEVD.AFC cleavage in hepatocyte lysates 133

Table 7.1 Proposed endonucleases involved in apoptosis 146

Abbreviations

anti-Dig	anti-digoxigenin-fluorescein Fab fragments
bp	base pairs
CAGE	conventional agarose gel electrophoresis
caspase	human ICE protease family members nomenclature
dig-11-dUTP	digoxigenin-11-2'-deoxyuridine 5'-triphosphate
DTT	dithiothreitol
EDTA	ethylenediaminetetraacetic acid
EGTA	ethyleneglyco-*bis*-(ß-aminoethyl)-*N,N,N',N'*-tetraacetic acid
FIGE	field inversion gel electrophoresis
H33258	Hoechst 33258
ICE	interleukin-1ß-converting enzyme
ISEL	in situ end-labelling
kbp	kilobase pair
PBS	phosphate-buffered saline
PI	propidium iodide
TdT	terminal deoxynucleotidyl transferase
TGF-$ß_1$	transforming growth factor-beta 1

1. Introduction

1.1 Modes of cell death

A large body of evidence has now been accumulated demonstrating the existence of a highly organised type of cell death. This mode of cell death called apoptosis is different from necrosis, which is the process of cell killing by a variety of harmful conditions and toxic stimuli. Cells undergoing necrosis typically exhibit distinctive morphological and biochemical features (reviewed in Trump et al., 1984). The earliest changes include the swelling of the cytoplasm and organelles, especially the mitochondria (high amplitude swelling) and this ultimately leads to organelle dissolution and rupture of the plasma membrane. These changes allow the leakage of the cellular contents into the extracellular space and the influx of extracellular Ca^{2+} across the membrane results in cytoskeletal alterations leading to membrane blebbing and activation of proteases, phospholipases and endonucleases (Orrenius et al., 1989). Necrosis typically affects groups of contiguous cells and is followed by inflammatory reactions (Schwartzman and Cidlowski et al., 1993).

In contrast, apoptosis or programmed cell death is a genetically controlled response for cells to commit suicide. Apoptosis is the Greek word that describes the dropping or falling of petals from flowers, or leaves from trees. This mode of cell death can be initiated and inhibited by a variety of stimuli, both physiological and pathological (Kerr et al., 1972). Cells undergoing apoptosis shrink, lose specialised cell surface elements such as microvilli and cell-cell junctions and eventually lose contact with their neighbouring cells. Ultrastructurally, dramatic changes occur within the nucleus leading to the compaction and margination of the nuclear chromatin, condensation of cytoplasm and variable convolution of nuclear and cellular outlines. The plasma membrane remains intact throughout this process thereby avoiding leakage of the cellular contents. This is highly significant as apoptotic cell death is not associated with inflammatory reactions. The cell ultimately separates into membrane bound fragments containing parts of the nucleus and intact organelles referred to as apoptotic bodies that are taken up by nearby cells or tissue macrophages. However, in cell cultures, apoptotic bodies usually escape phagocytosis and such bodies will undergo a process of degeneration called secondary necrosis (Wyllie, 1992). Current approaches to identification of apoptosis in cells and tissues involve morphological assessment. Although laborious and time consuming, this method is perhaps the ideal one. The methods used to detect the ultrastructural

morphological changes of chromatin condensation and nuclear fragmentation are electron microscopy, phase contrast or light microscopy (Patel and Gores, 1995). Furthermore, DNA binding dyes (i.e. propidium iodide, acridine orange, Hoechst 33258) can be used to identify the patterns of chromatin condensation and nuclear fragmentation in individual cultured cells by fluorescence and confocal microscopy. In this study, this method has been used to identify and quantify apoptosis in hepatocytes (see chapter 5).

The aims of this chapter are to summarise the current state of knowledge on apoptosis in the liver and pertinent findings from non-liver systems to address the relevant biochemical and molecular mechanisms in both the commitment and execution phases of this cell death programme. For a comprehensive survey on the subject of apoptosis, the reader is directed to recent reviews (Kerr, 1994; Thompson, 1995; Orrenius, 1995, Hale et al.,1996; McConkey et al., 1996).

1.2 Apoptosis in the liver

The first observation of apoptotic morphology termed as 'shrinkage necrosis' by Kerr (1971) was found to predominate in normal liver and mild ischaemic damage after ligation of its portal blood supply. Later studies have also demonstrated that apoptotic bodies can be found regularly in the normal liver parenchyma (Bursch et al., 1984; Bhathal and Gall, 1985), the rate of incidence being about one per 2000 hepatocytes (Bursch et al., 1985; Columbano et al., 1985). In addition, Benedetti et al. (1988) have reported that there is a preferential distribution of apoptotic bodies around the terminal hepatic venules (zone 3) in both human and rat liver. However, as described later there are a variety of physiological and toxicological stimuli which mediate apoptosis in the liver. These stimuli are illustrated in Figure 1.1.

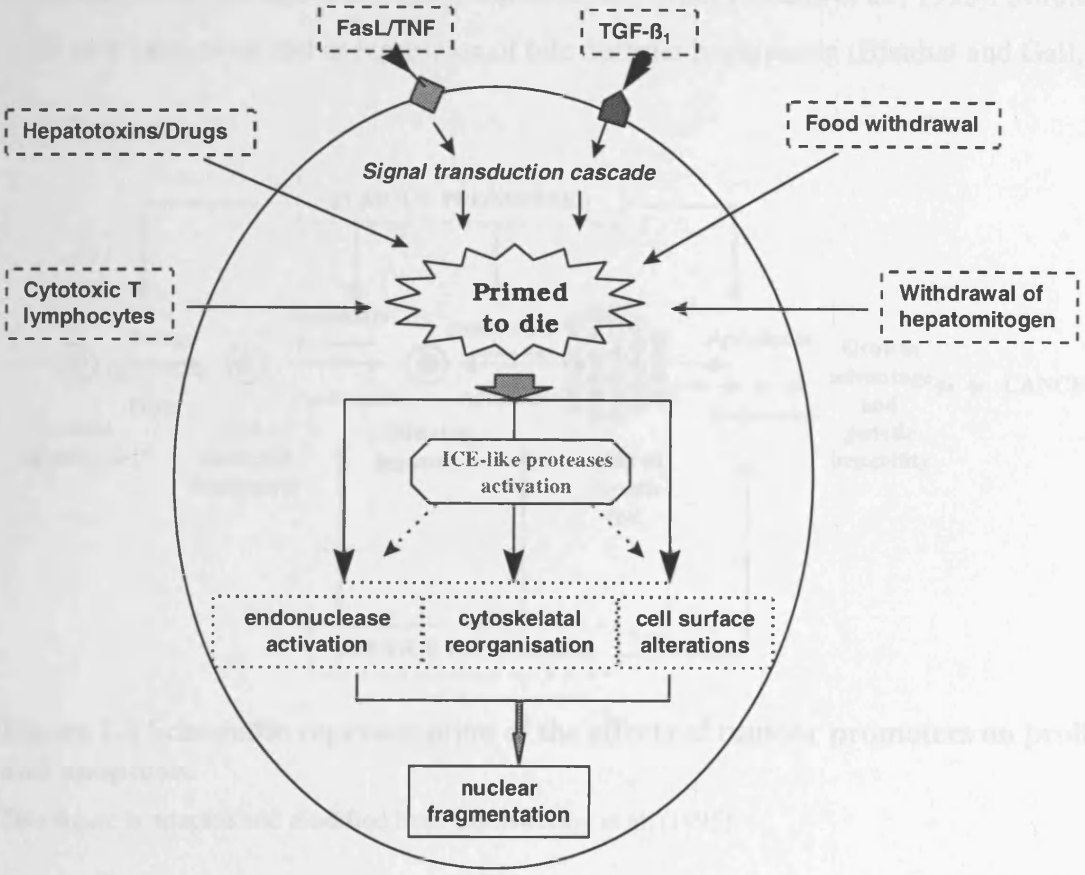

Figure 1.1 Schematic illustration of liver apoptosis induced by various physiological and toxicological stimuli.

1.2.1 Apoptosis and hepatocarcinogenesis

Both cell proliferation and apoptosis determine the net increase in the number of initiated cells and growth of precancerous cell populations in liver tumour development (Goldsworthy et al., 1995). Apoptosis represents an innate cellular defence against carcinogen induced cellular damage by removing and inhibiting survival and growth of altered cells at different stages of carcinogenesis (Goldsworthy et al., 1995). A simplistic schematic representation of the intricate regulation of apoptosis in carcinogenesis is shown in Figure 1.2. Hepatocarcinogenesis or liver growth can be induced by a variety of chemicals including phenobarbital (PB), α-hexachlorocyclohexane (α-HCH), the anti-androgen cyproterone acetate (CPA), ethinyl estradiol or peroxisome proliferators such as nafenopin or clofibrate (reviewed in Schulte-Hermann et al., 1995). Withdrawal of these agents produces tumour regression by stimulating apoptosis. Retreatment with these compounds can rescue the liver

from apoptosis (Bursch et al., 1984; Bursch et al., 1986; Roberts et al., 1995). Similar findings have also been observed in regression of bile ductular hyperplasia (Bhathal and Gall, 1984).

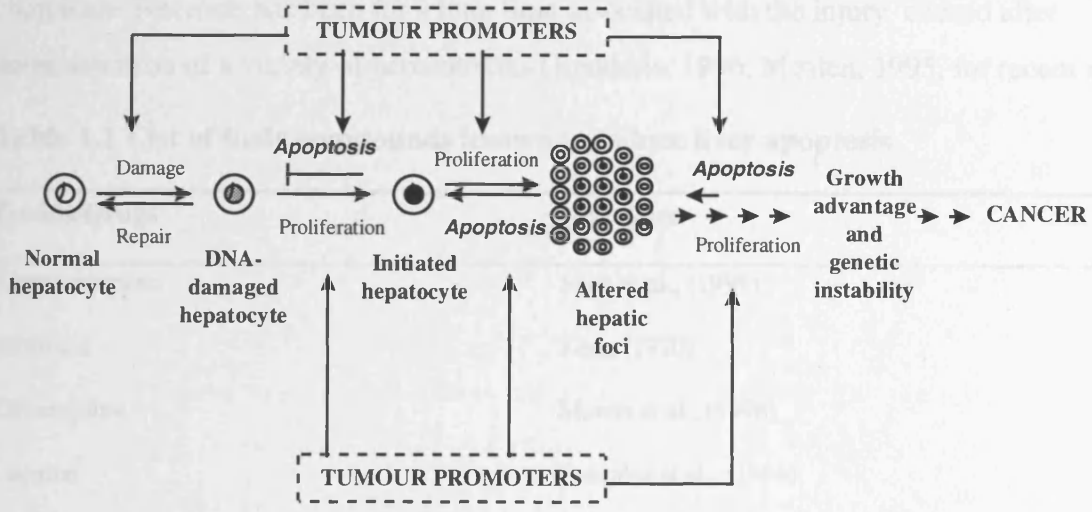

Figure 1.2 Schematic representation of the effects of tumour promoters on proliferation and apoptosis.

This figure is adapted and modified from Goldsworthy et al. (1995).

Tumour promoters such as TCDD may promote growth of the foci by specifically inhibiting apoptosis in hepatocytes of altered foci (Stinchcombe et al., 1995). In contrast, certain treatments can prevent preneoplastic growth and tumour development by enhancing lesion specific apoptosis especially by food restriction (Grasl-Kraupp et al., 1994) and monoterpene perillyl alcohol administration (Mills et al., 1995). Studies by Carthew et al. (1996) have shown that in tamoxifen treated liver of Wistar and Lewis strain rats, there is an increase in the labelling index of mitosis with significant increases in the number of apoptotic bodies. This is suggestive of the induction of apoptosis as a balance mechanism in controlling the mass of the liver.

Further elucidation of the effects of liver tumour promoters has been derived from studies using *in vitro* model system. Bayly et al. (1994) have demonstrated that nafenopin reversibly maintains the viability of primary rat hepatocytes and FaO hepatoma cell line by inhibiting apoptosis. In agreement, Oberhammer and Qin (1995) have also observed similar inhibitory effects of nafenopin on TGF-$ß_1$ induced apoptosis in hepatocytes. These results show that the effects seen *in vivo* can be reproduced *in vitro* and this will allow further dissection of the mechanisms involved in preventing apoptosis during hepatocarcinogenesis.

1.2.2 Toxin and drug induced liver apoptosis

It is not surprising that the liver, being the main organ for the detoxification of xenobiotics as well as endogenous compounds is subjected to the toxic actions of many chemicals. Necrosis has been for a long time associated with the injury caused after administration of a variety of hepatotoxins (Kedderis, 1996; Moslen, 1995, for recent reviews).

Table 1.1 List of toxic compounds known to induce liver apoptosis

Toxins/Drugs	Reference
Acetaminophen	Shen et al., (1991)
Albitocin	Kerr, (1970)
Chloroquine	Maeda et al., (1996)
Cocaine	Cascales et al., (1994)
Colchicine	Tsukidate et al., (1993)
Cycloheximide	Ledda-Columbano et al., (1992)
Cyclosporine A	Yokoyama et al., (1996)
1,1-Dichloroethylene	Reynolds et al., (1984)
Dimethylnitrosamine	Pritchards and Butler, (1989)
Ethanol	Benedetti et al., (1988)
Glycodeoxycholate	Patel et al., (1994)
Heliotrine	Kerr, (1969)
Leupeptin	Maeda et al., (1996)
Menadione	McConkey et al., (1988)
Polymyxin B	Sanchez et al., (1992)
Okadaic acid	Boe et al., (1991)
Staurosporine	Sanchez et al., (1992); Cain et al., (1996a)
Thapsigargin	Kaneko and Tsukamoto, (1994)
Thioacetamide	Ledda-Columbano et al., (1991)
Vinblastine	Tsukidate et al., (1993)

However a variety of compounds have been shown to induce apoptosis in the liver (Table.1.1). The induction of apoptosis by toxic agents is dose related. For example, HL-60 cells will undergo apoptosis after treatment with moderate concentrations of various drugs or low irradiation, whereas treatment with higher concentrations of these stimuli produces necrosis (Martin and Cotter, 1994). In the liver, a slightly different scenario was observed after *in vivo* administration of thioacetamide. At both the low (25mg/kg) and high dose (200mg/kg), morphological characteristics of apoptosis (chromatin condensation, cellular shrinkage, absence of inflammatory response, no change of the serum profile of transaminases) were seen initially (3 to 6h) in the absence of necrosis (Ledda-Columbano et al., 1991). Necrosis accompanied by massive inflammatory reactions was evident at 12h and even more pronounced at later time points (24 and 36h). This study indicates that apoptosis and necrosis may be induced sequentially by a single dose of thioacetamide. In addition other hepatotoxins such as 1,1-dichloroethylene (Reynolds et al., 1984) and diethylnitrosamine (Pritchard and Butler, 1989) may also induce apoptosis as well as necrosis. The co-existence of apoptosis and necrosis in the liver was also described by Kerr (1969; 1970) in animals treated with the pyrrolizidine alkaloid heliotrine and albitocin. Administration of a dose of cycloheximide that inhibits 80-85% of hepatic protein synthesis induced apoptosis in the rat liver (Ledda-Columbano et al., 1992). The incidence of apoptosis within 2h of giving the compound was not accompanied by changes in the levels of serum transaminases, necrosis and inflammatory reactions.

Many compounds have been reported to induce apoptosis in primary hepatocytes and hepatoma cell lines. For example, treatment with the microtubule antagonists such as vinblastine and colchicine induced apoptosis in cultured rat hepatocytes (Tsukidate et al., 1993). Exposure to menadione and the toxic bile acid glycodeoxycholate stimulated apoptosis at low doses whereas higher doses caused necrosis (McConkey et al., 1988; Patel et al., 1994). In another study, two protease inhibitors, leupeptin and chloroquine were found to induce apoptosis in hepatocytes (Maeda et al., 1996). On the other hand, thapsigargin, a non-phorbol ester type tumour promoter that specifically inhibits the endoplasmic reticulum Ca^{2+}-ATPase induced apoptosis in PLC/PRF/5 human hepatoma cells (Kaneko and Tsukamoto, 1994).

1.2.3 Viral and immune mediated apoptosis in the liver

There are a variety of viruses capable of infecting the liver, and elimination of these virus infected cells by apoptosis instead of necrosis is advantageous to the host. The infected cells can be eliminated either by direct viral cytotoxicity or by cytotoxic T lymphocytes (CTL) mediated immune responses to the viral antigens. Furthermore, the formation of apoptotic bodies with the intact membrane followed by phagocytosis prevents the dissemination and release of virions. In contrast, viral infected cells undergoing necrosis (lytic process) will lead to the spreading of the virions (Searle et al., 1987).

Characteristic histopathological evidence of apoptosis such as the presence of apoptotic bodies, previously known as acidophilic bodies or Councilman bodies are normally seen in viral hepatitis (Kerr et al., 1979). Cell mediated immune response occurs in hepatitis caused by both hepatitis B virus (HBV) and hepatitis C virus (HCV) (Searle et al., 1987; Ando et al., 1993; Mita et al., 1994; Hiramatsu et al., 1994). For example, in a transgenic mouse model of fulminant hepatitis B, hepatocytes underwent apoptosis immediately after a direct interaction with the hepatitis B surface antigen-specific CTL (Ando et al., 1993). In addition, liver biopsies taken from patients with chronic hepatitis C infection and fulminant hepatitis B also showed apoptosis occurring in the hepatocellular area (Hiramatsu et al., 1994; Takiya et al., 1995).

Apoptosis as a mechanism of cell death has also been observed in liver allograft rejection (Searle et al., 1987, Krams et al., 1995b). In a study by Searle et al. (1977), hepatocyte death in pig hepatic allograft rejection was found to parallel lymphoid infiltration of the parenchyma and to be exclusively apoptotic. These observations have been extended in biopsies of human liver transplants where numerous apoptotic bodies often associated with infiltrating mononuclear cells were seen in the parenchyma (Snover et al., 1984). In another study, Krams et al. (1995a) showed an increase in the incidence of apoptotic cells which paralleled mononuclear cell infiltration in allografts and did not occur in syngeneic grafts. Interestingly, there was an increase in transforming growth factor-beta1 (TGF-$ß_1$) expression which correlated with apoptosis in the liver allografts, supporting the role of this cytokine in hepatocyte apoptosis (see below).

1.2.4 Receptor mediated signalling in liver apoptosis

Apoptosis can be actively induced in many model systems by agonistic receptor engagement (Mc Conkey et al., 1996), such as by TGF-β_1, Fas/Apo-1, tumour necrosis factor (TNF) and steroids. There are a number of signal transduction pathways activated during apoptosis and these include the Ras signalling pathways, protein kinase C, calcium, ceramide, cAMP and transcriptional activation related to oxidative stress/oxygen radicals (reviewed in Hale et al., 1996). Although the apoptotic signalling pathways in the hepatobiliary system have not been extensively studied, triggering of apoptosis in the liver by three receptor mediated pathways i.e. TGF-β_1, Fas/Apo-1 and TNF-α has been characterised and will be discussed as described below.

1.2.4.1 Transforming growth factor-beta1 (TGF-β_1)

The initial identification of TGF-ß was based on its ability to induce reversible transformation of rodent fibroblasts (Moses et al., 1981; Roberts et al., 1981). The assay used to measure this activity, which provided the name for the peptide, was the ability of TGF-ß to induce normal rat kidney fibroblasts to grow and form colonies in soft agar in the presence of epidermal grawth factor. TGF-ß also stimulates anchorage-independent growth of other fibroblastic cell lines (Moses et al., 1981). It was first purified to homogeneity from human platelets with a molecular mass of 25 kDa (Assoian et al., 1983).

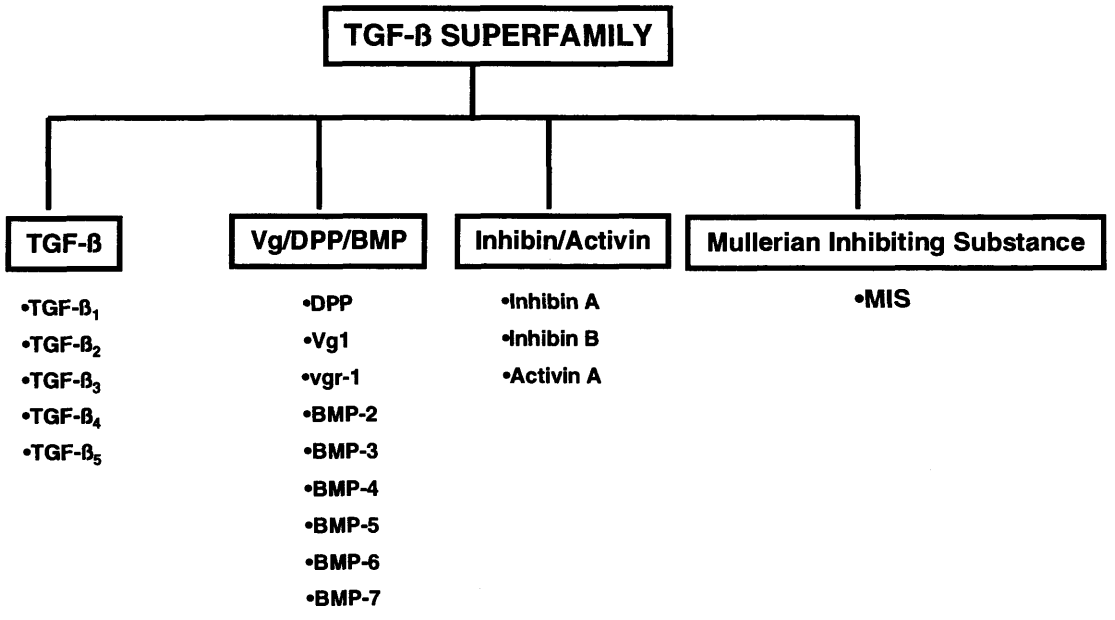

Figure 1.3 The members of TGF-ß superfamily

The members stated in this figure are of human origin with the exception of TGF-β_4 which is from chicken; TGF-β_5 and Vg1 from Xenopus; DPP from Drosophila.

Since the discovery of TGF-ß more than a decade ago, extensive protein characterisation and cDNA analyses have revealed a large group of structurally related factors, which are collectively termed the TGF-ß superfamily (Figure 1.3). This superfamily contains not only the mammalian TGF-ß isoforms (TGF-$ß_1$, TGF-$ß_2$ and TGF-$ß_3$), but includes the activins, inhibins, the bone morphogenetic proteins (BMPs), Mullerian inhibitory substance (MIS), the fruitfly *Drosophila* decapentaplegic protein (DPP) as well as other related proteins found in vertebrate species (reviewed in Massague, 1990).

1.2.4.1a Structure of TGF-$ß_1$

TGF-$ß_1$ is a disulphide linked dimer of two identical chains. Each chain is synthesised as a large precursor of 390 amino acids (Figure 1.4). This precursor contains an N-terminal signal peptide, a long pro-segment also called the latency associated peptide (LAP), and a 112 amino acid C-terminal polypeptide that constitutes the mature, bioactive TGF-$ß_1$ monomer (Massague, 1990).

The N-terminal signal peptide contains a hydrophobic signal sequence for translocation across the endoplasmic reticulum. Once in the endoplasmic reticulum, the long pro-segment is glycosylated at three glycosylation sites and two of the carbohydrate side chains are phosphorylated at a mannose residue forming mannose 6-phosphate (Purchio et al., 1988). This N-terminal modification is required for the secretion of TGF-$ß_1$, as deletion of the hydrophobic sequence and the two mannose 6-phosphate N-linked carbohydrates prevents TGF-$ß_1$ secretion (Lopez et al., 1992)

TGF-$ß_1$ is secreted in the latent form which is also known as TGF-$ß_1$-LAP. Although the mechanisms of its activation *in vivo* are not fully understood, evidence suggests that mannose 6-phosphate residues in the TGF-$ß_1$ pro-segment may tether the complex to the mannose 6-phosphate/insulin growth factor-II (M6P/IGF-II) receptors (Purchio et al., 1988). These receptors are involved in TGF-$ß_1$-latent complex activation which results in the release of the bioactive peptide. The precursor cleavage site is a sequence of four basic amino acids preceding the bioactive domain which constitutes the mature TGF-$ß_1$ monomer. Proteases such as plasmin and cathepsin have been implicated in the activation of latent TGF-$ß_1$ which is bound to M6P/IGF-II receptor (Derynck, 1994).

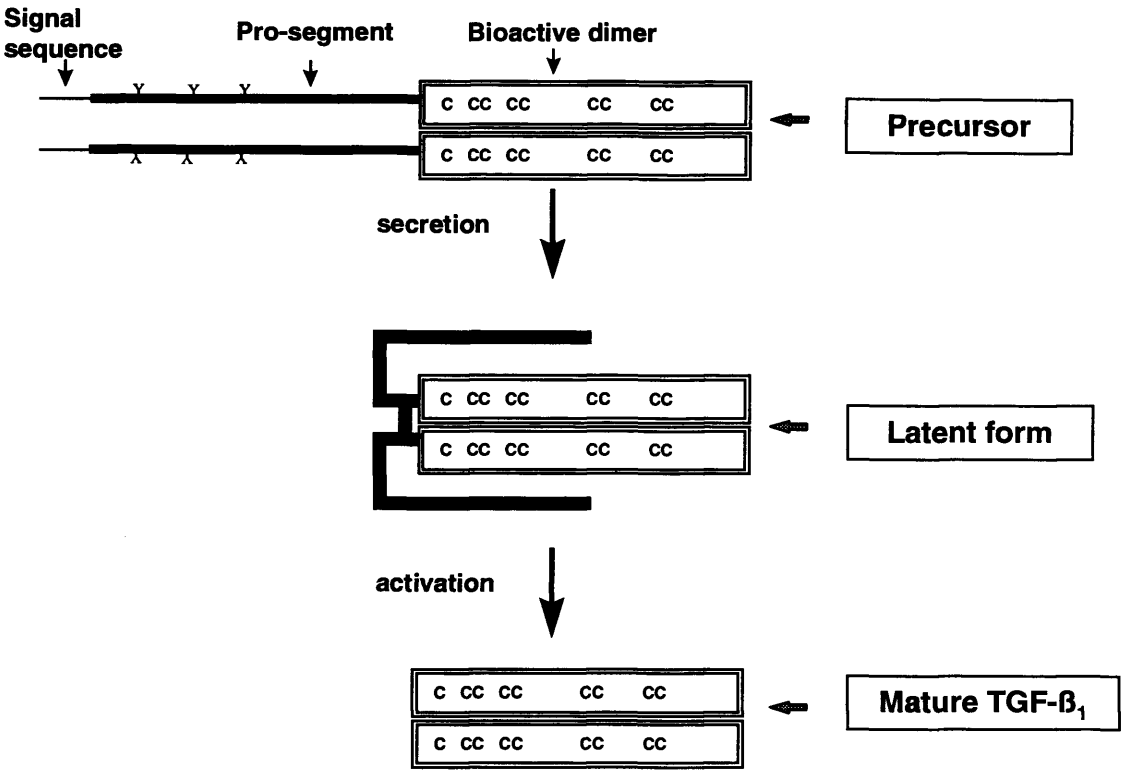

Figure 1.4 Schematic illustration of precursor, latent and bioactive forms of TGF-$ß_1$

The precursor, latent form and bioactive dimer of TGF-$ß_1$ are shown in this figure. The sites for N-linked glycosylation are indicated as 'Y' in the pro-segment region. The cysteines in the bioactive domain are shown as 'C'. TGF-$ß_1$ dimer remains in a biologically latent form after secretion. Upon activation, the mature bioactive form of TGF-$ß_1$ is released. This figure is adapted and modified from Massague,1990.

1.2.4.1.b Receptors of TGF-$ß_1$

There are three membrane bound receptors for TGF-ß called type I, II and III receptor (RI, RII and RIII respectively). RIII, also called betaglycan is a transmembrane proteoglycan with a short cytoplasmic domain (Derynck, 1994). No signalling motifs are found on RIII, consistent with the current belief that this receptor does not mediate TGF-ß signalling. Nevertheless, expression of betaglycan increases binding of TGF-ß to the type II receptor, but not type I receptor, which suggests that RIII may be involved in ligand presentation to RII (reviewed in Derynck, 1994).

The biological activities of TGF-$ß_1$ are mediated by its binding to a heteromeric receptor complex comprising RI and RII (Figure 1.5). The type II receptor is a transmembrane serine-threonine kinase with a short extracellular cysteine rich domain. The long cytoplasmic region comprises primarily the kinase domain, which is flanked by a carboxy-terminal extension

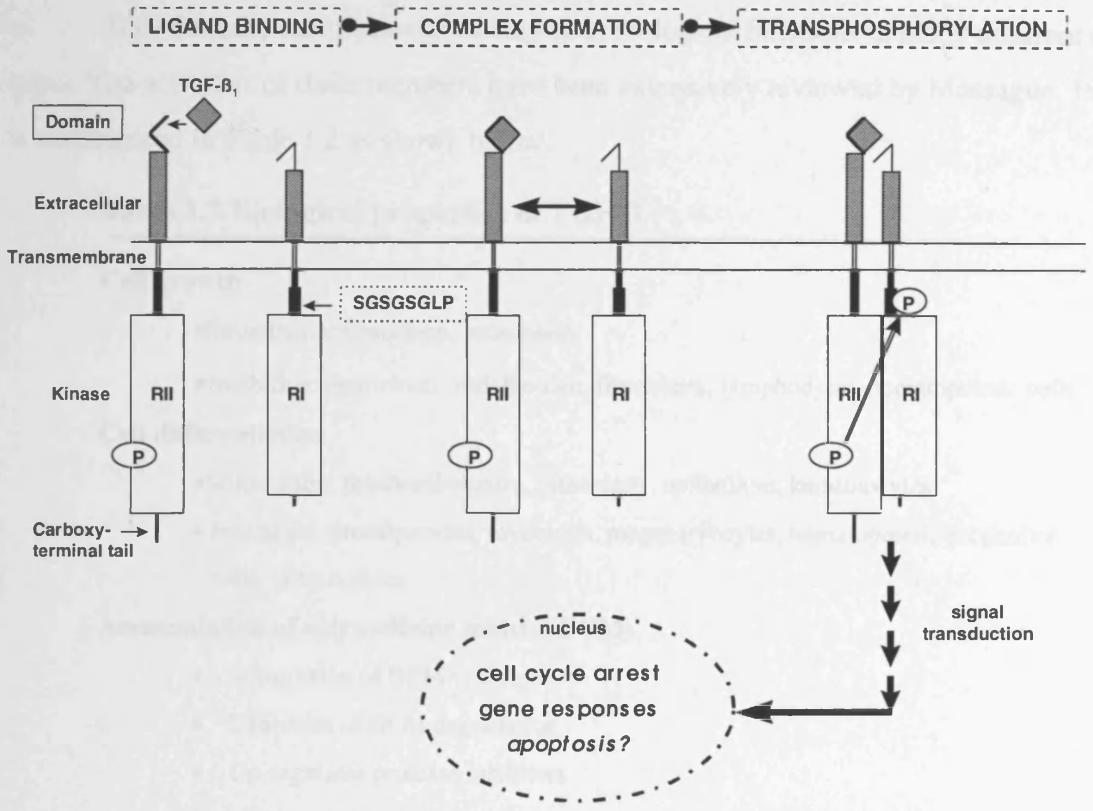

Figure 1.5 Activation of the heteromeric TGF-ß$_1$ receptor complex

TGF-ß$_1$ receptor complex involves binding of dimeric TGF-ß$_1$ to RII; recruitment of RI to the RII-TGF-ß$_1$ complex; phosphorylation of the GS domain of RI by the RII serine-threonine kinase. This allows RI kinase to propagate TGF-ß$_1$ signalling pathway. This figure is adapted and modified from Wrana et al., 1994.

and a spacer segment between the transmembrane and kinase sequences. Similar to RII, type I receptor is also a transmembrane serine/threonine kinase but with shorter extracellular and cytoplasmic domains. In contrast to RII, the type I receptor has only a few amino acids on the carboxy terminal region. The spacer regions between the transmembrane and kinase domains of RI contain a conserved SGSGSGLP motif, called the GS domain (Derynck, 1994).

The type II receptor, which is a constitutively active kinase can directly bind TGF-ß$_1$, but it is incapable of mediating TGF-ß$_1$ responses in the absence of a type I receptor. Unlike RII, the type I receptor at the cell surface is unable to bind TGF-ß from the medium. However, RII bound TGF-ß is recognised by RI, which as a result, becomes incorporated into the complex. Once in the complex, RI is transphosphorylated by RII at serine and threonine residues in the GS domain (Wrana et al., 1994). Phosphorylation of RI on these residues correlates with the activation of its kinase activity as mutations that interfere with this phosphorylation abrogate signal propagation (Wrana et al., 1994). Thus, phosphorylation of RI by type II receptor is an essential step in the TGF-ß$_1$ signalling pathway.

TGF-ß family members exert a variety of biological functions in many different cell types. The activities of these members have been extensively reviewed by Massague, 1990 and is summarised in Table 1.2 as shown below.

Table 1.2 Biological properties of TGF-ß

Cell growth

- •Stimulation: fibroblasts, osteoblasts
- •Inhibition: epithelium, endothelium, fibroblasts, lymphocytes, hematopoietic cells

Cell differentiation

- •Stimulation: prechondroblasts, osteoblasts, epithelium, keratinocytes
- • Inhibition: preadipocytes, myoblasts, megakaryocytes, hematopoietic progenitor cells, lymphocytes

Accumulation of extracellular matrix (ECM)

- • Stimulation of ECM synthesis
- • Inhibition of ECM degradation
- • Up-regulates protease inhibitors
- • Down-regulates proteolytic enzymes

Increases cell adhesion

- • Stimulates synthesis of integrin receptors
- • Stimulates integrin synthesis

Chemotaxis

- • Macrophages
- • Fibroblasts
- • Osteoblasts

Apoptosis

This table is adapted and modified from Terrell et al., 1993

TGF-$ß_1$ can stimulate growth of some cells, while causing growth arrest in other cells. For example, TGF-$ß_1$ has been shown to stimulate growth of fibroblasts (Tucker et al., 1983) and osteoblasts (Robey et al., 1987), whereas it inhibits growth of epithelial cells (Massague, 1990). It has also been shown to stimulate production of collagen and fibronectin and their incorporation into the extracellular matrix of fibroblasts (Ignotz and Massague, 1986). TGF-$ß_1$ inhibits adipogenesis, myogenesis and hematopoiesis, whereas it promotes chondrogenesis and epithelial cell differentiation (Sporn et al., 1987). This cytokine also plays an important role in

the inflammatory response by its ability to potently attract monocytes and fibroblasts (reviewed in Derynck, 1994)

The various functions of TGF-$ß_1$ indicate the involvement of this cytokine in many physiological and pathological conditions. However, in this chapter, I will discuss two relevant effects of TGF-$ß_1$, namely growth inhibition and apoptosis.

1.2.4.1c Growth inhibition by TGF-$ß_1$

As shown in Table 1.2, TGF-$ß_1$ inhibits growth in many cell types. The mechanism of TGF-$ß_1$ induced growth arrest differs in different cell types. Earlier studies have shown that growth inhibition of Mv1Lu lung epithelial cells by TGF-$ß_1$ is associated with the supression of retinoblastoma protein (RB) phosphorylation (Laiho et al., 1990). Hypophosphorylated RB binds to the transcription factor E2F; phosphorylation causes it to dissociate from E2F, enabling it to proceed with the activation of S phase genes (Weinberg, 1995; see Figure 1.6). These findings suggest that RB kinases are potential targets in TGF-$ß_1$ signalling pathway.

It has now been demonstrated that activation of these RB kinases requires accumulation of the activating subunit (cyclin) and the catalytic subunit (cyclin dependent kinase [CDK]), assembly of the cyclin/CDK complex, and CDK phosphorylation by the CDK-activating kinase (CAK) as illustrated in Figure 1.6 (Massague and Polyak, 1995). The activities of these kinases are now known to be regulated by members of the growing family of cyclin-dependent kinase inhibitors (CDI) (Sherr and Roberts, 1995).

TGF-$ß_1$ has been shown to down-regulate cyclin E, CDK2 and CDK4 expression in human keratinocytes (Geng and Weinberg, 1993). Furthermore, Hannon and Beach (1994) have demonstrated increased expression of p15, a cyclin dependent kinase inhibitor (CDI) in TGF-$ß_1$ treated human keratinocytes. p15 may function as an effector of TGF-$ß_1$ mediated cell cycle arrest through inhibition of CDK4 and CDK6 (Hannon and Beach, 1994). However in these cells, TGF-$ß_1$ had no effect on the expression of another CDI called p27. In contrast, inhibition of cyclin E/CDK2 complexes by p27 has been shown in TGF-$ß_1$ mediated growth arrest in Mv1Lu cells (Polyak et al., 1994). It has been suggested that p27 is released from cyclin D1-CDK4 complexes upon TGF-$ß_1$ treatment and subsequently associates with cyclin E-CDK2 complexes to block its kinase activity (Polyak et al., 1994).

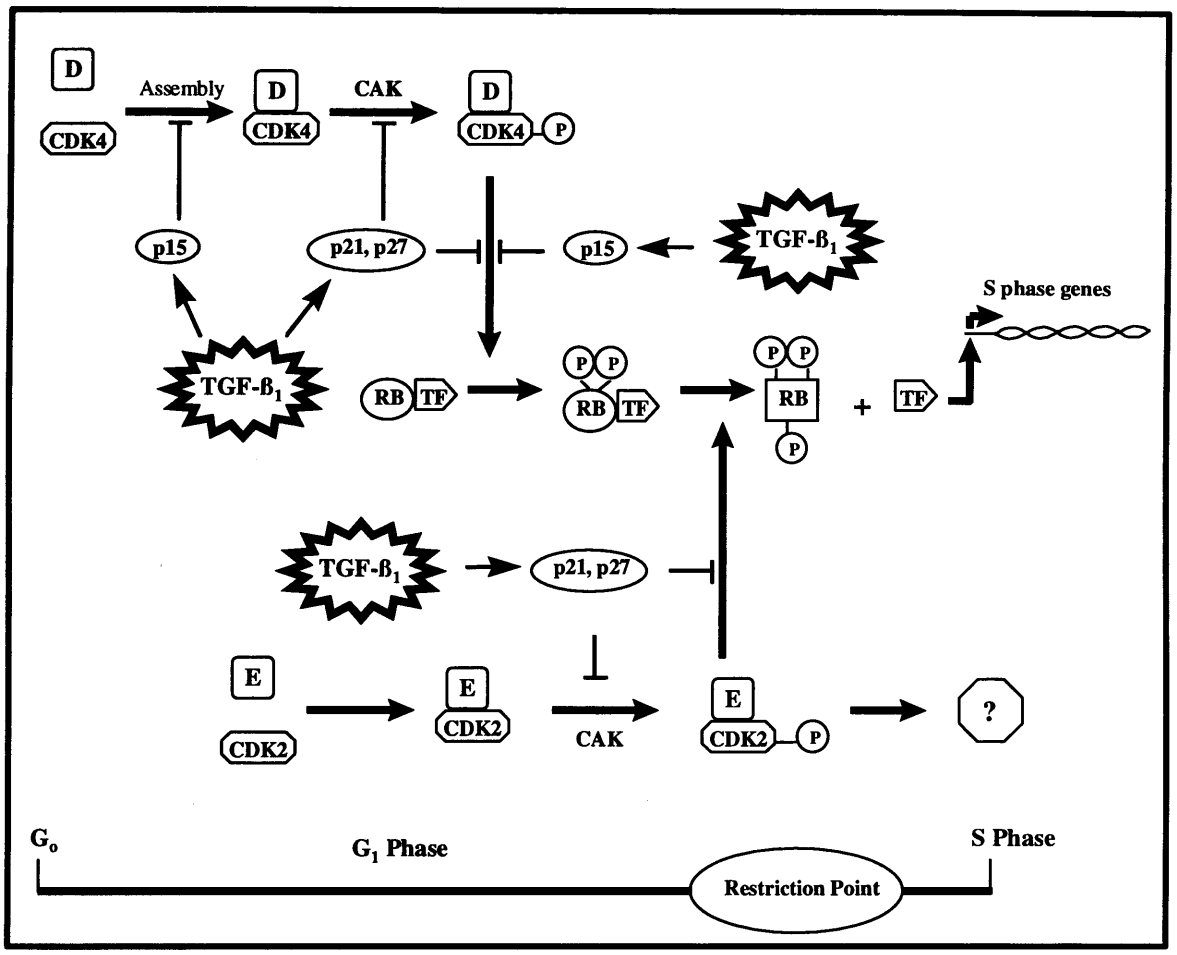

Figure 1.6 Targets of TGF-ß$_1$ in G$_1$ phase progression

In early G$_1$ phase, D-type cyclins assemble with CDK4 or CDK6 (not shown in this figure) and once assembled, they are phosphorylated by a CDK activating kinase (CAK). This complex now acquires catalytic activity which further phosphorylates retinoblastoma protein (Rb). Hyperphosphorylation of Rb results in the release of bound transcription factors (TF) such as E2F which activate genes required for S phase entry. Cyclin E-CDK2 complex which appears later in the G$_1$ has also been suggested to phosphorylate Rb as well as other substrates. The regulation of G$_1$ progression by TGF-ß$_1$ and cyclin dependent kinase inhibitors such as p21, p27 and p15 is discussed in the text. This figure is adapted and modified from Sherr and Roberts, 1995.

Datto et al. (1995) have proposed the involvement of yet another member of the CDI family called p21 in TGF-ß$_1$ treated human keratinocytes and MCF-7 breast epithelial carcinoma cells. In this study, they have demonstrated that induction of p21 leads to its increased association with cyclin D1 and CDK2. These results, together with the findings described above, clearly support the idea that TGF-ß$_1$ may affect the cell cycle progression by inducing the activities of multiple CDIs which ultimately leads to hypophosporylation of RB.

TGF-ß$_1$ has also been shown to mediate growth arrest in hepatocytes isolated from normal and regenerating rat liver (Nakamura et al., 1985; Carr et al., 1986; Strain et al., 1987). Furthermore, Whitson and Itakura (1992) have demonstrated that growth arrest in TGF-ß$_1$ treated WB rat epithelial cells is associated with hypophosphorylation of RB. These results

indicate that inhibition of RB phosphorylation may be a cause or a consequence of the G_1 arrest. Whether the induction of growth arrest and apoptosis share the same pathways remains to be identified.

1.2.4.1.d Apoptosis induced by TGF-$ß_1$

The results described in the previous section suggest that TGF-$ß_1$ is likely to play a central role in regulating normal cell growth and act as a negative regulator of hepatocyte proliferation. Further support for this hypothesis comes from studies by Oberhammer et al. (1992) who have demonstrated that TGF-$ß_1$ induces apoptosis in hepatocytes *in vitro* and after intravenous injection *in vivo*. In addition, Terrell et al. (1993) have observed liver involution in response to high dose systemic administration of TGF-$ß_1$ in rats. Oberhammer et al. (1993) have shown that this atrophy is caused by apoptosis. TGF-$ß_1$ induced apoptosis is much more effective in the regressing liver, after withdrawal of the mitogen cyproterone acetate (Oberhammer et al., 1993). Positive immunostaining of TGF-$ß_1$-LAP has been identified in apoptotic hepatocytes in regressing liver after CPA withdrawal but not in necrotic hepatocytes after CCl_4 treatment (Bursch et al., 1993). These findings suggest that hepatocytes synthesise the precursor of TGF-$ß_1$ prior to apoptosis or that other cells synthesise this cytokine which is released into the extracellular environment.

Involvement of this cytokine in hepatocyte apoptosis has been substantiated by studies in a transgenic mouse model in which mature TGF-$ß_1$ is overexpressed in the liver (Sanderson et al., 1995). Hepatocyte apoptosis has been frequently observed in all of the five transgenic lines, but is most pronounced in line 25 which has the highest plasma levels of TGF-$ß_1$. In addition, TGF-$ß_1$ has also been shown to induce apoptosis in foetal hepatocytes in primary culture demonstrating the ability of this cytokine to modulate the growth of foetal liver (Fabregat et al., 1996; Sanchez et al., 1996).

Activin A, another member of the TGF-ß superfamily has also been demonstrated to cause growth arrest and apoptosis in cultured hepatocytes (Yasuda et al., 1993; Schwall et al., 1993). Moreover, subcutaneous infusion of activin A has resulted in apoptosis in mice liver (Hully et al., 1994). These results suggest that activin A may be important in hepatic homeostasis.

Apoptosis mediated by TGF-β_1 has also been observed in nonliver systems including epithelium cells like prostate (Kyprianou and Isaacs, 1989), endometrial stromal cells (Rotello et al., 1991; Moulton et al., 1994), human papillomavirus type 16-immortalised human ectocervical epithelial cells (Rorke and Jacobberger, 1995) and in human breast adenocarcinoma cell lines, MCF-7 and MDA-231 (Perry et al., 1995). In addition, increased expression of TGF-β_1 has been demonstrated during apoptosis in oestrogen receptor-dependent tumours following oestrogen ablation (Kyprianou et al., 1990) and mammary gland involution (Strange et al., 1992).

Resistance to growth inhibition and apoptosis induced by TGF-β_1 has been implicated as a mechanism of carcinogenesis, although at present the mechanism of the resistance is not fully understood (Schulte-Hermann et al., 1995). In this respect, several hepatoma cell lines (e.g. Hep G2) have been shown to be resistant to TGF-β_1 induced apoptosis (Shirai et al., 1994, Lin and Chou, 1992) whereas others like FaO, Hep 3B and HuH-7 cells are susceptible (Bayly et al., 1994; Chuang et al., 1994; Fan et al., 1996 respectively). Peroxisome proliferators such as nafenopin supressed apoptosis mediated by TGF-β_1 in hamster, guinea pig and rat hepatocytes as well as FaO hepatoma cells (James and Roberts, 1996; Bayly et al., 1994). Similar results were obtained with phenobarbital treated hepatocytes (James and Roberts, 1996). In summary these results indicate the importance of apoptosis supression in liver tumour hyperplasia (also see section 1.2.1).

Increased TGF-β_1 intracellular concentrations in periportal hepatocytes but not in putative preneoplastic cells have been observed in phenobarbital promoted rat liver tumours (Jirtle and Meyer, 1991). On the other hand, patients with hepatocellular carcinoma have higher plasma levels of TGF-β_1 which reduced significantly upon treatment of this cancer (Shirai et al., 1994). This indicates the involvement of the cytokine in eliminating unwanted cells by apoptosis during tumour formation in the liver. Support to this suggestion comes from recent studies by Mullaeur et al. (1996). They have demonstrated that in the putative preneoplastic foci, the already-elevated basal apoptotic incidence is increased by TGF-β_1. Moreover, the apoptotic inducing activity is further enhanced by the additional treatment with the anti-oestrogen tamoxifen. These results show that tamoxifen increases the susceptibility of preneoplastic cells to undergo TGF-β_1 stimulated cell death.

It is possible that the tumour itself is resistant to apoptosis, and this process only occurs in the surrounding normal cells. A possible mechanism to explain this selective growth advantage is the down regulation of the mannose 6-phosphate/insulin-like growth factor II (M6P/IGF-II) receptor (which plays a role in controlling the level of active TGF-β_1) in preneoplastic hepatocytes but up-regulation in normal hepatocytes (Jirtle et al., 1994). Alternatively, the resistance to TGF-β_1 induced apoptosis could be due to loss of TGF-β_1 receptors I or II, as these receptors are involved in the signalling pathways leading to growth inhibition of epithelial cells (Wrana et al., 1994; Park et al., 1994). Furthermore, involvement of RB in apoptosis has now been demonstrated, in addition to its known effects in growth arrest (Fan et al., 1996). They showed that inhibition of RB phosphorylation and its expression by TGF-β_1 induced apoptosis in HUH-7 cells. Furthermore antisense RB treatment induced apoptosis in primary hepatocytes while overexpression of wild-type RB inhibited TGF-β_1 induced apoptosis in HUH-7 cells (Fan et al., 1996). These results provide insights into RB functions and suggest that this protein is involved in controlling a balance between growth and apoptosis in normal development and neoplastic transformation.

1.2.4.2 Fas/APO-1/CD95 and tumour necrosis factor (TNF)

Fas is a 45-kD cell surface protein belonging to the TNF/nerve growth factor receptor family. Engagement of Fas/APO-1 receptor with specific antibodies, or upon exposure to its natural ligand transduces an apoptotic signal to a variety of cell types (Nagata and Goldstein, 1995). Similar effects are also seen with TNFR-1, another member of the TNF receptor family. Fas and TNFR-1 share a region of homology termed the 'death domain' which has been identified as Fas-associating protein with death domain (FADD/MORT1) and TNFR-1 associated death domain (TRADD) respectively (reviewed in Cleveland and Ihle, 1995). These death domains function as the common signalling conduit for this cytokine mediated cell death.

Fas receptor is expressed in many normal and neoplastic cells or tissues. However its ligand is expressed mainly on activated cytotoxic T lymphocytes (CTLs) which play a pivotal role in the regulation of apoptosis in several systems including the liver. This observation poses a question as to why liver cells express the Fas receptor which can result in apoptosis and its relevance in the homeostasis and disease in the hepatobiliary system. In this respect, it has been demonstrated that intraperitoneal injection of monoclonal antibody against Fas antigen in mice induces hepatocyte apoptosis (Ogasawara et al., 1993). Similar findings have also been

described in studies employing primary mouse hepatocyte cultures (Ni et al., 1994). The high susceptibility of the liver to Fas-mediated apoptosis might be correlated with the absence of expression of bcl-2 in nontransgenic mice, as hepatic apoptosis is delayed and dramatically reduced in transgenic mice expressing the human bcl-2 gene product in hepatocytes (Lacronique et al., 1996). Further support for the role of Fas in the hepatobiliary system comes from a recent study by Galle et al. (1995) who demonstrated not only the ability of Fas to induce apoptosis in primary human hepatocytes but also the involvement of this receptor mediated cell death in liver damage. They found an increased expression of Fas receptor in hepatitis B virus related cirrhosis and acute liver failure and the Fas ligand expression was elevated mainly in areas with lymphocytic infiltration, suggesting killing of hepatocytes by T lymphocytes using the Fas receptor-ligand system. In agreement, Takatani et al. (1996) reported diffuse and strong expression of Fas on the plasma membrane of hepatocytes in patients with severe and chronic hepatitis.

The location of Fas expression is an important factor in its involvement in apoptosis. For example, it has been shown that hepatocellular carcinoma (HCC) tissues express Fas less frequently and more weakly than non-cancerous tissues (Higaki et al., 1996). The majority of non-cancerous specimens expressed Fas both on the surface and in the cytoplasm where the incidence of apoptosis was higher. In contrast, HCC tissues expressed Fas mainly in the cytoplasm where the incidence of apoptosis is significantly lower. This indicates a mechanism for the cancer cells to escape from Fas-mediated apoptosis.

Another cytokine that has been implicated in liver injury and apoptosis is TNF-α, a secretory product of macrophages and lymphocytes. Like Fas, TNF-α shares the ability to induce sphingomyelinase and evidence has been presented to suggest that the product, ceramide, is an inducer of apoptosis (reviewed in Nagata and Goldstein, 1995). TNF-α has been shown to induce apoptosis in rat and mouse hepatocytes and liver *in vivo* (Shinagawa et al., 1991; Leist et al., 1994). Interestingly, TNF-α requires a metabolic condition of transcriptional arrest in order to exert its apoptosis (Leist et al., 1994). In addition, Van Antwerp et al. (1996) have shown that cells with a block in NF-κB signalling by protein and RNA synthesis inhibitors (e.g. cycloheximide or actinomycin D) are more susceptible to TNF-α induced apoptosis. Thus, inhibition of NF-κB may be used by organisms as a means of killing TNF-α targeted cells.

Further elucidation of the Fas/TNF-α mediated apoptosis and the intricate interplay with other cytokines like TGF-$ß_1$ will provide insight into the receptor mediated signalling pathways and the downstream execution process culminating in hepatocyte apoptosis. Indeed in a recent study, pre-exposure of human malignant glioma cells to TNF-α has been shown to augment Fas/APO-1 dependent cytotoxicity (Weller et al., 1994). Furthermore, pre-treatment with TGF-$ß_2$ enhanced Fas-induced glioma cell apoptosis. Such augmentation in the hepatobiliary system remains to be identified.

1.3 Biochemical mechanisms of apoptosis

The last decade has seen a rapid growth of research in understanding the mechanisms of apoptosis. Among the various biochemical events observed in apoptosis, chromatin cleavage has been considered the biochemical hallmark of apoptosis. Although it has been demonstrated that denucleated cells undergo apoptosis suggesting that cell nucleus and DNA fragmentation are not required for apoptosis (Jacobson et al.,1994; Schulze-Osthoff et al., 1994), nuclear DNA degradation is still a cardinal feature of apoptosis in many cell types. More recent observations have alluded to the role of proteases involved in both the cytoplasm and nucleus in executing the apoptotic death programme which is believed to occur upstream and/or prior to the activation of the apoptotic endonucleases.

1.3.1 DNA cleavage during apoptosis

Although the generation of oligonucleosomal DNA fragments in rat liver nuclei was demonstrated by Hewish and Burgoyne (1973), it was Skalka et al. (1976) who first observed internucleosomal cleavage during apoptosis in lymphoid tissues of irradiated mice. Subsequently Wyllie (1980) reported in a landmark paper that an endonuclease was specifically activated during glucocorticoid induced thymocyte apoptosis. This enzyme cleaved DNA linker regions between nucleosomes and multiples of 180-200kbp DNA fragments were generated and seen as a ladder pattern upon gel electrophoresis (Wyllie,1980). Current opinion holds that the internucleosomal cleavage is a result of Ca^{2+}/Mg^{2+} endonuclease(s) activation (Compton,1992; Peitsch et al., 1994).

Direct evidence for the involvement of Ca^{2+} in triggering apoptotic endonuclease activation has been reported. Therefore treatment of hepatocytes with moderate doses of menadione resulted in a sustained increase in cytosolic Ca^{2+} concentration which preceded endonuclease activation and death (McConkey et al., 1988). Later studies by the same group

obtained similar results in glucocorticoid induced apoptosis in thymocytes (McConkey et al., 1989). In this study, they found that prevention of sustained Ca^{2+} elevation by either buffering cytosolic Ca^{2+} with quin 2 or incubation of thymocytes in 'Ca^{2+} free' medium, prevented endonuclease activation. Furthermore, exposure of human adenocarcinoma cells to TNF-α caused an increase in intranuclear Ca^{2+} accumulation and resulted in endonuclease activation and apoptosis (Bellomo et al., 1992).

The ionic requirements of endonucleases have been studied extensively and in this respect, Ca^{2+} has been shown to activate the constitutive endonuclease(s) in isolated nuclei resulting in apoptotic like-DNA cleavage (reviewed in Walker et al., 1995). The Ca^{2+} concentrations required to induce DNA fragmentation in isolated nuclei are normally in the milimolar range. However Jones et al. (1989) have shown that physiological concentrations of Ca^{2+} (nanomolar range) activate DNA cleavage in rat liver nuclei. This is achieved when ATP is included in the incubation to stimulate Ca^{2+} uptake into the nucleus (Nicotera et al., 1989; Jones et al., 1989).

However recent studies have demonstrated that morphological features typical of apoptosis occur in the absence of DNA laddering (Cohen et al., 1992; Oberhammer et al., 1993a,b). Furthermore, studies using pulse field gel electrophoresis have shown that the DNA is initially cleaved into ≥700kbp, 200-300kbp and 30-50kbp fragments which precedes internucleosomal cleavage (Filipski et al., 1990; Brown et al., 1993). These fragments appear to represent the loops (50kbp) and rosettes (300kbp) of the higher order chromatin structure (Filipski et al., 1990). Cytochemical localisation studies have shown that the loops are attached to the internal nuclear matrix at sites called the matrix attachment regions (Davie, 1995). Since topoisomerase II is a component of the internal nuclear matrix, it seems reasonable to predict that topoisomerase II is involved in the stability and degradation of these loops at the matrix attachment regions (Zlatanova and van Holde, 1992).The involvement of topoisomerase II in the attachment of the 50kbp loop domain to the matrix attachment regions has been shown to be important in promoting chromatin condensation or facilitating endonucleolytic digestion of the genome (Szabo et al., 1990). In contrast, recent findings have revealed that the formation of 50kbp fragments in HL-60 and MOLT-4 cells do not involve topoisomerase II (Beere et al., 1995). In agreement, Rusnak et al. (1996) have also demonstrated that the generation of

≥1Mbp and 450-600kbp DNA fragments in Du-145 is the result of endonuclease activation and not topoisomerase II /DNA interactions.

Although the mechanisms of the large fragments formation are not fully understood, the cationic requirements for this process have been demonstrated in studies employing isolated nuclei. Thus in nuclei isolated from liver, thymocytes, HL-60 and IL2-dependent CTLL cells, the formation of large kbp fragments of DNA is a Mg^{2+}-dependent process (Cain et al., 1994; Sun and Cohen, 1994; Walker et al., 1994). The cleavage of DNA into the large fragments precedes the activation of internucleosomal cleavage, which requires both Ca^{2+} and Mg^{2+}. Support for the role of Mg^{2+} comes from a recent study on bile acid induced hepatocyte apoptosis (Patel et al., 1994). In this study, the increased endogenous endonuclease activity during apoptosis has been associated with the elevation of intracellular Mg^{2+} concentration.

It is possible that proteolytic activation is involved in these multi-step DNA cleavage processes since topoisomerase II, lamins (components of nuclear matrix) and histones H1 are known targets of apoptotic proteases (reviewed in McConkey et al., 1996; see next section). Cleavage of these proteins may result in unfolding of chromatin and therefore increase the endonuclease accessibility to degrade DNA.

Although DNA cleavage has been shown to occur during apoptosis in many cell types under various stimuli (Bortner et al., 1995), several examples of apoptosis in the absence of DNA cleavage have been reported. In studies of embryonic cell death and metamorphosis of insects, internucleosomal cleavage was not observed (Zakeri et al., 1993). Similarly, Oberhammer et al. (1993) have demonstrated that endonuclease activation is not associated with chromatin condensation in TGF-$ß_1$ treated hepatocytes. This is an interesting observation as DNA laddering in hepatocytes has been shown to occur in apoptosis induced by activin A, a member of TGF-ß superfamily (Hully et al., 1994). Studies described in chapter 5 of this thesis have resolved the anomalous observation of TGF-$ß_1$ treated hepatocytes by using different methods of analysing DNA cleavage. In addition further characterisation of the multi-step DNA cleavage in the liver is also described in chapters 3, 4 and 5 of this thesis.

1.3.2 Proteolysis in apoptosis

Apoptosis involves a series of degradative processes which occur in an ordered and regulated manner. Until recently, many of the studies have been focused primarily in understanding the role of endonucleases in DNA degradation. However, burgeoning evidence

Table 1.3 Cleavage of proteins during apoptosis

Protein Identity	Cleavage products (kDa)	Cellular location	Reference(s)
Topoisomerase I	70	nucleus	Kaufmann, (1989) Casciola-Rosen et al., (1995)
U1-70kDa	40	nucleus	Casciola-Rosen et al., (1994)
PARP	85	nucleus	Kaufmann et al., (1993)
Histone H1	small fragments	nucleus	Kaufmann, (1989)
Histone 2B	small fragments	nucleus	Baxter et al., (1989)
DNA-PKcs	230, 160	nucleus	Teraoka et al., (1996) Casciola-Rosen et al., (1995)
Rb	68, 48	nucleus	An and Dou, (1996)
SREBP1/SREBP2	55, 70	ER/nucleus	Wang et al., (1996)
Lamin A/Lamin C	42	nuclear scaffold	Ucker et al., (1992) Lazebnik et al., (1995a)
Lamin B_1	45	nuclear scaffold	Kaufmann, (1989) Oberhammer et al., (1994)
Topoisomerase II	small fragments	nuclear scaffold	Kaufmann, (1989)
APC	90	cytoplasmic	Browne et al., (1994)
PKCδ	40	cytoplasmic	Emoto et al., (1995)
Terminin	small fragments	cytoplasmic	Hebert et al., (1994)
D4-GDI	23	cytoplasmic	Na et al., (1996)
Actin	30, 14	various	Kayalar et al., (1996)

This table has been adapted and modified from Kumar and Lavin (1996)

indicate that proteases, especially homologues of the interleukin-1ß converting enzyme (ICE) family play a central role as regulators and/or components of the cell death execution machinery (Martin and Green, 1995). Evidence implicating the involvement of proteases in apoptosis have evolved basically from studies using a variety of physiologic, biochemical and

genetic approaches. These include the observation of specific and reproducible proteolytic cleavage of cytoplasmic and nuclear proteins and the ability of certain protease inhibitors or viral proteins to block apoptosis. In addition, gene knockout or overexpression experiments have also added to the knowledge of the importance of proteases in apoptosis (Patel and Gores, 1995, Kumar and Lavin, 1996, for recent reviews)

Studies employing protease inhibitors have revealed several classes of proteases involved in apoptosis, including serine and cysteine proteases. N-tosyl-L-lysyl chloromethyl ketone (TLCK), a trypsin like serine protease inhibitor has been shown to inhibit apoptosis in etoposide treated HL-60 cells (Bruno et al., 1992; Kaufmann et al., 1993), a variety of apoptotic inducers in thymocytes (Weaver et al., 1993; Fearnhead et al., 1995) and in hepatocytes treated with glycodeoxycholate (Kwo et al., 1995). In thymocytes, N-tosyl-L-phenylalanine chloromethyl ketone (TPCK) a chymotrypsin like serine protease inhibitor has different effects from TLCK. While TLCK inhibits apoptosis prior to DNA cleavage or cytoplasmic changes, TPCK only blocks the internucleosomal cleavage and has no effects on the early morphological changes (Fearnhead et al., 1995) suggesting a proteolytic cascade in thymocyte apoptosis.

In agreement, Chow et al. (1995) have demonstrated that a mechanism based serine protease inhibitor 3,4-dichloroisocoumarin (DCI) and TPCK prevent the apoptotic nuclei promoting activity (ANPA) after Fas antigen ligation. In contrast, only TPCK inhibits chromatin degradation and morphological changes mediated by the ANPA in Jurkat T lymphocytes. In isolated rat thymocyte and liver nuclei, DCI, TPCK, TLCK and calpain inhibitors have been shown to inhibit certain stages of DNA cleavage by preventing proteolysis (Cain et al., 1995; Weaver et al., 1993; Zhivotovsky et al.,1994). In addition, a recently identified 24kDa serine like protease which is sensitive to TPCK has been shown to activate DNA cleavage (Wright et al., 1994).The activation of calpain, a calcium dependent cysteine protease has been demonstrated in dexamethasone treated thymocytes (Squier et al., 1994). In this study, they have shown an increase in calcium dependent proteolysis of a labelled casein substrate, as well as the simultaneous loss of the pro-form of one of the calpain isozymes. Degradation of many proteins has now been demonstrated to occur during apoptosis and their cellular location and cleavage products are summarised in Table 1.3.

1.3.2.1 ICE/CED-3 related proteases in apoptosis

Genetic studies in *Caenorhabditis elegans* have provided the most insight into the genes controlling death, of which 131 out of 1090 cells die at precise locations and times during development of the nematode (Ellis et al.,1991). The activities of two genes, *ced-3* and *ced-4* are essential for cells to undergo programmed cell death, since recessive mutations in *ced-3* or *ced-4* result in survival of cells which normally die during development (Yuan and Horvitz, 1990). In contrast, *ced-9* gene acts as a gatekeeper to prevent cells from activating the cell death program (Hengartner et al., 1992). The product of the ced-9 gene has been shown to be similar to the mammalian bcl-2 protein (Hengartner and Horvitz,1994). Although no mammalian homologues of *ced-4* gene product have been identified so far, *ced-3* has been found to encode a protein that shares extensive homology with mammalian ICE (Yuan et al., 1993).

ICE is a cysteine protease identified and isolated from a human monocytic cell line that can cleave the inactive 31kDa precursor of IL-1ß (pro-IL-1ß) at Asp^{116}-Ala^{117} to generate the active cytokine (IL-1ß, 17.5kDa) in response to a variety of inflammatory stimuli (Cerretti et al., 1992; Thornberry et al., 1992; Dinarello, 1991). Both CED-3 and ICE share a pentapeptide conserved sequence QACRG that is essential for their catalytic activities (Yuan et al., 1993). Like granzyme B, ICE and its family members have an unusual stringent specificity for cleaving after aspartate residues (Thornberry et al., 1992; Thornberry et al., 1995). Overexpression of ICE or CED-3 in Rat-1 fibroblasts induce apoptosis, suggesting that ICE is functionally as well as structurally, related to CED-3 (Miura et al., 1993). It is important to note that such evidence is only an association, since ectopic expression of a number of proteases (e.g. chymotrypsin, proteinase K, trypsin) can induce apoptosis significantly (Williams and Henkart, 1994).

Further evidence that ICE plays a critical role in apoptosis comes from the findings that CrmA, a potent inhibitor of ICE (Ray et al.,1992) have been shown to block apoptosis mediated by Fas/Apo-1 (Los et al., 1995, Enari et al., 1995b), TNF-α (Miura et al., 1995), serum deprivation (Wang et al., 1994) and in neurons deprived of nerve growth factor (Gagliardini et al., 1994). In addition, thymocytes from ICE-deficient mice were resistant to apoptosis induced by Fas antibody (Kuida et al., 1995). However, thymocytes from these ICE knockout mice underwent apoptosis in response to stimuli such as ionising radiation and

dexamethasone (Kuida et al., 1995). An explanation for this paradox is that ICE being the first described is not the sole mammalian homologue of CED-3. Therefore it does not have an autonomous role in causing apoptosis like CED-3 in the nematode.

Indeed, further studies have demonstrated that ICE/CED-3 is a family of aspartate-specific cysteine proteases and to date nine homologues of CED-3 and ICE have been identified. Kumar et al. (1992, 1994) first identified a mouse homologue of ICE, named Nedd2 [*N* (neural precursor cells) *e*xpressed *d*evelopmentally *d*own-regulated] and its human counterpart was subsequently cloned by Wang et al. (1994)

Table 1.4 Subfamilies of ICE related proteases

CED-3	
	• CED-3
	• CPP32/Yama/apopain (caspase-3)
	• ICE-LAP3/Mch3/CMH1 (caspase-7)
	• Mch2 (caspase-6)
	• Mch4 (caspase-10)
	• Mch5/FLICE/MACH (caspase-8)
	• ICE-LAP6 (caspase-9)
ICE	
	• ICE (caspase-1)
	• ICE_{rel}II/TX/Ich2 (caspase-4)
	• ICE_{rel}III/TY (caspase-5)
NEDD2	
	• Nedd2/Ich1 (caspase-2)

N.B. It is worth mentioning that the homologues described in this section are up-to date. No doubt experiments are currently underway to identify new members which will be reported in the literature soon.

called Ich-1 (*I*ce and *c*ed-3 *h*omologue). This was followed by the discovery of a 32kDa putative cysteine protease, CPP32 (Fernandes-Alnemri et al., 1994) which was named apopain and Yama by Nicholson et al. (1995) and Tewari et al. (1995b) respectively. Subsequently, two additional members of the ICE/CED3 family have been identified, ICE_{rel}II and ICE_{rel}III based on their close relatedness to ICE (Munday et al., 1995). ICE_{rel}II has also been cloned independently by two other groups called TX and Ich2, respectively (Faucheu et al., 1995; Kamens et al., 1995). Faucheu et al. (1996) have also cloned ICE_{rel}III and named it as TY.

Furthermore, Mch2 and Mch3 have been identified by the same group (Fernandes-Alnemri et al., 1995a,b). ICE-LAP3 and CMH1, both identical to Mch3 have been characterised by Duan et al. (1996a) and Lipkke et al. (1996) respectively. The pentapeptide sequence QACRG is conserved in all of these ICE homologues.

More recently, 3 other new members have been identified. ICE-LAP6 which is constitutively expressed in a variety of foetal and adult human tissues have been described by Duan et al. (1996b). Interestingly, ICE-LAP6 contains an active site QACGG pentapeptide, rather than the QACRG pentapeptide shared by other family members (Duan et al., 1996b). In addition, the other two new members identified were Mch4 and Mch5, which contain a QACQG pentapeptide as their putative active sites (Fernandes-Alnemri et al., 1996). This novel pentapeptide sequence in the ICE/CED-3 family has also been shown by two separate groups, Muzio et al. (1996) and Boldin et al. (1996) who have discovered a novel FADD/MORT1 interacting protease in Fas induced apoptosis named FLICE and MACH respectively. The sequence of MACH, FLICE and Mch5 are similar indicating that they are all the same ICE homologue. Phylogenetic analysis of the proteases based on the relatedness to each other has revealed three subfamilies that is called CED-3 subfamily, ICE subfamily and Nedd2 subfamily (reviewed in Chinnaiyan and Dixit, 1996; Kumar and Lavin, 1996) and members of each subfamily are shown in Table 1.4. In addition, the recently proposed human ICE/CED3 protease nomenclature called caspase is also indicated in this table for the members of this family (Alnemri et al., 1996).

1.3.2.2 Substrates of ICE-like proteases

Although many proteins are degraded during apoptosis (see Table 1.3), most of the proteases responsible for these cleavages have not been identified. However, there is now increasing evidence that ICE-like proteases can cleave some of these proteins. In addition, some members of the ICE-like family are able to auto-process and process other members. Furthermore, peptide inhibitors either of viral origin or synthetic can act as pseudo-substrates of ICE-like proteases and therefore inhibit its activity.

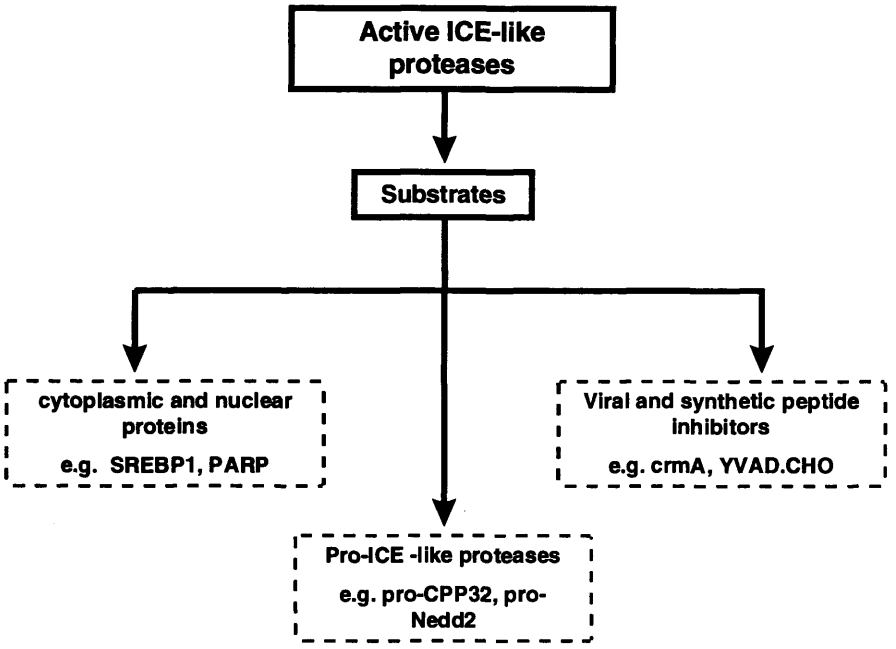

Figure 1.7 Substrates of ICE-like proteases during apoptosis

For the purpose of this review, the substrates of these proteases are divided into three categories as illustrated in Figure 1.7.

1.3.2.2a Cytoplasmic and nuclear proteins

Poly(ADP-ribose) polymerase (PARP, 113-116kDa) was the first protein to be identified as being cleaved during apoptosis by an ICE-like protease, termed prICE for protease resembling ICE (Lazebnik et al., 1994). Sequencing of the 89kDa fragment reveals that PARP is cleaved at the DEVD/G sequence. prICE is different from ICE because it does not cleave pro-IL-1ß, the ICE substrate. On the other hand, purified recombinant ICE does not degrade PARP (Lazebnik et al., 1994).

Subsequently, Yama and apopain have been demonstrated to cleave PARP *in vitro* (Tewari et al., 1995b; Nicholson et al., 1995). It is therefore possible that Yama/apopain is the protease responsible for the cleavage of PARP seen in prICE. However, it is interesting to note that the specific ICE inhibitor profile of purified apopain is not similar to prICE (Lazebnik et al., 1994). The irreversible ICE inhibitor Ac-YVAD.CMK (4μM) completely blocked prICE activity in the cell-free system as assessed by PARP cleavage, morphological changes and DNA laddering (Lazebnik et al., 1994). In contrast, the tetrapeptide aldehyde inhibitor of ICE, Ac-YVAD.CHO (1μM) failed to inhibit PARP cleavage activity in apoptotic osteosarcoma cells and it was a weak inhibitor of apopain ($K_{i\ CPP32}$=12μM versus $K_{i\ ICE}$=0.76nM).

Further studies have shown that co-expression of PARP with ICE, TX and Nedd2 result in its cleavage identical to that seen in apoptotic cells (Gu et al., 1995b). These results contradict previous findings by Lazebnik et al. (1994) and Nicholson et al. (1995) who reported that ICE itself was unable to cleave PARP. Other members of the ICE/CED-3 family such as Mch2 and Mch3 were capable of cleaving PARP and this activity was also observed in a recently identified member, ICE-LAP6 (Fernandes Alnemri et al., 1995a,b; Duan et al., 1996b respectively).

Why is PARP cleavage important during apoptosis? PARP is a nuclear enzyme which is activated during DNA damage (deMurcia and deMurcia, 1994). It contains two zinc fingers near its N-terminus which binds to DNA strand breaks. Once bound, the C-terminal catalytic domain becomes activated and further stimulate it to catabolize NAD and polymerise ADP-ribose onto the automodification domain (de Murcia and de Murcia, 1994). Since ATP is required for completion of apoptosis (Zhang et al., 1994), depletion of NAD and ATP levels might disrupt the apoptotic process as the formation of apoptotic bodies is an energy consuming process (reviewed in Earnshaw, 1995). Proteolytic cleavage of PARP results in the separation of the two zinc finger DNA binding domain from the automodification and catalytic domains and hence disables PARP from DNA repair and genome maintenance (Nicholson et al., 1995). Also the Ca^{2+}/Mg^{2+} dependent endonuclease implicated in DNA fragmentation during apoptosis is negatively regulated by ADP-ribosylation (Tanaka et al., 1984), therefore cleavage of PARP will allow activation of the endonuclease.

Is cleavage of PARP required for apoptosis? Recent studies have shown that PARP is not degraded in epidermal growth factor induced apoptosis in a breast cancer cell line. This indicates that PARP is not a crucial substrate in apoptosis (Armstrong et al., 1994). In agreement, PARP null mice developed normally suggesting that cleavage of PARP is not essential in apoptosis (Wang et al., 1995a). These results are also in agreement with the data presented in this thesis (chapter 6) where PARP cleavage was not observed in hepatocytes undergoing apoptosis.

The cleavage of lamin has been observed during apoptosis in many cell systems including etoposide treated leukaemia cells (Kaufmann, 1989), chicken hepatoma DU249, thymocytes treated with dexamethasone, TNF and campthothecin treated SN12C renal carcinoma cells (Lazebnik et al., 1993) and also in a cell free apoptosis system (Lazebnik et al.,

1995). Inhibition of the lamin protease with TLCK prevented the packaging of condensed chromatin into apoptotic bodies but did not affect PARP and DNA cleavage activities (Lazebnik et al., 1995). Like prICE, lamin protease was also inhibited by Ac-YVAD.CMK suggesting that this protease is a member of the ICE family. Further studies have revealed the cleavage site of lamin A which occurs at VEID/NG and that Mch2α possesses the lamin cleavage activity (Takahashi et al., 1996). Like Ac-YVAD.CMK, Zn^{2+} also inhibits cleavage of lamin A. In agreement, Orth et al. (1996a) have demonstrated that Mch2 cleaves lamin A and that this cleavage can be prevented by TLCK.

In another study, three distinct tiers of ICE-like activity were observed in Fas ligated Jurkat cells (Greidinger et al., 1996). The earliest cleavage detected was fodrin which was inhibited by benzyloxycarbonyl-Val-Ala-Asp fluoromethyl ketone (Z-VAD.FMK) an inhibitor of both ICE and ICE-like proteases. This was followed by cleavage of PARP, U1-70kDa and DNA-PK_{cs} which were all substrates of the CPP32-like proteases. These cleavages were inhibited by both Ac-DEVD.CHO and Z-VAD.FMK. Finally, lamin B cleavage was observed in the third phase which was abolished in the presence of Ac-YVAD.CHO, Ac-DEVD.CHO and Z-VAD.FMK. The sensitivity to Ac-YVAD.CHO is only observed in lamin B cleavage suggesting a cascade of ICE-like proteases participating in apoptosis (Greidinger et al., 1996). Also cleavage of lamin could result in disruption of its interactions with other proteins including retinoblastoma gene product (RB) (Ozaki et al., 1994) and recent studies have shown that cleavage of hypophosphorylated Rb occurs during apoptosis in chemotherapy treated HL-60 and U937 cells (An and Dou, 1996). It is suggested that Rb protease is a member of ICE family as addition of Ac-YVAD.CMK inhibits cleavage of this cell cycle protein.

Further studies by Casciola Rosen et al. (1996) have demonstrated that the cleavage of DNA-PK_{cs} and U1-70kDa is mediated by apopain, therefore abolishing their critical homeostatic functions in nuclear repair and the splicing of mRNA. CPP32 has also been shown to cleave sterol regulatory element binding protein-1 (SREBP-1) and sterol regulatory element binding protein-2 (SREBP-2) *in vitro* (Wang et al., 1995b), and also during apoptosis (Wang et al., 1996). In addition, the hamster equivalent of Mch3 called Mch3/SCA-2 has the ability to cleave both SREBP-1 and SREBP-2 (Pai et al., 1996). However the significance of these cleavages during apoptosis is not yet established.

1.3.2.2.b Auto-processing or cleavage of members of ICE family

Members of the ICE family are synthesised as proforms which require proteolytic cleavage to their active forms. It appears now that ICE and its homologues can auto-process or cleave other members of this family (Kumar and Harvey,1995, see Figure 1.8).

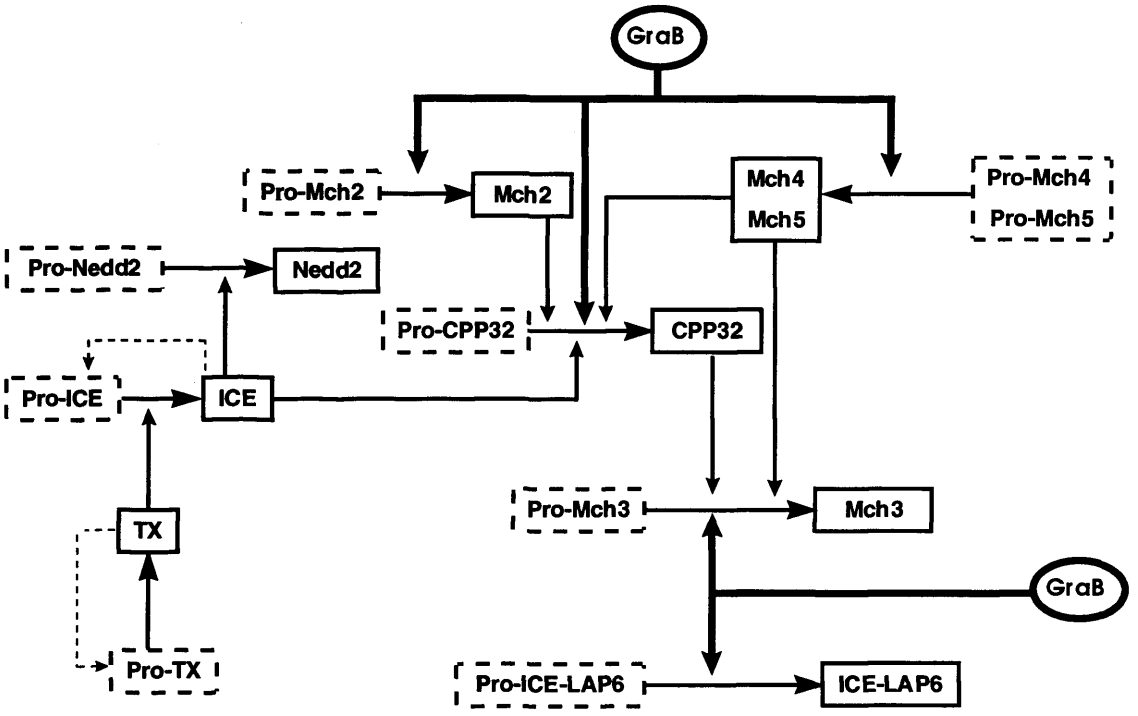

Figure 1.8 Processing of ICE family members

The pro-forms of the ICE members (in dashed-line boxes) are processed either by themselves (dashed arrow, e.g. pro-ICE) or by active ICE members (in boxes). Granzyme B (in circles) also cleaves the pro-forms to their mature forms (thick arrow).

In this respect, ICE itself has the ability to auto-process itself in addition to processing pro-Yama and pro-Nedd2 (Thornberry et al., 1992; Tewari et al., 1995b; Kumar and Lavin, 1996). The ICE pathway may be operational in the Fas mediated pathway because it is absent in ICE knockout experiments and CrmA abolished this pathway (Kuida et al., 1995; Enari et al., 1995b; Los et al., 1995). Moreover, in Fas induced apoptosis, the ICE-like activity preceded CPP32-like activity in studies using fluorogenic substrates specific for each type of activity respectively (Enari et al., 1996). Another novel human protease, TX cleaves itself and ICE (Faucheu et al., 1995) whereas Fernandes-Alnemri et al. (1995b) demonstrated the ability of CPP32 to cleave pro-Mch3α but not vice-versa suggesting that CPP32 is upstream of Mch3α in the protease cascade. In this respect, a CPP32 activating protease (CAP) has been identified and purified from hamster liver extract that specifically cleaves and activates CPP32

(Liu et al., 1996). The protein sequence of CAP reveals that CAP is the hamster homologue of Mch2α. Indeed Orth et al. (1996b) have confirmed that Mch2α not only activates pro-Yama but it is able to process pro-ICE-LAP3 as well. Also since recombinant ICE-LAP3 cannot cleave pro-Yama but Yama can cleave pro-ICE-LAP3, it is possible that Yama acts as an intermediate between Mch2α and ICE-LAP3.

Cytotoxic T lymphocyte-mediated cytotoxicity involves the release of perforin which aids the entry of granzymes into the cell. Granzyme B has been shown to have a specificity for cleaving after aspartic acid (P_1) and has been suggested to induce apoptosis by cleaving the precursor of ICE or members of its family (Greenberg and Litchfield, 1994). In this respect, ICE itself is not a substrate for granzyme B (Darmon et al., 1995) but pro-CPP32 can be cleaved by granzyme B and the active CPP32 can degrade PARP (Darmon et al., 1995). Similar results have also been obtained where granzyme B activates Mch2, pro-Yama, pro-ICE-LAP3 and pro-ICE-LAP6 (Orth et al., 1996a; Chinnayan et al., 1996; Gu et al.,1996; Duan et al., 1996). In another recent study, Fernandes-Alnemri et al. (1996) have demonstrated that granzyme B also cleaves pro-Mch3α, pro-Mch4 and pro-Mch5. The latter proenzymes, Mch4 and Mch5 contain an N-terminal FADD like death domain (see also section 1.2.4.2) which can be activated in Fas induced apoptosis. They have further shown that Mch4 and Mch5 cleave both CPP32 and Mch3α, suggesting a hierarchy of ICE-like proteases in apoptosis. Significantly, granzyme B can process FLICE to its active form indicating a possible mechanism for activation of ICE like protease(s) in granzyme B induced apoptosis (Muzio et al., 1996). Also overexpression of FLICE induces apoptosis in MCF-7 cells which can be abrogated by Z-VAD.FMK and CrmA. These findings suggest that FLICE/MACH is the most upstream enzymatic component in the Fas/Apo1 and p55-R death inducing signalling complex (Muzio et al., 1996; Boldin et al., 1996).

1.3.2.2.c Viral protein and peptide based inhibitors

Two viral proteins, CrmA and p35 have been identified as potent inhibitors of ICE-like proteases. CrmA (*c*ytokine *r*esponse *m*odifier A) was originally described as a cowpox virus serpin that modified host inflammatory responses due to its ability to inhibit ICE (Ray et al., 1992). Serpin proteins contain a reactive site loop (RSL) which can interact with protease active sites to allow inhibition. In this respect, CrmA contains an Asp residue within the ICE

recognition sequence LVAD at the critical RSL site. Therefore CrmA is a potent inhibitor of ICE (Ray et al., 1992).

In addition to ICE, CrmA has now been shown to inhibit CPP32 and block PARP cleavage both *in vitro* and in apoptotic cells (Tewari et al., 1995b). As mentioned earlier, overexpression of CrmA in a variety of mammalian cells prevents apoptosis induced by growth factor withdrawal, disruption of contacts with extracellular matrix, Fas and TNF pathways (Gagliardini et al., 1994; Boudreau et al., 1995; Los et al., 1995; Tewari and Dixit, 1995; Miura et al., 1995)

The other known viral inhibitor of ICE family proteases is from the insect baculovirus *Autographa californica* called p35 (Clem and Miller, 1994). Recent studies have shown that p35 blocks apoptosis by directly inhibiting ICE/CED-3 family members (Bump et al., 1995; Xue and Horvitz, 1995). The enzymic activity of ICE, Ich-1, Ich-2 and CPP32 were abolished by equal amounts of recombinant p35. Furthermore Rabizadeh et al. (1993) demonstrated that p35 transfected neuronal cell line did not undergo apoptosis upon serum withdrawal or treatment with a calcium ionophore.

Potent and selective reversible and irreversible peptide based inhibitors have been developed (Nicholson, 1996). More specific inhibitors based on the tetrapeptide sequence of the preferred substrate P_4-P_1 residues have proved to be useful in understanding the involvement of the ICE family members (Kaufmann, 1996). In this respect, inhibitors with YVAD motif have been synthesised to specifically inhibit ICE as this motif correspond to YVHD cleavage site within pro-IL-1ß (Thornberry et al., 1992). Peptide aldehydes, nitriles and ketones are reversible inhibitors while compounds that form thiomethylketone with the active-site cysteine are irreversible inhibitors (Thornberry et al., 1994). Both Ac-YVAD.CHO and Ac-YVAD.CMK have been shown to be potent inhibitors of apoptosis induced by different stimuli (Lazebnik et al., 1994; Chow et al., 1995; Enari et al., 1996; Los et al., 1995).

On the other hand, DEVD based compounds derived from the cleavage site in PARP are potent inhibitors of CPP32 (Nicholson et al., 1995). An aldehyde analogue, Ac-DEVD.CHO has been shown to inhibit campthothecin induced apoptosis in osteosarcoma cells (Nicholson et al., 1995). Furthermore this compound was a potent inhibitor of U1-70kDa, DNA-PK_{cs} and PARP cleavage in apoptotic HeLa lysates (Casciola-Rosen et al., 1996).

Another interesting peptide inhibitor is Z-VAD.FMK, which as described in the previous section, blocks apoptosis in many systems (Fearnhead et al., 1995; Zhu et al., 1996; Cain et al., 1996a; Greidinger et al., 1996). This compound is a tripeptide in which the P_1 Asp residue is esterified and this increases its membrane permeability (Henkart, 1996). An analogue of this compound, ZVAD based- [α-(2,6-dicholorobenzoyl)oxy) methyl ketone] has been shown to be a potent inhibitor of ICE (Dolle et al., 1994; Miller et al., 1995). In another study, Slee et al. (1996) have demonstrated that Z-VAD.FMK blocks apoptosis by preventing the activation of pro-CPP32 into its active form, rather than preventing the proteolytic action of CPP32 directly.

In conclusion, understanding the biochemical mechanisms involved in apoptosis offers insight into potential targets for therapeutic interventions. This has proven to be the case in the liver as a recent study has demonstrated that Ac-YVAD.CMK is a potent pharmacological agent in treating liver damage due to excessive apoptosis induced by anti-Fas antibody in mice and liver failure due to TNF-α injection (Rouquet et al., 1996).

1.4 Aims of study

Studies presented in this thesis are aimed towards understanding the execution mechanisms during apoptosis in the liver. Basically two model systems have been used in this study i.e. rat liver nuclei and primary hepatocytes culture. The aims of this thesis are as follows;

1) to characterise the mechanisms of DNA cleavage and involvement of protease(s) in rat liver nuclei as observed during apoptosis (chapters 3 and 4)

2) to characterise the mechanisms of TGF-$ß_1$ induced apoptosis and the DNA cleavage processes (chapter 5)

3) to characterise the involvement of ICE-like proteases in TGF-$ß_1$ mediated apoptosis in hepatocytes (chapter 6)

2. Materials and Methods

2.1 Materials

All chemicals unless stated otherwise were obtained from the Sigma Chemical Co., Poole, Dorset, U.K. Terminal deoxynucleotidyl transferase (TdT) and most culture reagents were from Gibco, Paisley, Scotland. Anti-digoxigenin-fluorescein Fab fragments (anti-dig), digoxigenin-11-2'-deoxyuridine-5'-triphosphosphate (Dig-11-dUTP), rat tail collagen, pronase, 3,4-dichloroisocoumarin (DCI), N-α-tosyl-L-lysyl-chloromethyl ketone (TLCK), N-α-tosyl-L-phenylalaninyl-chloromethyl ketone (TPCK) and collagenase were obtained from Boehringer Mannheim U.K., Lewes, East Sussex, U.K. Benzyloxycarbonyl-Asp-Glu-Val-Asp-7-amino-4-trifluoromethylcoumarin (Z-DEVD.AFC), benzyloxycarbonyl-Asp-Glu-Val-Asp (Ome)-fluoromethyl ketone (Z-DEVD.FMK), acetyl-Asp-Glu-Val-Asp-aldehyde (Ac-DEVD.CHO), benzyloxycarbonyl-Val-Ala-Asp (Ome)-fluoromethyl ketone (Z-VAD.FMK), benzyloxycarbonyl-Val-Ala-Asp-chloromethyl ketone (Z-VAD.CMK), benzyloxycarbonyl-Ala-Ala-Asp-chloromethyl ketone (Z-AAD.CMK), N-acetyl-Tyr-Val-Ala-Asp-chloromethyl ketone (Ac-YVAD.CMK), N-acetyl-Tyr-Val-Ala-Asp-aldehyde (Ac-YVAD.CHO) were from Enzyme Systems Inc., Dublin, California. Recombinant human TGF-ß$_1$ was obtained from R&D Systems Europe, Abingdon, Oxon, U.K. and dissolved in 4mM HCl containing 1mg/ml bovine serum albumin.

2.2 Methods

2.2.1 Isolation of nuclei in magnesium buffers

Nuclei were isolated from rat liver as reported previously (Jones *et al.*, 1989) with some modifications. Male F344 rats (180 - 200g, fed *ad libitum*, obtained from Harlan-Olac, Bichester, Oxfordshire, UK) were anaesthetized by intraperitoneal injection with 0.6ml of 60mg/ml sodium pentobarbitone (Sagattal, May and Baker) in isotonic saline and perfused *in situ* with 150ml ice-cold TKM solution (50mM Tris-HCl, 25mM KCl, 5mM $MgCl_2$, pH 7.5) to remove blood. The liver was removed, diced and homogenised in 40ml of STKM-1 (TKM solution containing 0.25M sucrose) with a glass Teflon homogeniser (9 strokes with motor-driven pestle). The homogenate was then filtered through successive layers of nylon bolting cloth (200µm and 70µm mesh size) before centrifuging at 700 x *g* for 10min in a Beckman JS13.1 rotor. The pellet was homogenized (5 strokes) in 40ml of STKM-1 and centrifuged

again at 700 x *g* for 10min. The nuclei pellet was resuspended by homogenization (3-5 strokes) in 24ml of STKM-1 and mixed with 48ml of TKM containing 2.3M sucrose (STKM-2) and then 18ml aliquoted into four centrifuge tubes each of which contained a 6ml cushion of STKM-2. The tubes were centrifuged at 47000 x *g* for 1h in a Beckman SW28Ti rotor. The upper layer and the sucrose cushion were removed by aspiration and resulting pellet gently resuspended in 10ml of STKM-1 before centrifuging at 1000 x *g* for 10min. Finally, the pellet was resuspended in 10ml of incubation buffer containing 125mM KCl, 2mM K_2HPO_4, 25mM Hepes and 4mM $MgCl_2$, pH 7.0.

2.2.2. Isolation of nuclei in spermidine/spermine buffers (SP-buffers)

Nuclei were isolated as described above, except that 4mM $MgCl_2$ was replaced with 0.15mM spermine, 0.5mM spermidine, 1.0mM EDTA and 0.1mM EGTA. The final incubation buffer contained polyamines but no EDTA and EGTA. All isolation procedures were performed at 0-4°C.

2.2.3 Autodigestion of isolated nuclei

Nuclei were incubated at a concentration of 10 x 10^6/ml in the appropriate buffer with or without the addition of the indicated concentrations of Mg^{2+} and/or Ca^{2+}. Autodigestion of nuclei was performed at 37°C for the indicated times in the presence of various ions/inhibitors. The reaction was stopped by adding an equal volume of ice-cold incubation buffer containing 20mM EGTA and aliquots taken for the analyses described below.

2.2.4 Isolation of hepatocytes

Hepatocytes were isolated from adult male F344 rats (180-200g, fed *ad libitum*) essentially as described by Seglen (1973). The rats were anesthetized intraperitoneally with 0.6ml of 60mg/kg (200mg/kg body weight) sodium pentobarbitone (Sagattal, May and Baker). The liver was then exposed by a midline incision and retraction of the stomach and intestines to expose the hepatic portal vein. The hepatic portal vein was cannulated using an argyle medicut intravenous cannular 16GA x 2in. (Arterial Medical Sciences) filled with 1ml of heparin (1000 U/ml) and ligated. The inferior vena cava was then cut and the liver was perfused with oxygenated 1x Ca^{2+}-Mg^{2+} free hanks balanced salt solution (HBSS) containing 1.65g/l of $NaHCO_3$ and 0.19g/l of EDTA prewarmed to 38°C at a steady flow rate of 50ml/min. During perfusion, the liver was dissected free from the animal and removed onto a platform and with no interruption of

flow, switched to closed circuit perfusion using 100 ml of oxygenated HBSS containing 0.03% collagenase and 5.3 mM $CaCl_2$, prewarmed at 38°C. The collagenase perfusion was allowed to proceed for approximately 20 min after which the liver was removed to a sterile petri dish (56 cm^2) containing 30ml Williams Medium E (supplemented with 10% foetal bovine serum {FBS}, 2mM glutamine, 100U/ml penicillin and 10µg/ml streptomycin). The liver was gently agitated, and the cells dispersed in the medium. The cells were then filtered through Nybolt mesh cloth (125µm, John Staniar & Co. Ltd) and the cell suspension washed 4 times by repeated low speed (50 x g) centrifugation for 3min followed by resuspension. The supernatant (containing the majority of Kupffer, endothelial, bile ductule cells and non-viable hepatocytes) was discarded. Finally the hepatocytes were resuspended in Wiliams Medium E supplemented with 1% FBS, 2mM glutamine, 100U/ml penicillin, 100µg/ml streptomycin, 6µM hydrocortisone, 1.4nM insulin and 14nM dexamethasone. Cell density and viability were determined by mixing 10µl of hepatocytes with 90µl of Trypan Blue solution in PBS and counting the number of non-viable (blue) and viable (no staining) hepatocytes in a hemocytometer. Hepatocytes were only used if the viability was > 85%.

2.2.5 Culturing of hepatocytes

Hepatocytes were grown as monolayers on collagen coated coverslips or in collagen coated plastic petri dishes at a density of 87,500 cells/cm^2 as described by Oberhammer et al. (1992). Cultures were incubated at 37°C in a 5% CO_2 humidified incubator. Viable hepatocytes attached within 3-4 h, after which the medium was aspirated and washed with an equal volume of PBS to remove the dead cells. Fresh medium was added and the cultures were then used for the appropriate experiments.

2.2.6 Isolation of nuclei from hepatocytes monolayer (enucleation method)

Nuclei were isolated from monolayer cultures according to the method of Otto (1990) with some modifications (Cain et al., 1996b). At the indicated times, the culture medium was aspirated and 10ml of ice-cold 1% (w/v) citric acid (free acid) pH 2.8 was added and gently swirled over the cells. The petri dishes were left at 4°C for 10min to achieve cell swelling. The citric acid buffer was then removed and 10ml of 1% citric acid containing 0.1% Tween 20 added and left for 20-25 min with an occasional agitation of the plate. The efficiency of the nuclei release from the cells into the buffer was monitored by a phase contrast inverted microscope and was routinely >90%. The nuclei were then transferred into a 25ml plastic tube and centrifuged at 1000 x g for 5min. The supernatant was aspirated and the pellet gently

resuspended in 10ml of PBS and recentrifuged at 1000 x g for 5min . The pellet was resuspended in 0.8ml of PBS and at this stage, a 10µl or 25µl aliquot was taken for cell counting (see below).

2.2.7 Preparation of hepatocyte lysates

Hepatocytes were cultured on collagen coated petri dish (56 cm^2). At the indicated times, the medium was aspirated and the cultures were washed twice with pre-cooled (4°C) Tris buffered saline (120mM NaCl, 25mM Tris-HCl, pH 7.6). Then 1.25ml of lysis buffer (50mM Tris-HCl, 120mM NaCl, 0.5% NP40, pH 8.0, 20µg/ml leupeptin, 5µg/ml pepstatin, 5µg/ml aprotinin, 2mM PMSF and 2mM EDTA) was added and the cells agitated at 4°C for 15 min. The crude lysate was transferred to an eppendorf tube and spun down at 13,000 rpm/15 min at 4°C. The supernatant (lysate) was removed and the protein determined by the Bradford Method before aliquoting in 50µl volumes and storing at -80°C.

2.2.8 Gel electrophoresis

2.2.8.a Conventional agarose gel electrophoresis (CAGE)

CAGE was carried out to detect DNA ladders as described by Sorenson *et al.* (1990). 5 x 10^5 rat liver nuclei or 1x10^6 hepatocyte nuclei were collected and spun at 200 x *g* for 5min. The supernatant was removed and the pellet was resuspended in 15µl of ultra-pure water. RNase A was added to give a final concentration of 10µg/ml and incubated at room temperature for 20min. Finally, 5µl loading buffer containing Ficoll and bromophenol blue was added. Samples were loaded onto a 1.8% agarose gel in TBE buffer (89mM Tris, 89mM Boric acid, 2.5mM EDTA, pH 8.3).The top panel of the gel above the wells was cut and a digestion gel (0.8% agarose, 2%SDS in TBE, 25mg/ml proteinase K) was poured. Initially, the gel was run at 20 V for 1h followed by 100 V for 3h. The size standards routinely used were a *Hin*dIII digest of lambda DNA and/or a 123bp ladder. DNA was visualised by staining in ethidium bromide (10ng/ml) and destaining in water for at least 1h. The gels were photographed on a transilluminator with UV light.

2.2.8.b Field inversion gel electrophoresis (FIGE)

FIGE was used to resolve large molecular weight DNA fragments. Agarose plugs were prepared by the method of Anand and Southern (1990). 2.5 x 10^6 rat liver nuclei or 5 x 10^6 hepatocyte nuclei were centrifuged at 1000 x *g* for 5 min. The supernatant was removed and

the pellet resuspended in 0.25ml of prewarmed PBS (at 50°C). A further 0.25ml of prewarmed 1% agarose L was added, then 100µl (i.e. containing 5 x 10^5 rat liver nuclei or 1 x 10^6 hepatocyte nuclei) aliquot was dispensed to each well of the insert mould to form the plugs which were left on ice for 30min. The DNA in the plugs was deproteinised by incubation in NDS solution (1% lauryl sarcosine, 0.5M EDTA and 10mM Tris, pH 9.5) containing 1mg/ml pronase for 48h at 50°C. FIGE was carried out as described by Brown et al. (1993) using a 15min continuous pulse, followed by a 2.4s forward and 0.8s reverse pulse cycle for 1h. A 1.5 ramp factor was applied, thereby increasing the respective pulse time ten-fold to 24s and 8s by the end of the 7h run. Under these conditions, DNA fragments in the 4.4 to 460 kbp range were separated. *Saccharomyces cerevisiae* chromosomes (243 - 2200 kbp, Clontech, Cambridge, UK) and pulse markers (0.1-200kbp, Sigma Chemical Co., Poole, UK) were used as standards.

2.2.9 In situ end labelling (ISEL) and Flow Cytometry

2.2.9.a ISEL on isolated rat liver nuclei

ISEL was carried out using a modified procedure of the method described by Gold et al. (1993). Nuclei (20 x 10^6 / 2ml) were incubated for the indicated times and the reactions were terminated by addition of 2ml ice-cold incubation buffer containing 20mM EGTA. The nuclei were centrifuged for 1000 x g for 5min, and resuspended in 100µl of PBS prior to fixation with 1ml of 1% formaldehyde (ice-cold) in Hanks Buffered Salt Solution with 20mM HEPES (pH 7.0) for 15 min. The nuclei were pelleted /resuspended in 100µl of PBS before adding 2ml of 70% ethanol (pre-cooled at -20°C) and permeabilised for 1h on ice. The nuclei were sedimented (1000 x g for 5 min) and resuspended in 1ml of 50mM Tris-HCl, 150mM NaCl, pH 7.6 buffer (TBS). At this stage, the nuclei were counted, sedimented and resuspended at a concentration of 2 x 10^6 in 100µl of TdT labelling buffer (100mM sodium cacodylate,10mM $CoCl_2$, 1mM DTT, pH 7.2). TdT enzyme(15 units) and 2µM dig-11dUTP were added to the nuclei (100µl) and incubated for 60min at 37°C. The reaction was terminated with 1ml of ice-cold TBS containing 5mM EDTA, pH 7.6. The nuclei were pelleted and resuspended in 0.5ml of anti-body labelling buffer (5% non-fat dried milk, 0.1% Triton X-100, 4x standard saline citrate, pH 7.2) and incubated for 15min at 4°C to block non-specific antibody binding before centrifuging at 1500 x g for 5min. The pellet was resuspended in 0.25ml of antibody labelling buffer containing a 1/125 dilution (1.6µg/ml) of anti-dig antibody

and incubated in the dark for 30 min at 37°C. Finally the nuclei were pelleted and resuspended in 1ml of 10µg/ml propidium iodide (PI) in PBS.

2.2.9.b ISEL on hepatocyte nuclei

Hepatocyte nuclei (0.8ml in PBS, as described in the enucleation method) were fixed with 3.2ml of ice-cold 1% formaldehyde on ice for 15min. The nuclei were sedimented at 1000 x g for 5min and the pellet was resuspended in 200µl of PBS before adding 2ml of 70% ethanol (pre-cooled at -20°C) and left on ice for 1h. The nuclei were then sedimented and resuspended in 1ml of TBS. From this stage onwards, the steps involved were the same as described above for isolated rat liver nuclei.

2.2.9.c Flow cytometry

A FACScan flow cytometer (Becton Dickinson, USA) was used to measure the red (PI) and green (fluorescein, anti-dig) fluorescence of labelled nuclei. Using doublet discrimination, data from 10^4 singlet nuclei were collected and displayed as bivariate cytograms of red versus green fluorescence. Typically this gives two populations which from the PI fluorescence corresponded to diploid (2N) and tetraploid (4N) nuclei. LYSYS II software was used to gate around these populations to measure the mean relative green fluorescence intensity (designated peak mean fluorescence, PMF) or to determine the numbers of normal and apoptotic nuclei.

2.2.10 Morphological assessment of apoptosis in hepatocytes culture

Hepatocytes were grown on collagen coated coverslips in 6 well plates as described by Oberhammer et al. (1992). At the indicated times, the culture medium was aspirated and hepatocytes were fixed with 1ml of 1% formaldehyde in PBS for 5-10min. The formaldehyde was removed and the hepatocytes washed twice with 1ml PBS. The cells were stained with 1ml of 10µg/ml Hoechst 33258 (H33258, in PBS) for 5min, followed by two washes with distilled water. The coverslips were removed and mounted on a slide with FluoroMount mounting medium.

In cases where cell viability were assessed, propidium iodide (PI, 10µg/ml) was added to the incubation medium and left for 10min in the incubator, prior to washing with PBS, followed by formaldehyde fixation and staining with H33258 as outlined above.

Fluorescent nuclei were visualized with an Olympus BH2 microscope and scored as either

i- normal cells (N) where the chromatin was uncondensed and uniformly spread over the nucleus.

ii- apoptotic nuclei (A) where the nucleus contained masses of condensed chromatin

Apoptotic bodies were not counted as it was difficult to estimate if they arose from one cell or many different cells. Approximately 2000-3000 nuclei (from duplicate treatments) were counted. The percentage of apoptotic cells were derived as follow;

$$\% \text{ apoptosis} = \frac{A}{(A + N)} \times 100$$

For the evaluation of cell viability, % of non-viable cells (NV) were reported as cells including PI.

$$\% \text{ non-viable cells} = \frac{NV}{\text{Total cells}} \times 100$$

2.2.11 Confocal Microscopy

Confocal microscopy was carried out with a Leica TCS 4D (Leica, U.K. Ltd) and apoptotic nuclei were examined under a 100x objective using excitation wavelengths of 568nm and 488nm for PI and anti-dig fluorescence respectively. Each panel in the confocal microscopy figures showed nuclei which have been optically sectioned into a 'gallery' of 16 slices (each approximately 0.5μm apart). This gives information on the spatial distribution on the fluorescence intensity and the combined 'maximum projection' image is essentially a 2D representation of the information within the 3D image stack.

2.2.12 Fluorimetric assay of proteolytic activity

A spectrofluorometric assay to measure CPP32 like activity was developed using a Perkin Elmer LS 50B Luminescence Spectrometer and the model fluorogenic substrate, benzyloxycarbonyl-Asp-Glu-Val-Asp-7-amino-4-trifluoromethylcoumarin (Z-DEVD.AFC).

Liberation of AFC from the substrate was monitored continuously in a fluorimeter essentially as described by Thornberry (1994) using an excitation wavelength (λ_{ex}) of 400nm and an emission wavelength (λ_{em}) of 505nm in a modified thermostatted cuvette (37°C) holder.

The fluorescence intensity was calibrated with standard concentrations of AFC. Lysates (25-50µg protein) were assayed in 1.25ml of 0.1% CHAPS, 10mM DTT, 100mM Hepes and 10% sucrose (pH 7.5) with and without protease inhibitors which were added in DMSO (maximum 10µl). The reaction was started with 20µM Z-DEVD.AFC substrate and the reaction followed for 10min (specific activity) or 25min (inhibition studies).The protease activity was calculated from the slope of the recorder trace and expressed as pmol/mg protein/min.

2.2.13 Kinetic studies of the proteolytic activity

The kinetic analysis of the progressive inhibition of lysate cleavage activity was carried out essentially as in the model described by Thornberry et al. (1994) in which an initial reversible complex (EI) is formed, followed by conversion to the inactivated enzyme EI*.

$$E+I \underset{k_2}{\overset{k_1}{\leftrightarrow}} EI \xrightarrow{k_3} EI^* \qquad \text{(equation 1)}$$

The observed rate of dissapearance of free enzyme (k_{obs}) was determined for each inhibitor from progression curves as described by Morrison (1982). In each case the progressive inhibition was followed for 25min and the k_{obs} values determined from the curves by a direct fit to the equation

$$[\text{AFC fluor'}] = v_s t + (v_o - v_s)[1 - \exp(-k_{obs}t)]/ k_{obs} \qquad \text{(equation 2)}$$

using a curve fitting program developed by Dr. V. Cunningham (MRC Cyclotron Unit) where v_o and v_s are the initial and steady state reaction velocities. The k_{obs} was then used to determine the k value which is the second order rate constant for inactivation of the enzyme. If the rate of inactivation is determined by the conversion to EI* (i.e. $k_3 \ll k_2$) then k value is defined by k_3/K_i where $K_i=k_2/k_1$. Alternatively, if the rate of inactivation is governed by the initial formation of EI (i.e. $k_3 \gg k_1 \cong k_2$) then the second order rate constant is equal to k_1 (i.e. k_{on} association constant). Depending on the type of inhibition the K_i and k values were determined according to the equations described by Thornberry et al. (1994).

2.2.14 Determination of protein concentration

Protein concentrations were assayed using the Bradford method (Coomasie Brilliant Blue G-250, Bio-Rad). Aliquots (1µl) of hepatocyte lysate were mixed in 1ml of diluted Bio-Rad reagent (1:5 dilution) and after a period of 5-60 min, the OD_{595} minus reagent blank was

measured. The assay was standardized using several dilutions of protein standard (bovine serum albumin) and unknowns were then read from a standard curve of OD_{595} versus protein concentration.

2.2.15 Coulter Counting

2.2.15.a Rat liver nuclei

Nuclei were counted using a Coulter-ZM cell counter and 256 Channelyser (Coulter Electronics, Luton, Beds. U.K.). Lower and upper thresholds were set to count between 3.52μm and 9.25μm for unfixed nuclei, and 2.8μm and 7.34μm for fixed nuclei which were smaller in size.

2.2.15.b Hepatocyte nuclei

Nuclei were counted and analyzed using a Casy 1 (Schärfe System, Reutlingen, Germany) cell counting and sizing system using a 150μm aperture for routine analysis.

2.2.16 Collagen coating of coverslips and petri dishes

Coverslips (Chance Propper Ltd., Warley, England, No 1.5, 22x22 mm) were rinsed in 70% ethanol followed by a rinse in acetone, prior to air drying. The coverslips were then placed into each well of a 6 well plate. Rat tail collagen (Boehringer Manheim Biochemica) was dissolved in sterile 0.2% v/v acetic acid to give a final concentration of 0.67mg/ml and 0.72ml aliquoted onto each coverslip. In the case of the $56cm^2$ and $125cm^2$ petri dishes, 4.2ml and 9.3ml of collagen solution were added respectively. This forms a collagen film of 50μg/ cm^2. The plates were then left overnight in an incubator followed by aspiration and air dried in a laminar flow hood.

2.2.17 SDS-PAGE gel electrophoresis and Western blotting

SDS-PAGE was carried out with 12% gels for CPP32 like protease as described by Slee et al. (1996) or 7.5% gels for the detection of PARP protein as outlined previously (Fearnhead et al., 1995). Protein lysate was used for CPP32 analysis whereas hepatocyte nuclei were used for the detection of PARP protein. Hepatocyte nuclei (1×10^6 nuclei) or protein lysate were solubilised in sample buffer (62.5mM Tris, 2% SDS, 15% glycerol, 0.005% bromophenol blue, 5% β-mercaptoethanol, pH 6.8) and boiled at 100°C for 3min. The nuclei were sonicated prior to boiling in order to aid disruption of DNA binding proteins (PARP).

Electrophoresis was performed at 30mA (for one gel) until the bromophenol tracking dye reached the interface of the upper and lower gel. Then the current was increased to 40mA and the electrophoresis was performed until the bromophenol tracking dye was 2cm from the bottom of the gel. A corner of the gel was cut away to mark the orientation of the samples and the gel rinsed in transfer buffer (25mM Tris/HCl pH 8.3, 192mM glycine and 20% methanol) for 20min to remove SDS.

A pre-cut Hybond nitrocellulose membrane was presoaked in transfer buffer prior to the assembly of the transfer sandwich. Then the membrane was laid over the gel and the two sandwiched between 3MM filter papers . A glass pipette was rolled across the surface to remove any trapped air bubbles and the sandwich was cushioned between 2 sponges. This sandwich cassete were then placed in a tank and blotting was carried out at 30V for 16h. After the transfer, the membranes were soaked in 1% Tris buffered saline (2mM Tris-HCl, 13.7mM NaCl, pH 7.6) + 0.1%Tween 20 (TBST) for 10min to remove methanol. Non-specific binding sites were blocked with blocking buffer containing TBST+ 5% Marvel (non-fat dried milk powder) with continuous agitation for 1h. The membrane was washed with TBST (15min once followed by two 5min washes). The membrane was then incubated for 1h with rabbit antiserum to PARP (diluted 1:8000 in TBST) or rabbit polyclonal antibody to CPP32 (diluted 1:10000 in TBST) which was raised to the P17 subunit. The antibody to PARP was a gift from Dr. G. Poirier, Quebec, Canada whereas the antibody to CPP32 was a gift from Merck Frost, Canada. Following the incubation with primary antibody, the membrane was blocked again for 15min followed by two 5min repeats with blocking buffer. This was followed by 15min and two 5min washes with TBST. Then the secondary antibody (goat anti-rabbit IgG) conjugated to horseradish peroxidase (diluted 1:2000 in TBST) was added for 1h and the wash procedure was carried out as for the primary antibody. Finally the membrane was soaked in 1% TBS and an ECL (Enhanced Chemiluminescence from Amersham, Bucks., UK) kit was used to detect the protein of interest.

3. Formation of large DNA fragments in rat liver nuclei is a Mg^{2+} and/or Ca^{2+}/Mg^{2+} dependent process

3.1 Introduction

Apoptosis, originally described as shrinkage necrosis (Kerr, 1971) is characterised by a marked condensation of chromatin, accompanied with shrinkage of the nucleus, compaction of cytoplasmic organelles, cell shrinkage and changes at the cell surface. Subsequently, the cell is phagocytosed and there is no inflammatory response (Wyllie et al., 1980; Arends and Wyllie, 1991). When cells undergo apoptosis a number of biochemical events takes place but the most striking characteristic is the fragmentation of DNA into internucleosomal fragments of 180-200 base pairs (bp) or multiples thereof which indicate that the chromatin has been cleaved at the linker DNA. These fragments are seen as a ladder pattern on conventional agarose gels (Wyllie, 1980). Internucleosomal cleavage is thought to arise from the activation of one or possibly more Ca^{2+}/Mg^{2+}-dependent endonucleases (Compton, 1992; Peitsch et al., 1994).

Evidence from a number of studies has shown that in cells undergoing apoptosis there is an increase in intracellular Ca^{2+} concentration. Thus, for example Wyllie et al. (1984) showed that the Ca^{2+} ionophore A23187 activated DNA cleavage and apoptosis in thymocytes whilst McConkey et al. (1989) demonstrated that glucocorticoids induced the endonuclease activity via an elevation of cytosolic Ca^{2+} levels. Similarly, apoptotic hepatocytes showed increases in intracellular Ca^{2+} levels (McConkey et al., 1988). The findings that buffering intracellular Ca^{2+} increases by chelation with quin-2AM prevented the activation of the endonuclease and apoptosis, demonstrates the Ca^{2+} requirement in apoptosis (McConkey et al., 1989;1990). Further evidence for the importance of Ca^{2+} in endonuclease mediated fragmentation has come from studies on isolated rat liver nuclei, which have been shown that Ca^{2+} activates an endonuclease, producing a DNA fragmentation pattern identical to that seen in apoptotic cells (Jones et al.,1989).

However, more recent studies (Walker et al., 1991; Brown et al., 1993) have demonstrated that DNA cleavage in apoptotic thymocytes involves an initial cleavage into high molecular weight fragments of approximately ≥700, 200-250 and 30-50kbp, followed by subsequent endonucleolytic cleavage into nucleosome or oligonucleosome sized fragments. Brown et al. (1993) proposed that the formation of large fragments of DNA represents a much

earlier event in the apoptotic process. In support to this conclusion, Oberhammer et al. (1993a) have shown that hepatocytes undergoing apoptosis with TGF-β_1 treatment exhibit the classical morphology of condensed chromatin but without DNA laddering. Furthermore, it was shown that in a variety of cell lines, apoptotic cell death occurs with cleavage of the DNA into 300 and/or 50 kbp fragments prior to, or in the absence of internucleosomal fragmentation (Oberhammer et al., 1993b).

In order to further understand the mechanisms of DNA cleavage occurring during liver apoptosis, rat liver nuclei were used as an in vitro model system since the DNA fragments generated in isolated nuclei are indistinguishable from those found during apoptosis (Wyllie, 1980). In this study, the specific cationic requirement on the DNA cleavage processes in rat liver nuclei was established. The methods used in this study were conventional gel electrophoresis (CAGE), field inversion gel electrophoresis (FIGE) and in situ end-labelling (ISEL) in conjunction with flow cytometry. CAGE which is used to establish the DNA ladder is restricted to the analysis of DNA fragments of less than 20kbp. Therefore the changes in DNA integrity must also be assessed by using FIGE which allows analysis up to 2Mbp fragments (Schwartz and Cantor , 1986). Although the gel electrophoresis method will allow assessment of the DNA integrity and cleavage products, it does not allow quantitation of the rate or extent of DNA cleavage. In this respect, the ISEL technique was established to detect/quantitate the number of DNA strand breaks involved in DNA degradation. A further advantage of this method was that the DNA cleavage in nuclei of different ploidy (i.e. diploid and tetraploid) state could be determined.

This study showed that DNA was initially cleaved into the large kbp DNA fragments in a sequential manner from ≥700, 200-250, 30-50kbp prior to internucleosomal cleavage. The formation of the large DNA fragments was a Mg^{2+} dependent process which was further accelerated in the presence of Ca^{2+}. However Ca^{2+} alone did not stimulate the cleavage of DNA. The subsequent degradation of DNA into nucleosomal cleavage had an absolute requirement for both Ca^{2+} and Mg^{2+}. Using ISEL, there was no difference in the sensitivity of the 2N and 4N nuclei populations to undergo chromatin cleavage. The results in this chapter support the hypothesis that the large kbp fragment formation and internucleosomal cleavage are two distinct processes with separate cationic specificities, which are involved in DNA degradation during apoptosis.

The results described in this chapter have previously been reported in:

Cain K., Inayat-Hussain S.H., Wolfe J.T. and Cohen G.M.(1994) DNA fragmentation into 200-250 and/or 30-50 kilobase pair fragments in rat liver nuclei is stimulated by Mg^{2+} alone and Ca^{2+}/Mg^{2+} but not by Ca^{2+} alone. FEBS Lett. 349: 385-391

3.2 Results

3.2.1 Isolation and autodigestion assays of rat liver nuclei in spermine/spermidine-containing buffers

Previous studies have shown that Ca^{2+} stimulates the endogenous endonuclease activity in isolated nuclei (see Schwartzman and Cidlowski, 1993 for review). In the case of thymocyte nuclei, relatively large non-physiological concentrations of Ca^{2+} (1-5mM) have been used to induce DNA laddering (Cohen and Duke, 1984) whereas in rat liver nuclei, micromolar concentrations have been reported to be effective at activating the endonuclease activity (Jones et al., 1989).

Preliminary studies of rat liver nuclei isolated in Mg^{2+} containing buffers confirmed that DNA ladders could be induced with as little as 50μM Ca^{2+}. As shown in Fig.3.1, rat liver nuclei incubated without the addition of Ca^{2+} for either 0 or 30min (lanes 1 and 2 respectively) showed no internucleosomal cleavage. Addition of 50μM Ca^{2+} (lane 3) resulted in DNA laddering. Increasing the Ca^{2+} concentration to 300μM Ca^{2+} led to a further cleavage of DNA into oligosomal fragments. However when DNA strand breaks were measured using ISEL technique (Table 3.1), it was noticed that even in rat liver nuclei incubated for 30min at 37°C (control nuclei), there was a significant amount of endogenous endonuclease activity detected (three fold increase in the number of DNA strand breaks as compared to unincubated nuclei). Addition of 50μM Ca^{2+} led to a further increase (2-3 fold) in the level of ISEL.

The instability of chromatin is well known and it has been shown that Mg^{2+}, which is normally used to stabilise the DNA in isolation media, can be replaced with polyamines (spermine and/or spermidine) (Kokileva, 1981; Filipski et al.,1990). Polyamines have important physiological functions and are essential for normal cell growth and differentiation. Spermine and spermidine, in particular stabilize chromatin and nuclear enzymes due to their ability to form complexes with organic polyanions such as negatively charged groups on proteins and

DNA (Heby and Persson, 1990), and are commonly used as stabilizing cations in chromatin isolation media as they are known to inhibit the autodigestion of DNA in isolated

Figure 3.1 CAGE analysis of DNA cleavage in rat liver nuclei stimulated with Ca^{2+}.

Rat liver nuclei were isolated and incubated in Mg^{2+} buffers as described in the methods chapter and subsequently analysed by CAGE. The first lane (std) contains markers of 123bp and multiples thereof. The remaining lanes are as follows: lanes 1 and 2 are the 0 and 30min controls respectively; lanes 3 and 4 are incubations of rat liver nuclei in the presence of 50μM Ca^{2+} and 300μM Ca^{2+}.

nuclei. Another important aspect is the exposure of liver nuclei during isolation to a milieu containing high concentration of cations (e.g. Mg^{2+} and Ca^{2+}) from blood and also disruption

of the cells, mitochondria and endoplasmic reticulum during isolation which may result in DNA autodigestion. Addition of metal ion chelators (e.g. EDTA and EGTA) to remove potential endonuclease and endoprotease activating cations (e.g. Ca^{2+}) results in nuclei preparations in which the DNA structure is resistant to strand breakage. On this basis, I have isolated rat liver nuclei in isolation media (SP-buffers) containing polyamines (spermine and spermidine) and metal chelators (EGTA and EDTA) [see chapter 2 for detailed method], however the latter were omitted in the incubation buffer. The results in Table 3.1 show that the nuclei isolated with SP-buffers have comparable levels of ISEL when compared to the Mg^{2+}-buffers. Most importantly, nuclei isolated in SP-buffers after further incubations for 30min at 37°C did not exhibit an increase in the peak mean fluorescence, indicating that under these conditions the nuclei and DNA structure were stable. This is in contrast to nuclei isolated in Mg^{2+} buffers. Addition of 50μM Ca^{2+} alone did not affect the amount of ISEL in nuclei isolated in SP-buffers but co-incubation with 4mM Mg^{2+} produced a significant increase in the amount of strand breakage. This strand breakage was not sufficient to cleave the DNA into oligonucleosomal fragments as shown in Fig. 3.1. However, co-incubation with 50μM Ca^{2+} and 4mM Mg^{2+} increased the amount of ISEL (Table 3.1) and the addition of 300μM Ca^{2+} with 4mM Mg^{2+} resulted in internucleosomal DNA cleavage seen as a ladder pattern on the gel (Fig. 3.2). As a result of these preliminary experiments all the subsequent experiments were with nuclei isolated and incubated in SP-buffers.

Table 3.1. The effect of spermine and spermidine on ISEL in rat liver nuclei

	Peak Mean Fluorescence			
Treatment	**Mg^{2+} buffers***		**SP-buffers****	
Incubation	2N nuclei	4N nuclei	2N nuclei	4N nuclei
0min	7	11	6	9
30min	21	35	5	8
30min + 50μM Ca^{2+}	57	96	6	11
30min + 50μM Ca^{2+} + 4mM Mg^{2+}	-	-	12	22

Rat liver nuclei were isolated as described in the methods with Mg^{2+} (4mM) containing buffers* or alternatively with SP-buffers** in which Mg^{2+} was replaced with 0.15mM spermine, 0.5mM spermidine, 1mM EDTA and 0.1mM EGTA. ISEL was carried out as described and the nuclei analysed by flow cytometry. The data in the table are taken from a typical experiment.

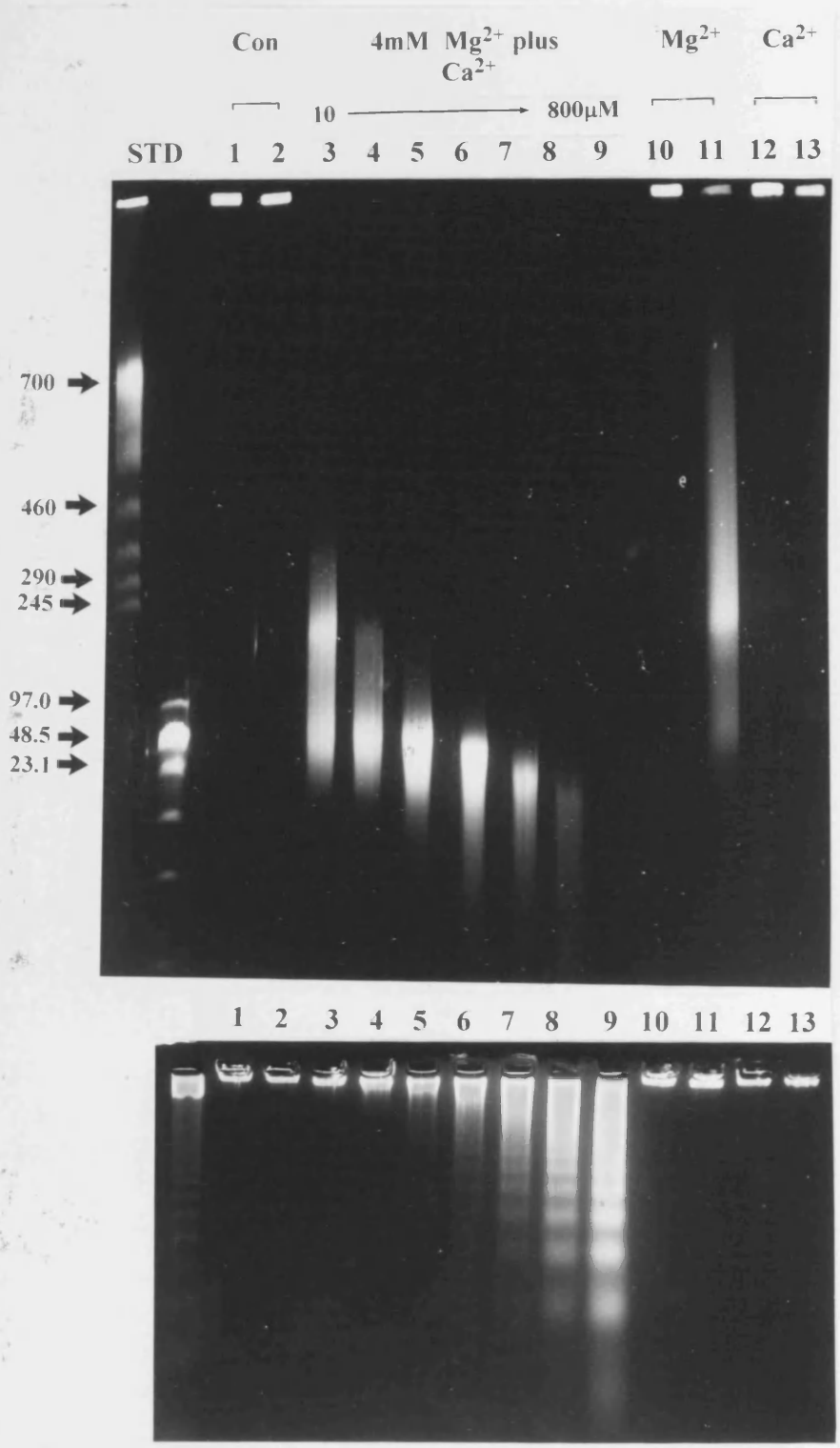

Figure 3.2. CAGE and FIGE of rat liver nuclei after Mg^{2+} and Mg^{2+} plus Ca^{2+} activation.

Rat liver nuclei were isolated and incubated in SP-buffers and subsequently analysed by FIGE (upper panel) and CAGE (lower panel) as described in materials and methods. In the FIGE gel the first two lanes contain *S. cerevisiae* chromosome standards (243-2200 kbp) and 0.1-200 kbp standards, respectively, and key sizes are indicated. The remaining 13 lanes are as follows: con (1 & 2) = 0min and 30min control without Ca^{2+} and Mg^{2+}; Ca^{2+} plus Mg^{2+} (3-9) = 10, 25, 50, 100, 200, 400, 800µM respectively with constant 4mM Mg^{2+}; Mg^{2+} (10 & 11) = 0 and 30min with 4mM Mg^{2+}; Ca^{2+} (12 &13) = 0 and 30min with 200µM Ca^{2+}. In the agarose gel the first lane contains markers of 123bp or multiples thereof. The remaining lanes are as for the FIGE gel.

3.2.2 Effects of Mg^{2+} and Ca^{2+}/Mg^{2+} on DNA fragmentation in rat liver nuclei

As described above, nuclei incubated in SP-buffers without Ca^{2+}/Mg^{2+} for 30min at 37°C showed no endogenous DNA cleavage, as shown by ISEL (Table 3.1), CAGE and FIGE (Fig. 3.2, lanes 1-2). However the addition of 4mM Mg^{2+} alone (Fig. 3.2, lanes 10-11) resulted in the formation of large fragments of DNA with an approximate size of 200-250kbp and without any detectable DNA laddering. Ca^{2+} on its own did not induce large fragment formation or internucleosomal cleavage (Fig. 3.2, lanes 12-13).

However, when Ca^{2+} was added with 4mM Mg^{2+}, there was a much faster rate of DNA cleavage and the size spectrum of DNA fragments produced was markedly dependent on the concentrations of Ca^{2+} (Fig. 3.2, lanes 3-9). Thus the concentration-response curve with Ca^{2+} showed that between 10-25μM Ca^{2+} (lanes 3-4) there was initial cleavage into 200-250 and 30-50kbp fragments without any internucleosomal cleavage. Between 50-100μM Ca^{2+} (lanes 5-6), DNA cleavage was accelerated further and predominantly 30-50kbp fragments were detected with a small amount of DNA laddering. Above 100μM Ca^{2+}, smaller amounts of large fragments were detected, accompanied by a progressive increase in internucleosomal cleavage until ultimately only the classical DNA ladder (Fig. 3.2, lanes 7-9) was detected. This data demonstrate that Ca^{2+} facilitates or potentiates the Mg^{2+} dependent DNA degradation.

3.2.3 Size distribution of DNA fragments after Mg^{2+} dependent degradation

The gel electrophoresis data in Fig. 3.2 (lanes 12-13) highlighted an interesting finding in that Ca^{2+}, in the absence of Mg^{2+} did not activate the mechanisms responsible for either the formation of large kbp fragments or internucleosomal cleavage. However, 4mM Mg^{2+} without Ca^{2+} activated the formation of 'large fragments' of DNA (approximate size 200-250kbp, Fig. 3.2, lane 11).

Varying the Mg^{2+} concentration significantly affected the size distribution of large kbp sized DNA fragments (Fig. 3.3). Thus at 1mM Mg^{2+} (Fig. 3.3, lane 3), no DNA fragmentation was detected on gels. With 2mM Mg^{2+} (lane 4), the DNA was degraded into very large fragments, i.e. mainly ≥700kbp and at 4mM Mg^{2+} (lane 5), both the ≥700kbp as well as 200-250kbp size DNA fragments were seen. The latter size predominated after incubation with 8mM Mg^{2+} (lane 6) although there were fragments seen in the range of 30-50kbp. When the

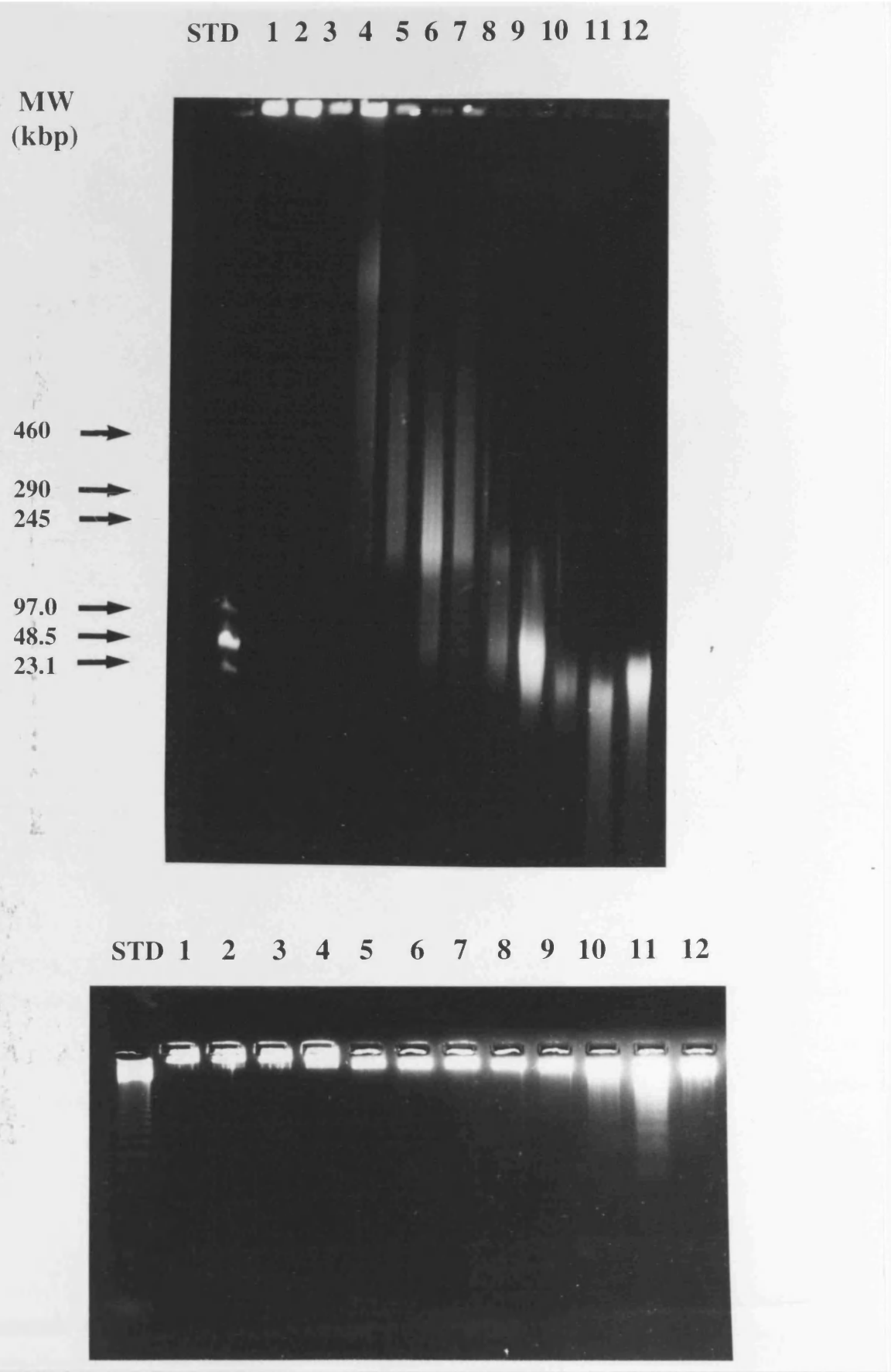

Figure 3.3. CAGE and FIGE of Mg^{2+} induced DNA fragmentation in rat liver nuclei

Rat liver nuclei prepared as described in Figure 3.2 were analysed by FIGE (upper panel) and CAGE (lower panel) as described above. In the FIGE gel, first lane contains standards (STD) as described in Figure 1 and key sizes are indicated with arrows. Lanes 1 & 2 are the 0 and 30min controls respectively; lanes 3-7 are 1, 2, 4, 8, 16mM Mg^{2+} minus Ca^{2+}; lanes 8-12 are 1, 2, 4, 8 and 16mM Mg^{2+} plus 200μM Ca^{2+}. In CAGE the first lane is the 123bp standards and lanes 1-12 are as described for FIGE.

Mg^{2+} concentration was increased to 16mM (lane 7), the major DNA species was the 200-250kbp fragments suggesting that the increased concentration of Mg^{2+} was inhibiting the formation of the 30-50kbp fragments. No DNA laddering was detected on CAGE with the Mg^{2+} concentrations (1-16mM) used above.

When the Mg^{2+} concentration was varied in the presence of a fixed concentration of Ca^{2+} (200μM), a markedly different profile of DNA large fragments was seen (Fig. 3.3, lanes 8-12). Thus at 1mM Mg^{2+} (lane 8), 30-50kbp fragments predominated with a small amount of 200-250kbp size DNA being detected. Only 30-50kbp sized fragments were detected with 2mM Mg^{2+} (lane 9) whereas at 4 and 8mM Mg^{2+} (lanes 10-11), the major fragments were <30kbp and this was accompanied by DNA laddering. At 16mM Mg^{2+} (lane 12) there was a small amount of DNA laddering, suggesting that the internucleosomal cleavage was inhibited at high Mg^{2+} concentrations. Thus in the presence of Mg^{2+} and Ca^{2+}, a more extensive cleavage of DNA was observed than in the presence of Mg^{2+} alone.

3.2.4 In situ end labelling (ISEL) and flow cytometry as a semi quantitative measure of DNA strand breakage in rat liver nuclei

Although the gel electrophoresis experiments gave valuable information on the size of the DNA fragments, it was difficult to quantify the extent or rate of the DNA cleavage. In order to overcome these deficiencies, an ISEL technique was developed in order to quantitate the extent of DNA strand breakage in isolated rat liver nuclei and thereby assess the relative effects of Mg^{2+} and Mg^{2+}/Ca^{2+} on DNA degradation.

A typical cytogram is shown in Fig. 3.4 in which the data are displayed as 3D contour plots with DNA content (PI, red fluorescence) in the x-axis (linear scale) and anti-Dig labeling (green fluorescence) which is a measure of DNA strand breaks in the z-axis (log scale). The cytogram demonstrates that this technique gives information on both the 2N and 4N nuclei populations. The level of ISEL in nuclei incubated for 30min (without any divalent cations) at 37°C was very low (Fig. 3.4A) and was equivalent to non-incubated nuclei (see Table 3.1). However when 8mM Mg^{2+} was added there was a small but measurable increase in the ISEL (Fig. 3.4B). In contrast, the addition of 200μM Ca^{2+} (Fig. 3.4C) alone did not produce any increase in ISEL. This increase was not seen even when the Ca^{2+} concentration was increased to 800μM (data not shown). However the addition of 200μM Ca^{2+} plus 8mM Mg^{2+} produced the greatest increase in ISEL (Fig. 3.4D). Interestingly, all the nuclei treated with the cation(s)

moved as a cohort as seen in Figs 3.4C & D and in all cases the level of ISEL in the two populations of nuclei was related to the DNA content, i.e. end labeling in tetraploid nuclei was approximately double that of the diploid nuclei. Thus the ploidy of the nuclei did not alter the susceptibility of the DNA to cationic stimulated degradation.

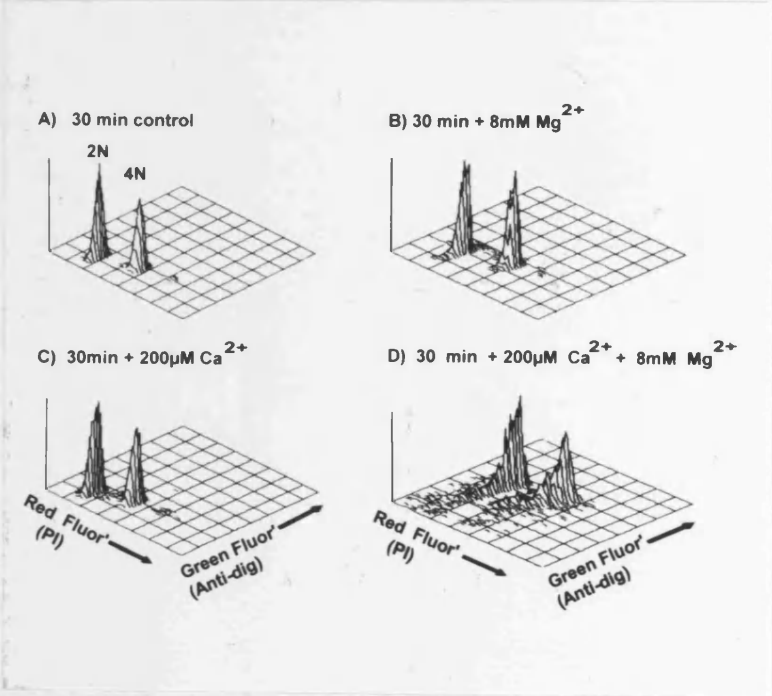

Figure 3.4 Flow cytometric detection of DNA fragmentation in isolated rat liver nuclei using ISEL

Rat liver nuclei were isolated in SP-buffers as described in methods and then incubated as indicated, i.e. A) 30min control with no Mg^{2+} or Ca^{2+} at 37°C, B) as A) but with the addition of 8mM Mg^{2+}, C) as A) but with the addition of 200µM Ca^{2+}; D) as A) but with the addition of 200µM Ca^{2+} and 8mM Mg^{2+}. The reactions were terminated and the DNA strand breakage determined by ISEL and flow cytometry as described in methods. The figure shows the data represented as a 3D cytogram with relative PI fluorescence (DNA content) and green fluorescence (anti-Dig) plotted as indicated.

3.2.5 The effect of Mg^{2+} and Ca^{2+} on ISEL in rat liver nuclei

As shown above, end labeling provided a measure of the DNA strand breakage and the influence of Mg^{2+} on this was investigated further. Increasing concentrations of Mg^{2+} caused an increase in the level of ISEL with a maximum peak mean fluorescence at 8mM Mg^{2+}, followed by a decrease at 16mM Mg^{2+} (Fig. 3.5B). These results were in good agreement with the electrophoresis data described in Fig. 3.3, because as the DNA was cleaved into smaller fragments there would be a proportionate increase in the number of DNA strand breaks and hence a higher level of ISEL. This conclusion was further supported by the data obtained after nuclei were incubated with a fixed concentration of Ca^{2+} (200µM) and varying Mg^{2+} concentrations (Fig. 3.5A). A marked increase (10-fold) in the intensity of the green

fluorescence was observed as compared to that produced by Mg^{2+} alone (see Fig. 3.5A, B). This increased level of ISEL corresponded to the increase in both the 30-50kbp and oligonucleosomal fragments. The data demonstrated that Ca^{2+} and Mg^{2+} together produced a far greater amount of DNA strand breakage than did Mg^{2+} alone.

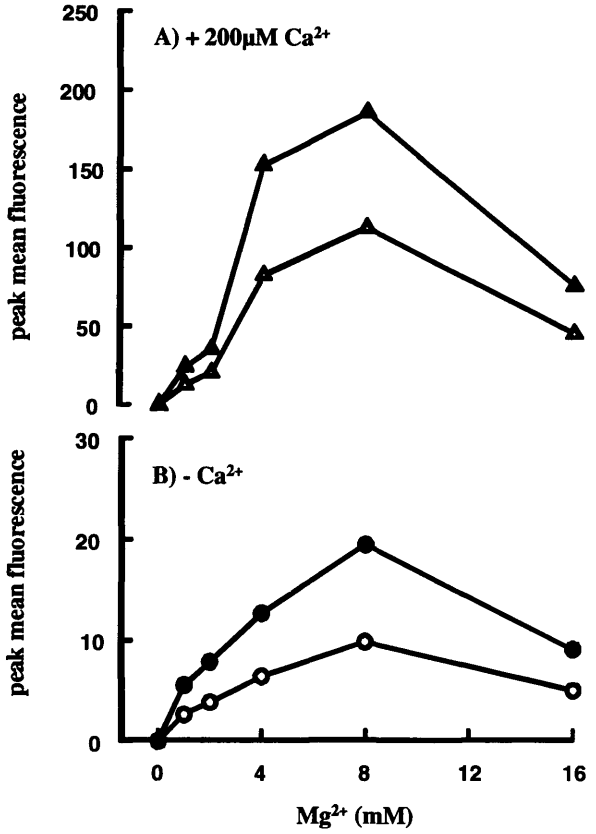

Figure 3.5 Effects of Ca^{2+} on Mg^{2+} induced ISEL cleavage in rat liver nuclei

Rat liver nuclei were prepared as described in Figure 1 and then incubated for 30min at 37°C in SP-buffers supplemented with (A) and without 200μM Ca^{2+} (B), and containing increasing concentrations of Mg^{2+}. DNA cleavage was measured with ISEL and flow cytometry as described in materials and methods. Open and solid symbols represent 2N and 4N nuclei, respectively.

3.2.6 Time dependence of Mg^{2+} dependent DNA cleavage

The studies shown above indicated that the Mg^{2+} dependent degradation of DNA progressed through a series of intermediate steps which generate successively smaller sized fragments. The profile of DNA cleavage products of the Mg^{2+} process was investigated further by performing a time course study as shown in Fig. 3.6. Degradation of DNA was not observed in the control experiment (i.e. 0.5 or 4h incubation without Mg^{2+}). However, with 8mM Mg^{2+}, there was initially a formation of large fragments in the range of ≥700kbp and 200-

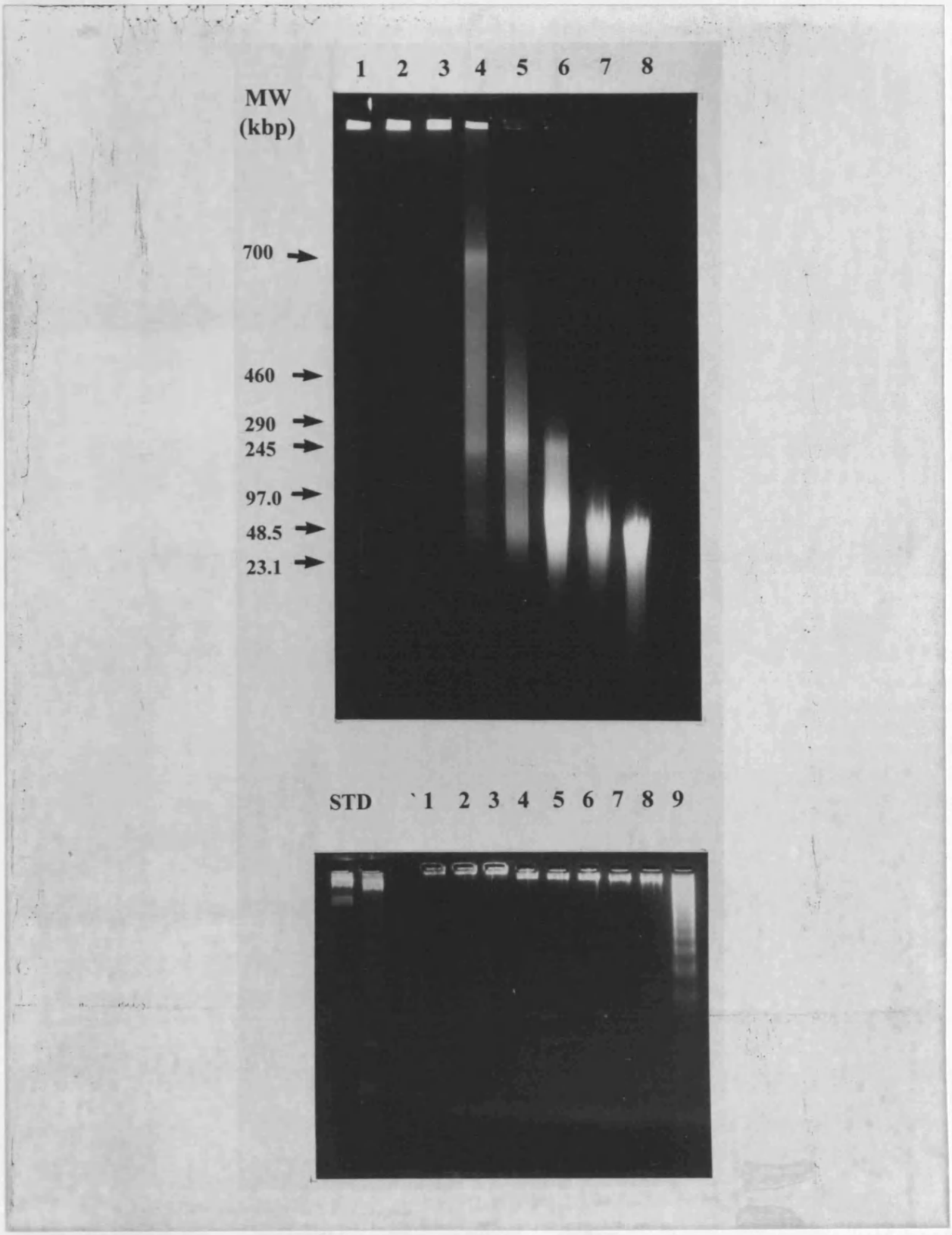

Figure 3.6 Time course for Mg^{2+} induced DNA cleavage in rat liver nuclei

Rat liver nuclei were prepared and incubated at 37°C for 0-4h with or without 8mM Mg^{2+}. At the indicated times, the reactions were terminated and the DNA fragmentation patterns were determined by FIGE (upper panel) and CAGE (lower panel). In both FIGE and CAGE, lanes 1-3 were nuclei incubated without Mg^{2+} for 0, 0.5 and 4h respectively, and lanes 4-8 show the effect of nuclei incubated with 8mM Mg^{2+} for 0.5, 1, 2, 3 and 4h respectively. Lane 9 shows the effect of 8mM Mg^{2+} + 400μM Ca^{2+} after 30min as a positive control for DNA laddering.

250kbp at 30 min. By 1h, most of the DNA was degraded predominantly to 200-250kbp but by 2h most of these fragments (i.e. 200-250kbp) were degraded to 30-50kbp sized fragments.

By 3h, only the 30-50kbp DNA fragments were detected which were unaltered even at 4h. Significantly, internucleosomal cleavage was not observed on CAGE, confirming that Mg^{2+} activated only the formation of large fragments in a step wise manner from intact DNA to ≥700kbp→200-250kbp→30-50kbp. The ISEL results (Fig. 3.7) complement the gel data in that at 30min the nuclei have low peak mean fluorescence values which progressively increased with time. The increase in fluorescence was consistent with the expected increase in DNA strand breaks. Thus for example, at 1h the majority of the DNA fragments was 200-250kbp size which by 4h has been degraded into 30-50kbp. This process should generate a 4-6 fold increase in the number of DNA strand breaks and in both the 2N and 4N nuclei there were a similar increase in peak mean fluorescence values.

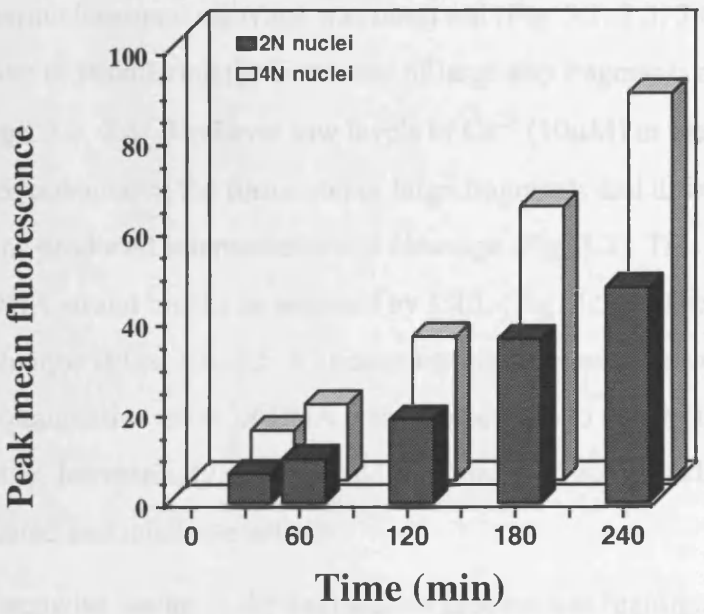

Figure 3.7 Time course of Mg^{2+} induced DNA cleavage as measured by ISEL

Rat liver nuclei were prepared as described in Figure 3.6 and incubated for 0, 60,120, 180 or 240min in SP-buffers containing 8mM Mg^{2+}. The reactions were terminated and DNA strand breaks determined by ISEL as described in methods.

3.3 Discussion

Endonuclease cleavage of DNA into nucleosomal fragments, which can be seen as a DNA ladder after agarose gel electrophoretic separation, has long been regarded as the biochemical hallmark of apoptosis (Wyllie, 1980). However, recent studies (Walker et al.,

1991; Brown et al.,1993; Oberhammer et al.,193b) have shown that there is an initial cleavage of DNA into ≥700,200-300 and 30-50kbp fragments, prior to internucleosomal degradation. The size of the large fragments are similar to the 'loops' (30-50kbp) and rosettes (200-300kbp), which has been suggested by Filipski et al. (1990) to be essential components of higher order chromatin structure. A fuller understanding of the mechanisms/enzymes catalysing the formation of the large fragments is of fundamental importance to the study of apoptosis. Since the DNA fragments generated in isolated nuclei are indistinguishable from those found during apoptosis, nuclei provide an ideal model to investigate this phenomenon.

The results in this study show how a combined approach using conventional agarose gel electrophoresis, FIGE and ISEL can be used to investigate the DNA fragmentation process. Initially, the DNA was degraded into ≥700kbp sized fragments which were subsequently cleaved in a Mg^{2+} concentration, time dependent and stepwise manner into 200-250kbp and 30-50kbp fragments (Figs. 3.2, 3.6). When this process was catalysed by Mg^{2+} alone, no internucleosomal cleavage was observed (Fig. 3.2, 3.3, 3.6). Also, Ca^{2+} on its own was ineffective in stimulating the formation of large kbp fragments or internucleosomal cleavage (Figs. 3.2, 3.4). However low levels of Ca^{2+} (10μM) in the presence of 4mM Mg^{2+} accelerated or potentiated the formation of large fragments and ultimately at higher Ca^{2+} concentrations produced internucleosomal cleavage (Fig. 3.2). This produced a much greater number of DNA strand breaks as assessed by ISEL (Fig. 3.5A). The data obtained with the end labelling technique (Figs. 3.4, 3.5, 3.7) demonstrated the potential of this technique to provide both a semi-quantitative assay of DNA cleavage but also to discriminate between nuclei with different ploidy. Interestingly, both diploid and tetraploid nuclei had the same susceptibility to cation stimulated endonuclease activity.

The stepwise nature of the degradation process was highlighted by the time course experiments (Fig. 3.6). The progression with 8mM Mg^{2+} involved an initial cleavage to the large ≥700kbp fragments. Subsequently, these were cleaved into 200-250kbp fragments and then ultimately to the 30-50kbp fragments. In the absence of Ca^{2+} there was no further cleavage. The data supported the idea that the breakdown of the DNA was an ordered process which was related to DNA structure.

The addition of Ca^{2+} (Figs. 3.2-3.5) in the presence of Mg^{2+} appeared to have two effects. Firstly, it enhanced the production of the 30-50kbp fragments from the larger ≥700kbp

and 200-250kbp fragments, and secondly it activated internucleosomal cleavage. Both of the effects may be produced by the same enzyme/mechanism which is activated by Mg^{2+} but is accelerated or facilitated in the presence of Ca^{2+}. Alternatively, DNA fragmentation could be as a result of two separate and distinct processes or enzymes. In this context, it is of interest that Wyllie et al.(1992), using a plasmid cutting assay have shown that a constitutive nuclease extracted from the nuclei of thymocytes, which are particularly susceptible to apoptosis can be activated by Mg^{2+} and that this activity is further facilitated by the addition of Ca^{2+}. In addition, Patel et al. (1994) have recently demonstrated that the rate of glycodeoxycholate mediated apoptosis in rat hepatocytes is dependent on increases in cytosolic free Mg^{2+}, suggesting regulation of endonuclease activity by cellular Mg^{2+} concentrations. Further studies showed that the in vitro endonuclease activity present in soluble protein extracts from rat hepatocyte nuclei was predominantly Mg^{2+} dependent. In this respect, Walker et al.(1995) have also studied the cationic requirement for the complete pattern of DNA cleavage in nuclei and suggest that the whole process may be catalyzed by two pools of Mg^{2+} activated/ Ca^{2+} modulated DNase I-like enzyme activities. Regardless of the mechanisms involved, the role of Mg^{2+} has to be reappraised in the apoptotic process. Previously, the absence of DNA laddering in apoptotic cells (Brown et al.,1993; Oberhammer et al.,1993a;1993b) was interpreted as evidence that internucleosomal cleavage was an 'end stage' or 'down stream' event. Clearly, from my data this only occurs at moderately high Ca^{2+} concentrations or at a late stage (time) in the process. However, it is equally clear that low levels of the Ca^{2+} in conjunction with Mg^{2+} will catalyse the rapid and the irreversible degradation of the DNA into large fragments which precedes nucleosomal cleavage.

It should be emphasised that this study provides information on the constitutive nucleases of the isolated rat liver nuclei and strictly speaking this is not apoptosis. However, as discussed earlier the fragmentation patterns produced in isolated nuclei are similar to those observed in thymocytes induced to undergo apoptosis by topoisomerase II inhibitors (Filipski et al.,1990; Walker et al., 1991) and dexamethasone (Brown et al., 1993). Thus isolated nuclei would appear to be a valid model for looking at the DNA fragmentation in apoptosis. These results together with other studies with rat thymocytes (Walker et al., 1991, Brown et al., 1993) and isolated rat thymocyte nuclei (Sun and Cohen, 1994) demonstrate that this progressive, multi-step, degradation is a common feature of apoptosis.

3.4 Summary

Internucleosomal cleavage of DNA has often been regarded as the biochemical hallmark of apoptosis. However, the results in this chapter demonstrate that in isolated rat liver nuclei the DNA is initially cleaved into ≥700, 200-250 and 30-50kbp fragments via a multi-step process, which is activated by Mg^{2+} and Mg^{2+} + Ca^{2+} but not Ca^{2+} alone. The subsequent internucleosomal cleavage requires both cations. These findings demonstrate that a key down stream event in the apoptotic process is the fragmentation of DNA into large kbp fragments by either a Mg^{2+}-dependent process (which can be potentiated by Ca^{2+}) and/or by a Mg^{2+}/Ca^{2+} activated endonuclease.

4. Multi-step DNA cleavage in rat liver nuclei is inhibited by thiol reactive agents

4.1 Introduction

Various observations have suggested that the activation of proteases is required for DNA fragmentation in both isolated nuclei and intact cells. Thus for example, it has been reported by Bruno et al. (1992) that co-incubation of thymocytes with inducers of apoptosis and serine protease inhibitors prevented the appearance of DNA ladders as well as the typical changes in the flow cytometric distribution of treated cells. Furthermore, several serine proteases that could be involved in nuclear destabilisation during apoptosis have been described recently. Tian et al. (1991) purified and cloned a widely expressed nuclear RNA-binding protein homologous to the CTL granule serine protease TIA-1, while Gaziev and Kutsyi (1992) have described a nuclear matrix associated PMSF sensitive protease in liver nuclei, whose activity is elevated subsequent to gamma irradiation. In addition, Clawson et al. (1992) have recently described a nuclear scaffold, calcium dependent serine protease in rat liver nuclei with a predominantly chymotryptic-like substrate preference and its activity shows extensive similarities to multicatalytic proteinase complex. Furthermore, the degradation of lamin B_1 has also been proposed to promote the formation of large fragments of DNA by allowing the release of matrix attachment regions to give access for endonucleases in apoptotic thymocytes and isolated thymocyte nuclei (Neamati et al., 1995). Studies in immature thymocytes undergoing apoptosis (Weaver at al., 1993) showed that serine protease inhibitors prevent the internucleosomal DNA cleavage but not the initial stages of nuclear collapse and DNA degradation. In addition, Fearnhead et al. (1995) have demonstrated that TLCK inhibits the formation of large fragments in apoptotic thymocytes but not in isolated thymocytes nuclei suggesting that proteolysis is required for the initial cleavage of intact DNA to the large kbp fragments or at some earlier stage in the apoptotic process. In contrast, TPCK inhibits the internucleosomal cleavage but not the chromatin condensation suggesting a proteolytic cascade might be involved in thymocyte apoptosis. Zhivotovsky et al. (1994) have shown that inhibitors of serine proteases (TPCK and TLCK) prevented the formation of 50kbp fragments as well as the internucleosomal cleavage in rat liver nuclei. Further evidence also comes from assays of protease activity which revealed that nuclear serine protease activity increases during bile salt-induced hepatocyte apoptosis (Kwo et al., 1995). In addition, studies by Wright et al.

(1994) showed that a 24kDa protease purified from TNF or uv-induced apoptosis in U937 cells activated DNA fragmentation in U937 nuclei. Collectively, these studies suggest that proteases are involved in facilitating endonucleolytic DNA fragmentation.

The results in chapter 3 demonstrated the multi-step DNA cleavage pattern and its cationic requirement in rat liver nuclei. Initially, DNA is degraded into large kbp fragments (700, 200-250 and 30-50kbp) in a Mg^{2+} dependent process which can be potentiated by Ca^{2+}. However, the subsequent and terminal internucleosomal cleavage which produces mono/oligo-nucleosomes is a Ca^{2+}/Mg^{2+} dependent process. These results can be interpreted as being evidence for either two or more separate enzymes with different cationic requirements or alternatively as a single endonuclease which has both Mg^{2+} and Ca^{2+} binding sites that can activate or modify the catalytic activity of the enzyme. If there are separate and distinct enzymes, it should be possible to preferentially block one without affecting the other. One can also envision the potential roles for proteases in this multi-step DNA cleavage; i.e proteolytic activation of an endonuclease precursor (a pro-endonuclease) or enhancement of the accessibility of target DNA by degradation of proteins that guard the DNA, thereby allowing the apoptotic endonuclease(s) to function.

The results presented in this chapter are divided into two sections. The first section provides further evidence for this stepwise degradation by examining the effects of heavy metals (Cd^{2+} and Hg^{2+}). Furthermore, I have also investigated the possibility of the involvement of proteases in the multi-step DNA cleavage process by using serine protease inhibitors including TLCK, TPCK and DCI. TLCK irreversibly inhibits trypsin-like serine proteases, which require a basic amino acid in the P_1 position according to the nomenclature of Schecter and Berger, while TPCK irreversibly inhibits chymotrypsin-like serine proteases, which requires an aromatic amino acid in the P_1 position (Beynon and Bond, 1994). DCI is a mechanism based serine protease inhibitor (Harper et al., 1985) and recent studies have shown that DCI will also inhibit a thiol protease (Foreman et al., 1993). As some of the inhibitors mentioned above (Cd^{2+}, Hg^{2+} and DCI) have shown to be potent inhibitors of the multi-step DNA cleavage and that these compounds share a common feature that is an affinity to bind to sulphydryl group, I have used a classical -SH alkylating agent, NEM and found that it is also a potent inhibitor of DNA cleavage in rat liver nuclei. These results suggest that a critical thiol(s) is involved in the DNA cleavage reactions which are a feature of the apoptotic process.

The second section in this chapter provides further evidence that the multi-step DNA cleavage is carried out by a single endonuclease or a class of endonucleases whose cleavage activity is modified according to cation availability. This was achieved by using Mn^{2+} to replace Mg^{2+} in rat liver nuclei which the results showed that Mn^{2+} mimicked the effects of both Mg^{2+} and Ca^{2+}/Mg^{2+}. Low concentrations of Mn^{2+} mimicked the effects of Mg^{2+} in producing the large kbp fragments and higher concentrations of Mn^{2+} duplicated the effects of both Ca^{2+}/Mg^{2+} producing internucleosomal cleavage in isolated nuclei. Both these processes were inhibited by DCI and NEM. Another well-known endonuclease inhibitor, Zn^{2+} also prevented the multi-step DNA cleavage. The results are discussed and a general scheme for the multi-step DNA cleavage and the effects of the inhibitors in these process(es) in rat liver nuclei is proposed.

The data presented in this chapter have been published in the following journals;

1) Kelvin Cain, Salmaan H. Inayat-Hussain, Ludmilla Kokileva, Gerald M Cohen (1994) DNA cleavage in rat liver nuclei activated by Mg^{2+} or Ca^{2+} + Mg^{2+} is inhibited by a variety of structurally unrelated inhibitors. Biochem. Cell Biol., 72; 11-12; 631-638

2) Kelvin Cain, Salmaan H. Inayat-Hussain, Ludmilla Kokileva, Gerald M Cohen. (1995) Multi-step DNA cleavage in rat liver nuclei is inhibited by thiol reactive agents. FEBS Lett. 358; 255-261

SECTION I

4.2 Results

4.2.1 Inhibition of Mg^{2+} and Ca^{2+}/Mg^{2+} induced DNA cleavage in isolated rat liver nuclei by Hg^{2+} and Cd^{2+}

A recent study by Lohmann and Beyersmann (1993) has shown that Cd^{2+} and Hg^{2+} are potent inhibitors of Ca^{2+}/Mg^{2+} internucleosomal cleavage. However the effect of these heavy metals on large fragment formation had not been investigated and the experiments described below not only confirmed that Hg^{2+} and Cd^{2+} were very potent inhibitors of internucleosomal cleavage but also shows that they were effective at blocking the large fragment formation.

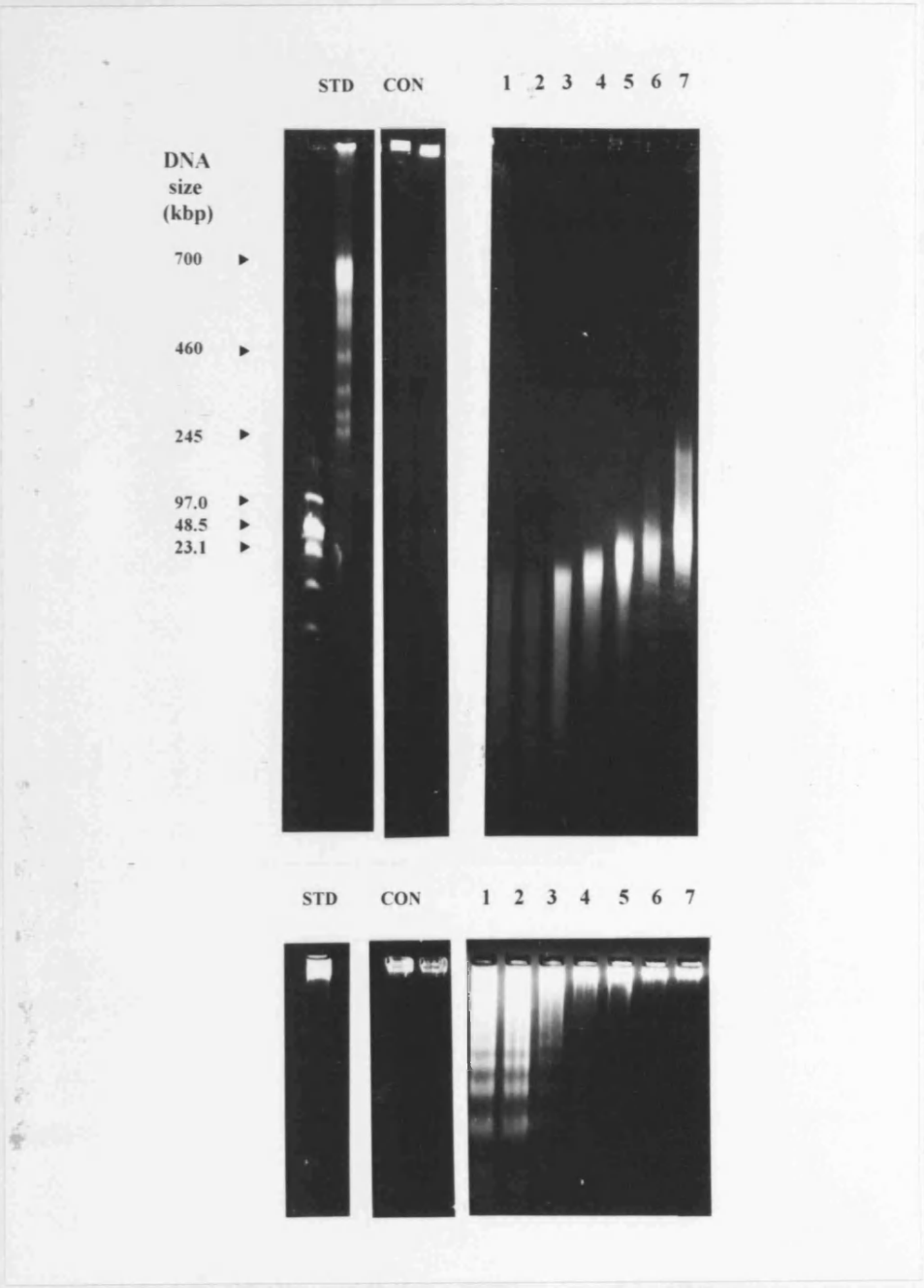

Figure 4.1 Cd^{2+} inhibition of Ca^{2+}/Mg^{2+}-activated DNA cleavage in rat liver nuclei

Rat liver nuclei were isolated and incubated for 30 minutes as described in methods with a range of Cd^{2+} concentrations (0-800μM) in the presence of 100μM Ca^{2+} and 8mM Mg^{2+}. The reactions were terminated and the nuclei were subjected to FIGE (A) and CAGE (B) as described. Lanes 1 - 7 contain 0, 25, 50, 100, 200, 400 and 800μM Cd^{2+} respectively.

The effects of Cd^{2+} on DNA cleavage after Ca^{2+}/Mg^{2+} activation is demonstrated in Fig. 4.1. FIGE and CAGE showed nuclei activated by 100μM Ca^{2+}/8mM Mg^{2+} exhibited extensive internucleosomal cleavage (DNA laddering) with only a small amount of <30kbp fragments (Fig. 4.1, lane 1). The inhibition of DNA cleavage produced by a range of Cd^{2+} concentrations (25-800μM) produced a progressive, incremental increase in the size of the large fragments (Fig. 4.1A, lanes 2-7), ranging from 30-50 and 200-250kbp fragments to intact DNA. This was accompanied by the abolition of internucleosomal cleavage (Fig. 4.1B). These results further support the view that chromatin is degraded via a stepwise process, which involves the generation of DNA fragments of a defined and successively smaller size. The electrophoresis data also showed that while DNA laddering was completely abolished at low inhibitor concentrations, there was still extensive DNA cleavage, which produced the large kbp fragments. Thus, CAGE should not be used as the sole criterion for determining whether or not DNA fragmentation has been inhibited or abolished.

Hg^{2+}, which is also a heavy metal in group IIB demonstrated a more potent inhibition of the Ca^{2+}/Mg^{2+} stimulated DNA cleavage than Cd^{2+} as shown in Fig. 4.2. The inhibitory effects of Hg^{2+} were produced over a narrow concentration range (i.e. between 10-15μM, Fig. 4.2A&B). The inhibition of DNA fragmentation by Hg^{2+} blocked the internucleosomal cleavage (Fig. 4.2B) and resulted in the appearance of large DNA fragments of increasing sizes, comprising 200-250≥700kbp and intact DNA (Fig. 4.2).

Both Cd^{2+} and Hg^{2+} were effective inhibitors of large fragment formation in nuclei incubated with 8mM Mg^{2+} alone for 1h at 37°C. Under these conditions, FIGE revealed that in the absence of the heavy metals the DNA was cleaved into 30-50 and 200-250kbp sized fragments (zero lanes, Fig. 4.2C&D). The inhibition of the formation of these large fragments was accompanied by marked effects on the size of the fragments. Thus between 25-100μM Cd^{2+} there was a change in the DNA size distribution with the appearance of intact DNA in the sample well and an increased amount of 200-250kbp fragments. This was accompanied by a corresponding decrease in the smaller 30-50kbp fragments. At higher Cd^{2+} concentrations (200 and 400μM), the inhibition was greater and resulted in the DNA being partially cleaved into 200-250 and ≥700kbp fragments with more of the intact DNA remaining in the sample well. The highest concentration of 800μM Cd^{2+} produced an almost total inhibition of cleavage leaving virtually all of the DNA retained at the origin of the gel. The inhibitory effects of Hg^{2+}

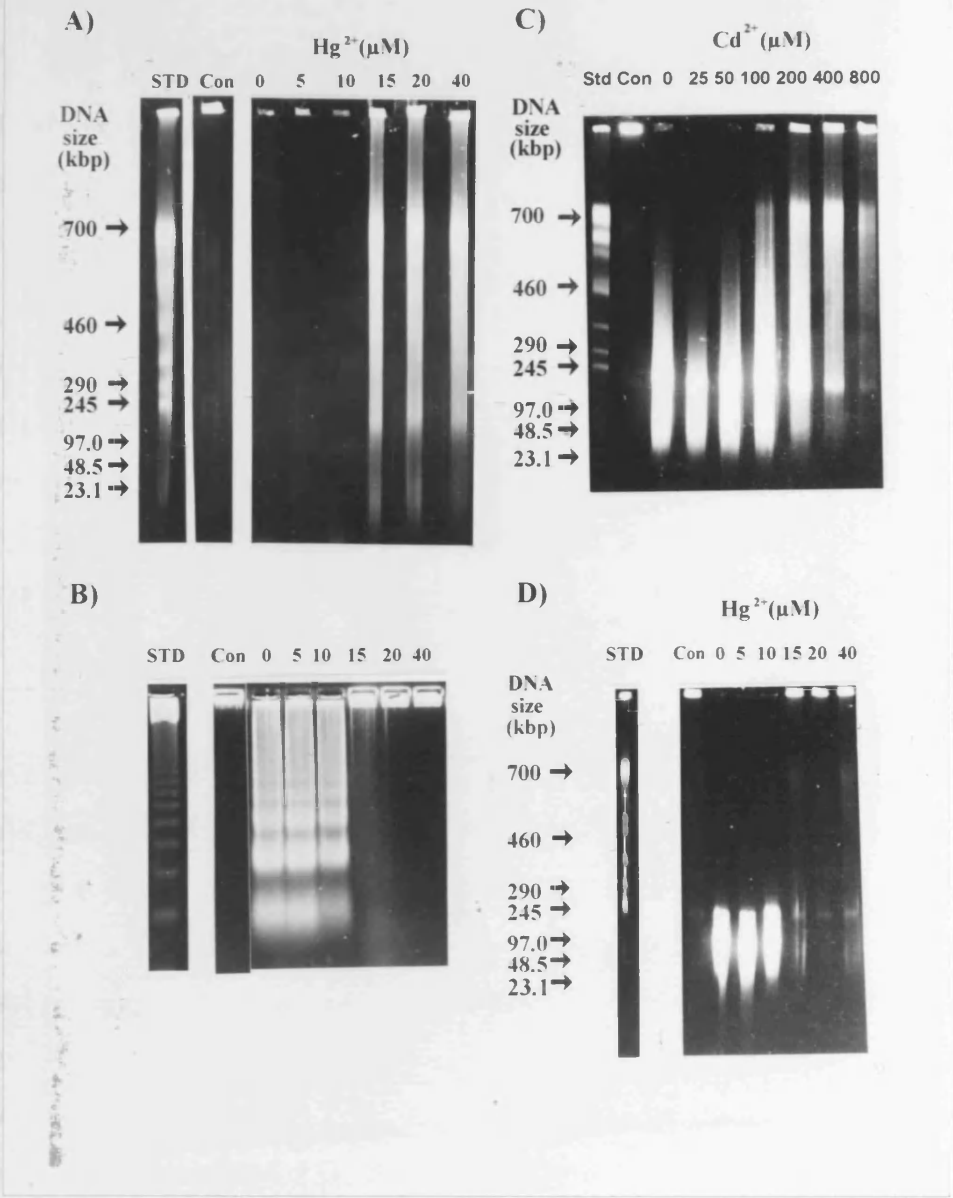

Figure 4.2 Cd^{2+} and Hg^{2+} inhibition of DNA cleavage in rat liver nuclei

Rat liver nuclei were isolated and incubated with and without inhibitors with either 100μM Ca^{2+}/8mM Mg^{2+} for 30 minutes or 8mM Mg^{2+} for 60 minutes as described. The reactions were terminated and the nuclei from the incubations analysed by FIGE and/or CAGE. The effect of Hg^{2+} on Ca^{2+}/Mg^{2+}-activated cleavage is shown in panel A (FIGE) with the corresponding internucleosomal cleavage shown in the panel B below. The effect of Cd^{2+} and Hg^{2+} on large fragment formation as stimulated by 8mM Mg^{2+} alone is shown in panels C and D. In these cases, there was no internucleosomal cleavage and the CAGE results are not shown. The 'con' lanes refer to nuclei incubated without cations for the appropriate and thus demonstrates that in the absence of added cations, there was no endogenous cleavage. In FIGE gels (A, C and D) *S. cerevisiaes* chromosomal DNA markers are shown as 'STD' with the sizes indicated by arrows. In the CAGE (B) the 'STD' lane refers to laddering standards of 123bp or multiples thereof. The concentrations of Hg^{2+} and Cd^{2+} are as indicated in the legends above the gel.

on Mg^{2+} activated DNA cleavage were produced over a narrow concentration range (10-15μM) and were accompanied by an abrupt shift in the DNA size from 30-50 and 200-250kbp fragments to intact DNA (Fig. 4.2D). As with Cd^{2+}, both the Mg^{2+} and Ca^{2+}/Mg^{2+}-dependent DNA cleavage reactions were inhibited by similar concentrations of Hg^{2+}.

4.2.2 Inhibition of Ca^{2+}/Mg^{2+} induced DNA fragmentation in isolated rat liver nuclei by protease inhibitors

There is increasing evidence for the role of proteases in apoptosis and recently, Weaver et al., 1993 have reported that the serine protease inhibitors TPCK and DCI inhibited DNA laddering but not large fragment formation in apoptotic thymocytes. They also reported that these inhibitors did not block internucleosomal cleavage or the formation of large fragments in isolated nuclei obtained from rat thymus and rat liver. However, in contrast Zhivotovsky et al. (1994) have shown that TPCK and another serine protease, TLCK inhibited DNA fragmentation in isolated rat liver nuclei.

In this study, the effects of DCI, TPCK and TLCK on cation stimulated DNA cleavage were investigated with the more usual gel techniques, and also with the ISEL technique which was used to quantify the inhibitory potency of these agents. This is shown in Fig. 4.3 which demonstrates that DCI was a potent inhibitor of Ca^{2+}/Mg^{2+} stimulated DNA cleavage. The end labelling experiments (Fig. 4.3C) showed that the I_{50} value for this protease inhibitor was 10-12μM and that the cleavage of the DNA was almost completely blocked at approximately 50μM DCI. The gel electrophoresis studies demonstrated that inhibition of ISEL was accompanied by the abolition of internucleosomal cleavage (Fig. 4.3B, lanes 2-5) and the concomitant appearance (Fig, 4.3A, lanes 2-5) of the larger kbp sized fragments of DNA. The size of these fragments was determined by the extent of the inhibition which was accompanied by a step-wise increase in the size of the large fragments which progressed from <30kbp (lane 1, no inhibitor), to 30-50 and 200-250kbp (lane 2; 11.5μM DCI), to 30-50, 200-250 and ≥700kbp and intact DNA (lanes 3-5, 29-115μM DCI). TPCK was a poor inhibitor of both ISEL, DNA laddering and large fragment formation (Fig. 4.3A&B, lanes 7-11).

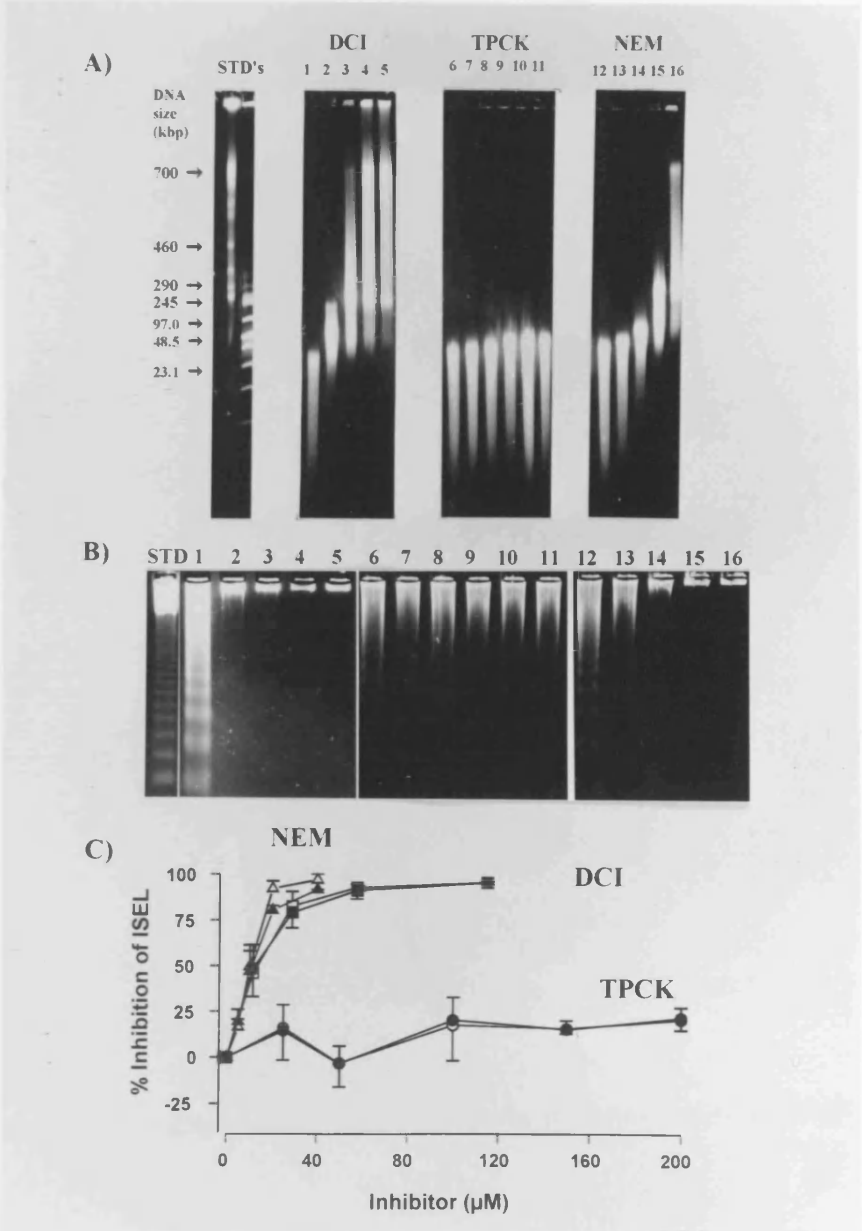

Figure 4.3 Effects of NEM and protease inhibitors on DNA cleavage in rat liver nuclei

Rat liver nuclei were incubated in the presence of 100 μM Ca^{2+}/8 mM Mg^{2+} with or without NEM and protease inhibitors for 30 min. The reactions were terminated and aliquots taken for FIGE (A), CAGE (B) and ISEL (C) which were carried out as described in methods. The lanes for the inhibitors are as follows: DCI (lanes 1-5) = 0, 11.5, 28.8, 57.7 and 115 μM; TPCK (lanes 6-11) = 0, 25, 50, 100, 150 and 200 μM; NEM (lanes 12-16) = 0, 5, 10, 20, and 40 μM. Analysis of ISEL was carried out as described previously, from bivariate cytograms of propidium iodide (DNA content) versus green (anti-Dig) fluorescence. The peak mean fluorescence values, which were a measure of the end (anti-dig) labelling of the 2N (open symbols) and 4N (closed symbols) nuclei, were corrected for control fluorescence values (i.e. nuclei incubated without cations). The corrected values were expressed as a % of the uninhibited cleavage and are shown as the mean ±S.E.M. of 3 separate nuclei preparations.

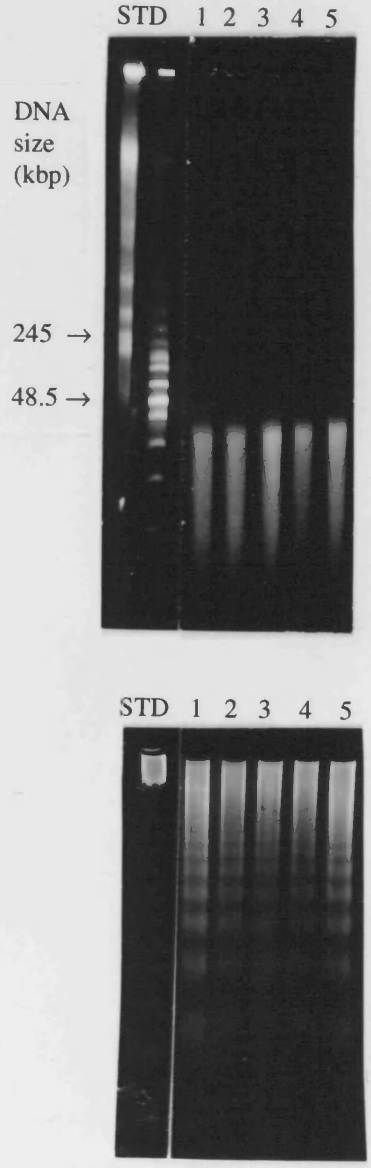

Figure 4.4 The effect of TLCK on Ca^{2+}/Mg^{2+}-activated DNA cleavage in rat liver nuclei

Rat liver nuclei were isolated and incubated for 30min as described in methods with a range of TLCK concentrations (0-100μM) in the presence of 100μM Ca^{2+} and 8mM Mg^{2+}. The reactions were terminated and the nuclei were subjected to FIGE (upper panel) and CAGE (lower panel) as described. Lanes 1-5 contain 0, 10, 25, 50 and 100μM TLCK respectively.

However, TLCK which is a trypsin like serine protease inhibitor did not inhibit the Ca^{2+}/Mg^{2+} stimulated DNA cleavage as seen on CAGE and FIGE (Fig. 4.4).

As DCI has been reported to inhibit thiol protease (Foreman et al., 1993) and the heavy metals Cd^{2+} and Hg^{2+} are known to have great affinity for thiols (Vallee and Ulmer, 1972), it

was possible that a crucial thiol was involved. This possibility was examined by the effects of sulphydryl blocking agent on the Ca^2/Mg^{2+} dependent DNA cleavage. The results of these studies are shown in Fig. 4.3 which demonstrated that NEM was also a potent inhibitor of DNA cleavage. The inhibition of end labelling by NEM (I_{50}=10-12μM) was accompanied by the abolition of internucleosomal cleavage (Fig. 4.3B, lanes 13-16) and a step-wise increase in the size of the large fragments (Fig. 4.3A, lanes 13-16) from <30kbp, to 30-50kbp and 200-250kbp, ≥700kbp and intact DNA. NEM produced an almost total (90-95%) inhibition of ISEL (Fig. 4.3C). All the inhibitors used did not have any effect on DNA structure when incubated with nuclei in the absence of cations.

4.2.3 Inhibition of Mg^{2+} dependent degradation of DNA into 'large fragments' by protease inhibitors and N-ethylmaleimide

As shown in Fig. 4.5, large fragment formation activated by Mg^{2+} alone was inhibited by DCI and as the end labelling data demonstrates (Fig. 4.5B), the sensitivity of this process (I_{50}= 12-14μM) to the inhibitor was similar to that shown by the Ca^{2+}/Mg^{2+} dependent cleavage reaction (Fig. 4.3C). In the presence of Mg^{2+}, only the large 30-50 and 200-250kbp sized fragments were produced which were detected by FIGE (Fig. 4.5A, lane 1) and increasing inhibition of the cleavage process was accompanied by a step-wise increase in the size of the DNA fragments (lanes 2-5). TPCK partially inhibited the Mg^{2+} stimulated DNA cleavage (compare with the Ca^{2+}/Mg^{2+} activated process, Fig. 4.3C), producing a maximum of 50% inhibition and only a small increase in the size of the DNA fragments (Fig. 4.5A, lanes 7-10). TLCK was ineffective at inhibiting the Mg^{2+}-dependent DNA cleavage as shown in Fig. 4.6. However, NEM was a potent inhibitor of the end labelling stimulated by Mg^{2+} (I_{50} = 6-8μM, Fig. 4.5B) and as shown in Fig. 4.5A (lanes 12-15) this inhibition was accompanied by a step wise increase in the size of cleaved DNA fragments.

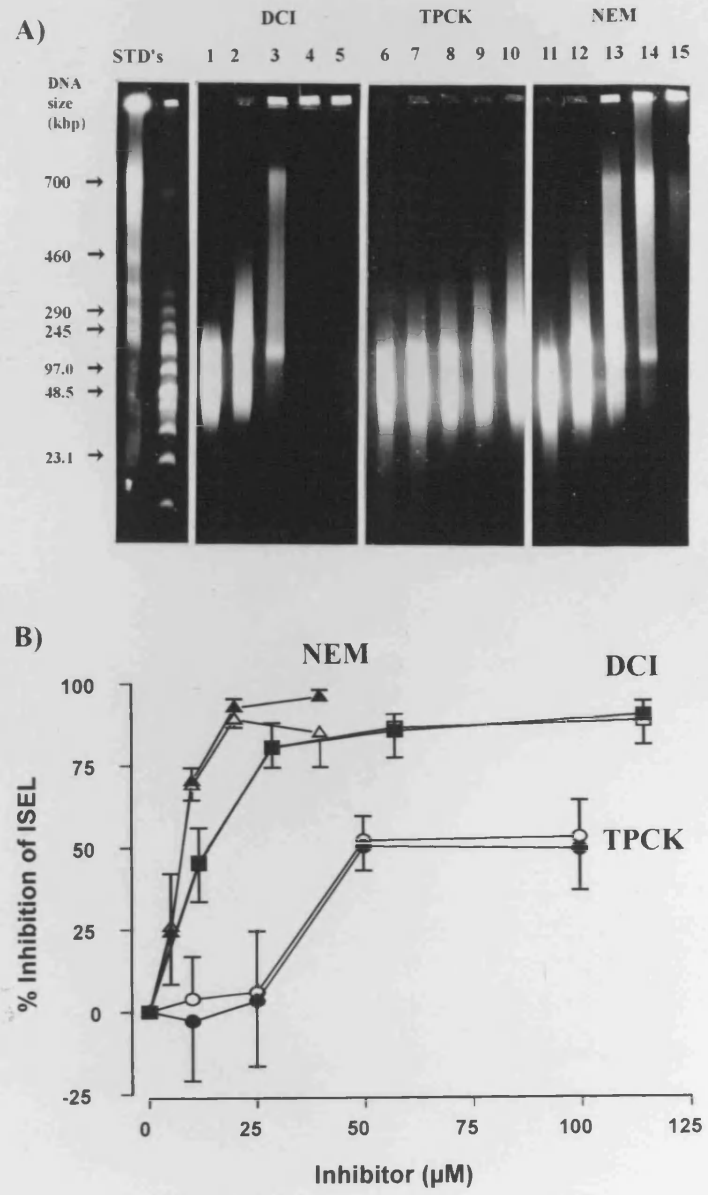

Figure 4.5 The effect of NEM and protease inhibitors on Mg^{2+}-activated DNA cleavage

TPCK, DCI and NEM were incubated with rat liver nuclei in the presence of 8mM Mg^{2+} for 60min. The reactions were terminated and aliquots taken for FIGE (A) and ISEL (B) which were carried out as described in methods. The concentrations for the inhibitors were; DCI (lanes 1-5) = 0, 11.5, 28.8, 57.7 and 115μM; TPCK (lanes 6-10) = 0, 25, 50, 100, 150 and 200μM; NEM (lanes 11-15) = 0, 5, 10, 20, and 40μM. Inhibition of end-labelling was carried out as described in methods and the results are expressed as the mean ± S.E.M. of 4-6 separate nuclei preparations.

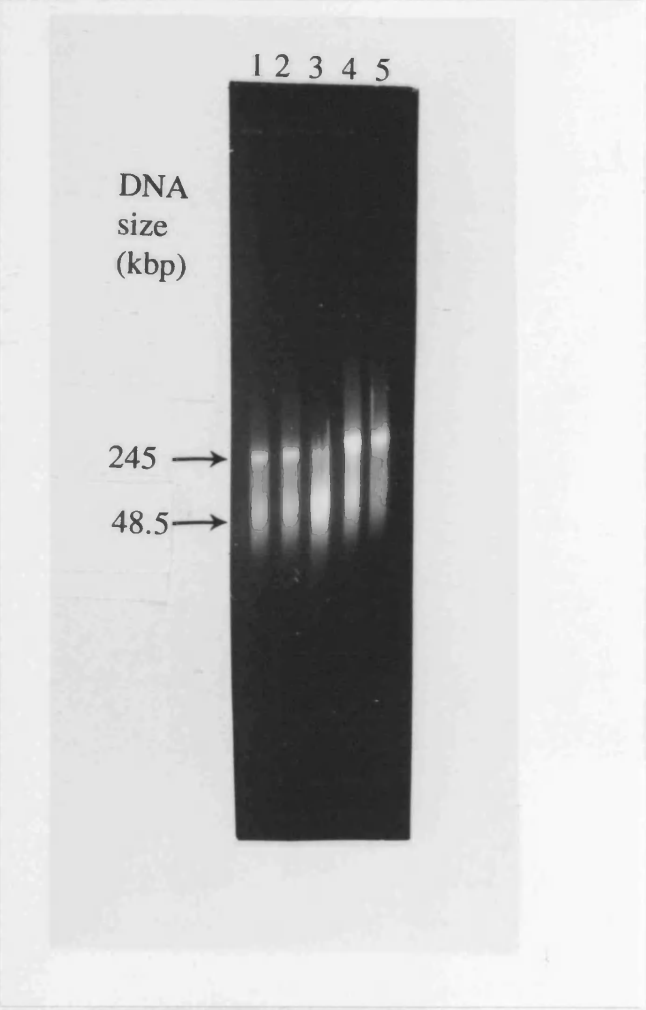

Figure 4.6 The effect of TLCK on Mg^{2+}-dependent DNA cleavage

Rat liver nuclei were incubated with/without TLCK in the presence of 8mM Mg^{2+} for 60min. The reactions were terminated and aliquots were taken out for FIGE. The lanes (1-5) are as follows; 0, 10, 25, 50 and 100μM TLCK. No internucleosomal fragments were detected by CAGE (data not shown).

4.2.4. Effect of dithiothreitol on DCI and NEM inhibition of DNA cleavage

The results of the above studies clearly showed that DCI was a potent inhibitor of DNA cleavage and contrasted with the results of Weaver et al. (1993) who maintained that the Ca^{2+}/Mg^{2+} endonuclease activity of nuclei isolated from thymocytes and rat liver (data not shown) was not inhibited by DCI. However it should be noted that in the latter experiments the

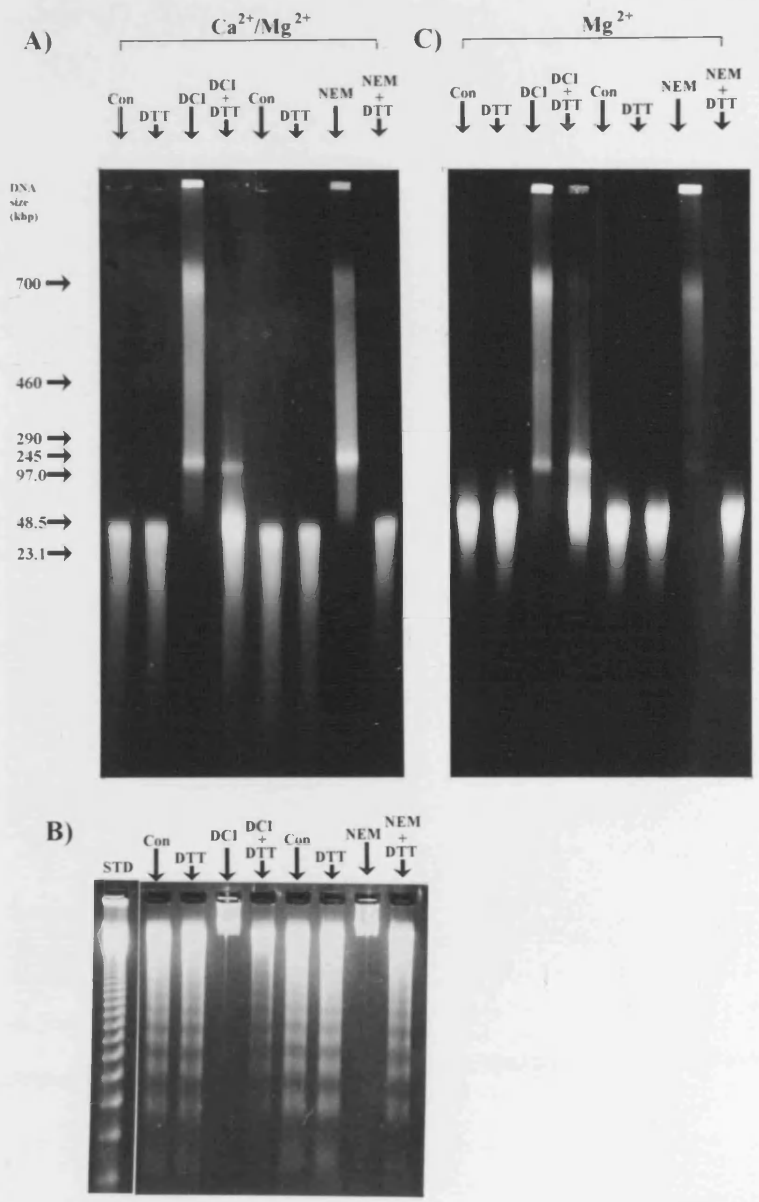

Figure 4.7 The effect of DTT on the inhibition of DNA cleavage by NEM and DCI

Nuclei activated with either 100μM Ca^{2+}/8mM Mg^{2+} for 30 min (A,B) or 8mM Mg^{2+} for 60min (C) and were inhibited with either 40μM NEM or 115μM DCI in the presence or absence of DTT (i.e. 500μM for DCI and 200μM for NEM). The reactions were terminated and DNA cleavage analysed by FIGE (A and C) and CAGE (B). The control lanes are from nuclei incubated with the appropriate cations, without any other additions. The remaining lanes are as the con lanes except that the nuclei have incubated with the indicated additions. The standards are not shown for the FIGE gels, although key sizes are labelled with arrows.

incubation buffer contained 0.2mM dithiothreitol (DTT) which has been shown to inactivate DCI and thereby prevent its inhibition of the proteolytic activity of the multi-proteinase complex (Djaballah et al., 1992). It was therefore possible that DTT could also block the effects of DCI on DNA cleavage and the experiments shown in Fig. 4.7 verify the hypothesis. Thus, incubation of nuclei with 100μM Ca^{2+}/8mM Mg^{2+} (Fig. 4.7A, con lane) for 30min/37°C produced a typical DNA ladder with a small amount of ≥30kbp large fragments. The same fragmentation pattern was obtained in the presence of 500μM dithiothreitol (DTT lane) demonstrating that this dithiol did not effect the fragmentation process. DCI (115μM) blocked the internucleosomal cleavage (Fig. 4.7B) and resulted in most of the DNA being retained in the sample well of the FIGE gel with only a small amount of the chromatin degraded into ≥700 and 200-250kbp fragments. Co-incubation of DTT with DCI essentially blocked the inhibitory effect of DCI on the internucleosomal cleavage and large fragment formation. DTT (200μM) also blocked the inhibitory effect of NEM (Fig. 4.7A,B) which is a potent thiol reagent. The blocking affect of DTT on the inhibitory effects of DCI and NEM on large fragment formation were also observed in nuclei activated with 8mM Mg^{2+} (Fig. 4.7C).

4.3 Discussion

In this study, a variety of compounds with widely different structures have been shown to inhibit both Mg^{2+} and Ca^{2+}/Mg^{2+} dependent DNA cleavage reactions. Although the compounds in this study have little or no structural relationships, it is clear that the inhibitory effects produced by all these compounds were remarkably similar. Thus, increased inhibition was always correlated with a sequential, step-wise increase in the size of the DNA fragments and in many respects the size distribution pattern was the exact opposite of that produced by the normal step-wise degradation process which have been described for thymocytes and rat liver nuclei (Walker et al.,1991; Sun and Cohen, 1994; Walker et al., 1994). The latter studies suggested that DNA cleavage is an ordered and step-wise process which progressively reduces the size of the DNA into its constituent higher order structural components. The inhibitor studies support this conclusion and lend support to the hypothesis that the sizes of the large fragments are similar to the 'loops' (30-50 kbp), which have been suggested by Filipski et al. (1990) to be essential components of higher order chromatin structure. It is therefore possible that the DNA cleavage patterns which are seen in these inhibitor studies are results of these compounds blocking the degradation process at the various stages in the unravelling of the

DNA. This would suggest that the various stages of degradation are catalysed by different enzymes and Weaver et al. (1993) have reported that in thymocytes treated with dexamethasone, DCI will block internucleosomal cleavage but not the large fragment formation or the morphological signs of apoptosis. Furthermore, Walker et al. (1994) have reported that in liver nuclei, DCI will block DNA laddering but not the large fragment formation. These results have been interpreted as evidence that proteases are involved in internucleosomal cleavage but not large fragment formation. The results presented here, however do not support this concept and the data in Figs 4.3 and 4.5 clearly show that DCI will inhibit large fragment formation whether stimulated by Ca^{2+}/Mg^{2+} or Mg^{2+} alone . Furthermore, the ISEL data show that the sensitivity of both these cation stimulated processes is the same.

The identity of the enzyme(s) which cleave DNA during apoptosis is as yet unknown and as reviewed by Peitsch et al. (1994), various candidates have been put forward. These include; NUC-18 (M_r 18 kDa) which requires Ca^{2+}/Mg^{2+} for activity and has recently been shown by Montague et al. (1994) to have considerable homology with the cyclophilin; DNase I (M_r 32-37kDa) which requires Ca^{2+}/Mg^{2+} or Mn^{2+} for activity; DNase II (M_r 29kDa) which does not require cations for its activity. The data presented in this and the previous chapter provide evidence for either a Mg^{2+} dependent enzyme whose activity is markedly altered and stimulated in the presence of Ca^{2+}, or for two (or more) enzymes, one (or group) catalysing the large fragment formation and the other, the internucleosomal cleavage. If there were separate enzymes it is likely that they would show differential sensitivity to inhibitors. However, the findings described in this chapter demonstrate that Cd^{2+}, Hg^{2+}, NEM and DCI were equally effective at inhibiting the Mg^{2+} and Ca^{2+}/Mg^{2+} activated DNA cleavage. Only TPCK appeared to have differential effects in that it was slightly more potent at inhibiting the Mg^{2+} process. But even in this case the maximum inhibition of approximately 50% was much less than that produced by DCI or NEM which gave 80-100% inhibition. Therefore these results suggests that both Mg^{2+} and Ca^{2+}/Mg^{2+} activities are catalysed by the same endonuclease enzyme.

Both the Mg^{2+} and Ca^{2+}/Mg^{2+} activated DNA cleavage were inhibited by Cd^{2+} and Hg^{2+} which are noted for their affinity for -SH groups (Vallee and Ulmer, 1972). It is therefore likely that they are targeting a critical thiol group(s) on the endonuclease. DNA cleavage was also blocked by concentrations of DCI which are similar to the levels used for inhibiting serine

proteases (Powers and Harper, 1986) and would suggest that the most likely target was a protease. However, TLCK a trypsin like serine protease inhibitor did not inhibit DNA degradation and TPCK a chymotrypsin like serine protease inhibitor was a weak inhibitor of the Mg^{2+} dependent DNA fragmentation. DCI is believed to be a general serine protease inhibitor in that it inhibits both chymotrypsin and trypsin like proteases (Harpers et al.,1985). Furthermore, recent studies have shown that DCI will also inhibit calpain I, a thiol protease (Foreman et al., 1993) and the finding that DTT inactivates the inhibitor (Djaballah et al., 1992) suggests that DCI reacts with sulphydryl groups. It is therefore significant that NEM which is well known for its reactivity towards thiol (Riordan and Vallee, 1972; Jocelyn, 1987) was also a potent inhibitor of DNA fragmentation. Furthermore, co-incubation with DTT blocked the inhibitory effects of NEM and also those of DCI. The protective effect of DTT suggests that DCI and NEM were reacting with a thiol and I have also found that diamide (data not shown) which oxidises protein-SH groups to disulphides (Kosower and Kosower,1987) also protects against the inhibitory effects of these compounds. These results, coupled with the findings with Cd^{2+} and Hg^{2+} which are classical sulphydryl inhibitors, strongly suggest that a critical thiol is involved in the DNA fragmentation process. The thiol group may be located on the endonuclease itself as Nikonova et al. (1993) have reported that three nucleases extracted from thymocyte nuclei were inhibited by NEM and iodoacetamide. Also Ribeiro and Carson (1993) have described the purification of a Ca^{2+}/Mg^{2+} endonuclease from human spleen, which was partially inhibited by NEM. Alternatively, the sensitive thiol group may be located on a protease. There is some confusion and contradiction as to the precise effects of protease inhibitors and it is likely that more than one protease is involved. In this respect, it is of interest that Motizuki et al. (1984) have reported the purification of a thiol protease from rat liver nuclei which was activated by dithiothreitol and inhibited by iodoacetamide.

It is also significant that calpain which is a ubiquitous thiol protease is activated by low concentrations of Ca^{2+} (3μM) and hydrolyses nuclear matrix proteins (Mellgren et al., 1993). However the proteolytic action of calpain is abolished if the nuclear DNA has been removed by DNase I. Conversely, adding back DNA to DNase I treated nuclei restores the proteolytic action of calpain. These studies suggest that there may be proteases which require DNA for activity and hence may have an active role in DNA cleavage. It is therefore possible that thiol proteases either in the nucleus or alternatively after migration from the cytoplasm are directly

involved in the constitutive endonuclease activity which is responsible for DNA fragmentation. In this respect it is of interest that DCI has been shown to inhibit calpain I (Foreman et al., 1993), however I have found that both calpain inhibitor I (N- Ac-Leu-Leu-norleucinal) and calpain inhibitor II (N-Ac-Leu-Leu-normethioninal) did not inhibit either Mg^{2+}or Ca^{2+}/Mg^{2+} activated DNA cleavage in rat liver nuclei.

The results of this study provide evidence that DCI and NEM may be targeting a critical thiol group which is essential for endonuclease activity and suggests that these compounds will be useful probes for further investigating this important element of the apoptotic process.

SECTION II

4.4 Results

4.4.1 Mn^{2+} activates 'large fragment' formation and internucleosomal DNA cleavage in rat liver nuclei

Nuclei incubated with low concentrations of Mn^{2+} (10-50μM) for 1 hour did not exhibit DNA cleavage (Figure 4.8A, lanes 1-3 respectively). However, when nuclei were treated with 100μM Mn^{2+} (Figure 4.8A, lane 4), the DNA was cleaved into mostly ≥700 kbp sized fragments and with 200μM Mn^{2+} (Figure 4.8A, lane 5), DNA cleavage was more extensive as shown by the appearance of 200-300kbp fragments. At 400μM Mn^{2+} the DNA was further cleaved into predominantly 30-50kbp fragments (lane 6). Concentrations of Mn^{2+} up to 400μM (Figure 4.8B, lanes 1-6) did not induce any internucleosomal DNA cleavage as detected by conventional agarose gel electrophoresis. However, when nuclei were incubated with 800 and 1000μM Mn^{2+} the DNA was further degraded into mostly <30kbp sized fragments (Figure 4.8A, lanes 7 and 8) and also into mono-/oligonucleosomes which gave a characteristic 'DNA ladder' (Figure 4.8B, lanes 7-8).

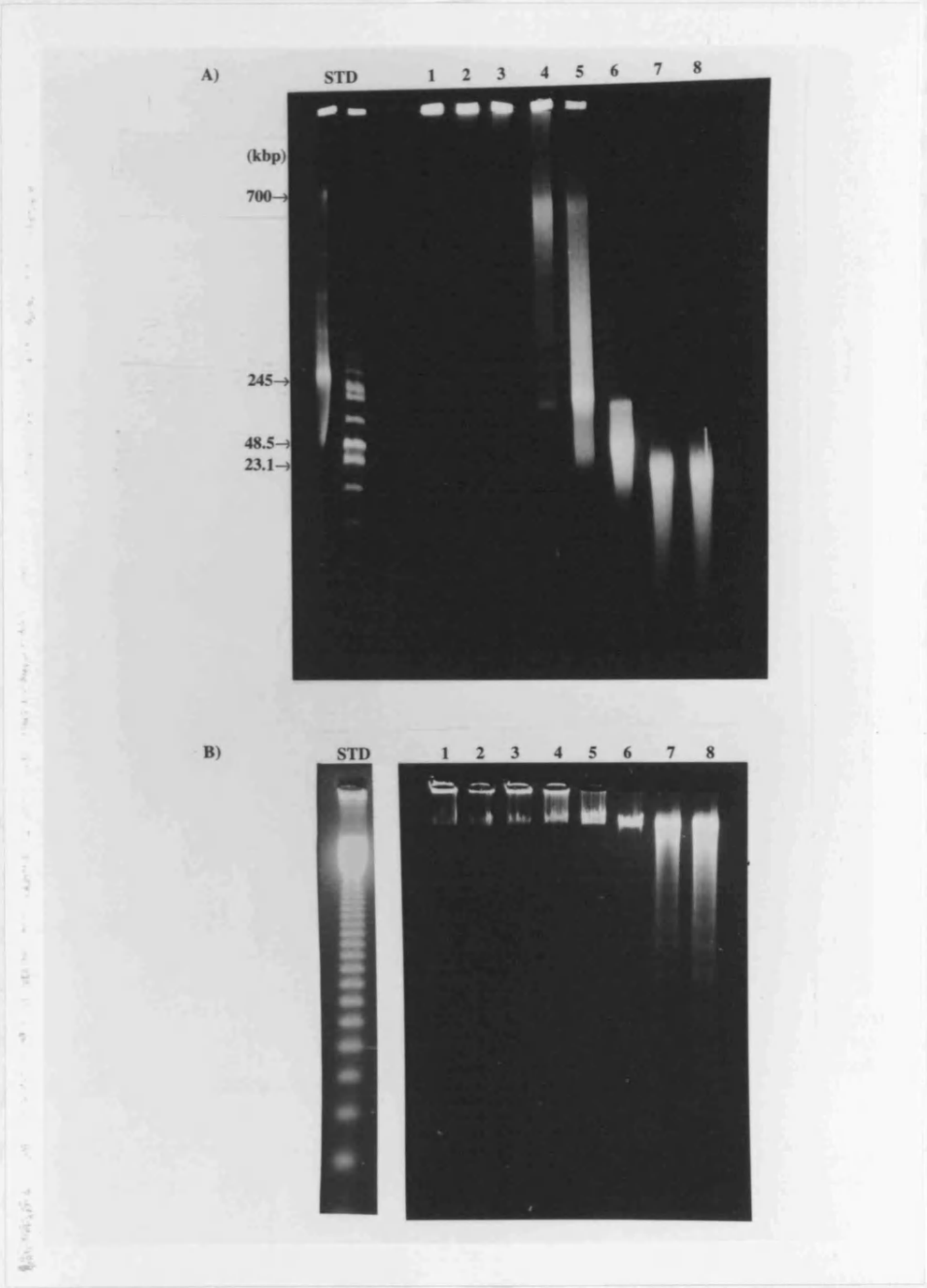

Figure 4.8 Mn^{2+} dependent DNA cleavage in rat liver nuclei

Rat liver nuclei were isolated and incubated for 1 hour with a range of Mn^{2+} concentrations and the DNA cleavage analysed by A) FIGE and B) CAGE as described in the Methods. In the FIGE gels the STD lanes contain *S. cerevisiae* chromosome standards and 0.1-200 kbp standards, respectively with the sizes indicated by the arrows. The remaining lanes (1-8) show the DNA size profiles from nuclei incubated with 10, 25, 50, 100, 200, 400, 800 and 1000μM Mn^{2+} respectively. In the conventional agarose gel the STD lane contains markers of 123bp or multiples thereof and the remaining lanes (1-8) are as described for the FIGE gel.

4.4.2 Time course of Mn^{2+} dependent DNA cleavage

As shown above, Mn^{2+} induced DNA cleavage in a concentration dependent manner and from this experiment it appeared that lower concentrations of Mn^{2+} only activated the 'large fragment' formation. This possibility was investigated further by following the time course for DNA cleavage using 100 and 200μM Mn^{2+} which did not induce internucleosomal cleavage in rat liver nuclei after a 1 hour incubation (Figure 4.8). Figure 4.9A shows that when nuclei were incubated with 100μM Mn^{2+} over 4 hours there was a progressive but limited cleavage of the DNA into predominantly 200-300kbp fragments. With 200μM Mn^{2+} (Figure 4.9C), cleavage was more extensive and over the 4 hour time period the DNA was further reduced in size to 30-50 kbp fragments. Internucleosomal cleavage was not observed with either 100 or 200μM Mn^{2+} (Figure 4.9B&D). In this respect the results with low concentrations of Mn^{2+} (i.e. 100 and 200 μM) over a 4 hour incubation were similar to the results which showed that 8mM Mg^{2+} stimulated the formation of 'large fragments' (chapter 3). However, Mn^{2+} is approximately 40-fold more potent than Mg^{2+} as only 200μM Mn^{2+} was required to give the same degree of DNA cleavage.

Treatment of nuclei with 400μM Mn^{2+} produced a different pattern of cleavage and after an hour incubation the DNA was cleaved into 200-300kbp and 30-50kbp fragments (Figures 4.8 and 4.10) without internucleosomal cleavage. After 2 hours most of the larger fragments were reduced in size to 30-50kbp fragments (Figure 4.10A) and a small amount of internucleosomal cleavage (Figure 4.10B) was detected. At 3 hours there was increased 'DNA laddering' (Figure 4.10B) and a further reduction in the size of the large fragments to >30kbp (Figure 4.10A). Finally, by 4 hours only a small amount of the 'large fragments' was detected as most of the DNA at this stage was now degraded to mono-/oligonucleosomes (Figure 4.10B).

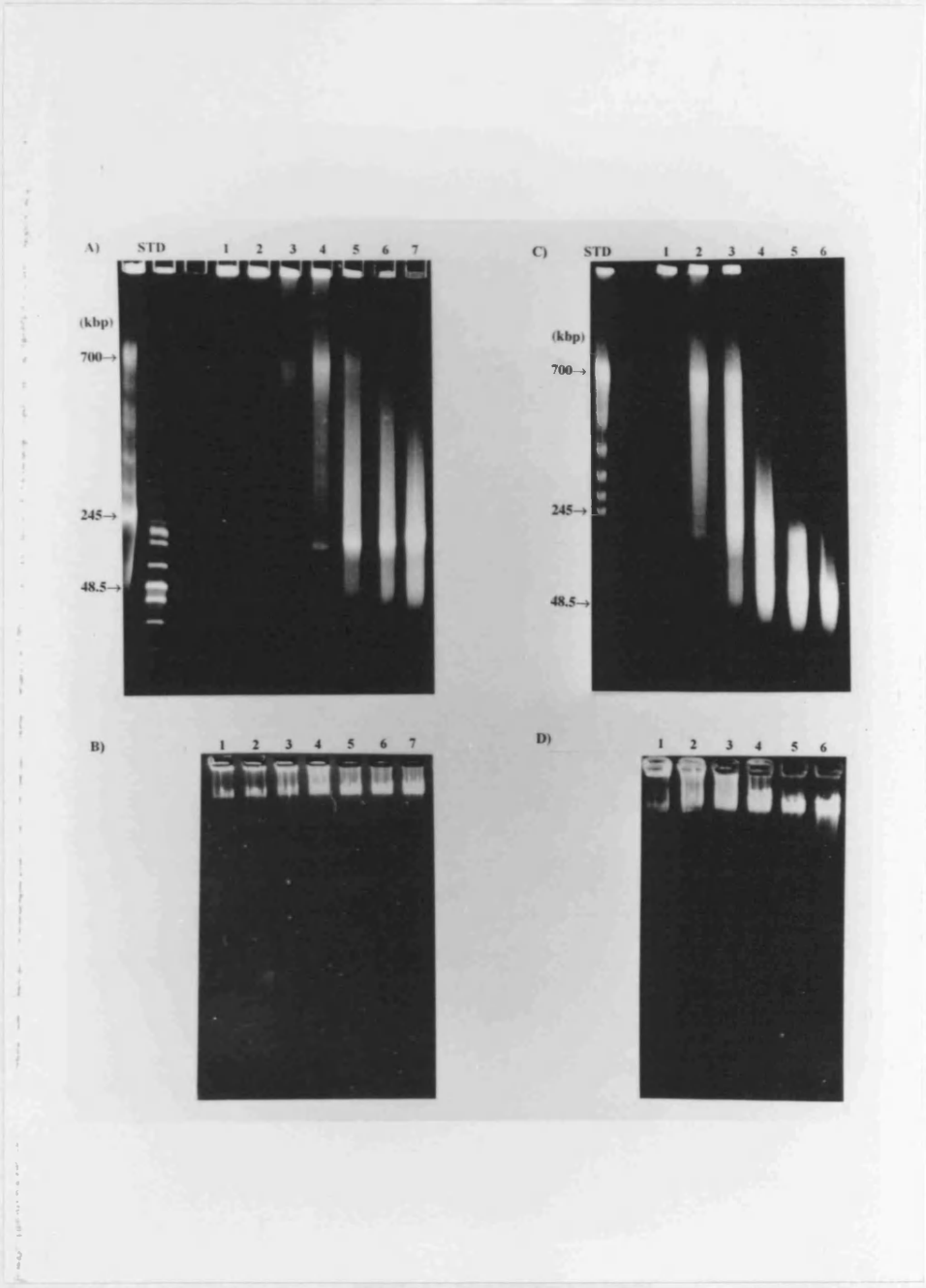

Figure 4.9 Time course of DNA cleavage in rat liver nuclei activated with 100μM and 200μM Mn^{2+}

Rat liver nuclei were prepared and incubated at 37°C for 0-4 hours with 100μM and 200μM Mn^{2+}. At the indicated times, the reactions were terminated and the DNA fragmentation patterns were determined by FIGE (A and C) and CAGE (B and D). STD lanes are indicated as described in Figure 4.8. In A) and B) lanes 1 and 2 show the DNA cleavage patterns from control nuclei incubated for 0 and 4 hour respectively without Mn^{2+}. Lanes 3-7 show the cleavage of DNA when the nuclei were incubated with 100μM Mn^{2+} for 30min, 1, 2, 3 and 4 hours respectively. In panels C) & D) lane 1 is DNA from nuclei incubated without Mn^{2+} for 4 hours and lanes 2-6 are from nuclei incubated with 200μM Mn^{2+} for 30 min, 1 ,2, 3 and 4 hours respectively.

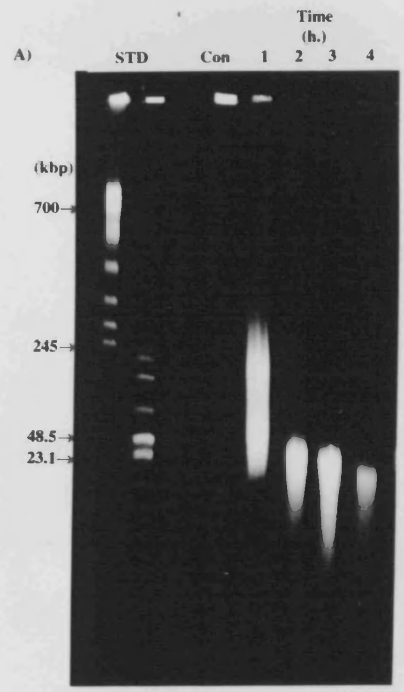

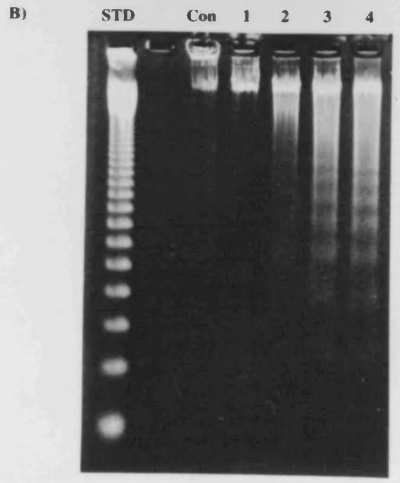

Figure 4.10 Time course of DNA cleavage in rat liver nuclei activated with 400μM Mn^{2+}

Rat liver nuclei were prepared and incubated at 37°C for 0-4 hours with 400μM Mn^{2+}. At the indicated times, the reactions were terminated and the DNA fragmentation patterns of the treated nuclei were analysed by FIGE (A) and CAGE (B). The standards (STD) used were as described in the legend to Figure 4.8. Con refers to nuclei incubated for 4 hours without Mn^{2+} and the remaining lanes for nuclei incubated with 400μM Mn^{2+} for the indicated times.

4.4.3 Mn^{2+} activated cleavage of DNA into 'large fragments' and mono-oligonucleosomes is inhibited by Zn^{2+}

Zn^{2+} is an inhibitor of the Ca^{2+}/Mg^{2+} endonuclease involved in internucleosomal fragmentation (Cohen and Duke, 1984) and recent work has demonstrated that Zn^{2+} also partly inhibits the formation of 'large fragments' and mono/oligonucleosomes in isolated nuclei (Cohen et al., 1994; Zhivotovsky et al., 1994). These findings were confirmed and extended in the present study and Figure 4.11 A (lanes 1 and 2) shows that 8mM Mg^{2+} induced DNA cleavage into 30-50kbp was blocked by 400μM Zn^{2+} and the DNA was only cleaved into 200-250kbp DNA fragments. This concentration of Zn^{2+} also inhibited DNA laddering induced by 100μM Ca^{2+} and 8mM Mg^{2+} and resulted in an increase in the size of the large fragments from ≤30 to 30-50kbp (Fig. 4.11A and B, lanes 3 & 4 respectively). Zn^{2+} thus completely inhibits DNA laddering but only partially blocks the formation of large fragments and this suggests that the latter is resistant to the effects of this cation. However, when a lower concentration of Mg^{2+} (4mM) was used to stimulate DNA cleavage into only 700 and 200-250kbp fragments (Fig. 4.11C) and using a higher concentration of Zn^{2+} (1000μM), it was possible to inhibit the cleavage of the DNA into both the 700kbp and 200-250kbp (Fig. 4.11 C, lanes 1 and 2 respectively).

Furthermore, Zn^{2+} was also a potent inhibitor of Mn^{2+} activated DNA cleavage as shown in Figure 4.12. Incubation of control (no Zn^{2+}) rat liver nuclei for 1hour with 400μM Mn^{2+} resulted in cleavage of the DNA to 200-300kbp and 30-50kbp fragments (Figure 4.12A, lane 1) without internucleosomal cleavage. However, in the presence of 250μM Zn^{2+} (Figure 4.12A, lane 2) most of the DNA was intact and remained at the origin of the gel. The cleaved DNA was resolved mainly as ≥700kbp fragments but there was a small amount of cleavage to 200-300kbp fragments. Incubation with 500 and 1000μM Zn^{2+} (Figure 4.12A, lanes 3 and 4) produced an even more pronounced inhibition and only a small amount of the DNA was cleaved to the ≥700kbp sized fragments. Furthermore, when 200μM Mn^{2+} was used (data not shown) to activate the endonuclease(s), Zn^{2+} totally inhibited the cleavage of DNA into ≥700 kbp.

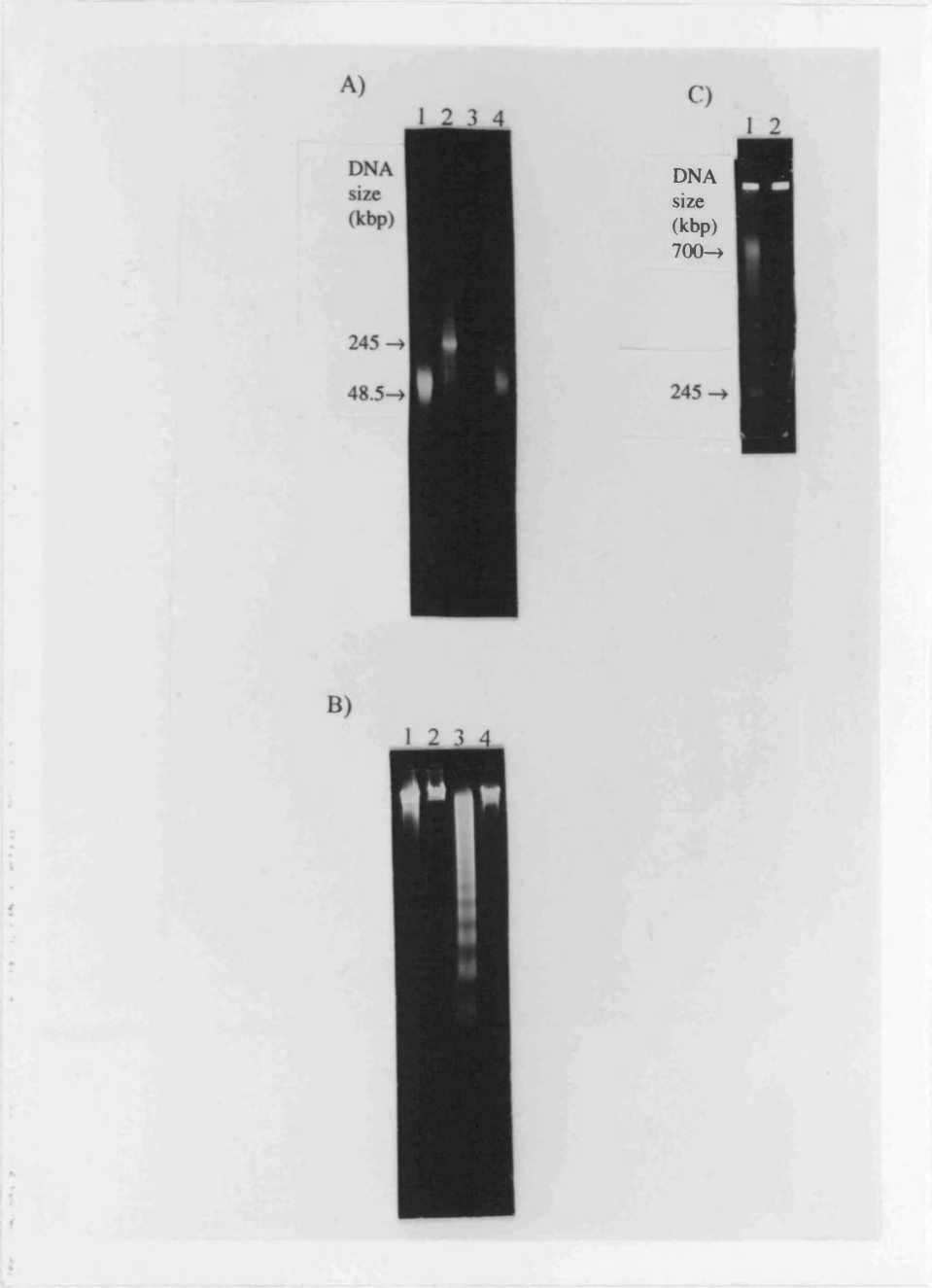

Figure 4.11 Inhibition of Mg^{2+} and Ca^{2+}/Mg^{2+} dependent DNA cleavage by Zn^{2+}

Rat liver nuclei were incubated at 37°C for 1hour in the presence of 8mM Mg^{2+} with or without 100μM Ca^{2+} (panel A and B) and whereas panel C is incubation of nuclei with 4mM Mg^{2+}. Either 400μM Zn^{2+} (panel A and B) or 1000μM Zn^{2+} (panel C) were used to inhibit DNA cleavage. Reactions were terminated and DNA analysed by FIGE (panel A and C) and CAGE (panel B). In panel A and B, the lanes are as follows; lanes 1 and 2 are nuclei with 8mM Mg^{2+} in the presence of 0 and 400μM Zn^{2+} respectively; lanes 3 and 4 are nuclei with 100μM Ca^{2+}/8mM Mg^{2+} in the presence of 0 and 400μM Zn^{2+} respectively. In panel C, lanes 1 and 2 are with 4mM Mg^{2+} in the presence of 0 and 1000μM Zn^{2+} respectively.

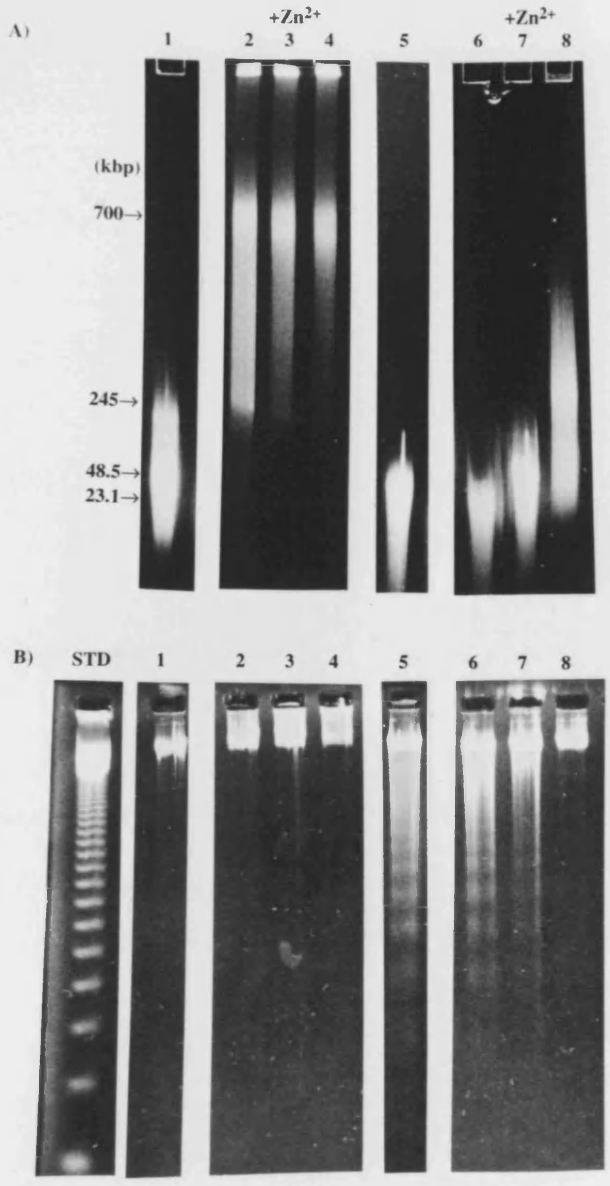

Figure 4.12 Zn^{2+} inhibition of Mn^{2+}-activated DNA cleavage

Rat liver nuclei were incubated at 37°C for 1 hour with various additions and the reactions terminated. DNA cleavage was analysed by FIGE (A) and CAGE (B) as described in the methods. Lanes 1-4 and 5-8 were from nuclei incubated with 400μM and 1000μM Mn^{2+} respectively, and co-treated with 0, 250, 500 and 1000μM Zn^{2+} (lanes 1-4 and 5-8 respectively). In the FIGE gel the kbp sizes are indicated by arrows and in the CAGE, the STD lane refers to markers of 123bp or multiples thereof.

When nuclei were incubated with 1mM Mn^{2+} the DNA was cleaved into ≤30kbp fragments and was accompanied by extensive internucleosomal cleavage (Figure 4.12, lane 5) which was inhibited by Zn^{2+}. Thus, 250μM Zn^{2+} (Figure 4.12, lane 6) slightly inhibited 'DNA laddering' whilst 500μM Zn^{2+} (lane 7) produced a greater inhibition of internucleosomal cleavage coupled with a corresponding increase in the size of the large fragments from ≤30 to 30-50kbp. At 1mM Zn^{2+} (lane 8) internucleosomal cleavage was completely blocked and was accompanied by the appearance of 200-300kbp fragments in the FIGE gel, but neither the ≥700kbp fragments or intact DNA was detected. On the basis of the FIGE and CAGE experiments it would appear that DNA cleavage activated by high concentrations of Mn^{2+} was less sensitive to Zn^{2+} inhibition.

4.4.4 DCI and NEM inhibit multi-step DNA cleavage induced by Mn^{2+}

NEM and DCI are equally effective at inhibiting both the Mg^{2+} and Ca^{2+}/Mg^{2+} dependent DNA cleavage reactions in rat liver nuclei as shown in section I (this chapter). These inhibitors also proved to be active against Mn^{2+}-induced cleavage as shown in Figure 4.13. Thus, with 1mM Mn^{2+}, the DNA of control nuclei (lane 1) was cleaved to ≤30kbp fragments and mono/oligonucleosomes, and 50μM NEM blocked internucleosomal cleavage with concomitant appearance of large (≥700kbp) fragments and intact DNA in the FIGE gel. At 100μM NEM, DNA cleavage was almost totally inhibited with most of the DNA remaining intact and in the well of the gel (Figure 4.13A, lane 3), although some of the DNA was still cleaved to ≥700kbp fragments. A similar result was obtained with 100μM and 150μM DCI in which increasing inhibition was accompanied by abolition of DNA laddering and the appearance of intact DNA at the origin of the FIGE gel (Figure 4.13 A,B, lanes 4 and 5). In other experiments (results not shown) when 200μM Mn^{2+} was used to activate cleavage, it was found that NEM and DCI completely blocked DNA cleavage.

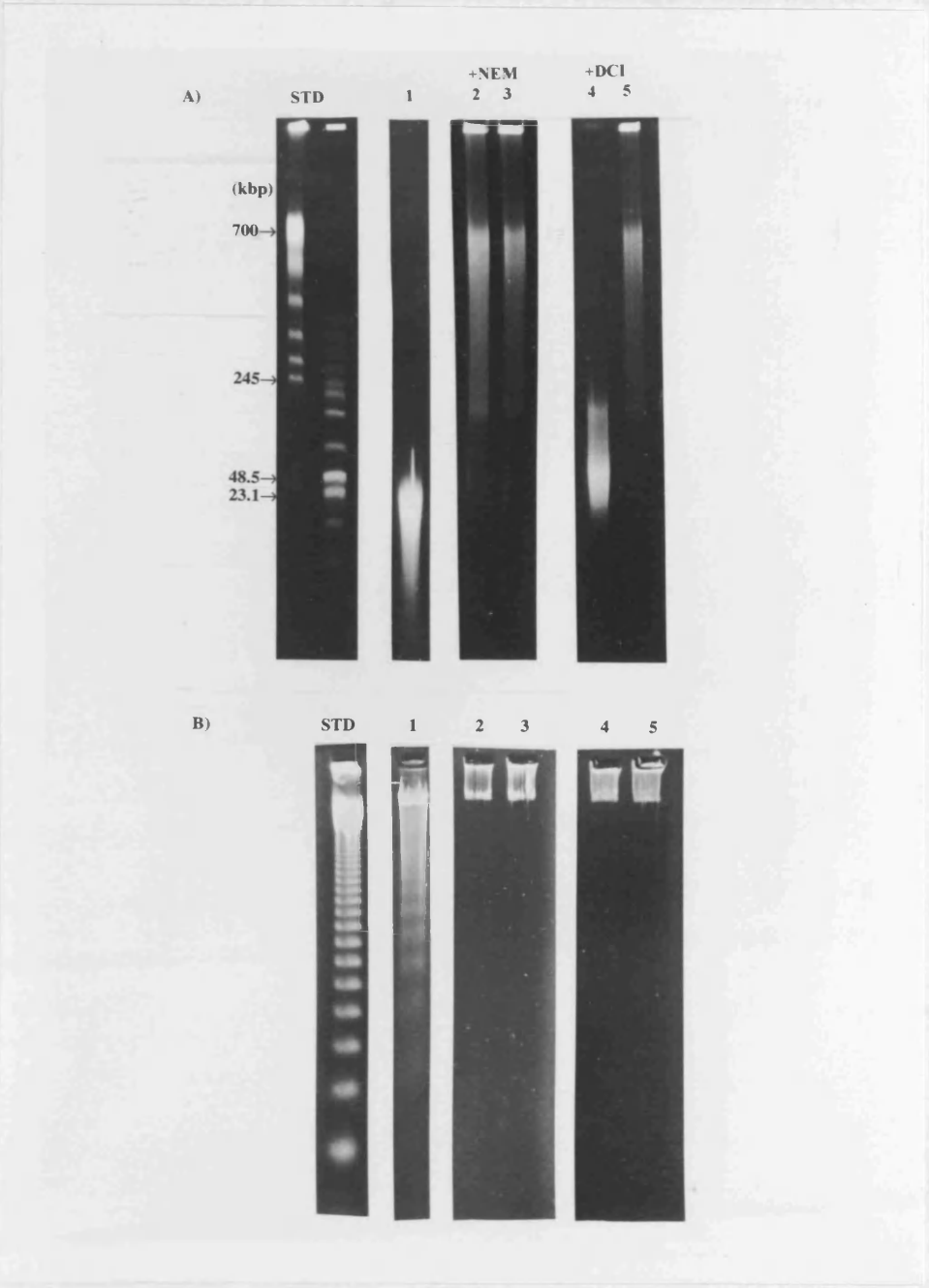

Figure 4.13 Inhibition of Mn^{2+}-activated DNA cleavage by DCI and NEM

NEM and DCI were incubated with rat liver nuclei in the presence of 1000μM Mn^{2+} for 1hour. The reactions were then terminated and the nuclei analysed by FIGE (A) and CAGE (B) as described in the methods. STD lanes are as described for Figure 4.8 and lane 1 is DNA from the control nuclei incubated without inhibitor. Lanes 2 and 3 shows the DNA cleavage in nuclei treated with 50 and 100μM NEM respectively, and lanes 4 and 5 are for the nuclei treated with 100 and 150μM DCI respectively.

4.4.5 Mn^{2+} induces high levels of ISEL in rat liver nuclei

DNA cleavage induced by Mg^{2+} and Ca^{2+}/Mg^{2+} in nuclei can be quantified using ISEL (chapter 3) and this method was used to compare the effects of Mn^{2+} with those produced by Mg^{2+} and Ca^{2+}/Mg^{2+}. Typical cytograms are shown in Figure 4.14, with the x-axis denoting the DNA content (PI, red fluorescence) and the z-axis showing the amount of ISEL (anti-digoxigenin labelling, green fluorescence) which as discussed in chapter 3 is a measure of DNA strand breakage.

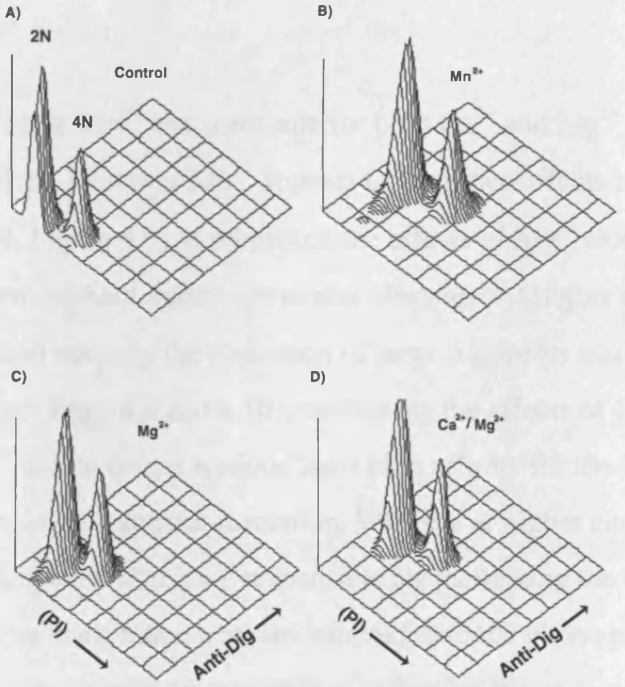

Figure 4.14 Flow cytometric detection of DNA fragmentation in isolated rat liver nuclei using *in situ* end labelling (ISEL)

Rat liver nuclei were isolated as described in the methods and then incubated as indicated i.e., A) 1 hour control with no added cations; B) as A) but the addition of 1000μM Mn^{2+}, C) as A) but with the addition of 8mM Mg^{2+}; D) as A) but with the addition of 100μM Ca^{2+} and 8mM Mg^{2+}. The reactions were then terminated and the DNA strand breakage assayed by ISEL and flow cytometry as described in the methods section. The figure shows the data represented as 3D cytograms with relative propidium iodide fluorescence (DNA content) and green fluorescence (anti-Dig) plotted as indicated. The cytograms show two peaks which correspond to the 2N and 4N nuclei.

Figure 4.14A shows the cytogram of control nuclei incubated for 1 hour in the absence of any divalent cations and the level of ISEL is very low in both the diploid (2N) and tetraploid (4N) nuclei. However, the addition of 1mM Mn^{2+} (Figure 4.14B) caused a marked increase in ISEL in both the 2N and 4N nuclei populations. Note that as in the previous experiments

(chapter 3) all the nuclei are affected when treated with a particular cation. This high level of ISEL is consistent with the gel electrophoresis studies shown in Figure 4.8 which demonstrated that 1mM Mn^{2+} produced extensive internucleosomal cleavage (many DNA strand breaks). In comparison, 8mM Mg^{2+} (Figure 4.14C) produced a small but significant increase in ISEL which is in agreement with studies in the previous chapter (chapter 3) which showed that in this situation the end-labelling is measuring the formation of 'large fragments'. In contrast, incubation of liver nuclei with both 100μM Ca^{2+} and 8mM Mg^{2+} (Figure 4.14D) resulted in a large increase in end-labelling comparable to that produced by Mn^{2+} alone and was due to extensive internucleosomal cleavage.

4.5 Discussion

This study shows that Mn^{2+} can substitute for both Ca^{2+} and Mg^{2+} in a concentration dependent manner (Fig.4.8). However Mn^{2+} appears to have two effects in that at low concentrations (≤200μM, Figure 4.9), it mimicked the effects of Mg^{2+} alone by stimulating 'large fragment' formation without internucleosomal cleavage. At higher concentrations (≥400μM), Mn^{2+} facilitated not only the formation of large fragments but also stimulated internucleosomal cleavage (Figs. 4.8 and 4.10), mimicking the effects of Ca^{2+}/Mg^{2+}. These results suggest that Mn^{2+} at low concentrations has a high affinity for the Mg^{2+} binding sites which are responsible for large fragment formation. Whereas at higher concentration, Mn^{2+} binds to those Ca^{2+} binding sites which are responsible for facilitating the formation of large fragments and also to those sites which activate internucleosomal cleavage. Thus, Mn^{2+} depending on the concentration used was capable of activating the endonuclease(s) responsible for multi-step DNA cleavage.

The effects of Zn^{2+} on the apoptotic process were described by Cohen and Duke (1984) who showed that DNA laddering was inhibited by Zn^{2+}. Later studies (Cohen at al., 1992; Barbieri et al., 1992) demonstrated in thymocytes , that although Zn^{2+} blocked internucleosomal cleavage it did not inhibit some of the morphological features of dexamethasone induced apoptosis. Moreover, in these thymocytes the DNA was still cleaved into large fragments (Brown et al., 1993) suggesting that this process was not inhibited by Zn^{2+} and studies by Walker et al (1994) have shown that the Mg^{2+} dependent endonucleolytic activity in nuclei isolated from liver, thymocytes, HL60 and IL2-dependent CTLL cells is apparently insensitive to Zn^{2+}.

The different cleavage patterns which are produced by the different cations raises the possibility that there are cation specific endonucleases and in this respect, Walker et al. (1995) have proposed that the initial Mg^{2+}-dependent cleavage of DNA occurs at rare sites which are spaced at 300-1000kbp intervals and insensitive to Zn^{2+}. This suggests that the enzyme catalysing this step is a separate endonuclease. However, my results now provide evidence that all the steps involved in the cleavage of DNA to oligonucleosomes are susceptible to Zn^{2+}. Thus, with Mn^{2+}-activated cleavage, Zn^{2+} inhibited the cleavage reactions responsible for degrading DNA to ≥700kbp→200-300kbp →30-50kbp fragments and also blocked internucleosomal cleavage (Figure 4.12). Only when high Mn^{2+}, Mg^{2+} or Ca^{2+}/Mg^{2+} concentrations were used was the cleavage of intact DNA to ≥700kbp fragments not inhibited by Zn^{2+} (or DCI and NEM). This is reminiscent of my previous studies presented in section I of this chapter which showed that on the basis of FIGE, DCI and NEM did not completely inhibit the formation of the ≥700kbp fragments when Ca^{2+}/Mg^{2+} were used to activate DNA cleavage. However, when Mg^{2+} alone or low Mn^{2+} were used it was possible to completely inhibit DNA cleavage with Zn^{2+}, DCI and NEM. When ISEL was used to quantify the inhibition of Mg^{2+}- and Ca^{2+}/Mg^{2+}-activated cleavage, it was found that the I_{50} values for DCI and NEM respectively for both cleavage processes were the same. Thus, the apparent insensitivity of the initial cleavage step to ≥700kbp to Zn^{2+} is only seen when there is a high rate of cleavage. The findings that Mn^{2+}, Mg^{2+} and Ca^{2+}/Mg^{2+} activated DNA cleavage have the same inhibitor sensitivity to Zn^{2+}, DCI and NEM supports the concept that Mn^{2+} is activating the same endonuclease(s) as Mg^{2+} and Ca^{2+}.

From these results it is possible to formulate a mechanism to explain DNA cleavage in isolated nuclei and this is shown in Figure 4.15. In this model, it is envisaged that there is a single/class of enzymes with multiple cation binding sites.

The extent, pattern and rate of cleavage is then determined by the species and concentration of the activating cation(s). Thus, one class of binding sites requires Mg^{2+} (or low Mn^{2+}) and activates the formation of 30-50kbp fragments but these binding sites do not stimulate internucleosomal cleavage activity (Figure 4.15A) and under these conditions DNA cleavage can be totally inhibited by Zn^{2+} or DCI or NEM. This type of DNA fragmentation

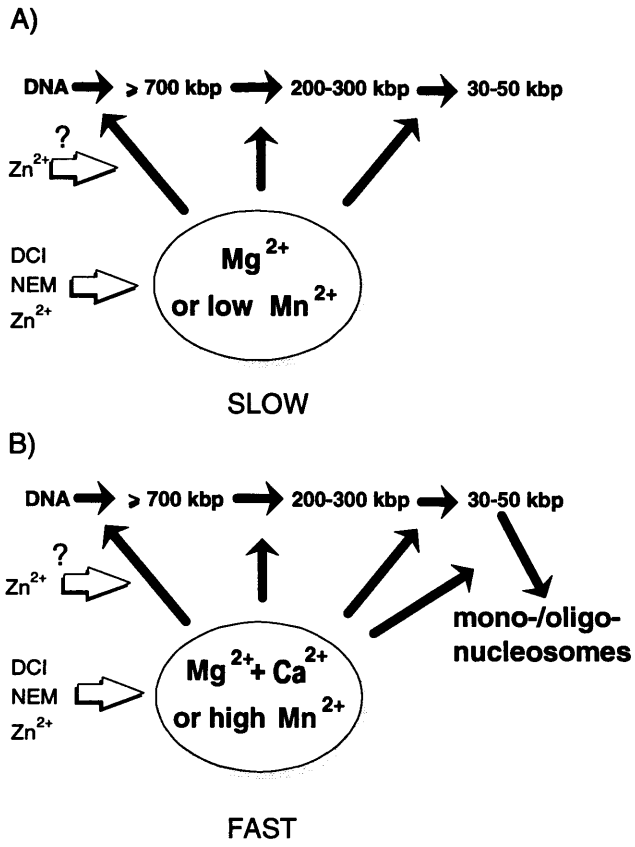

Figure 4.15 Scheme for DNA cleavage in isolated liver nuclei

In this scheme the endonucleases are represented as a single pool of enzymes capable of acting at all possible cleavage sites. This does not rule out the possibility that there are separate cation-specific enzymes.

requires a relatively small number of DNA strand breaks to cleave the DNA into 30-50kbp fragments and only a small increase in endonuclease activity is required. A second class of binding sites requires Ca^{2+} (or high Mn^{2+}) and with the Mg^{2+} sites facilitate the initial 'large fragment' formation and also stimulate the terminal internucleosomal steps (Figure 4.15B). DNA cleavage into 'large fragments' requires a lower endonucleolytic activity than is necessary for internucleosomal cleavage which requires many more strand breaks (250-fold, i.e., if 50kbp fragments were cleaved to 180-200bp nucleosomes). For this type of cleavage the enzymic activity is obviously much greater and it follows that this process will be very sensitive to inhibition as detected by conventional agarose gel electrophoresis. However, the cleavage of DNA into 'large fragments' requires fewer strand breaks and even if the Ca^{2+}/Mg^{2+} or high Mn^{2+} -dependent process were 95% inhibited, there would still be sufficient residual enzyme activity to cleave the DNA into 'large fragments' which would be detected by FIGE.

The actual mechanisms of multi-step DNA cleavage inhibition by DCI, NEM and Zn^{2+} are still far from being understood. Although apoptotic endonuclease(s) is a very likely target of these inhibitors, one could not ignore the possibility of these compounds inhibiting protease(s) that is required to either activate the endonuclease or alternatively degrade proteins that interact or inhibit the endonuclease or those rendering the DNA inaccessible to the nuclease (see Patel and Gores, 1995, for review). In this respect, Helgason et al. (1995) have demonstrated that proteinases are involved in initiating DNA fragmentation during CTL-mediated target cell killing. They showed that DCI significantly reduced the inhibition of DNA fragmentation by aurin tricarboxylic acid, an endonuclease inhibitor and suggested that one or more proteases is involved in the early stage of DNA fragmentation process, i.e. upstream of the endonuclease. In the same context, Kwo et al. (1995) demonstrated a twofold increase in nuclear serine like protease activity during bile acid induced apoptosis in hepatocytes accompanied by a 2.5 fold decrease in non-nuclear serine like protease activity, suggesting a translocation of of the protease from cytosol to the nucleus. Interestingly, Zn^{2+} inhibited this nuclear serine like protease activity.

The identity of the endonucleases is as yet unknown and several candidates have been proposed as the enzymes responsible for 'DNA laddering' (Compton, 1992; Peitsch et al., 1994). The mechanism of action and substrate specificity of one possible candidate, DNase 1 varies according to whether or not Mg^{2+}, Ca^{2+} or Mn^{2+} are the activating cations (Walker et al., 1995). The cation dependent cleavage reactions in isolated nuclei are consistent with this type of enzyme and it may be that the endonucleases involved in apoptosis are homologues of this enzyme.

4.6 SUMMARY

This chapter describes the use of several structurally unrelated compounds to inhibit the multi-step DNA cleavage and the results show that inhibition produces an increase in the size of the DNA fragments, from mono/oligonucleosomes to 30-50, 200-250, ≥700kbp and finally to intact DNA.The effects of two potent inhibitors used in this study, DCI and NEM were blocked by dithiothreitol, suggesting that a critical thiol(s) is involved in the DNA cleavage reactions. Further characterisation of the cationic requirement shows that Mn^{2+} can replace both Ca^{2+} and Mg^{2+} and produce a multi-step DNA cleavage and this is also inhibited by NEM and DCI. Furthermore Zn^{2+}, a putative endonuclease inhibitor blocked all the DNA

degradation processes. Using ISEL to determine if there is any preferential difference in the inhibitory effects of NEM and DCI showed that the compounds have similar I_{50}s for the Mg^{2+} dependent and Ca^{2+}/Mg^{2+} dependent processes. These results and the finding that Mn^{2+} dependent DNA cleavage can be blocked by Zn^{2+}, DCI and NEM suggests that the DNA cleavage is catalysed via a single endonuclease or a class of endonuclease(s) whose catalytic activity is modified when the appropriate cations are present.

5. Characterisation of TGF-β_1 induced apoptosis in primary hepatocytes culture

5.1 Introduction

Hepatocytes can die by either apoptosis or necrosis, in the latter case, cell death is accompanied by cell swelling, leakage of cell content, nuclear disintegration and an influx of inflammatory cells. In contrast, apoptosis is characterised by cell shrinkage, nuclear fragmentation, the formation of apoptotic bodies and a lack of inflammatory response. Apoptosis is rarely detected in the adult healthy liver, however upon treatment with cytokines or chemicals (e.g. TGF-β_1, anti-Fas/APO-1 antibody, cycloheximide), during liver regression or in certain clinical conditions (e.g. viral hepatitis), a significant increase in the percentage of apoptosis can be observed (Schulte-Hermann et al., 1995). As the liver is the largest internal organ of the body which performs a wide range of vital biochemical processes, the occurrence of uncontrolled apoptosis may cause impaired hepatic functions and this could lead to aberrations in other organ systems and ultimately to death as have been observed with Fas administration (Ogasawara et al., 1993). An insight into the mechanisms of apoptosis in hepatocytes may provide therapeutic strategies for amelioration of liver diseases.

Investigating the mechanisms underlying apoptosis in the liver *in vivo* is difficult as the duration of apoptosis in rat liver is only 3h (Bursch et al., 1990). This explains the relatively rare observation of apoptosis in histological sections even in states of considerable cell loss. Hepatocytes which are parenchymal cells of the liver occupy about 60% of this organ (Telford and Bridgman, 1995). Apoptosis can be induced in primary cultures of hepatocytes by a variety of compounds including staurosporine, a protein kinase C inhibitor (Sanchez et al., 1992; Cain et al., 1996a), growth inhibitors such as TNF-α (Shinagawa et al., 1991), Fas antibody (Ni et al., 1994) and TGF-β_1 (Oberhammer et al., 1992; 1993a). These compounds produce chromatin condensation and all except TGF-β_1 result in DNA cleavage and it is now recognised that during apoptosis the chromatin is degraded, initially into 200-300 and/or 30-50kbp fragments, prior to internucleosomal cleavage (Walker et al., 1991; Brown et al., 1993; Cohen et al., 1994; Oberhammer et al., 1993b). The 'large fragments' can be detected with field inversion gel electrophoresis (FIGE) and the small DNA fragments by conventional agarose gel electrophoresis (CAGE) as described in the previous chapters. Gel electrophoresis

techniques give an aggregate picture of all cells (i.e. gel profiles are a combination of both apoptotic and normal nuclei) and do not give quantitative information on the number of cells or the stages of apoptosis. Such information is normally obtained by staining the nuclei of the cells with the DNA binding dye (e.g., Hoechst 33258) and counting the normal (uncondensed chromatin) and apoptotic (condensed chromatin) nuclei (Oberhammer et al., 1992; Oberhammer et al., 1993a). Alternatively, apoptosis can be detected in individual cells by in situ tailing or end-labelling (ISEL) followed by conventional microscopy (Oberhammer et al., 1996). These methods (as does the dye-binding technique) require time consuming morphological analysis to give a quantitative assay of apoptosis.

In contrast, apoptosis in single cell suspension cultures can be more easily analysed by a combination of ISEL and flow cytometry as has been demonstrated for example by Gorczyca et al. (1992) with thymocytes and HL-60 cells. Unfortunately, these methods are not easily applied to monolayer cultures, where the cells first have to be detached from the substratum. In this respect, I have tried various techniques including mild collagenase treatment, to detach hepatocytes from the monolayer. However, the resulting cell suspensions were not suitable for flow cytometry and for this reason another approach was adopted which involved isolation of the nuclei, followed by detection of DNA strand breaks with ISEL. The enucleation technique, which uses a combination of citric acid and detergent, was optimised for hepatocyte cultures and was adapted from a method used by Otto (1990) for isolating nuclei from fixed tissue. DNA strand breaks were detected by ISEL and flow cytometry as described in the previous chapter for isolated rat liver nuclei. In addition, analysis of DNA cleavage by gel electrophoresis can be performed on the nuclei isolated by this enucleation technique. In this study the combined enucleation / end-labelling technique has been used to investigate TGF-$ß_1$ induced apoptosis in hepatocytes. The results showed that the method is both sensitive and quantitative. However, the ISEL method detected a greater number of cells which were undergoing apoptosis than were detected by the standard morphological method. This indicated that DNA strand breakage could be induced in the chromatin before overt condensation changes were detected. This was confirmed by examining the end-labelling nuclei with confocal microscopy, which showed that the nuclei with high levels of ISEL exhibited a wide range of morphologies. Some of these nuclei had an obvious apoptotic morphology while others had little or no chromatin condensation. Furthermore the confocal microscopy also showed that normal hepatocytes had a low but detectable level of DNA strand breakage which

progressively increased throughout the time of culture. The DNA cleavage process was markedly enhanced in TGF-$ß_1$ treated hepatocytes.

In contrast to a previous finding by Oberhammer et al. (1993a) that endonuclease activation is not associated with TGF-$ß_1$ induced apoptosis in hepatocytes, I have found that apoptosis in hepatocytes treated with this cytokine resulted in DNA cleavage similar to the multi-step pattern seen in rat liver nuclei discussed in the previous chapters. In order to further characterise the effects of TGF-$ß_1$ on hepatocytes, I have investigated two commonly used but unrelated compounds, cycloheximide and zinc diacetate (hereafter referred to as Zn^{2+}) which are known to modulate apoptosis. Cycloheximide, which is a protein synthesis inhibitor blocked all the features of apoptosis as assessed by morphology, FIGE, CAGE and ISEL. In contrast, Zn^{2+} a well known endonuclease inhibitor prevented the appearance of apoptotic nuclei as quantitated by morphology and ISEL but the gel electrophoresis profile showed inhibition of only the internucleosomal cleavage not the large fragments induced by TGF-$ß_1$.

Some of the results in this chapter have been published in the following publication;

Kelvin Cain, Salmaan H. Inayat-Hussain, Carole Couet, Hong-Min Qin and Franziska A Oberhammer (1996) A novel method for detecting apoptosis shows that hepatocytes undergo a time dependent increase in DNA cleavage and chromatin condensation which is augmented after TGF-$ß_1$ treatment. Cytometry 23;312-321

5.2 Results

5.2.1 TGF-$ß_1$ induced apoptosis in primary hepatocytes

In agreement with previous studies (Oberhammer et al., 1992), TGF-$ß_1$ was shown to be a potent inducer of apoptosis in primary hepatocytes. Figure 5.1A shows untreated hepatocytes in a high density culture incubated for 16h and then fixed and stained with a DNA binding dye, Hoescht 33258 (H33258). When hepatocytes were treated with 1ng/ml TGF-$ß_1$ for 16h and stained with H33258, the nuclear morphology of apoptosis was observed as shown by the arrows.

There is a range of morphologies seen, from the earlier chromatin condensation to apoptotic bodies. In order to confirm that there was no necrosis in TGF-$ß_1$ treated hepatocytes, the cultures were pre-treated with propidium iodide (PI) prior to staining with H33258 and the number of cells including PI (necrosis) counted. The results as shown in

A)

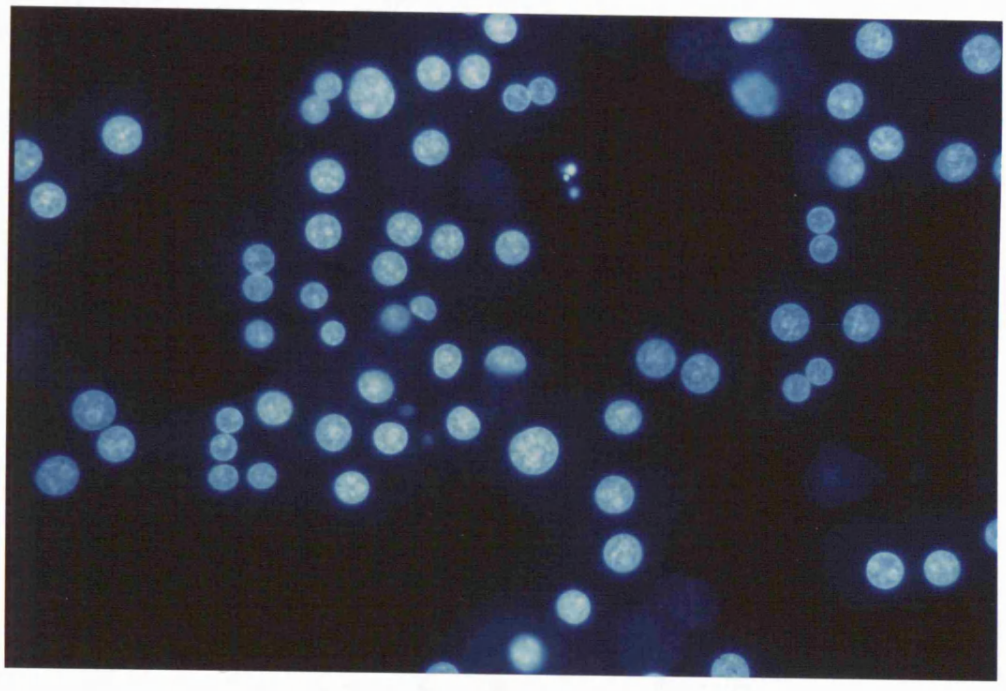

B)

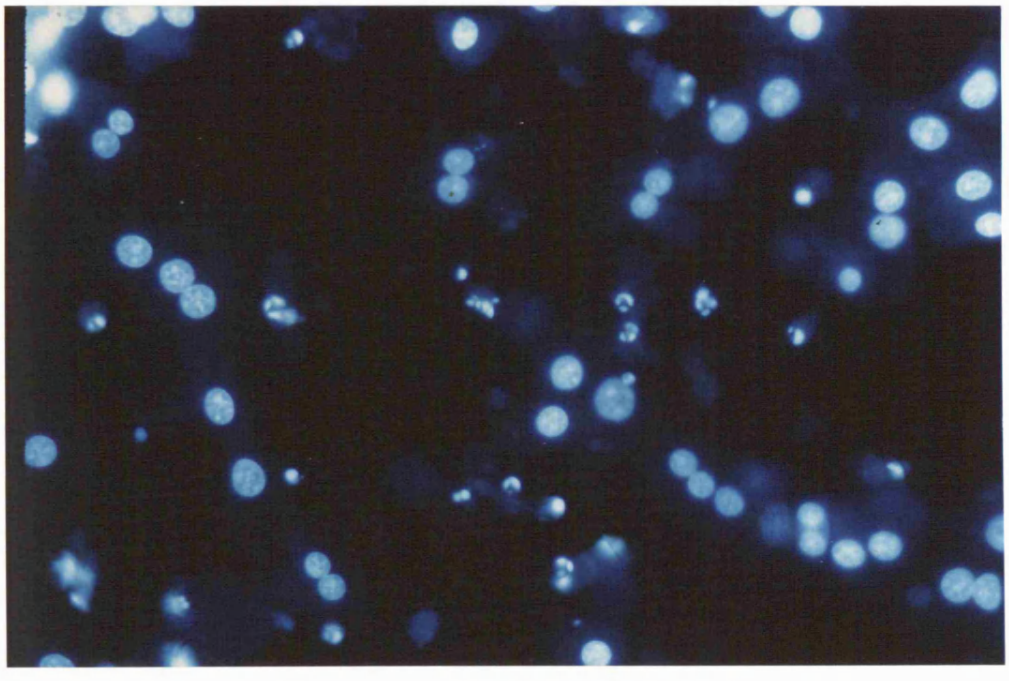

Figure 5.1 TGF-ß$_1$ induced apoptosis in primary culture hepatocytes

Hepatocytes were grown on collagen coated glass coverslips and incubated in the presence or absence of TGF-ß$_1$ and at 16h time point, the cells were fixed and stained with H33258. Photograph were taken using a fluorescence microscopy and panel A) shows control hepatocytes and panel B) shows TGF-ß$_1$ treated hepatocytes.

Figure 5.2A & B confirmed that treatment with TGF-ß$_1$ induced apoptosis and did not induce necrosis in primary hepatocytes culture.

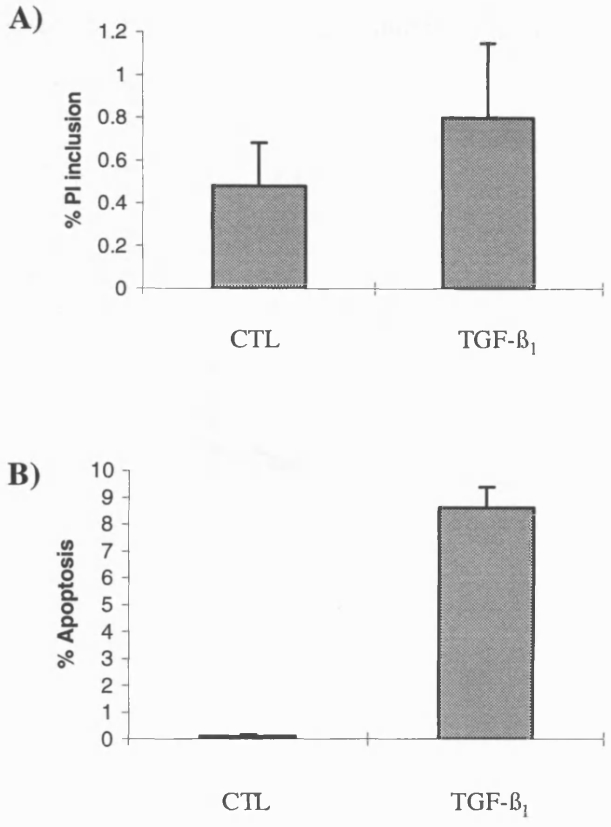

Figure 5.2 Effects of TGF-ß$_1$ on the mode of cell death in primary hepatocytes

Hepatocytes were cultured on collagen coated glass coverslips as described in methods chapter with each treatment carried out in duplicate. Cells were incubated with either vehicle (CTL) or 1ng/ml TGF-ß$_1$ and the cultures left for 16h before staining with PI (panel A) and H33258 (panel B). A minimum of ten fields (approx. 200 cells/field) for each coverslips was examined and the average number of nuclei/field calculated.

5.2.2 Isolation of nuclei from hepatocyte monolayers

Initial experiments were carried out to develop a rapid and gentle method for isolating nuclei from hepatocyte monolayers with a minimum of damage. However, conventional methods using hypotonic buffer and detergents showed that although nuclei were easily isolated from monolayers 4h after plating it proved more difficult to isolate the nuclei after longer periods in culture (i.e. 24 or 48h). I have therefore applied a method established by F.A. Oberhammer and H.M. Qin at the Institute of Tumorbiology and Cancer Research, University of Vienna which was adapted from Otto (1990) for the isolation of nuclei from cells pre-fixed with ethanol, which used 4% citric acid and 0.5% Tween-20. Preliminary experiments were

carried out with various concentrations of citric acid and different non-ionic detergents to determine the optimal isolation conditions. The best results were obtained when the cells were pre-treated with 1% citric acid to achieve cell swelling and then subsequently lysed with 1% citric acid and 0.1%Tween-20. The integrity of the nuclei was examined by size analysis and this is shown in Figure 5.3. The initial 'harvest' nuclei suspension (Fig. 5.3A), i.e. before

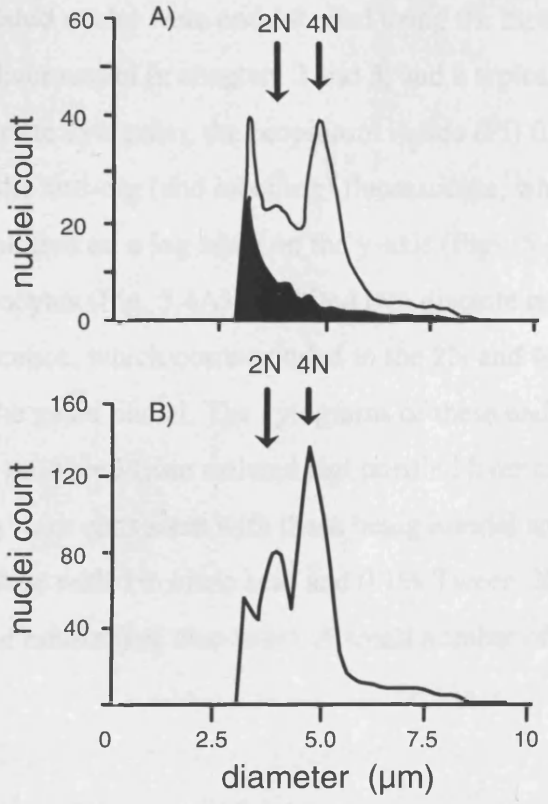

Figure 5.3 Size profile of nuclei isolated from monolayer hepatocytes

Hepatocytes were isolated and cultured as described in the methods. After 48h the nuclei were isolated with 1% citric acid (w/v), 0.1% Tween -20 for 20-25min. The nuclei were sedimented and resuspended/washed in PBS. Aliquots were taken for cell counting and sizing after diluting 1:400 (A) or 1:1000 (B) with Casyton™. Panel A shows the size profiles for the initial 'harvest' nuclei suspension, i.e. after isolation with 1% citric acid, 0.1% Tween-20 and the supernatant (filled-in profile) obtained after spinning down the nuclei. B shows the profile of the nuclei after washing and resuspending in PBS. The volumes corresponding to the 2N and 4N peaks were 29.5 and 52fl, respectively.

centrifugation contained 2N and 4N nuclei peaks and a third peak of smaller sized particles which represents contamination from cellular debris and organelles. The latter remained in the supernatant after centrifugation (filled in profile, Fig. 5.3A). The nuclei pellet after washing and resuspending in PBS was remarkably clean and relatively uncontaminated with cell debris (Fig. 5.3B). The modal volume of the 2N and 4N nuclei were 29.5 and 52fl, respectively. Similar

size profiles were obtained from isolated liver nuclei which had been purified by a sucrose gradient method as described in chapters 3 and 4 with the modal volumes of 2N and 4N peak for these nuclei were 27 and 54 fl, respectively. It is clear on the basis of these studies that the isolation procedure produced a relatively clean preparation of intact hepatocyte nuclei.

5.2.3 ISEL of DNA strand breaks in nuclei isolated from hepatocyte monolayers treated with TGF-β_1

The isolated nuclei were end-labelled using the method that was previously described for isolated rat liver nuclei in chapters 2 and 3; and a typical example of this is shown in Figure 5.4. In this bivariate cytogram, the propidium iodide (PI) fluorescence was plotted linearly on the x-axis, and the anti-dig (end labelling) fluorescence, which is a measure of the DNA strand breakage, was plotted on a log scale on the y-axis (Figs. 5.4A & B). Nuclei isolated from untreated hepatocytes (Fig. 5.4A) exhibited two discrete regions of PI fluorescence with low anti-dig fluorescence, which corresponded to the 2N and 4N nuclei and accounted for 97% (Fig. 5.4A) of the gated nuclei. The cytograms of these end-labelled isolated nuclei were similar to those produced from isolated and purified liver nuclei (chapter 3) and the low levels of end-labelling were consistent with these being normal and non-apoptotic nuclei. The isolation procedure with 1% citric acid and 0.1% Tween-20, therefore did not induce any artifactual strand breaks (see also later). A small number of nuclei (approx. 3%) exhibited enhanced, i.e. high anti-dig fluorescence (Fig. 5.4A) and were tentatively assessed as being from apoptotic cells. However, after treatment with TGF-β_1 for 24h, only 72% of the nuclei isolated from hepatocytes had low levels of end labelling, which were separated into the 2N and 4N peaks (Fig. 5.4B). The remaining nuclei (28%) had 'high levels' of ISEL and an extremely variable DNA content as measured by PI fluorescence (Fig.5.4B). In several different hepatocyte cultures, TGF-β_1 (1ng/ml) increased the number of nuclei containing elevated levels of DNA cleavage to 28.6±5.8% (mean ± S.E.M, n=5) at 16h and 66.6±3.3% (n=4) at 40h.

The extremely variable DNA content of the apoptotic nuclei may be due to the method detecting nuclear fragments, as well as whole nuclei, and this possibility was investigated by analysing the size of the labelled nuclei. Thus, in control cultures, approximately 55-70% of the total numbers of events detected by flow cytometry were gated as 2N and 4N nuclei. The

remaining events were either nuclei with >4N ploidy and/or debris. The size distribution of the gated nuclei is shown in Fig. 5.4C in which forward scatter (i.e. size) is plotted against PI

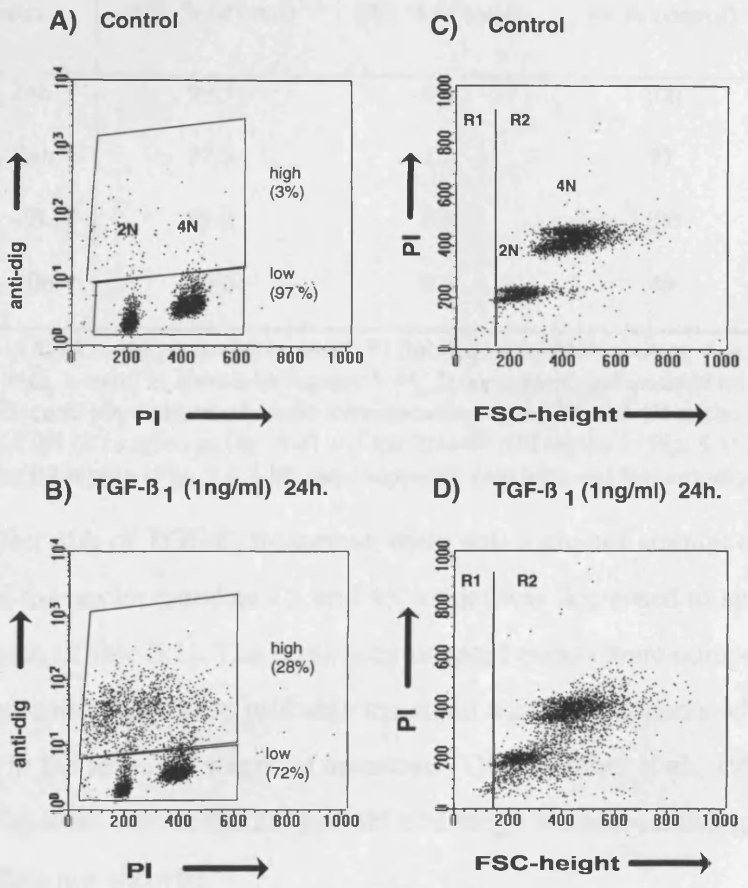

Figure 5.4 ISEL of DNA strand breaks in nuclei isolated from hepatocyte monolayers treated with TGF-$ß_1$

Hepatocytes were isolated and cultured with and without 1ng/ml TGF-$ß_1$ for 24h and nuclei isolated and end-labelled as described in the methods. The bivariate cytograms in A and B are dot-plots showing the PI fluorescence (i.e. DNA content) versus the level of DNA strand breakage (i.e., as measured by the amount of anti-dig fluorescence). The PI fluorescence (red) is plotted linearly on the x-axis and the anti-dig fluorescence (green) is plotted logarithmically on the y-axis. LYSIS II software was used to count the numbers of normal nuclei with low anti-dig fluorescence and apoptotic nuclei with high anti-dig fluorescence. In C and D, the PI content of the nuclei is plotted against the forward scatter (FSC-height), i.e., the size of the nuclei. The numbers of the fragmented <2N (R1) and the 2N + 4N (R2) nuclei were counted and expressed as a percentage of the total gated nuclei (see also Table 5.1)

content (i.e. DNA content). Most of the gated nuclei (approximately 99%) from untreated hepatocytes after 24h of culture were detected as two discrete populations, i.e., 2N and 4N nuclei. The number of nuclei gated in the 2-4N region after treatment with TGF-$ß_1$ for 24h was very similar to the control value (Table 5.1). However, the size versus PI cytogram (Fig. 5.4D) showed that although 97.3% of the nuclei populations within the 2-4N range (Table 5.1) the nuclei populations were more dispersed (Fig. 5.4D) due to variations in the DNA content.

Table 5.1 Effects of TGF-ß$_1$ on size and number of nuclei containing DNA strand breaks

Treatment	Intact nuclei (R2, % of total)	Nuclei fragments (R1, % of total)	Number of nuclei (% of control)	High anti-dig nuclei (% of total)
-TGF-ß$_1$ 24h	99.3	0.5	100	3.6
+TGF-ß$_1$ 24h	97.3	1.2	97	29.3
-TGF-ß$_1$ 40h	99.2	0.9	100	1.0
+TGF-ß$_1$ 40h	90.6	8.0	49	55.0

Cytograms of ISEL labelled nuclei in which PI fluorescence (DNA content, y-axis) was plotted against forward scatter (i.e. size, x-axis) as shown in Figures 5.4 C,D were gated and counted on Lysis II software. The dot plots gave discrete populations of nuclei corresponding to the 2N and 4N nuclei. The number of fragmented nuclei, i.e., < 2N (R1 region in Fig. 5.4) and the 2N+4N (R2 region in Fig. 5.4) nuclei were determined . Nuclei in the R2 region (Fig. 5.4 A,B) were separated into high and low anti-dig fluorescence.

After 40h of TGF-ß$_1$ treatment, there was a greater amount of apoptosis and the number of the nuclei gated as 2N and 4N nuclei was decreased to approximately 50% of the control value (Table 5.1). The remaining ungated events were composed of debris and <2N sized fragments which were probably the small nuclear fragments which are known to be produced in the terminal stages of apoptosis (Oberhammer et al., 1992). Almost 91% of the gated nuclei were within the 2N and 4N size range but had a much greater variation in DNA content (data not shown).

To investigate whether the increase in nuclei with high levels of DNA strand breaks was induced in a concentration dependent manner, nuclei were isolated from hepatocyte monolayers treated with various concentrations of TGF-ß$_1$. A saturable concentration effect curve was observed (Fig. 5.5) and showed the maximum effect of TGF-ß$_1$ was produced at a concentration of 1ng/ml.

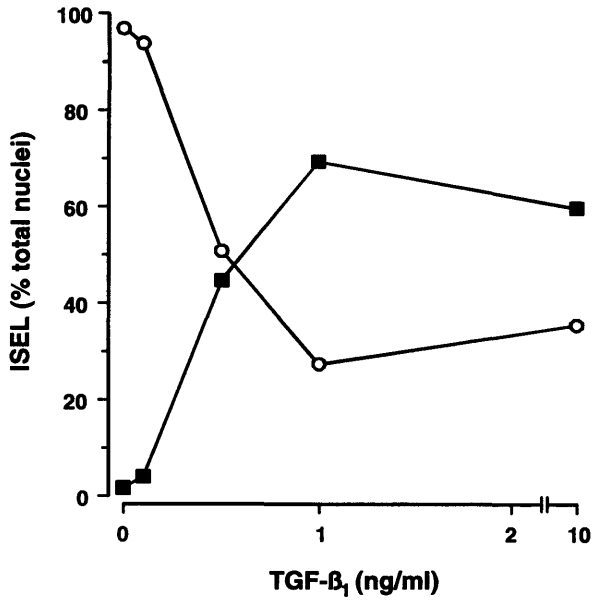

Figure 5.5 Concentration response curve of TGF-ß$_1$ treated hepatocytes as assessed by ISEL

In this experiment, apoptosis was induced in hepatocytes with varying concentrations of TGF-ß$_1$ and after 40h the amount of ISEL determined as described in methods. Normal nuclei with low (filled circles) and apoptotic nuclei with high anti-dig fluorescence (filled squares) are shown as a percentage of the total gated nuclei.

5.2.4 TGF-ß$_1$ induced apoptosis in hepatocytes is associated with multi-step DNA cleavage

Oberhammer et al. (1993a) have demonstrated the absence of internucleosomal fragmentation in TGF-ß$_1$ mediated apoptosis in hepatocytes. However, the data in this chapter using ISEL confirmed that DNA is extensively cleaved during TGF-ß$_1$ induced apoptosis and it was important to investigate how the DNA was cleaved. Nuclei isolated from hepatocyte monolayers treated with various concentration of TGF-ß$_1$ were therefore analysed by CAGE and FIGE and the electrophoresis data is shown in Fig. 5.6. In the control nuclei (lane 1), no internucleosomal cleavage was observed on CAGE (lower panel) whereas on FIGE (upper panel), there was a background level of large fragments of 700, 200-250 and 30-50kbp DNA fragments. These DNA fragment sizes are similar to the ones obtained in isolated rat liver nuclei (chapters 3 and 4). TGF-ß$_1$ (0.1ng/ml) did not induce any marked DNA cleavage as detected by both FIGE and CAGE and the cleavage patterns were essentially similar to the control. However addition of TGF-ß$_1$ from 0.5, 1.0 and 10ng/ml caused an increase in 30-50kbp fragments with a concomitant increase in internucleosomal cleavage (Fig.5.6). The DNA cleavage observed on gels mirrored the ISEL results seen in Figure 5.5.

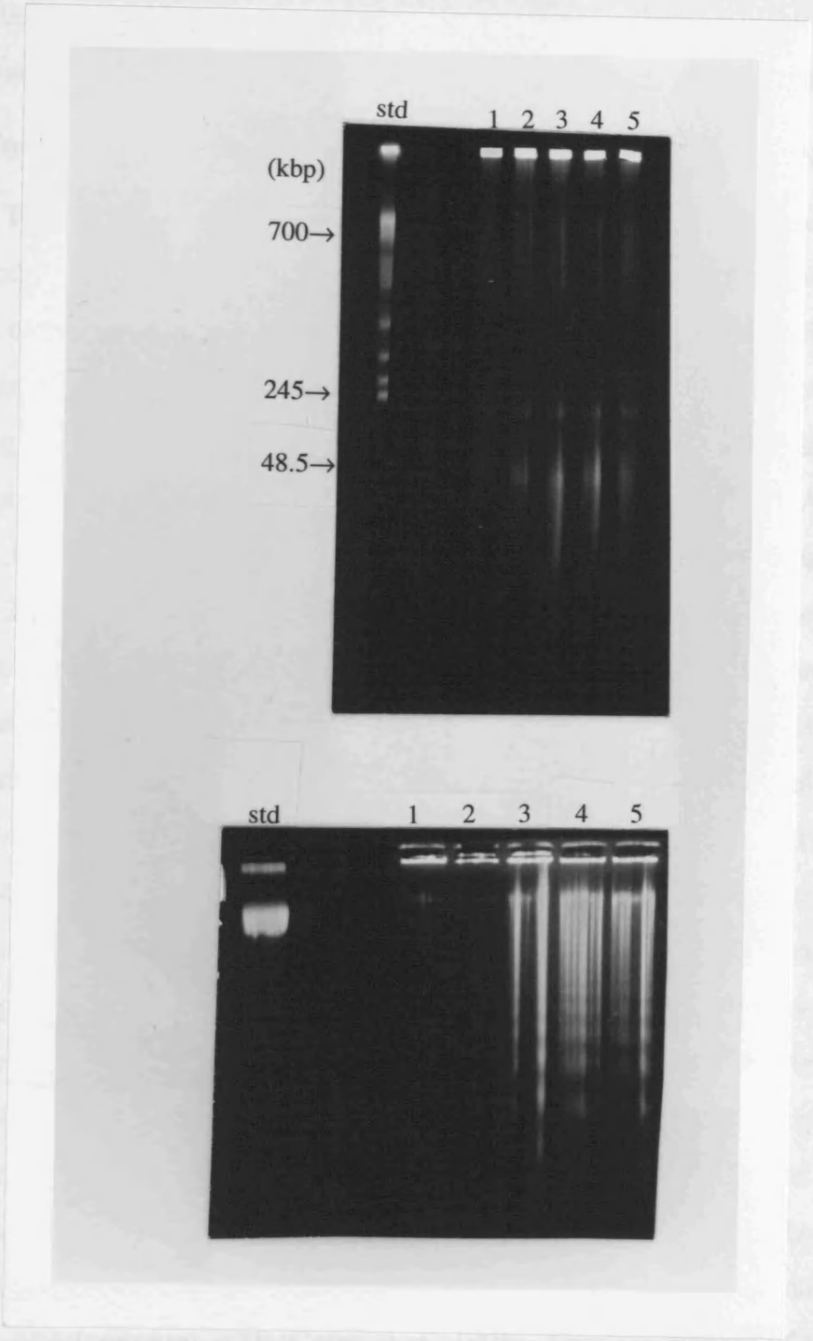

Figure 5.6 TGF-ß$_1$ treated hepatocytes induced multi-step DNA cleavage

Hepatocytes were isolated and cultured with and without TGF-ß$_1$ for 16h and nuclei isolated from these cultures. DNA cleavage was analysed by FIGE (upper panel) or CAGE (lower panel). The lanes are as follows; lane 1 is control (vehicle control), lanes 2-5 are 0.1, 0.5, 1.0 and 10ng/nl TGF-ß$_1$ respectively.

Thus, at 0.1ng/ml TGF-$ß_1$, the level of ISEL is similar to control level and increasing the concentrations of TGF-$ß_1$ (0.5-10ng/ml) caused an increase in the DNA strand breaks. It is important to note that electrophoresis technique will only provide information of the pattern of DNA cleavage which has occurred; they do not provide quantitative information. Hence a combination of the gel and ISEL technique provide both qualitative and quantitative data.

5.2.5 Comparison of morphological and ISEL methods for assessing apoptosis

The enucleation/end-labelling method provides a quantitative method for determining the amount of apoptosis in hepatocyte monolayers, and it was important to ascertain how this method compared with the standard morphological assay using a H33258 dye binding method. This was carried out by examining the time course of induction of apoptosis after treatment with 1ng/ml TGF-$ß_1$ and the results are shown in Figure 5.7. In untreated cultures the number of morphologically identifiable apoptotic nuclei was 1-2% (Fig.5.7A). After treatment with TGF-$ß_1$ the number of nuclei with apoptotic morphology increased from 6-7% at 16h and 16-18% at 24h, before plateaueing at 18-19% at 40 and 48h. This was accompanied by a corresponding and proportionate decrease in the number of normal (non-apoptotic) nuclei. With the ISEL method, the number of nuclei detected with elevated DNA strand breakage from untreated cultures was 2-3% (Fig.5.7B). In the TGF-$ß_1$ treated cultures the number of nuclei with high levels of end-labelling increased in a linear manner from 15-16% at 16h to 88% at 48h. This was accompanied by a parallel decrease in the number of nuclei (non-apoptotic) with low end-labelling. Thus at all times the proportion of nuclei with high end-labelling was greater than the numbers of nuclei detected with an apoptotic morphology. In addition the number of nuclei containing high levels of DNA strand breaks was still increasing after 24h even though the incidence of morphologically identifiable apoptotic nuclei had plateaued. This discrepancy could be due to the reduced energy level of the cells as the medium in the time course experiments was not changed. Therefore, the DNA strand breaks which occurred and labelled with ISEL were not accompanied by the nuclear morphological changes which requires ATP (Chow et al., 1995). Thus, the amount of apoptosis as assayed by the ISEL method was clearly greater than that detected by the H33258 dye binding method and this suggested that the end-labelling method was detecting nuclei which were not morphologically recognisable as apoptotic. This was an unexpected finding as previous studies with liver sections and fixed preparations of monolayer hepatocyte cultures after TGF-$ß_1$ treatment have shown that end-labelling was only detected in those nuclei with an obvious

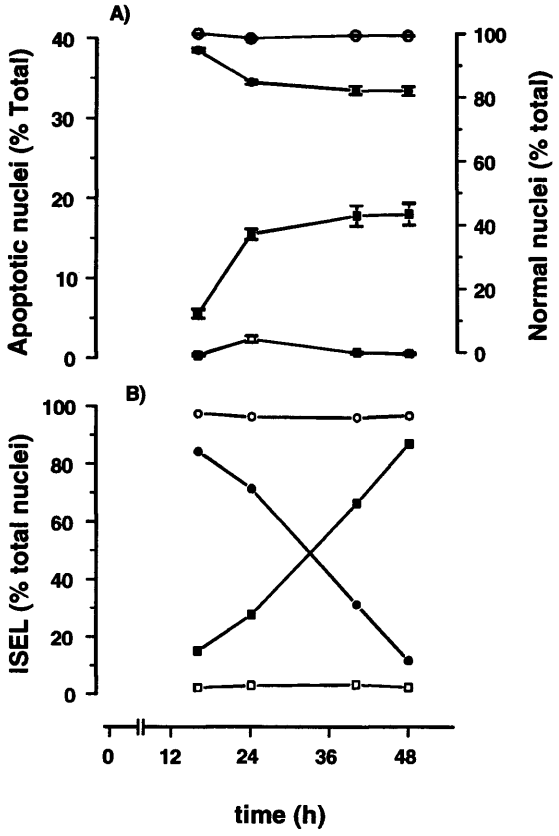

Figure 5.7 Comparison of the time course of apoptosis as assessed by morphology and ISEL

Apoptosis in hepatocytes treated with TGF-β_1(1ng/ml) was determined by two separate methods. The first method (A) used the morphological approach in which the nuclei were stained with H33258 and the number of apoptotic nuclei counted as described in the methods section. The second method (B) used the ISEL technique as described in Fig. 5.5. In the morphology assay, 10 separate fields on each coverslip (2 per treatment) were counted at x 200 magnification and values are given as mean (SEM, n=20). The normal nuclei from control (open circles) and TGF-β_1 treated (filled circles), and the apoptotic nuclei from control (open squares) and TGF-β_1 treated (filled squares) hepatocytes are shown as % of the total nuclei. In the ISEL experiments in B, normal (low anti-dig fluorescence) nuclei from control (open circles) and TGF-β_1 (filled circles) treated cells are shown as a percentage of the total gated nuclei. The apoptotic (high anti-dig fluorescence) nuclei from control (open squares) and TGF-β_1 (filled squares) treated are also expressed as a percentage of the total gated nuclei.

5.2.6 Confocal Microscopy of end-labelled nuclei

The morphologies of the end-labelled nuclei were examined by confocal microscopy, which allowed the simultaneous analysis of both chromatin condensation (PI fluorescence) and DNA strand breakage (anti-dig fluorescence) and thus produces an image showing the co-localisation of condensation and DNA cleavage. Nuclei isolated from untreated hepatocytes after 16h and 40h were sorted by flow cytometry and those nuclei with low anti-dig fluorescence (approx. 98% of the nuclei population) separated into 2N and 4N nuclei. Nuclei, representative of the 4N population after 16h culture , had a very low level of fluorescence

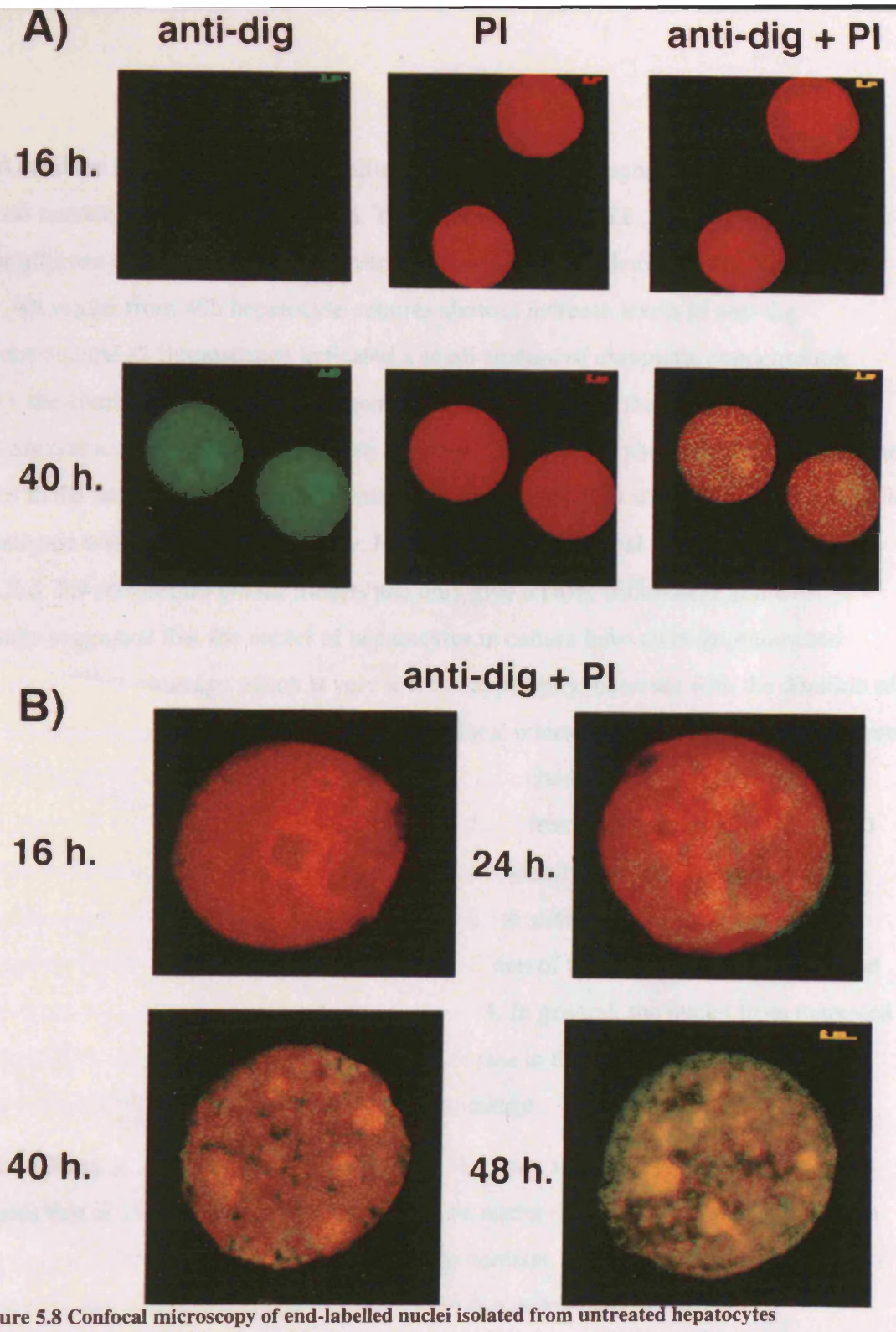

Figure 5.8 Confocal microscopy of end-labelled nuclei isolated from untreated hepatocytes

Nuclei were isolated and end-labelled as described in methods from hepatocytes cultured for 16-48h. The nuclei were analysed by flow cytometry (Fig.5.7B) and then examined by confocal microscopy. The panels, which are maximum projections images, show in A) 4N end-labelled nuclei from hepatocytes cultured for 16h and 40h respectively, and then sorted by flow cytometry into 2N and 4N nuclei. The nuclei were examined under a 40x objective. Each panel shows the green (anti-dig) and red (PI) fluorescence, respectively, and then both red and green combined (anti-dig + PI) fluorescence. B) the combined (anti-dig+PI) fluorescence for representative nuclei examined with a x100 objective after 16, 24, 40 and 48h culture. The size bars are 2μm. It should be noted that the colours in the confocal photographs are pseudo-colours and only give relative intensity not absolute differences. In the case of each experiment the colour intensity was maximised on the sample with the most fluorescence.

(Fig. 5.8A) and the PI fluorescence was uniformly distributed throughout the nuclei without any obvious condensation of the chromatin. The combined image (i.e., anti-dig fluorescence + PI) was largely red in colour, reflecting a very low level of DNA cleavage (Fig. 5.8A). However, 4N nuclei from 40h hepatocyte cultures showed increase levels of anti-dig fluorescence and the PI fluorescence indicated a small amount of chromatin condensation (Fig.5.8A). the combined image was orange/red in colour reflecting the increased DNA cleavage. Similar results were obtained with separated 2N nuclei. It should be stressed that the differences in the anti-dig fluorescence of nuclei from untreated cells were very small and could only be detected with confocal microscopy. Furthermore, the confocal images shown in Figures 5.8 & 5.9 are pseudo-colour images and only give relative differences in intensity. These results suggested that the nuclei of hepatocytes in culture have an endogenous and ongoing rate of DNA cleavage which is very low but apparently increases with the duration of culture. This possibility was confirmed by using confocal microscopy to look at the nuclei from the control hepatocytes in the time course experiment described in Fig.5.7. The combined images in Fig.5.8B show representative 4N nuclei isolated from hepatocytes after 16, 24, 40 and 48h. Over the time period the images of the nuclei gradually changes from red/orange (16h) to yellow/green (48h) indicating an increase in DNA strand breaks. This was accompanied by an increase in the granularity/condensation of the chromatin which appeared to occur in small foci distributed throughout the nucleus. In general, the nuclei from untreated hepatocytes exhibited a small but time-dependent increase in the heterochromatin content which was accompanied by increased DNA strand breakage.

The effects of TGF-$ß_1$ on the nuclear morphology are shown in Fig.5.9 which demonstrates that at 16h the low anti-dig fluorescence nuclei (Fig.5.9A) were very similar to the nuclei from untreated hepatocytes (Fig. 5.8A). In contrast, a typical example of high anti-dig fluorescent (apoptotic) nucleus showed that there is a much more intense green fluorescence which was co-localised with very discrete areas of chromatin condensation (Fig. 5.9B) and is typical of an early stage apoptotic nuclei (Oberhammer et al., 1992). After 40h, apoptosis was more extensive and the nuclei exhibited a range of morphologies with varying degrees of chromatin condensation, and the three examples (Fig. 5.9C) shown are representative of different stages in the apoptotic process. A nucleus from a 48h culture is shown in Fig. 5.9D and illustrates a late stage apoptotic morphology in which the chromatin

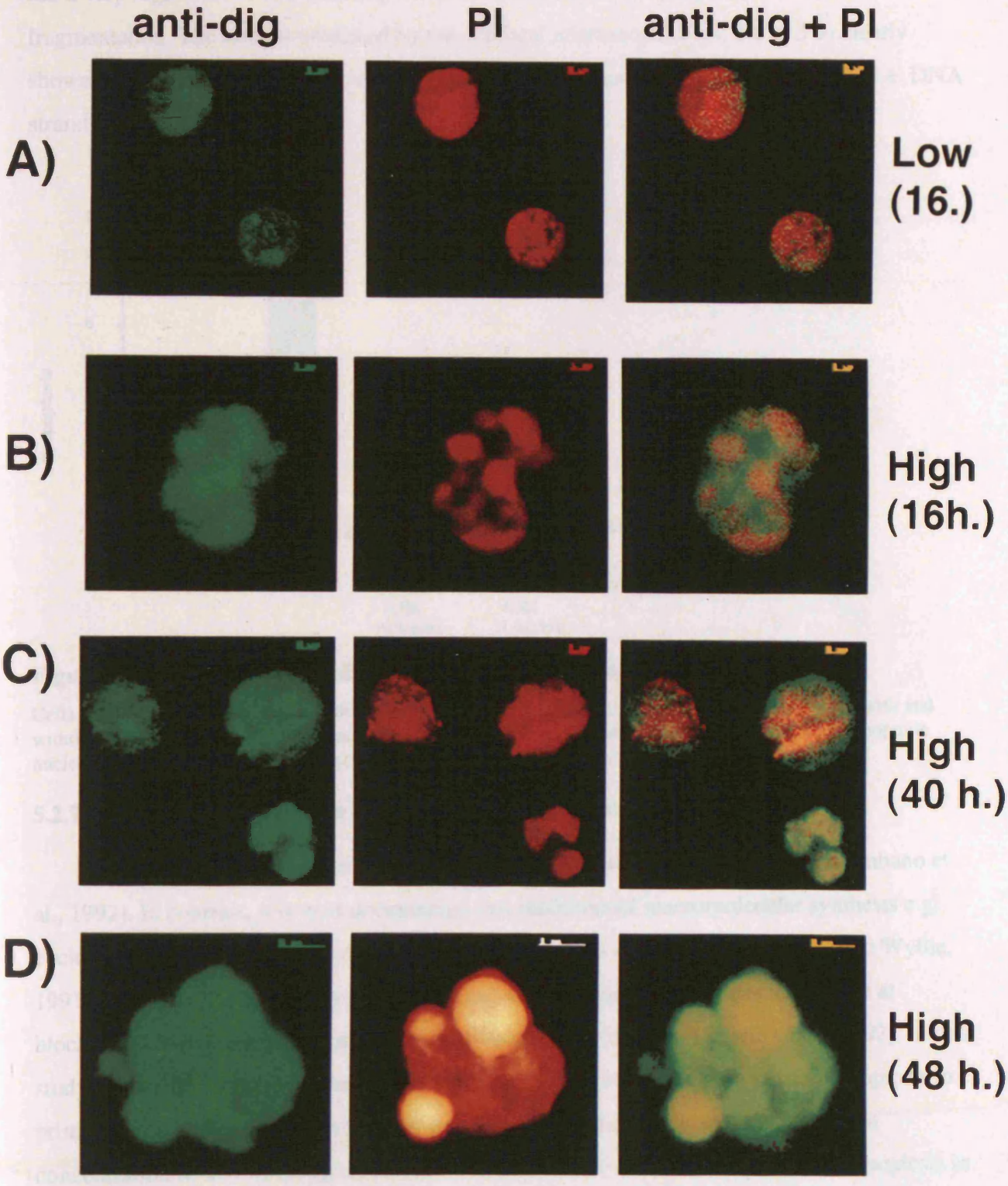

Figure 5.9 Confocal microscopy of end-labelled nuclei from TGF-ß$_1$ treated hepatocytes

Nuclei were isolated and end-labelled as described in Fig. 5.8 from hepatocytes cultured with (1ng/ml) TGF-ß$_1$ for 16, 40 and 48h. The nuclei from 16 and 40h (A-C) were analysed and separated by flow cytometry into low anti-dig fluorescence and high fluorescence nuclei which were then examined by confocal microscopy. The maximum projection images left to right show anti-dig (green), propidium iodide (red), and combined (anti-dig + PI) fluorescence images of typical examples. D shows a nucleus with high anti-dig fluorescence isolated after 48h of culture and viewed with a x100 objective. The size bars are 2µm.

has a very high level of end-labelling and is condensed into clumps, prior to nuclear fragmentation. The images produced by the confocal microscope (Figs. 5.8 & 5.9) clearly showed that condensation of the chromatin was proportioned to the amount of ISEL, i.e. DNA strand breakage.

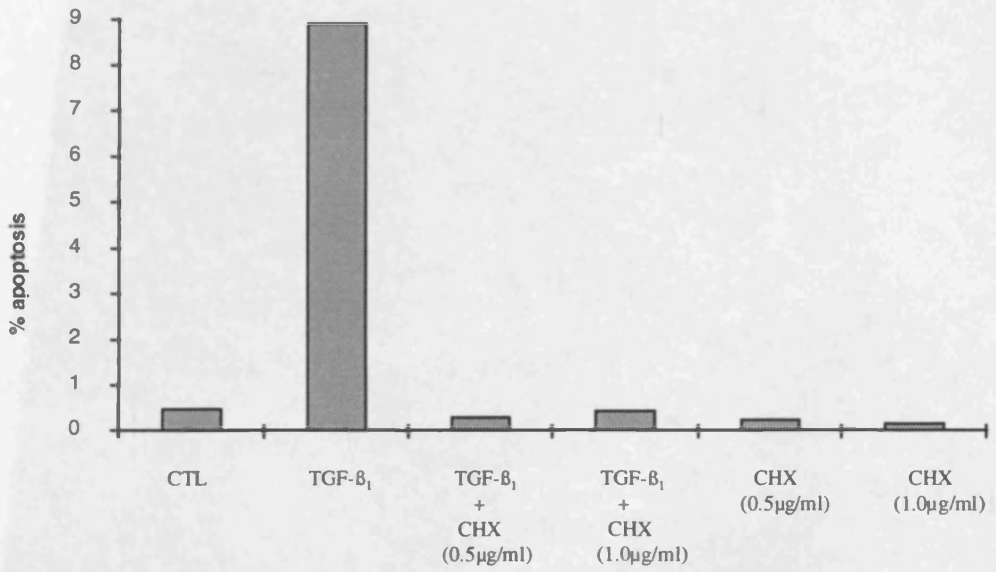

Figure 5.10 Cycloheximide inhibition of TGF-$ß_1$ induced apoptosis

Cells were pre-treated for 30min with the indicated concentration of cycloheximide before treating with and without 1ng/ml TGF-$ß_1$. After 16h incubations, the cells were fixed and stained with H33258 and apoptotic nuclei counted. Results shown are mean from 2 separate experiments

5.2.7 Effects of cycloheximide and Zn^{2+} on TGF-$ß_1$ induced apoptosis

Cycloheximide has been shown to induce apoptosis in the liver *in vivo* (Columbano et al., 1992). In contrast, it is well documented that inhibitors of macromolecular synthesis e.g. cycloheximide can block glucocorticoid induced apoptosis in thymocytes (Arends and Wyllie, 1991, for review). Interestingly, it has been reported that cycloheximide is ineffective at blocking TGF-$ß_1$ induced apoptosis in human hepatoma cell lines (Lin and Chou, 1992). In this study, I have found that cycloheximide was a potent inhibitor of TGF-$ß_1$ induced apoptosis in primary hepatocytes. As shown in Figure 5.10, preincubation of cycloheximide with a concentration as low as 0.5µg/ml prior to addition of TGF-$ß_1$ completely inhibited apoptosis in this TGF-$ß_1$ treated hepatocytes as assessed by the dye binding assay, H33258. Furthermore, using ISEL for the quantitation of the apoptotic nuclei also revealed similar results in that cycloheximide (0.5-1.0µg/ml) completely blocked the end-labelled nuclei in TGF-$ß_1$ treated hepatocytes as shown in Figure 5.11A. Cycloheximide on its own did not induce apoptosis as

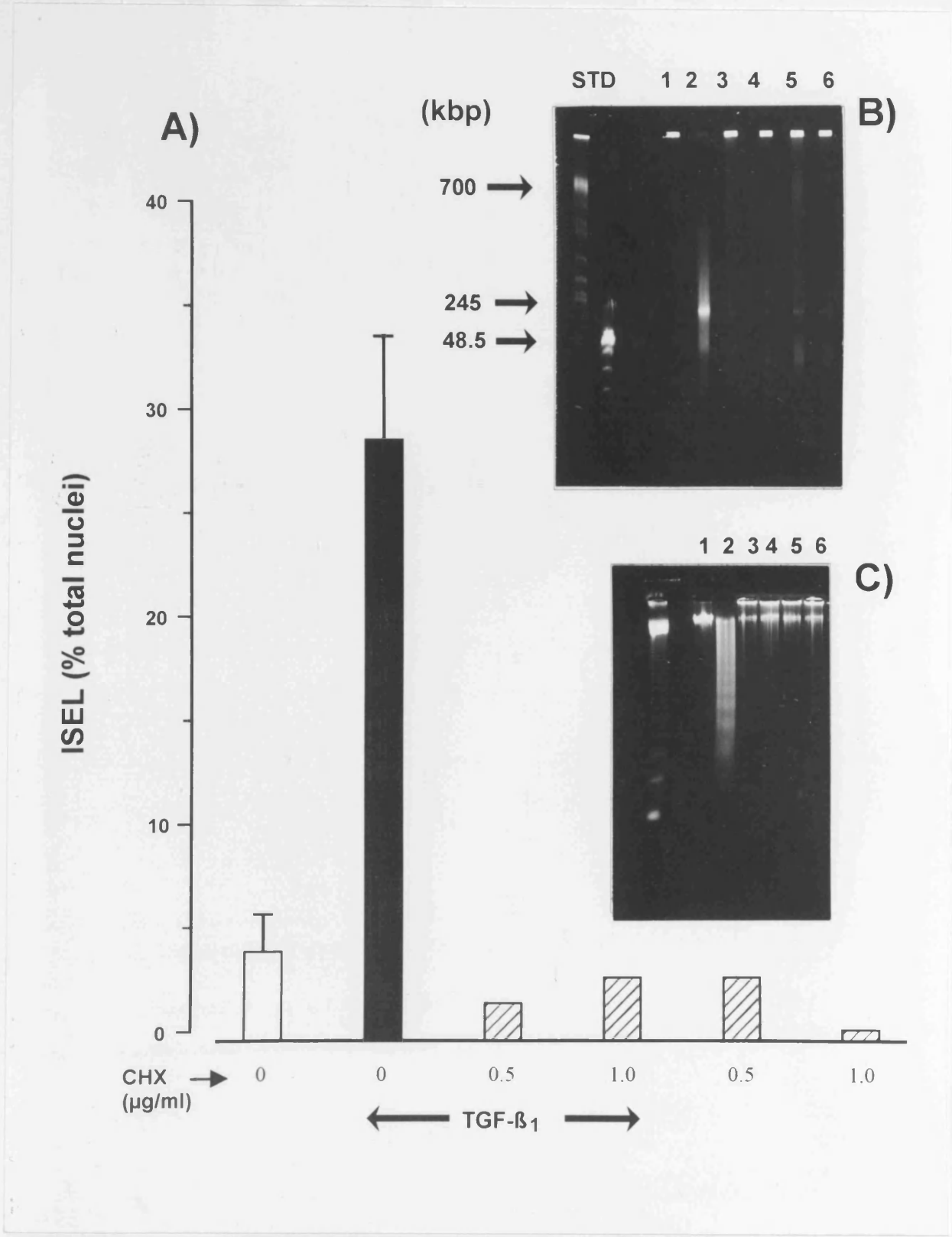

Figure 5.11 Cycloheximide inhibition of TGF-ß$_1$ induced DNA fragmentation.

Hepatocytes were pre-treated for 30 min with the indicated concentrations of cycloheximide before treating with and without 1ng/ml TGF-β_1 as described in the Materials and Methods. Nuclei were isolated from the hepatocyte cultures and analysed by ISEL (A), field inversion gel electrophoresis (B) and conventional agarose gel electrophoresis. In (A) the apoptotic nuclei are expressed as a % of the total nuclei. In (B) kilobase pair (kbp) DNA standards are indicated and in (C) the unmarked lane shows the laddering standards of 123bp and multiples thereof.

assessed by both H33258 and ISEL (Figures 5.10 & 5.11A respectively). When the DNA cleavage profile was analysed by FIGE (Fig.5.11B) or CAGE (Fig.5.11C), the large kbp and nucleosomal fragments detected in TGF-$ß_1$ treated hepatocytes were completely blocked by cycloheximide (Fig. 5.11B & C, lanes 3 and 4 respectively). In agreement with the morphology and ISEL, cycloheximide on its own did not result in DNA cleavage (Fig. 5.11B & C, lanes 5 and 6).

Several laboratories have now confirmed the initial finding by Duke et al. (1983) that Zn^{2+} is an inhibitor of the Ca^{2+}/Mg^{2+} dependent endonuclease, generally thought to be responsible for the internucleosomal DNA fragmentation in apoptosis (reviewed by Zalewski and Forbes, 1993). In this study, Zn^{2+} was also shown to be a potent inhibitor of Ca^{2+}/Mg^{2+} stimulated DNA cleavage in rat liver nuclei (chapter 4). The effects of Zn^{2+} on TGF-$ß_1$ mediated apoptosis in hepatocytes are shown in Fig.5.12, and it can be seen that 100µM Zn^{2+} completely blocked the apoptotic nuclear morphological changes as assessed by H33258. At this concentration, Zn^{2+} alone did not induce apoptosis.

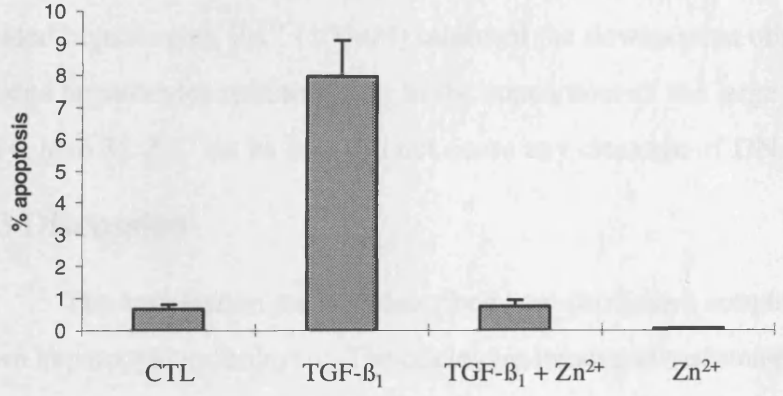

Figure 5.12 Effects of Zn^{2+} on TGF-$ß_1$ mediated apoptosis in hepatocytes as assessed by H33258

Hepatocytes were pre-treated for 30min with 100µM Zn^{2+} before treating with or without 1ng/ml TGF-$ß_1$ and the cultures were left for 16h. At this time, the cells were fixed and stained with H33258 and the number of apoptotic nuclei were counted.

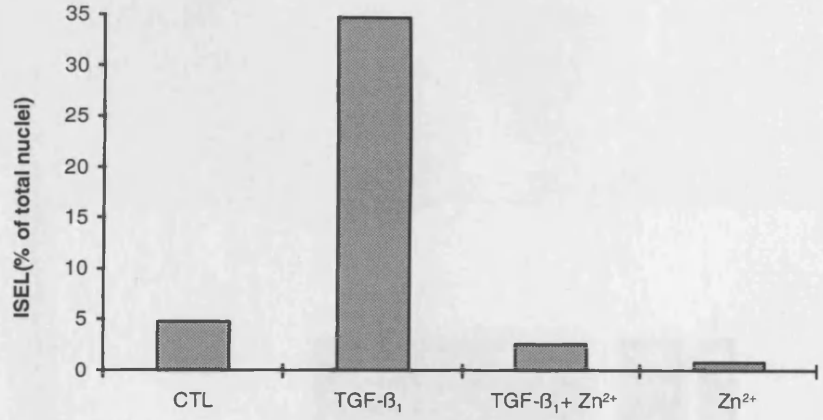

Figure 5.13 Effect of Zn^{2+} on ISEL of nuclei extracted from TGF-$ß_1$ treated hepatocytes

Hepatocytes were cultured and treated as described in Figure 5.12. Essentially, the cells were preincubated with and without 100µM Zn^{2+} and 1ng/ml TGF-$ß_1$ was added 30min later. After 16h incubation, the nuclei were extracted and end-labelled as described in methods. The values given are mean from 2 separate experiments.

Moreover, ISEL showed that Zn^{2+} inhibited apoptosis as shown in Fig. 5.13 and again Zn^{2+} on its own did not cause apoptosis. In contrast, when nuclei isolated from the hepatocyte cultures were subjected to gel electrophoresis (Fig. 5.14), there was a significant degradation of DNA into both the large kbp and nucleosomal fragments (Fig. 5.14, lane 2) in TGF-$ß_1$ treated hepatocytes. Zn^{2+} (100µM) inhibited the downstream oligosomal cleavage in TGF-$ß_1$ treated hepatocytes resulting only in the appearance of the large kbp sized fragments (Fig. 5.14, lane 3). Zn^{2+} on its own did not cause any cleavage of DNA (lane 4).

5.3 Discussion

The enucleation method described here provides a simple method for isolating nuclei from hepatocyte monolayers. The nuclei are intact and undamaged as assessed by the size profile. The method used in this study is a much gentler technique than used in an earlier study in which the hepatocytes were sonicated in a Triton X-100/citrate buffer (Davies et al., 1990). The flow cytometric analysis showed that in control cells the majority of the nuclei were separated into 2N and 4N populations which had low levels of end-labelling. In the case of anti-dig content versus PI cytogram (Fig. 5.4A&B) these populations were homogenous. However the PI content versus forward scatter (size) cytogram showed a bimodal distribution, this is perhaps not unexpected as the nuclei are derived from both mononucleated and binucleated cells. Consequently, a 2N and 4N nucleus can be derived from a hepatocyte with a single nucleus or alternatively from a binucleated cell with two nuclei. Thus, each 2N and 4N population is a mixture of two populations of nuclei.

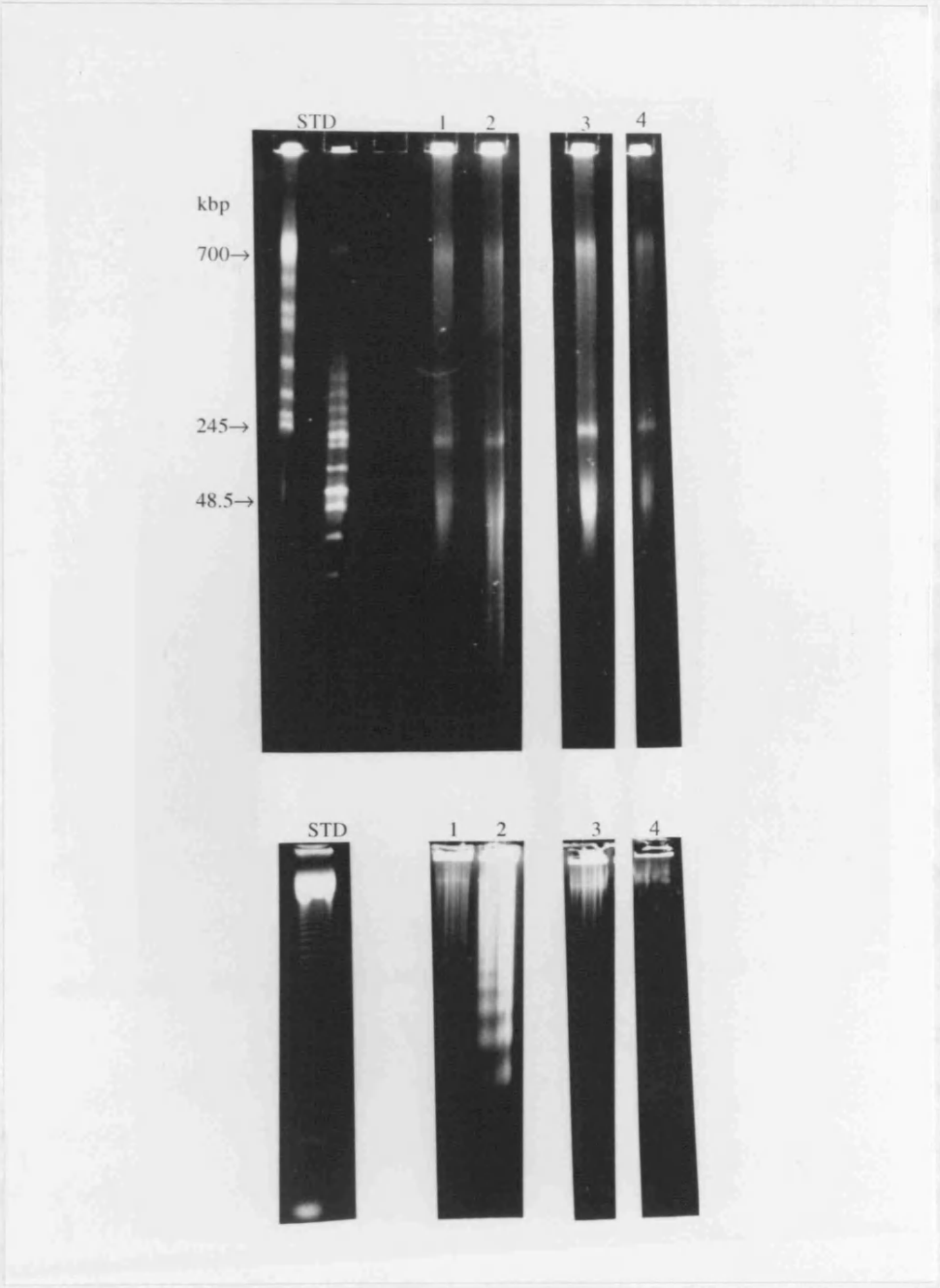

Figure 5.14 Effect of Zn^{2+} on TGF-$ß_1$ mediated apoptosis as analysed by gel electrophoresis

Nuclei were extracted from hepatocytes incubated for 16h as described in Figure 5.13 and DNA cleavage was analysed by FIGE (upper panel) and CAGE (lower panel). Lane 1, nuclei from solvent control for TGF-$ß_1$, lane 2 is the effect of 1ng/ml TGF-$ß_1$, lane 3 is 100μM Zn^{2+} added 30min prior to 1ng/ml TGF-$ß_1$ and lane 4 is 100μM Zn^{2+} alone.

Nuclei isolated from untreated hepatocytes which have been cultured for 0-48h have a very low level of ISEL as measured by flow cytometry. However, analysis of these nuclei with confocal microscopy showed that although the level of DNA strand breaks was low in control hepatocytes, there was a small and time dependent (i.e. duration of culture) increase in the amount of DNA cleavage (Fig. 5.7). This process was markedly enhanced after addition of TGF-β_1 and DNA strand breaks were detected in areas of condensed chromatin in nuclei with an apparent normal size (Table 5.1 and Fig. 5.9). The apoptotic nuclei (Fig. 5.4 and Table 5.1) as observed by PI staining had a diverse range of DNA contents. This was probably due to extensive internucleosomal DNA cleavage producing small nucleosome-sized fragments of DNA which can leak from the nucleus (Gorcyzca et al., 1992) rather than the method detecting nuclear fragments which should be accounted for by the 'gating'.

The increased levels of ISEL produced after TGF-β_1 treatment indicates that this can be used as a reliable measure of apoptosis. This conclusion is further supported by the data presented above which showed that cycloheximide, a protein synthesis inhibitor can block TGF-β_1 induced apoptosis (Figures 5.10 & 5.11). Cycloheximide not only abolished the morphological effects of TGF-β_1 but also completely blocked the increase in ISEL. However the detection of DNA strand breaks by ISEL in nuclei with an apparent normal morphology is in contrast to previous studies with monolayer hepatocyte cultures and liver sections from animals treated with TGF-β_1 (Oberhammer et al., 1996). In these experiments, detection of DNA strand breaks with the use of DNA polymerase and terminal transferase was carried out on monolayers or sections fixed with paraformaldehyde or formalin and access to the DNA was achieved by pre-treatment with a chaotropic agent followed by proteinase K. Using this method only those cells with an apoptotic morphology were positive for DNA strand breaks with most of them being DNA double strand breaks. DNA single or double strand breaks were not detected in nuclei with an apparently normal morphology. The detection of a greater number of nuclei with DNA cleavage as seen in the current study may be due to the treatment of the unfixed cells with citric acid, as it has been shown by Darzynkiewicz et al. (1979; 1990) that a brief treatment of ethanol fixed cells with citric acid partially denatures the DNA , i.e., unwinds the double helix. Under these conditions acridine orange binds to single DNA and double stranded DNA emitting red and green fluorescence respectively, and cells can be sorted according to both the DNA content and the sensitivity of the chromatin to denaturation. In general, condensed chromatin is more sensitive to acid denaturation and consequently mitotic

and quiescent cells with condensed chromatin (e.g. resting lymphocytes [Darzynkiewicz et al., 1977; 1984]), can be separated from cycling cells. Thus under acid conditions condensed chromatin is preferentially denatured and more accessible to ISEL. In the normal hepatocyte nuclei observed by confocal microscopy there was a very small increase in the heterochromatin content and this presumably under acid conditions would be denatured and more accessible to ISEL.

The use of confocal microscopy to examine the end-labelled nuclei demonstrates that in normal hepatocytes there is a low level of DNA cleavage which increases according to the time in culture (Fig. 5.8). This DNA cleavage process appears to be localised around a small areas of chromatin condensation. In the presence of TGF-$ß_1$ there is a marked enhancement of this process which occurs in parallel with the induction of apoptosis.

Several lines of evidence suggest that the appearance of apoptotic nuclear morphology, characterised by chromatin condensation is not necessarily accompanied by internucleosomal cleavage and may instead reflect the higher order chromatin cleavage into large kbp fragments of DNA. These reports include studies on DU-145 prostatic carcinoma cells (Oberhammer et al., 1993b), oligodendrocytes (Barres et al., 1992), MOLT-4 human lymphoblastoid cells (Beere et al., 1995) and hepatocytes treated with TGF-$ß_1$ (Oberhammer et al., 1993a). However, in my study, I found that endonucleolytic cleavage of DNA giving rise to both the large kbp and nucleosomal fragments occurred in TGF-$ß_1$ treated hepatocytes when analysed by gel electrophoresis (Fig.5.6). These fragments are similar to cationic stimulated DNA cleavage observed in rat liver nuclei. Cycloheximide , which is a protein synthesis inhibitor, blocked all the criteria used to assess apoptosis in study. Gant et al. (1992) have demonstrated 80% inhibition of protein synthesis in primary rat hepatocytes by 0.6µg/ml cycloheximide, which is very similar to the concentration used in this study. In different systems, cycloheximide has been shown to have different effects. Thus for example, in Hep3B cells, the cytocidal effect of TGF-$ß_1$ was not altered by cycloheximide (Lin and Chou, 1992). On the other hand, exposure of cycloheximide to JB1 rat hepatoma cells prevented the engagement of apoptosis induced by cisplatin (Evans and Dive, 1993). Although it is tempting to speculate that cycloheximide prevents the synthesis of 'suicide proteins' which is rapidly turned over, it is interesting to note that cycloheximide did not prevent staurosporine (a general protein kinase C inhibitor) induced apoptosis in hepatocytes (data not shown). This differences may suggest that cycloheximide is interacting with TGF-$ß_1$ signalling pathway. In this respect, cycloheximide is

also able to activate a subfamily of protein kinases (Stress-Activated Protein Kinases, SAPKs) related to MAP-kinases in hepatic cells (Kyriakis et al., 1994). The exact mechanism of inhibition by cycloheximide requires further studies (see later, chapter 6).

Previous studies have shown that chelation of intracellular Zn^{2+} by TPEN triggers apoptosis in thymocytes (McCabe et al., 1993) and Zn^{2+} has been shown to inhibit the Ca^{2+}/Mg^{2+} dependent endonuclease (Duke et al., 1983). I have demonstrated in this study that Zn^{2+} inhibited the apoptotic nuclear morphologic changes as assessed by H33258 staining and it also blocked the formation of end-labelled nuclei. However, when the DNA cleavage was visualised by gel electrophoresis, Zn^{2+} inhibited the internucleosomal cleavage seen in TGF-$ß_1$ treated hepatocytes but not the large fragments. This result suggests that Zn^{2+} has a major inhibitory effect on the downstream DNA cleavage processes. In this respect, Cohen et al. (1992) have shown that the key apoptotic feature in dexamethasone treated thymocytes still occur in the absence of endonuclease activation producing DNA laddering. The ISEL results is interesting since the large fragments were detected on FIGE but without any increase in end-labelled nuclei. This could be explained by the small amount of strand breaks formed in the large fragments (e.g. 300kbp) which is 1500 times less than that formed in DNA ladder (180bp) and the LYSIS II software used to gate the nuclei population cannot discriminate this small increase in labelling. In this respect, recent studies by Hara et al. (1996) have shown that HL-60 cells exposed to campthothecin underwent apoptosis which were protected by TPCK and zinc sulfate as measured by the TdT assay. However, TPCK whilst inhibiting TdT labelling and internucleosomal cleavage, it did not prevent the initial step of DNA cleavage, resulting in DNA fragments ≥50kbp. Another possible explanation is that Zn^{2+} induces a conformational change of the chromatin and does not allow the labelling of the nuclei. Alternatively, a role for topoisomerase II in the formation of the large fragments have been suggested by Filipski et al. (1991) and recent studies have shown that continuous treatment with a topoisomerase II inhibitor, etoposide, resulted in apoptosis and a transient additional band of >600kb (Beere et al., 1995). However, using ISEL, they were not able to label the strand breaks. This was explained as topoisomerase II covalently binds to the 5'-phosphate group of DNA and conceals the 3'-OH ends. The TdT reactions depends on the availability of free 3'-OH DNA ends and therefore concealment of the strand breaks by associated protein would prevent the incorporation of deoxynucleotides. Hence DNA fragment ends produced by and associated with topoisomerase II would not be labelled. Further studies to confirm if any morphological

changes have taken place at the electron microscopy level would be required to further understand the effects of Zn^{2+} on TGF-$ß_1$ treated hepatocytes.

5.4 SUMMARY

This study describes a method for quantitating apoptosis in hepatocyte monolayers in which nuclei were isolated from the cells and DNA strand breaks detected by in situ end-labelling and flow cytometry. This technique detected DNA cleavage in nuclei which did not have an obvious apoptotic morphology. Using confocal microscopy, nuclei from untreated hepatocytes contained low levels of DNA cleavage, which were localised in areas of condensed chromatin and increased according to the time in culture. Thus hepatocytes undergo a progressive and cumulative process of DNA cleavage/chromatin condensation which is markedly enhanced by TGF-$ß_1$. Gel electrophoresis analysis of TGF-$ß_1$ treated cells showed the formation of both large fragments and DNA laddering. Cycloheximide blocked apoptosis in TGF-$ß_1$ treated hepatocytes as assessed by ISEL, morphology and gel electrophoresis suggesting the synthesis of protein(s) is required for the signalling of cell death by this cytokine. On the other hand, Zn^{2+}, an endonuclease inhibitor, abrogated the nuclear condensation and DNA laddering but not the formation of large fragments suggesting its effects on the endonuclease which acts downstream in the execution phase of apoptosis.

6. ICE-like proteases are involved in TGF-β_1 treated hepatocytes

6.1 Introduction

The importance of apoptosis in the liver was first recognised by Kerr et al. (1971) who described the morphology of hepatocytes undergoing programmed cell death after portal vein ligation. Since this early finding, apoptosis has been observed in the liver after administration of acetaminophen (Shen et al., 1991), ethanol (Benedetti et al., 1988), thioacetamide (Ledda-Columbano et al., 1991), during hepatitis virus infection (Searle et al., 1987) and involution or regression of the liver after withdrawal of the mitogen, cyproterone acetate (Bursch et al., 1986). Apoptosis may also be involved in the physiological control of liver size as there is increasing evidence that apoptosis in the liver can be induced by external signalling factors/cytokines. A good example of this is the anti-Fas antibody which binds to the Fas receptor and produces an extensive and lethal apoptotic response in mouse liver (Ogasawara et al., 1993). The other important cytokine involved in controlling liver apoptosis is transforming growth factor-β_1 (TGF-β_1) which is a member of a family of proteins that inhibit growth in a variety of developing cells. However, TGF-β_1 has also been shown to cause liver atrophy after intra-venous injection (Terrell et al., 1993) and parallel studies by Oberhammer et al. (1993) showed that this liver atrophy was due to apoptotic cell death. Significantly, TGF-β_1 was even more effective at inducing apoptosis in the regressing liver after mitogen withdrawal (Oberhammer et al., 1993). Furthermore, TGF-β_1 is also a potent inducer of apoptosis in rat hepatocyte cultures (Oberhammer et al., 1992) and human (Lin and Chou, 1992) and rat hepatoma cell lines (Fukuda et al., 1993).

TGF-β_1 has been shown to bind co-operatively to type-I and type-II receptors and triggers a serine/threonine kinase cascade (Derynck, 1994). Although TGF-β_1 has been shown to induce G_1-growth arrest in epithelial cells (e.g. hepatocytes) and this effect is related to the hypophosphorylation of retinoblastoma protein (Geng and Weinberg, 1993), the mechanisms by which TGF-β_1 produces apoptosis in hepatocytes are as yet unclear. It could be envisaged that there are two phases of TGF-β_1 effects, firstly is the commitment phase and this is followed by the execution phase. The commitment phase will involve a myriad of signalling events possibly receptor mediated which will culminate in priming the cell to die. Once this stage has taken place, the execution phase machinery will be activated in order to complete the cell death programme (reviewed in Earnshaw, 1995). Recent attention has focused on

understanding this commitment phase and a critical role for intracellular proteases has been put forward as key control points in the initiation of apoptosis.

One of the major pieces of evidence for a role of proteolysis came from genetic studies which showed that the product of the *ced-3* gene is a mediator of cell death in the nematode *Caenorhabditis elegans* and has a high degree of homology with interleukin-1ß-converting enzyme (ICE), a mammalian cysteine protease (Yuan et al., 1993). Mutants of *C. elegans* lacking the ced-3 did not undergo programmed cell death (Ellis et al., 1991) and transfection/overexpression of ICE/CED-3 proteases induced apoptosis in a variety of host cells (reviewed in Kumar, 1995). Over the recent years, an increasing number of ICE-like proteases, including Nedd 2 (Kumar et al., 1992), its human homologue ICH-1 (Wang et al., 1994), CPP32/Yama/apopain (Fernandes-Alnemri et al., 1994; Tewari et al., 1995; Nicholson et al., 1995), TX/ICH-2/ICE rel-II (Faucheu et al., 1995; Kamens et al., 1995; Munday et al., 1995), ICE rel-III (Munday et al., 1995), Mch2 (Fernandes-Alnemri et al., 1995a), Mch3α/CMH-1/ICE-LAP3 (Fernandes Alnemri et al., 1995b; Lipke et al., 1996; Duan et al., 1996a) and ICE-LAP6 (Duan et al., 1996b) have been identified.

All of these proteases cleave substrates which must have an aspartic acid in the P_1 position and in ICE the specificity is determined by four amino acids (including aspartic acid) to the left of the cleavage site, the preferred motif being Tyr-Val-Ala-Asp (Thornberry and Molineux, 1995). In the case of CPP32 which is believed to be an important protease involved in apoptosis the substrate motif is Asp-Glu-Val-Asp (Nicholson et al., 1995) which is homologous to the cleavage site on poly (ADP-ribose) polymerase (PARP), a protein whose cleavage is believed to be a marker for apoptosis (Kaufmann, 1996). It is likely that each ICE-like protease will recognise and have a preferred affinity for a specific tetrapeptide motif and this property has been utilised in designing a number of specific peptide inhibitors (Table 6.1). These include N-acetyl-Tyr-Val-Ala-Asp aldehyde (Ac-YVAD.CHO) a specific ICE inhibitor (Thornberry et al., 1992) and N-acetyl-Asp-Glu-Val-Asp-aldehyde (Ac-DEVD.CHO) a potent inhibitor of CPP32 (Nicholson et al., 1995) and Mch3α (Fernandes-Alnemri et al., 1995b). Other peptide inhibitors with less than 4 amino acids are even more potent ICE inhibitors (Dolle et al., 1994) but have less specificity for ICE and can be regarded as inhibitors of both ICE and ICE-like proteases. Benzyloxycarbonyl-Val-Ala-Asp-$CH_2O(CO)[2,6\text{-}(Cl_2)]Ph$ (Z-VAD.DCB) is the most active (Dolle et al., 1994) and has been shown to block IL-1β

production in murine macrophages (Miller et al., 1995). Z-VAD.FMK has the same tri-peptide motif and blocks the apoptotic nuclei promoting activity in Jurkat T cells after Fas antigen

Table 6.1. Properties of various tetra/tripeptide inhibitors

Inhibitor	Peptide Motif	Predicted enzyme specificity	Predicted or known mode of inhibition	Comments
Ac-DEVD.CHO	DEVD	CPP32/Mch3α	Reversible competitive	
Z-DEVD.FMK	DEVD	CPP32/Mch3α	Covalent irreversible	OMe group enhances cell permeability
Ac-YVAD.CHO	YVAD	ICE	Reversible competitive	higher concentrations inhibit CPP32
Ac-YVAD.CMK	YVAD	ICE/CPP32-like	Covalent irreversible.	Inhibits many ICE-like proteases at higher concentrations
Z-VAD.DCB	VAD	ICE/CPP32-like	Covalent irreversible	
Z-VAD.FMK	VAD	ICE/CPP32-like	Covalent irreversible	Potent inhibitor of apoptosis in many systems.
Z-AAD.CMK	AAD	ICE/CPP32-like	Covalent irreversible	Inhibitor of murine and human granzyme B

ligation (Chow et al., 1995), Reaper mediated apoptosis in *Drosophila melanogaster* (Pronk et al., 1996) and apoptosis in THP.1 cells (Zhu et al., 1995), thymocytes (Fearnhead et al., 1995) and in a large variety of mammalian cell types (Jacobson et al., 1996). Furthermore, in a recent study in this laboratory, Z-VAD.FMK has been shown to block the processing of CPP32 in apoptotic THP.1 and Jurkat cells (Slee et al., 1996).

In addition to the growing family of ICE/CED-3 related proteases, possible roles for other proteases have been implicated in apoptosis. Evidence for these came from studies on the effects of various protease inhibitors in different model of apoptosis. Thus for example, TLCK, a serine protease has been shown to inhibit apoptosis in etoposide treated HL-60 cells (Kaufmann et al., 1993) and bile salt treated hepatocytes (Kwo et al., 1995). In thymocytes, TLCK inhibits all the characteristic changes of apoptosis including large fragment formation

and cytoplasmic alteration, indicating that the inhibited protease(s) is an effector of early apoptotic changes. In contrast, TPCK inhibits internucleosomal DNA cleavage but not the early morphological changes such as chromatin condensation suggesting a proteolytic cascade might be involved in thymocyte apoptosis (Fearnhead et al., 1995).

The aim of this study was to investigate the involvement of protease(s) during TGF-$ß_1$ induced apoptosis in hepatocytes. To achieve this, a combination of methods was applied in this study. This includes using a variety of serine and ICE-like protease inhibitors, fluorogenic substrates with high specificity and immunoblotting.

Some of the results in this chapter have been reported in:

Cain, K., Inayat-Hussain, S. H., Couet, C, Cohen, G.M. (1996) A cleavage-site-directed inhibitor of interleukin-1ß-converting enzyme-like proteases inhibits apoptosis in primary cultures of rat hepatocytes. Biochem J;314:27-32

6.2 Results

6.2.1 A serine protease(s) is not involved during apoptosis in TGF-$ß_1$ treated hepatocytes

In this study, the involvement of serine proteases during apoptosis in TGF-$ß_1$ treated hepatocytes was investigated by using specific inhibitors such as TLCK, TPCK and DCI. As shown in Figure 6.1, apoptosis induced in TGF-$ß_1$ treated hepatocytes was not significantly inhibited by pre-incubation with TLCK. These results are in contrast to previously described experiments (Kwo et al., 1995) who demonstrated that TLCK potently inhibited bile-acid induced hepatocyte apoptosis. However, it is worth noting that TGF-$ß_1$ induced apoptosis occurred after a lag phase of 8-16 hours which was much longer than that required for bile-acid (4h). Therefore the results with TLCK must be interpreted with caution as the lack of inhibition could be due to the inactivation/instability of the inhibitor itself in the culture medium. Alternatively, the protease might not be activated until later times in TGF-$ß_1$ treated hepatocytes and at this time of activation, TLCK may have already been degraded in the medium, thus could not inhibit apoptosis. To investigate these problems, TLCK was added at different time points in the culture, i.e. 4 or 8h after addition of TGF-$ß_1$. However, the results showed that TLCK was still not able to block apoptosis after TGF-$ß_1$ treatment (Fig. 6.1). In conclusion, no inhibition of apoptosis was observed with TLCK. Similar results were obtained with TPCK (data not shown).

conclusion, no inhibition of apoptosis was observed with TLCK. Similar results were obtained with TPCK (data not shown).

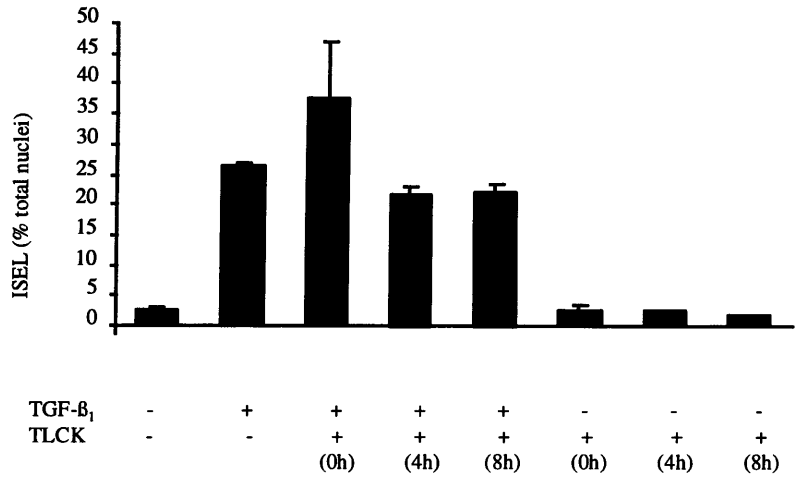

Figure 6.1 Effect of TLCK on TGF-$ß_1$ treated hepatocytes as assessed by ISEL

Hepatocytes were cultured on collagen coated petri dishes as described in methods. Hepatocytes were pre-treated with 100μM TLCK for 30min [shown as (0h)] prior to addition of 1ng/ml TGF-$ß_1$ or the inhibitor added 4h or 8h [shown as (4h) and (8h) respectively] after treatment with TGF-$ß_1$. After 16h, the nuclei were extracted from the cultures and ISEL was performed as described in methods.

The effects of DCI, a general mechanism based serine protease inhibitor was also determined in TGF-$ß_1$ treated hepatocytes. DCI was a very potent inhibitor of multi-step DNA cleavage in rat liver nuclei (see chapter 4). Therefore it was important to determine if this inhibitor would prevent apoptosis in TGF-$ß_1$ mediated apoptosis in hepatocytes. However the results obtained with DCI were inconclusive, i.e. in some experiments it inhibited apoptosis mediated by TGF-$ß_1$ whereas in others, it potentiated apoptosis (data not shown). In marked contrast, Z-VAD.FMK, an ICE-like protease inhibitor abrogated TGF-$ß_1$ mediated apoptosis in hepatocytes and this inhibition was reproducible in every experiment and the mechanisms of this inhibitor was investigated and is described in the next section (see below).

6.2.2 ICE-like protease inhibitors blocks chromatin condensation in apoptotic hepatocytes

Apoptosis was assessed in monolayer hepatocyte cultures after the chromatin had been stained with Hoechst 33258 and using fluorescence microscopy to count nuclei with classical apoptotic morphology. After 16h of culture, TGF-$ß_1$ (1ng/ml) induced about 9% apoptosis (Figure 6.2) and this was accompanied by a 10% decrease in the total number of cells on the

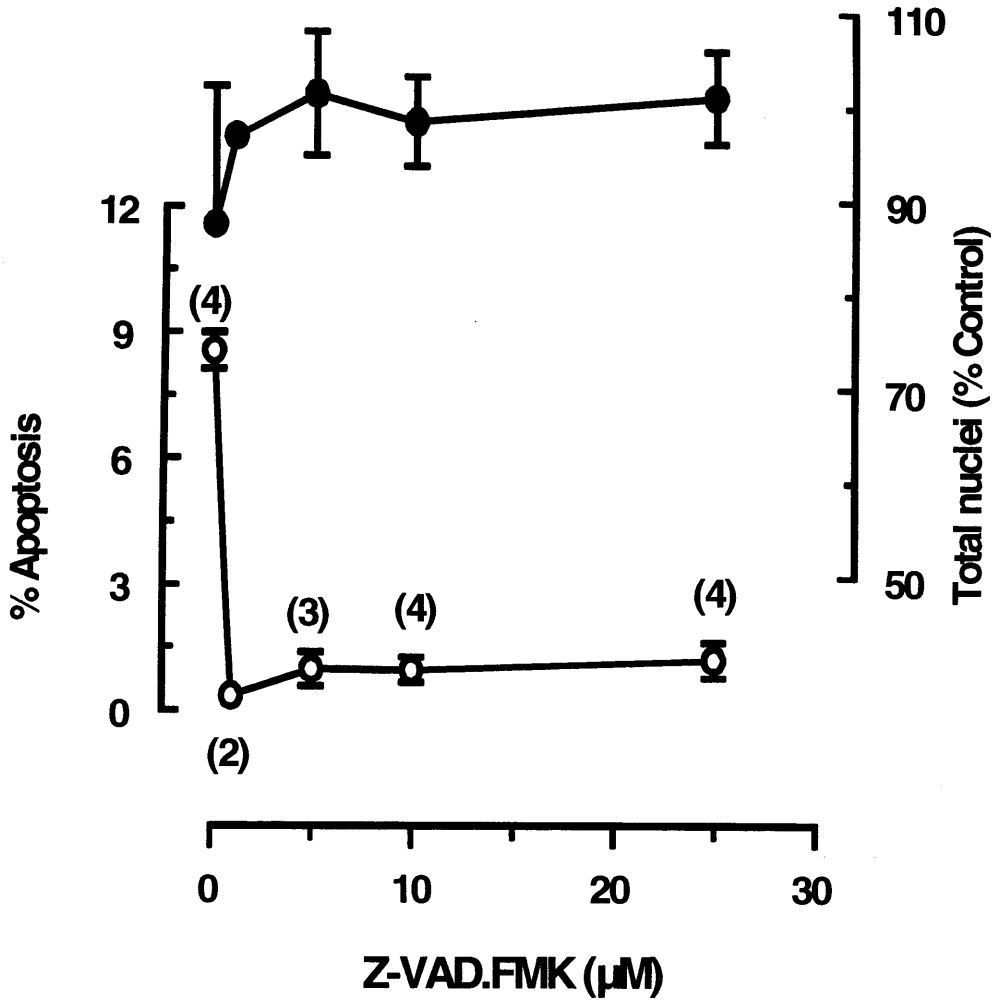

Figure 6.2 Effect of Z-VAD.FMK on TGF-ß$_1$ induced apoptosis in hepatocytes

Hepatocytes were cultured on collagen coated glass coverslips as described in methods section with each treatment carried out in duplicate. Cells were incubated with 1ng/ml TGF-ß$_1$ and the Z-VAD.FMK was added 4h later. After 16h, the number of normal and apoptotic nuclei were determined as described in the methods. A minimum of 10 fields (approx. 200 cells/field) for each coverslip was examined and the average number of nuclei/field calculated. The results are shown where appropriate as the mean ± S.E.M. with the number of experiments in parentheses. Total nuclei (i.e. normal + apoptosis) were expressed as a percentage of the control, i.e. untreated hepatocytes. Apoptotic nuclei were expressed as a percentage of the total nuclei and in control cells this was 0.6 ± 0.3% (n=4). Z-VAD.FMK on its own produced little or no effect. Solid and open symbols refer to total and apoptotic cells respectively.

Thus this loss of cells was due to the apoptotic cells rounding up and detaching from the substratum. Z-VAD.FMK (1-5 μM) totally blocked TGF-ß$_1$ induced apoptosis and reversed the cell loss, demonstrating that this inhibitor was particularly potent at blocking the changes in the morphology of apoptotic nuclei (Figure 6.2). In order to further confirm that the inhibition was not due to the general alkylating effect of the fluoromethyl ketone moiety on the

changes in the morphology of apoptotic nuclei (Figure 6.2). In order to further confirm that the inhibition was not due to the general alkylating effect of the fluoromethyl ketone moiety on the peptide inhibitor (Z-VAD.FMK), but the inhibition requires an aspartic acid residue on the P_1 position, I used two other compounds which have the chloromethyl ketone moiety but an aspartic residue in the P_1 position, i.e. Z-VAD.CMK and Z-AAD.CMK.

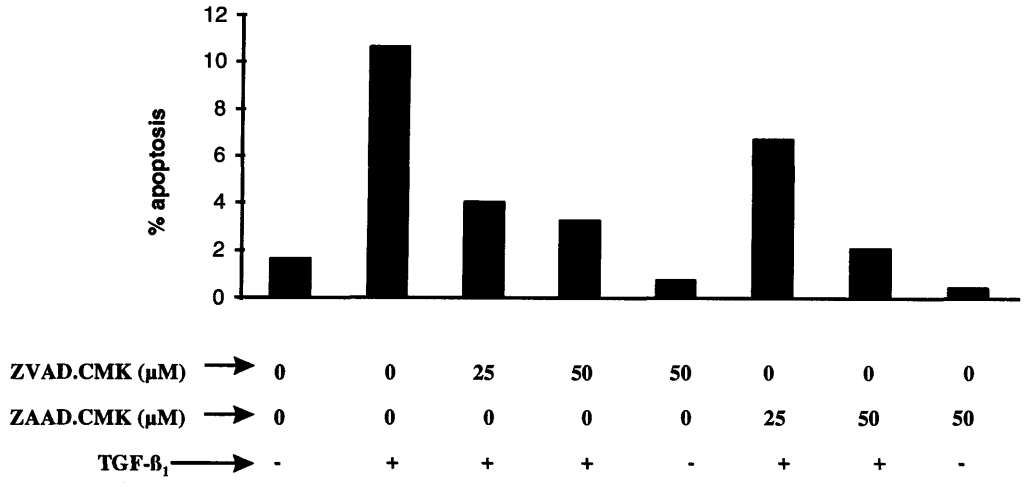

Figure 6.3 Effect of Z-VAD.CMK and Z-AAD.CMK on TGF-ß$_1$ induced apoptosis in hepatocytes

Hepatocytes were cultured as described in Fig.6.1 and each treatment was carried out in duplicate. The cells were pre-incubated with and without the inhibitors and 1ng/ml TGF-ß$_1$ was added 30min later. The cells were fixed and stained with H33258 after 16h as described in methods and the number of apoptotic nuclei counted and expressed as a percentage of the total nuclei. The results shown were mean from two separate experiments.

These compounds, however are not methyl ester derivatives (i.e. the P_1 position of aspartic acid is not methylated) unlike Z-VAD.FMK. Figure 6.3 shows that TGF-ß$_1$ induced apoptosis in hepatocytes was blocked by these compounds albeit at higher concentrations. Thus, 50μM of both Z-VAD.CMK and Z-AAD.CMK were required before 70-80% inhibition of TGF-ß$_1$ induced apoptosis was observed. The higher concentration required by these two compounds (i.e. Z-VAD.CMK and Z-AAD.CMK) is probably due to poor permeability into the cells as they are not methylated and the carboxyl group on the aspartic acid residue renders it more hydrophobic. It is interesting to note that inhibition by Z-AAD.CMK, which has alanine instead of valine at the P_3 position, was similar to Z-VAD.CMK suggesting that the P_3 position is relatively unimportant for the inhibitory effects of these tri-peptide inhibitors.

Ac-YVAD.CMK, which on the basis of its tetrapeptide structure should be a more specific ICE inhibitor, also blocked the morphological changes in the nucleus induced by TGF-ß$_1$ (Figure 6.4A). However, Ac-YVAD.CMK was much less potent than Z-VAD.FMK as even

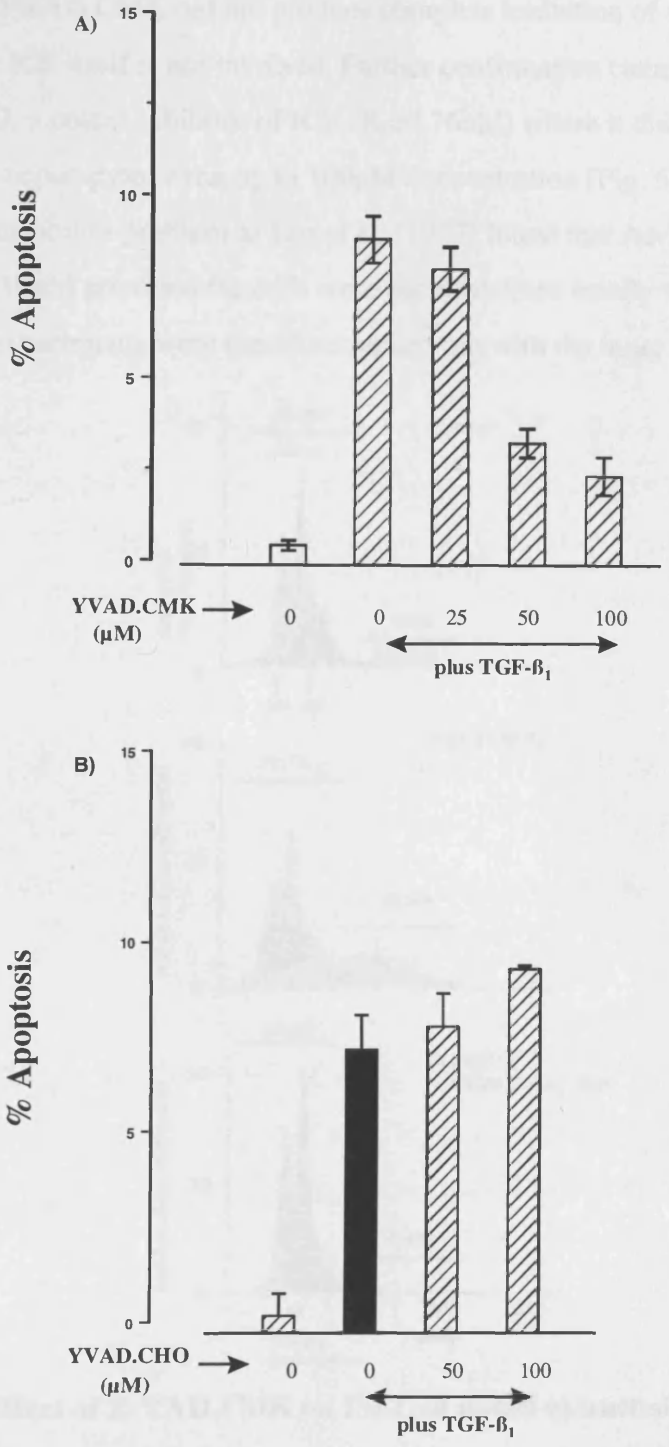

Figure 6.4 Effect of Ac-YVAD.CMK and Ac-YVAD.CHO on TGF-$ß_1$ induced apoptosis in hepatocytes

Hepatocytes were cultured as described in methods and each treatment was carried out in duplicate. In A) the cells were pre-incubated with and without Ac-YVAD.CMK and 1ng/ml TGF-$ß_1$ was added 30min later. In B), similar regime for treatment was carried out except the inhibitor was Ac-YVAD.CHO. The cells were fixed and stained after 16h and the number of apoptotic nuclei counted and expressed as a percentage of the total nuclei. The results from one experiment are shown; essentially the same results were obtained from a separate hepatocyte preparation. The values given are means ± S.E.M from a minimum of ten fields and thus show the interfield variation.

100μM Ac-YVAD.CMK did not produce complete inhibition of apoptosis and this may indicate that ICE itself is not involved. Further confirmation came from studies using Ac-YVAD.CHO, a potent inhibitor of ICE (K_i=0.76nM) where it did not inhibit TGF-$ß_1$ induced apoptosis in hepatocytes even up to 100μM concentration (Fig. 6.4B). However, this may reflect a permeability problem as Los et al. (1995) found that Ac-YVAD.CHO inhibited apoptosis at 10nM provided the cells were permeabilized briefly with hypotonic shock. Remaining experiments were therefore carried out with the more potent, Z-VAD.FMK.

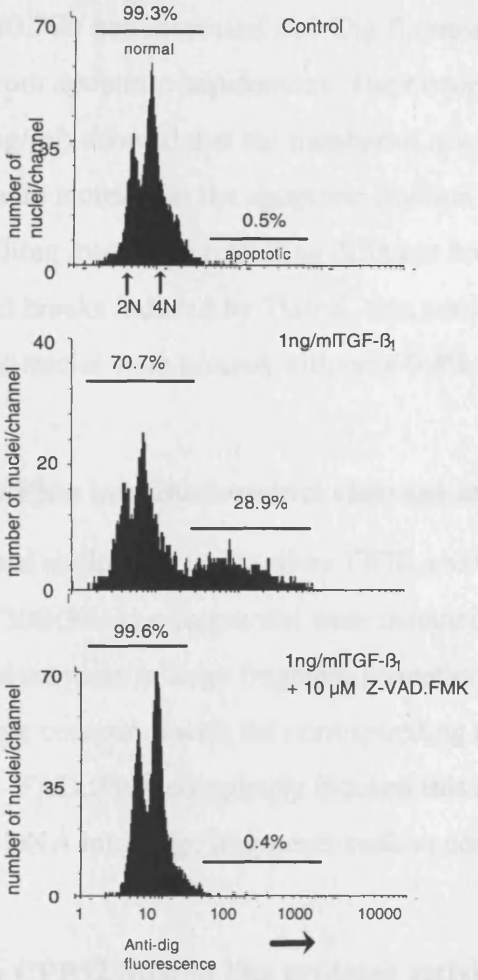

Figure 6.5 Effect of Z-VAD.FMK on ISEL of nuclei extracted from hepatocytes treated with TGF-$ß_1$

Hepatocytes were prepared as described in methods and incubated for 16 h without additions (control), with 1ng/ml TGF-$ß_1$ or with 1ng/ml TGF-$ß_1$ plus 10μM Z-VAD.FMK. The nuclei were isolated and end-labelled as described in the methods section. A univariate frequency histogram is shown with anti-Dig antibody fluorescence (the amount of DNA cleavage) plotted as a logarithmic scale on the x-axis and the number of nuclei per channel plotted on the y-axis. For analytical purposes only the 2N and 4N nuclei were gated (i.e. higher ploidy nuclei and debris were excluded) and in the control this accounted for approx. 60% of the total number of nuclei (i.e. 10^4) counted. The normal and apoptotic nuclei are given as percentage of the gated nuclei and are shown as horizontal bars. The position of the diploid (2N) and tetraploid (4N) nuclei are indicated with arrows.

6.2.3 Z-VAD.FMK blocks ISEL in apoptotic hepatocytes

The induction of apoptosis involves activation of endonucleases that generate DNA-strand breaks with 3'-OH and which can be detected by end labelling. Nuclei were extracted from the monolayer cultures and the DNA strand breaks were labelled as described in chapter 5. The frequency histograms (Fig. 6.5) showed two main peaks of low anti-Dig fluorescence, corresponding to the diploid (2N) and tetraploid (4N) nuclei. In the control, nearly all (i.e. 99.3%) of the gated nuclei were in this region and were normal non-apoptotic nuclei. Only a small number of nuclei (0.5%) had increased anti-Dig fluorescence (note the log scale) and were considered to be from apoptotic hepatocytes. The histogram for nuclei from hepatocytes treated with TGF-$ß_1$ (1ng/ml) showed that the number of normal nuclei had decreased to 70.7% concomitant with an increase in the apoptotic fraction to 28.9%. The apoptotic nuclei had a wide range of labelling intensities reflecting different levels of cleavage. However, the high level of DNA strand breaks induced by TGF-$ß_1$ was completely blocked by Z-VAD.FMK (10μM) and 99.6% of the nuclei were normal with only 0.4% of nuclei showing enhanced ISEL (Figure 6.5).

6.2.4 Z-VAD.FMK abolishes internucleosomal cleavage and large fragment formation

DNA from isolated nuclei was analysed by FIGE and CAGE (Figure 6.6). With the control, 30-50 kbp and 200-300 kbp fragments were detected (Figure 6.6A & B, lane 1). TGF-$ß_1$ produced a small increase in large fragment formation and a marked increase in internucleosomal cleavage compared with the corresponding control (Figure 6.6A & B, compare lanes 1 & 2). Z-VAD.FMK completely blocked this internucleosomal cleavage and reduced the cleavage of DNA into large fragments back to control levels (Figure 6.6A & B, lane 3).

6.2.5 TGF-$ß_1$ induces a CPP32/Mch3α like protease activity in hepatocytes

As shown above, Z-VAD.FMK (5 μM) totally abolished TGF-$ß_1$ induced apoptosis whilst Ac-YVAD.CMK which on the basis of its YVAD motif would be predicted to be a specific ICE inhibitor was a much less effective blocker of apoptosis (i.e. 50% inhibition at 50 μM). Furthermore, Ac-YVAD.CHO, the peptide aldehyde which is believed to be specific (Thornberry et al., 1994) for ICE was also ineffective at inhibiting TGF-$ß_1$ induced apoptosis even at concentrations up to 100 μM (Fig. 6.4). These results therefore suggested that TGF-$ß_1$

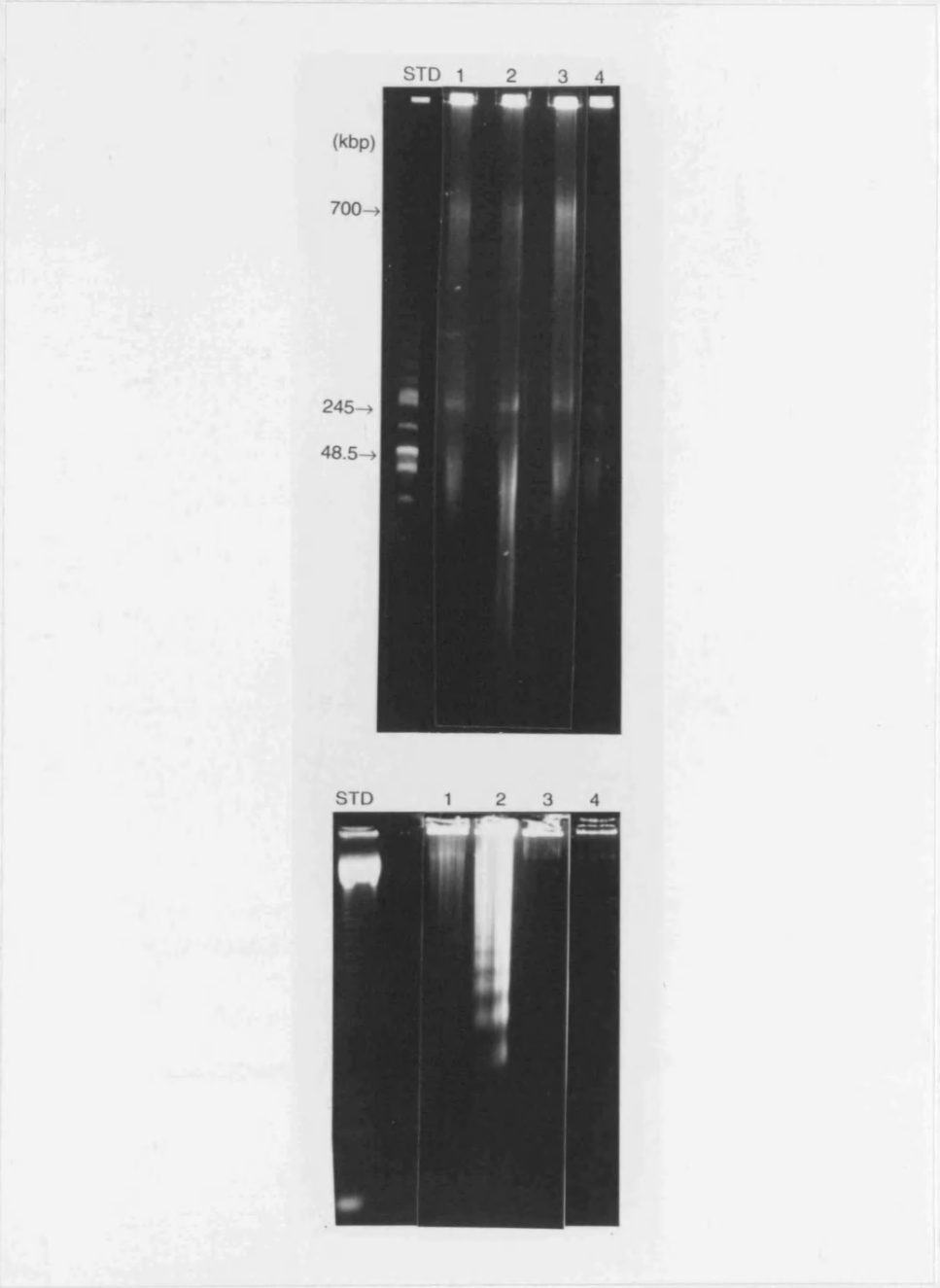

Figure 6.6 FIGE and CAGE of nuclei from hepatocytes treated with TGF-ß$_1$ with and without Z-VAD.FMK

Nuclei were isolated from hepatocytes as described in methods and DNA cleavage was analysed by FIGE (A) and CAGE (B). In the FIGE gel, the STD lane refers to the kbp sizes indicated by arrows and in CAGE , the STD lane refers to markers of 123bp or multiples thereof. Lane 1, nuclei from vehicle treated control hepatocytes, lanes 2 &3, nuclei from hepatocytes treated with 1ng/ml TGF-ß$_1$ and 1ng/ml TGF-ß$_1$ + Z-VAD.FMK (10µM) respectively. Z-VAD.FMK (10µM) alone is shown in lane 4.

was activating an ICE-like protease other than ICE itself and to investigate this Z-DEVD.AFC, an analogue of Ac-DEVD.AMC, was used to measure the protease activity in the lysates isolated from treated cells. These fluorescent tetrapeptide substrates contain DEVD which corresponds to the sequence in PARP and is cleaved by CPP32 (Nicholson et al., 1995) and Mch3α (Fernandes-Alnemri et al., 1995b). The Z-DEVD.AFC analogue has been shown to have identical kinetic properties as Ac-DEVD.AMC with recombinant CPP32 (K. Cain, personal communication).

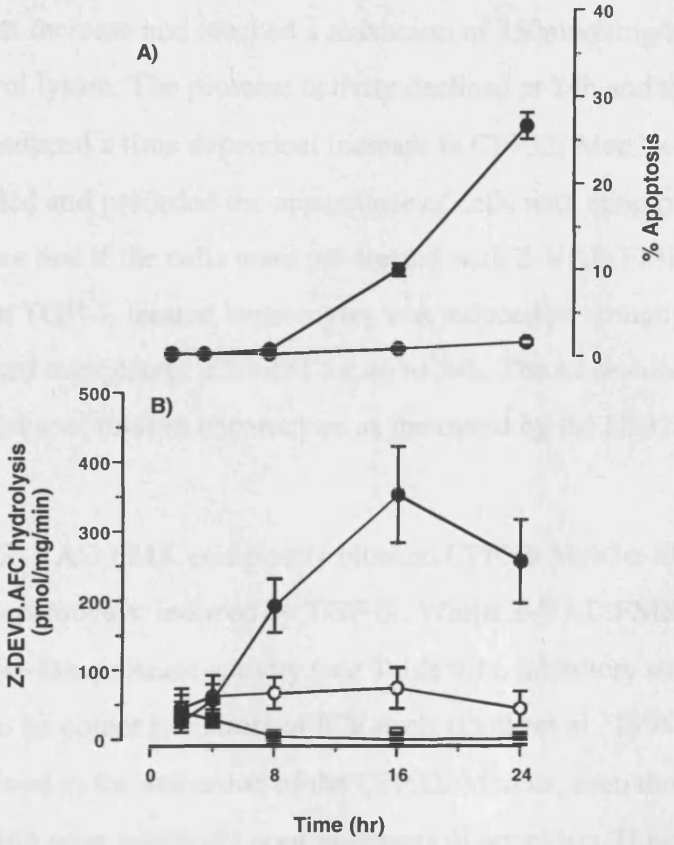

Figure 6.7 Time dependent increase in Z-DEVD.AFC cleavage in lysates isolated from hepatocytes treated with TGF-ß$_1$

Hepatocytes were grown on collagen coated cover slips and treated with 1ng/ml TGF-ß$_1$ as described in the Materials and Methods. At various times, cells were either fixed and assayed for apoptosis using the Hoechst 33258 dye binding method or cell lysates prepared from cells and the Z-DEVD.AFC cleavage activity assayed as described in the Materials and Methods. Panel (A) shows the % apoptosis expressed as the mean ± S.E.M from 20 fields counted i.e. ten fields counted from each cover slip at 200x magnification (total number of cells counted was approx. 2000-3000). Closed circles are from TGF-ß$_1$ treated cells and open circles are control cells. Panel (B) shows the proteolytic activity in lysates isolated from control (○), TGF-ß$_1$ (●), 5μM Z-VAD.FMK (□) and TGF-ß$_1$ + 5μM Z-VAD.FMK (■). The results are shown as the mean ± S.E.M from 4 separate experiments.

In these experiments (Fig.6.7), lysates (cell cytosol) were isolated from hepatocyte cultures at various times after TGF-β_1 (1ng/ml) addition and the Z-DEVD.AFC cleavage activity assayed and compared with the amount of apoptosis as measured by the H33258 dye binding method. As shown in Fig.6.7A, significant apoptosis (9-10%) induced by TGF-β_1 was first detected at around 16h and reached approximately 25% at 24h. The control rate of apoptosis was approx. 1-2% and did not vary over the 24h period. The Z-DEVD.AFC cleavage activity in lysates from control cultures was approximately 30-50pmol/mg/min and remained constant throughout the time course and presumably represents the background level of apoptosis. In contrast the activity in lysates from TGF-β_1 treated hepatocytes showed a time dependent increase and reached a maximum of 350pmol/mg/min at 16h, a 7-fold increase over the control lysate. The protease activity declined at 24h and these results clearly showed that TGF-β_1 induced a time dependent increase in CPP32/ Mch3α-like proteolytic activity which paralleled and preceded the appearance of cells with apoptotic nuclei. Furthermore, Fig.6.7B shows that if the cells were pre-treated with Z-VAD.FMK then the protease activity in lysates from TGF-β_1 treated hepatocytes was reduced to virtually non-detectable levels by 8h and remained completely inhibited for up to 24h. The same concentration of Z-VAD.FMK totally inhibited apoptosis in hepatocytes as measured by the H33258 dye binding method (Fig. 6.2).

Thus, Z-VAD.FMK completely blocked CPP32/ Mch3α-like protease activity and apoptosis in hepatocytes induced by TGF-β_1. Whilst Z-VAD.FMK is a potent inhibitor of CPP32/ Mch3α-like protease activity (see Table 6.1), inhibitors with the Z-VAD motif could be predicted to be potent inhibitors of ICE itself (Dolle et al., 1994) and it is possible that ICE could be involved in the activation of the CPP32/ Mch3α, even though Ac-YVAD.CMK and Ac-YVAD.CHO were relatively poor inhibitors of apoptosis. However, I could not detect any ICE activity using Ac-YVAD.AMC (data not shown), a specific ICE fluorogenic substrate.The conclusion that a CPP32/ Mch3α like protease was being activated was further strengthened by the experiments described in Fig.6.8. In this experiment (Fig.6.8B), Ac-DEVD.CHO, a specific, potent reversible inhibitor of CPP32 (Nicholson et al., 1995) inhibited TGF-β_1 induced apoptosis, although it was less potent than Z-VAD.FMK. However another DEVD analogue, Z-DEVD.FMK was a much more potent inhibitor of apoptosis as 10μM Z-DEVD.FMK completely blocked TGF-β_1 induced apoptosis (Fig.6.8A). Thus, this compound which is

presumably (because of the OMe group) more lipid soluble than Ac-DEVD.CHO was of at least a comparable potency to Z-VAD.FMK.

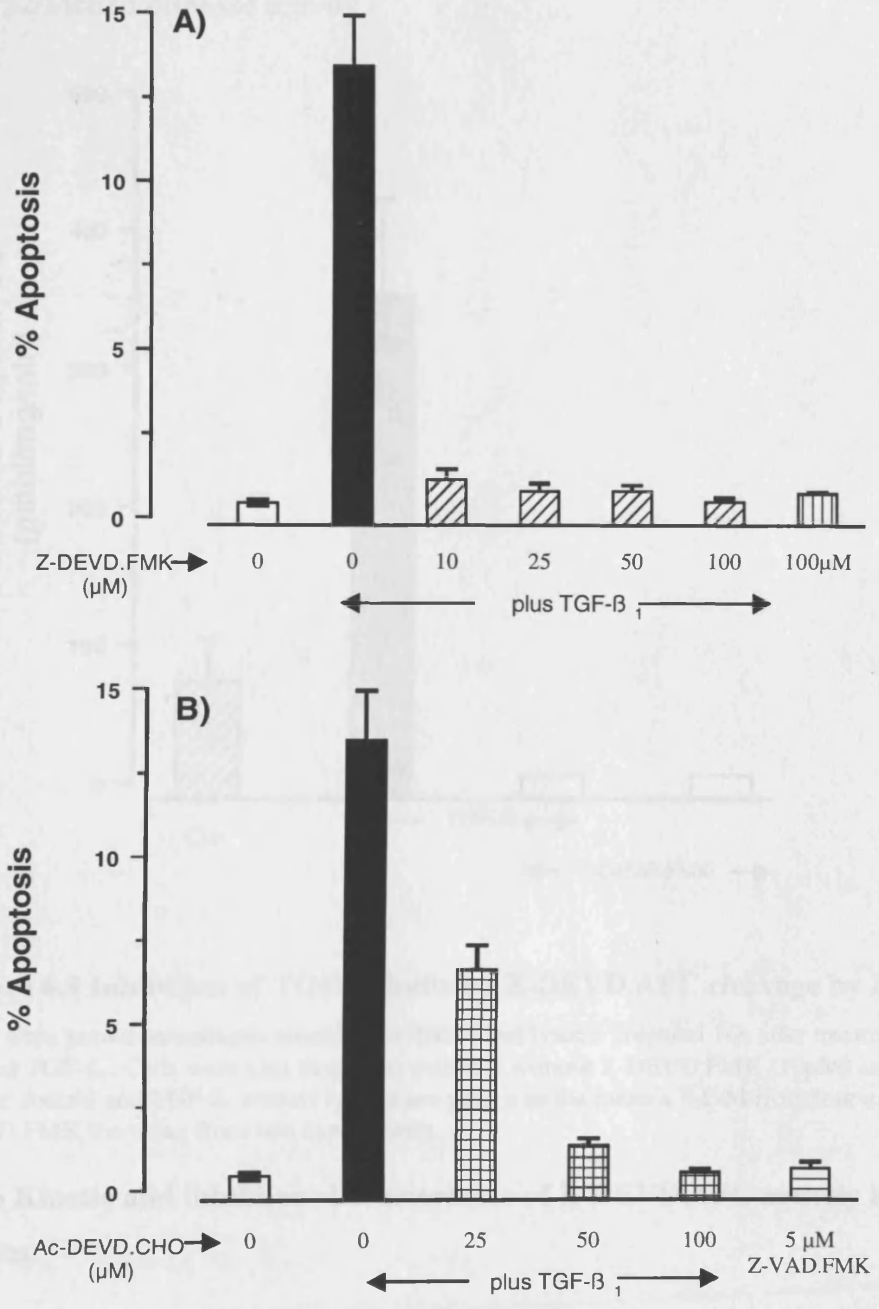

Figure 6.8 Inhibition of TGF-$ß_1$ induced apoptosis by Ac-DEVD.CHO and Z-DEVD.FMK

Hepatocytes were cultured as described in Figure 6.1 and each treatment was carried out in duplicate. The cells were pre-incubated for 30min with the indicated concentrations of Z-DEVD.FMK before adding 1ng/ml TGF-$ß_1$. The cells were fixed and stained after 16h with H33258 as described in Figure 6.1 and the % apoptosis determined from 20 separate fields.

Furthermore, the Z-DEVD.AFC cleavage activity in lysates isolated from hepatocytes treated with TGF-$ß_1$ in the presence of Z-DEVD.FMK was completely inhibited (Fig.6.9), demonstrating that this DEVD analogue was inhibiting apoptosis by inactivating the CPP32/Mch3α protease activity.

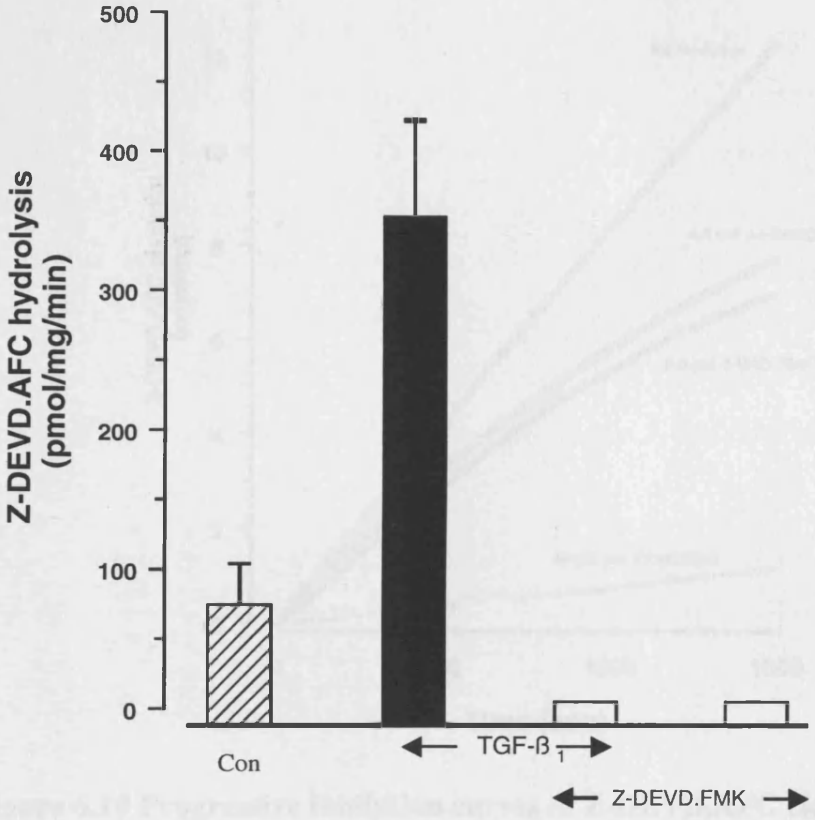

Figure 6.9 Inhibition of TGF-$ß_1$ induced Z-DEVD.AFC cleavage by Z-DEVD.FMK

Cells were grown on collagen coated petri dishes and lysates prepared 16h after treatment with and without 1ng/ml TGF-$ß_1$. Cells were also incubated with and without Z-DEVD.FMK (10μM) as indicated. The results for the control and TGF-$ß_1$ treated lysates are shown as the mean ± S.E.M from four experiments and the Z-DEVD.FMK the mean from two experiments.

6.2.6 Kinetic and inhibitor characteristics of Z-DEVD.AFC activity in hepatocyte lysates.

The differential sensitivity of TGF-$ß_1$ induced apoptosis to the effects of the various peptide inhibitors may be due to either permeability differences and/or differences in the potency/selectivity of the compounds as inhibitors of ICE-like proteases. However, detailed analysis of the inhibitory characteristics of the inhibitors used in this study could provide some insights into the mechanisms and characteristics of the enzymes involved. Studying the relative potency of these compounds as inhibitors of Z-DEVD.AFC cleavage in lysates from cells

treated with TGF-$ß_1$ for 16h (Fig.6.10 & Table 6.2) negates any permeability problems. Equation 1 (see chapter 2, section 2.2.13) describes the situation whereby the inhibitor is essentially acting as a suicide substrate. As discussed by Thornberry and Molineaux (1995),

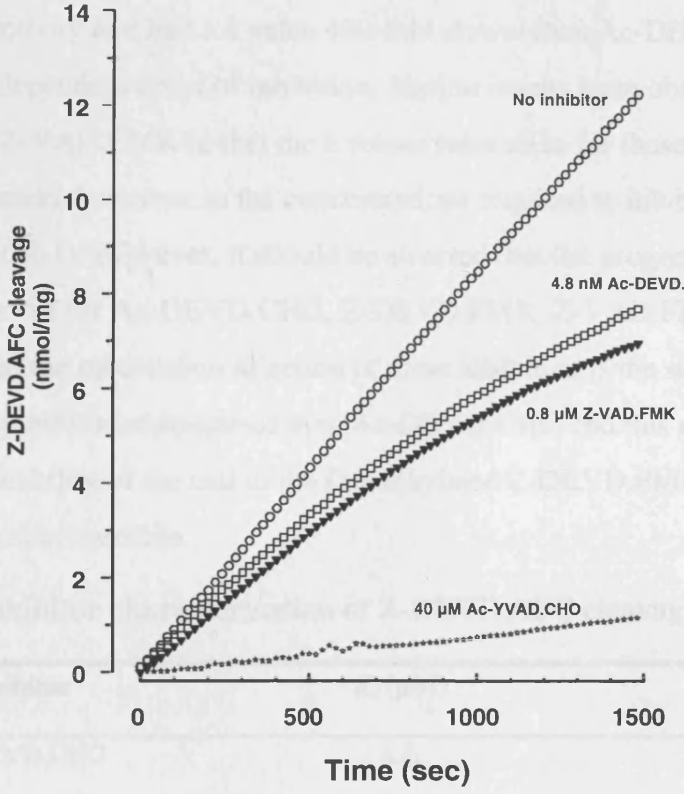

Figure 6.10 Progressive inhibition curves of Z-DEVD.AFC cleavage in activated cell lysate by ICE-like protease inhibitors

Cell lysates were prepared from hepatocytes treated for 16h with (1ng/ml) TGF-$ß_1$ as described in the Methods and incubated with and without the indicated concentrations of inhibitor. The reaction was initiated with enzyme and the production of free AFC monitored for 25 min.

peptide inhibitors of ICE (and ICE-like enzymes) fall into two categories; A) peptide aldehydes which are competitive and reversible inhibitors and B) peptide α-substituted ketones of the general structure R-CO-CH_2 -X , where X is a halogen (halomethylketone), diazonium ion (diazomethylketone) or carboxylate (acyloxymethylketone) leaving group. These inhibitors inactivate cysteine proteases by expulsion of the leaving group X to form a thiomethylketone with the active cysteine. Both reversible and irreversible selective inhibitors of ICE and CPP32 (Nicholson et al., 1995; Thornberry et al., 1994) exhibit slow binding to form the EI complex and a fast transformation step to produce the inactivated enzyme EI* as shown by the time-dependent progression to equilibrium and inhibition. This is illustrated for hepatocyte lysates by the two examples shown in Fig.6.10 for Z-VAD.FMK and Ac-DEVD.CHO. Similar curves

were obtained at different concentrations of both inhibitors and also for Z-DEVD.FMK (data not shown). The second order rate constant (k) was calculated and these are shown in Table 6.2. Both Ac-DEVD.CHO and Z-DEVD.FMK were more potent inhibitors of Z-DEVD.AFC cleavage activity than Z-VAD.FMK which required μM concentrations to inhibit the proteolytic activity and had a k value 400-fold slower than Ac-DEVD.CHO in which there was a slow time dependent onset of inhibition. Similar results were obtained with Z-VAD.CMK, an analogue of Z-VAD.FMK in that the k values were alike for these two compounds (Table 6.2) despite the marked contrast in the concentrations required to inhibit apoptosis in hepatocytes (see section 6.2.1). However, it should be stressed that the progressive time dependent inhibition curves for Ac-DEVD.CHO, Z-DEVD.FMK, Z-VAD.FMK and Z-VAD.CMK are indicative that the mechanism of action of these inhibitors is the same. Z-DEVD.FMK was a more potent inhibitor of apoptosis than Ac-DEVD.CHO and this may be a reflection of the greater permeability of the cell to the O-methylated Z-DEVD.FMK and also perhaps because this inhibitor is irreversible.

Table 6.2 Inhibitor characterisation of Z-DEVD.AFC cleavage in hepatocyte lysates

Inhibitor	K_i (μM)	k ($M^{-1}s^{-1}$)
Ac-DEVD.CHO	n.d.	1.94×10^5
Z-DEVD.FMK	n.d.	2.97×10^4
Z-VAD.FMK	n.d.	5.19×10^2
Z-VAD.CMK	n.d.	6.59×10^2
Ac-YVAD.CHO	12.63	n.d.
Ac-YVAD.CMK	0.6	n.d.
Z-AAD.CMK	2.69	n.d.

Lysates from hepatocytes treated for 16h with TGF-$ß_1$ (1ng/ml) were prepared and Z-DEVD.AFC cleavage activity assayed as described in the materials and methods . The K_m value used in the calculations was calculated by direct fit to a V against S plot using a commercially available curve fitting program (Fig P for Windows, Biosoft, Cambridge, U.K.) and was 37.7 ± 3.0μM. Inhibition studies were carried out with the reaction initiated by the addition of enzyme to buffer containing substrate and inhibitor. The progressive inhibition curves were analysed as described in the Materials and Methods whereas the K_i and k (second order rate constant for inactivation of the enzyme) values where appropriate were determined as described by Thornberry et al., (1994) and Morrison (1982). n.d.: not determined

The third inhibition curve shown in Fig 6.10 demonstrates that Ac-YVAD.CHO also inhibits Z-DEVD.AFC cleavage activity, however, unlike Z-VAD.FMK, Z-DEVD.FMK, Ac-DEVD.CHO and Z-VAD.CMK, there was no progressive inhibition of the cleavage activity and much higher concentrations were needed to inhibit the activity. This is essentially a classical competitive type of inhibition in which the binding of the inhibitor to the enzyme to form the EI complex is relatively fast and the subsequent transformation to the EI* complex is slow or non-existent. The same type of inhibition was found for Ac-YVAD.CMK and Z-AAD.CMK and as shown in Table 6.2, it was not possible to calculate the k values. However, the more appropriate K_i value could be calculated and the results show that the Ac-YVAD.CMK and Z-AAD.CMK compounds were 21-fold and 5-fold more potent than the aldehyde analogue Ac-YVAD.CHO. The difference in the potency explains why these compounds were much more potent than Ac-YVAD.CHO. The compounds with the YVAD motif has been shown to inhibit ICE itself in a progressive manner and this has been demonstrated for Ac-YVAD.CHO which inhibits purified ICE in a progressive manner with a k_{on} value of 3.8×10^5 $M^{-1}s^{-1}$ (Thornberry, 1994). The inhibition of CPP32-like cleavage activity by both the YVAD analogues does not follow this mechanism and there was no evidence of progressive time-dependent inhibition. Essentially these compounds are inhibiting the enzymes by binding to the active site and competing with the substrate. Significantly, Z-VAD.FMK has been shown to inhibit mouse ICE and human CPP32 in a progressive manner with a k values of 1.5×10^5 $M^{-1}s^{-1}$ and 6.6×10^3 $M^{-1}s^{-1}$ respectively (Armstrong et al., 1996). This result demonstrates that the Z-VAD motif can be recognised by both ICE and CPP32-like enzymes which catalyse the conversion to the inactivated thiomethyl ketone, albeit with different inactivation rates. Also Table 6.2 shows that the presence of the CMK group as compared to FMK group makes no difference to the Z-VAD's ability to inhibit Z-DEVD.AFC cleavage.

The inhibition data suggested that the increased ICE-like activity detected in hepatocyte lysates was due to either CPP32 or Mch3α. Furthermore, both these enzymes have been characterised kinetically and the K_m for Ac-DEVD.AMC for recombinant Mch3α and CPP32 expressed in bacterial lysates has been reported to be 51μM and 13μM respectively (Fernandes-Alnemri et al., 1995b) and the K_m for purified human CPP32 was shown to be 9.7 ± 1.0μM (Nicholson et al., 1995). In the case of Z-DEVD.AFC, the K_m for recombinant CPP32 and Mch3α have been shown to be 21 and 61.5μM respectively (K. Cain, personal

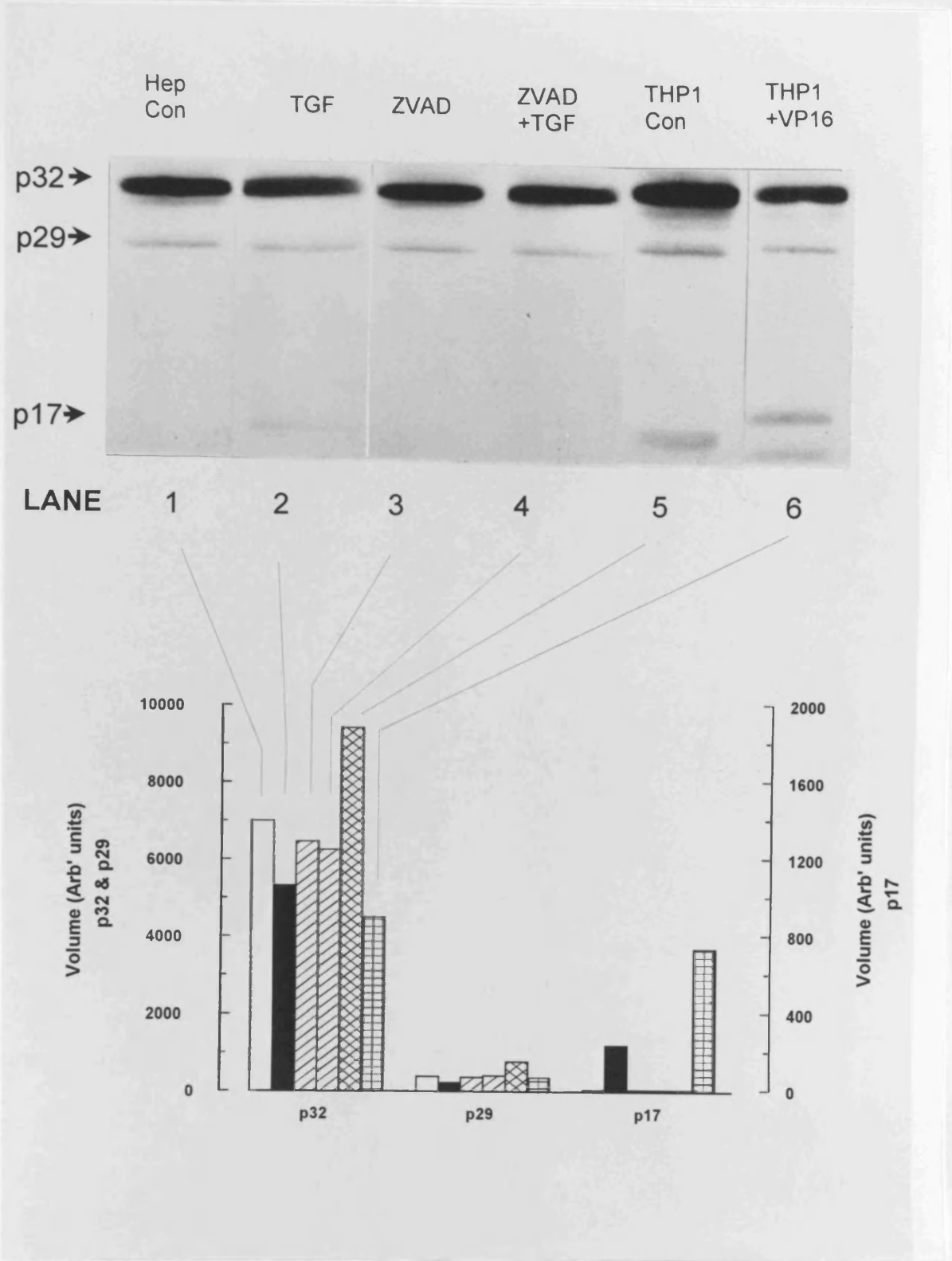

Figure 6.11 Limited processing/activation of CPP32 in hepatocytes

Cell lysates were prepared from hepatocytes cultured with and without 1ng/ml TGF-$ß_1$ for 16h and the processing/activation of CPP32 determined by SDS-PAGE and Western blotting as described in the Materials and Methods. The p32, p29 and p17 proteins are indicated with arrows. The immunoblot was quantitated using a Molecular Dynamics densitometer and Image Quant 3.3 software. The volume of each band is shown in arbitrary units with different scales for (p32+p29) and p17 subunits. All the samples loaded onto the gel contained 100 µg protein and lanes 5 & 6 are from control and etoposide (25µM for 4h) treated THP.1 cells. The remaining lanes (1-4) are hepatocyte lysates with the indicated treatments. The quantitation of the immunoblots is shown in the bar graph and the indicated key for p32 also applies to the p20 and p17.

communication). The K_m for Z-DEVD.AFC in hepatocyte lysates was 37.7 ± 3.0 μM (Table 6.2), indicating that both CPP32 and Mch3α could be involved.

6.2.7 Identification of ICE-like proteases in activated hepatocyte lysates

In order to determine the involvement of CPP32, an antibody to the p17 subunit was used in immunoblotting of the activated hepatocyte lysate for evidence of CPP32 processing. THP1 cells were used to validate the immunoblotting procedure and as can be seen in Fig.6.11, control cells (lane 5) contained predominately unprocessed CPP32, with a small amount of the partially processed enzyme, i.e. without the prodomain and corresponding to the p29 fragment. In the apoptotic THP1 cells (30% apoptosis) which were used as positive control, there was a marked decrease in the p32 and p29 (lane 6) fragments and this was accompanied by the appearance of a p17 band which is one of the subunits of the active enzyme (Nicholson et al., 1995). A slightly smaller band which may be a degradation product derived from the p17 was also detected. In the case of the hepatocyte lysates, only intact p32 and a small amount of p29 was detected in the control cells (lane 1). Lysates from TGF-$ß_1$ treated cells (12% apoptosis) showed an approximate 15% decrease in the amount of p32 (lane 2) and a small increase in the p17 subunit, demonstrating occurrence of a small but limited amount of processing of the inactive enzyme to its active form. This processing was blocked in lysates isolated from cells pre-treated with 10μM Z-VAD.FMK in the presence or absence of TGF-$ß_1$ (lanes 3 and 4 respectively). Similar results (data not shown) were also obtained with both Z-VAD.FMK and Z-DEVD.FMK when total cell proteins were used for immunoblotting.

6.2.8 PARP cleavage is not detected in apoptotic hepatocyte cultures

The activation of CPP32 would indicate that PARP should be cleaved during TGF-$ß_1$ induced apoptosis. However, I was not able to verify this in hepatocyte cultures. Thus, in preliminary experiments with SDS-PAGE and immunoblotting using total cell proteins (data not shown) neither intact nor the cleaved products of PARP were detected. One possible explanation for this result was that the antibody protocol was not detecting PARP. However the validity of the immunoblotting was confirmed by analysing normal and apoptotic rat thymocytes (Fig 6.12A, lanes 1&2) and THP.1 cells (Fig. 6.12B, lanes 3&4) which were used as positive controls. As can be seen in this figure, there was extensive PARP cleavage in both cell types. An alternative explanation was that the level of PARP is very low. However, PARP

is a nuclear protein and the levels should be higher in the isolated organelles and easier to detect. Therefore nuclei were isolated from treated cells and analysed for PARP as shown in Fig.6.12A. In control hepatocyte nuclei (lane 3), a band was detected similar to but slightly higher in molecular weight than the intact 116kDa protein which was clearly visible in the rat

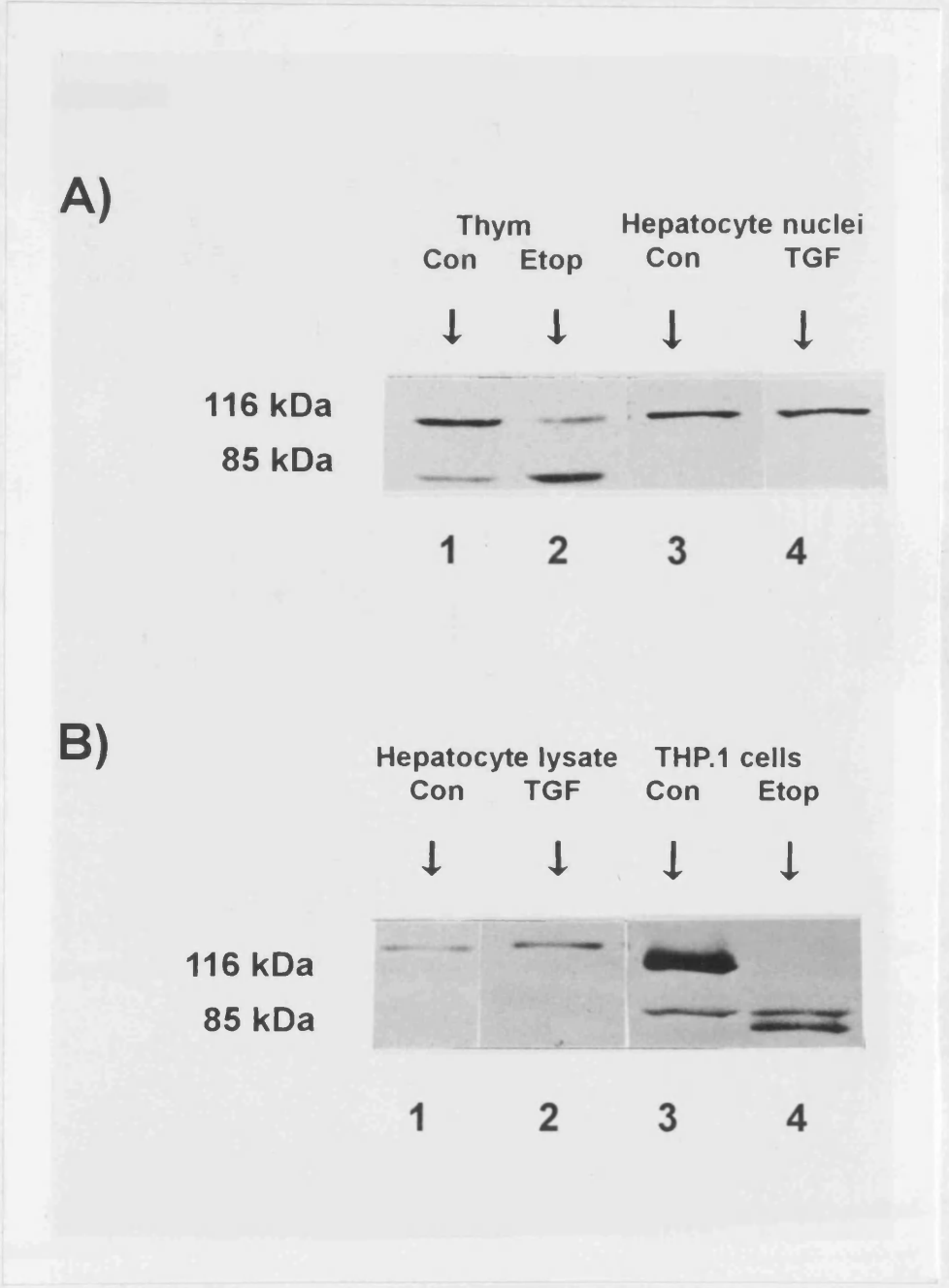

Figure 6.12 PARP cleavage is not detected in hepatocyte nuclei and cell lysates

Cell lysates and nuclei were prepared and analysed by SDS-PAGE and immunoblotting for PARP as described in the Materials and Methods. In panel A, control and apoptotic thymocytes (treated for 4h with 10μM etoposide) were used as positive controls (lanes 1 and 2). In the case of the cell lysates (panel B), THP.1 cells treated as described in Fig.6.11 were used as positive controls (lanes 3 and 4). In both experiments, hepatocytes were treated with and without 1ng/ml TGF-$ß_1$ for 16h.

thymocyte preparation (lane 1). In the thymocytes which have a high level of endogenous apoptosis (10 %) the cleaved 89kDa product was also detected. This band was increased in etoposide treated thymocytes (40-50% apoptosis) with a corresponding decrease in the intact PARP (Fig.6.12A, lane 2). No comparable band was detected in nuclei isolated from hepatocytes (lanes 3-4). The possibility that the cleaved PARP product had leached from the nuclei was then investigated by analysing the lysates for intact PARP. The lysates all contained the slightly higher molecular weight band that was detected in the nuclei (Fig.6.12B, lanes 1-2) but no cleavage products were detected which corresponded to the cleavage product seen in apoptotic THP.1 cells (Fig.6.12B, lane 4).

6.2.9 Cycloheximide blocks TGF-$ß_1$ induced apoptosis and activation of Z-DEVD.AFC cleavage but is not an inhibitor of CPP32/ Mch3α-like proteases.

Cycloheximide is a protein synthesis inhibitor which induces apoptosis in the liver *in vivo* (Faa et al., 1994). In other systems eg. thymocytes (see Schwartzman and Cidlowski, 1993) it blocks apoptosis. However, it has been reported that cycloheximide is ineffective at blocking TGF-$ß_1$ induced apoptosis in a human hepatoma cell line (Lin and Chou,1992).

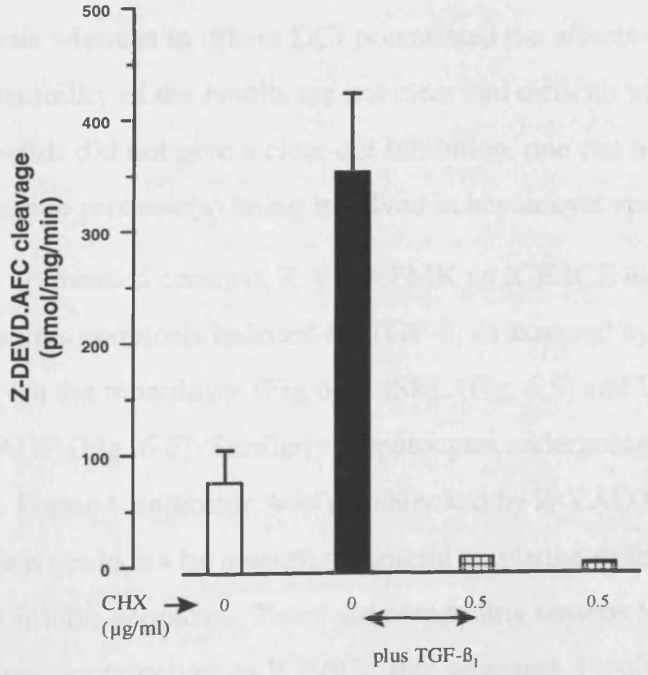

Figure 6.13 Cycloheximide inhibition of TGF-$ß_1$ induced Z-DEVD.AFC cleavage activity

Cells were pre-treated for 30min with the indicated concentrations of cycloheximide before treating with and without 1ng/ml TGF-$ß_1$ as described in the Materials and Methods. Z-DEVD.AFC cleavage activity in cell lysates was quantitated as described in the legends to Figures. 6.7.

In contrast, in rat hepatocytes, I found that cycloheximide was a potent inhibitor of TGF-$ß_1$ induced apoptosis as assayed by the dye binding assay (Fig.5.10 in chapter 5) and the same concentrations completely blocked DNA cleavage as measured by ISEL, field inversion and conventional agarose gel electrophoresis (Fig.5.11 in chapter 5). Significantly, the increased Z-DEVD.AFC cleavage activity in lysates prepared from TGF-$ß_1$ treated hepatocytes was completely blocked if the cells were pre-incubated with 0.5µg/ml cycloheximide (Fig. 6.13). However this concentration of cycloheximide did not inhibit the Z-DEVD.AFC cleavage activity of activated lysates (data not shown) and clearly the action of cycloheximide on cells was not a direct effect on the ICE-like proteases, but rather was an upstream event which prevented the activation of ICE-like proteases.

6.3 Discussion

The involvement of proteases in TGF-$ß_1$ mediated apoptosis in primary hepatocytes was investigated by employing a variety of protease inhibitors. Preliminary studies using serine like protease inhibitors, TLCK (Fig. 6.1) and TPCK (data not shown) did not block TGF-$ß_1$ induced apoptosis. In addition, results obtained with DCI (data not shown), a mechanism based serine like protease inhibitor, was inconclusive as in some experiments it blocked apoptosis whereas in others DCI potentiated the effects of TGF-$ß_1$. This inconsistency in the reproducibility of the results are not clear and difficult to interpret. Although all these compounds did not give a clear-cut inhibition, one can not rule out the possibility of some other serine protease(s) being involved in hepatocyte apoptosis.

In marked contrast, Z-VAD.FMK an ICE/ICE like protease inhibitor prevented hepatocytes apoptosis induced by TGF-$ß_1$ as assessed by chromatin condensation and loss of cells from the monolayer (Fig.6.2), ISEL (Fig. 6.5) and DNA fragmentation analysed by FIGE and CAGE (Fig. 6.6). Similarly, hepatocytes undergoing apoptosis induced by staurosporine, a protein kinase C inhibitor, was also blocked by Z-VAD.FMK (Cain et al., 1996a). The inhibition could not be a result of general alkylation of the halomethyl ketone moiety as TLCK did not inhibit apoptosis. There are compelling reasons to suggest that Z-VAD.FMK and its analogues are targeting an ICE/ICE like proteases. Firstly, the design and specificity of cleavage site directed inhibitor, such as Z-VAD.FMK, is based on the fact that peptide substrate specificity studies with ICE (Thornberry et al., 1992) have shown an almost absolute requirement for aspartic acid in the P_1 position. For substrates of ICE, four amino acids are

required to the left of the cleavage site and liberal substitution can be accommodated in the P_2 position, valine is preferred in P_3 and hydrophobic amino acids particularly tyrosine are required in the P_4 position (see also Table 6.1). However in the case of CPP32 the preferred substrate is DEVD (Nicholson et al., 1995) and this suggests that the substrate specificity of ICE like proteases is determined by the P_2, P_3, and P_4 amino acids. The most potent ICE inhibitor is the reversible competitive inhibitor Ac-YVAD.CHO the specificity of which has been demonstrated by the fact that an affinity ligand, Ac-Tyr-Val-(biotin)-Lys-Asp-$CH_2OC(O)$-[2,6-$(CH_3)_2$]Ph inhibits >99.99% of the ICE activity (which constitutes only <0.001% of the total protein) of THP.1 cell cytosol without labelling any other proteins (Thornberry et al., 1994). However, the inhibition of apoptosis by the ICE specific inhibitors, Ac-YVAD.CHO and Ac-YVAD.CMK in hepatocytes were very poor as shown in Fig. 6.4. Other peptide inhibitors with less than 4 amino acids are even more potent ICE inhibitors (Mashima et al., 1995) but have less specificity (Dolle et al., 1994) for ICE and perhaps can be regarded as inhibitors of both ICE/ICE like proteases. Z-VAD.acyloxy methyl ketone is the most active (Dolle et al., 1994) and has been shown (Miller et al., 1995) to block IL-1ß production in murine macrophages.

In order to further characterise the protease(s) involved in hepatocytes, I have used two approaches, firstly using fluorogenic substrates, Ac-YVAD.AMC and Z-DEVD.AFC for the detection of ICE or CPP32 like protease activity respectively. The second approach was to determine the activation/processing of CPP32 and also PARP by immunoblotting. The results in this study showed that apoptosis in hepatocytes induced by TGF-$ß_1$ initiated the processing/activation of a CPP32-like proteolytic cascade which was detected in the cytosol of apoptotic cells. The increase in Z-DEVD.AFC cleavage was detectable within 4 hr of TGF-$ß_1$ treatment and reached a maximum at 16 hr before declining at 24 hr. Thus, this increase in proteolytic cleavage preceded the onset of apoptosis as detected by the dye binding assay which is essentially detecting apoptosis, via the nuclear chromatin changes. Pre-treatment with Z-VAD.FMK, a covalent inhibitor of ICE/ICE-like inhibitors showed that when the increase in Z-DEVD.AFC cleavage was blocked (Fig.6.7) then there was no apoptosis in hepatocytes. This is the first unequivocal evidence that TGF-$ß_1$ induced apoptosis in hepatocytes occurs by a mechanism which requires the processing and therefore activation of one or more ICE-like proteases. Significantly, other studies in our laboratory have demonstrated that staurosporine

induced hepatocyte apoptosis also occurs via the processing/activation of ICE-like proteases (C.Couet, S.H. Inayat-Hussain and K.Cain, unpublished results).

The precise identification of the proteases responsible for the increased Z-DEVD.AFC activity is as yet a difficult problem. The *Km* data (Table 6.2) suggested that both CPP32 and Mch3α were activated. In the case of CPP32, this was proven by the Western blotting shown in Fig.6.11 which demonstrated that rat hepatocytes contained CPP32 and that there was a small amount of processing as detected by the appearance of the active p17 form. However, the amount of processing did not seem to be sufficient to explain the increased Z-DEVD.AFC cleavage. In this respect using an antibody raised against recombinant Mch3α (unpublished results, C. Couet, S.H. Inayat-Hussain, X-M. Sun, E.S. Alnemri, G.M. Cohen and K. Cain), we have shown the processing of Mch3α during hepatocyte apoptosis induced by either TGF-$ß_1$ or staurosporine. Whilst these results imply that both CPP32 and Mch3α were activated during apoptosis, the possible involvement of other ICE-like proteases could not be ruled out.

An unexpected finding in this study was the lack of PARP cleavage in hepatocytes after TGF-$ß_1$ treatment. A possible explanation for this result is that the level of PARP in hepatocytes which are non-proliferating cells is very low and therefore it could not be detected. However, the rat thymocytes which were used as positive controls were predominantly quiescent cells (85%) (Ritter and Crispe, 1992) and the degradation of PARP was clearly demonstrated (Fig. 6.12, lane 2). An alternative explanation was that the major ICE-like protease(s) activated in hepatocytes is able to cleave Z-DEVD.AFC but this may not be its preferred or usual substrate. This is not unreasonable as Z-DEVD.AFC has been shown to be cleaved by a number of recombinant ICE-like proteases (K. Cain, personal communication). This raises the question whether or not PARP cleavage is a necessary or an essential target during apoptosis and in this respect it has been reported that PARP knock out mice develop normally (Wang et al., 1994).

This study also presents an attempt to try and rationalise the inhibitor potency/selectivity of peptide inhibitors with their effects on apoptosis in intact cells. In this type of analysis, there are two factors to consider; absolute potency and cell permeability of the inhibitor, which in the absence of reliable assay procedures is very difficult to judge. However, in the case of the ICE type inhibitors based on the YVAD motif, both Ac-YVAD.CMK and Ac-YVAD.CHO were relatively poor inhibitors of Z-DEVD.AFC cleavage in cell lysates with

Ki 's of 0.6μM and 12.63μM respectively. Higher concentrations were needed to block apoptosis in the cells but the inhibitory potency ratio of Ac-YVAD.CMK >Ac-YVAD.CHO was maintained. Taken together these results suggest that these inhibitors can penetrate the cell but they are only effective at higher concentrations which inactivate CPP32-like proteases, non-specifically. Furthermore, these results seem to rule out the involvement of ICE itself in TGF-β_1 induced apoptosis in hepatocytes as the K_i for Ac-YVAD.CHO for ICE is 0.73 nM (Thornberry and Molineux,1995) which is significantly lower than the μM concentrations required for inhibiting Z-DEVD.AFC cleavage.

In contrast, Ac-DEVD.CHO and Z-DEVD.FMK were potent inhibitors of Z-DEVD.AFC cleavage. The progressive inhibition of the Z-DEVD.AFC cleavage is evidence that the inactivated enzyme is produced via the normal proteolytic mechanism further supports the use of these inhibitors as selective blockers of CPP32/Mch3α-like enzymes. In this respect in whole cells 25μM Ac-DEVD.CHO was required to give 50% inhibition of apoptosis whereas Z-DEVD.FMK produced virtually complete inhibition at 10μM. However, this is still approximately 5000 times the concentration for inhibiting Z-DEVD.AFC cleavage in lysates and this would suggest that even the OMe compound has a very poor cell permeability. This is perhaps not surprising given the polar nature of the amino acids in the P_3 and P_4 positions.

Z-VAD.FMK inhibited Z-DEVD.AFC cleavage in lysates at very similar concentrations to those required for blocking apoptosis. The progressive inhibition produced by Z-VAD.FMK would suggest that this compound was sufficiently like the normal substrate to be recognised and catalysed by the active site of the enzyme(s). The fact that Z-VAD.FMK has been shown to block apoptosis in a number of different cell systems and with diverse inducers of apoptosis (Chow et al., 1995; Pronk et al., 1996; Zhu et al., 1995; Fearnhead et al., 1995; Jacobson et al., 1996; Cain et al., 1996a) supports the view that this inhibitor is an important tool for investigating the role of ICE-like proteases in apoptosis. However, it should be emphasised with the Z-VAD.DCB analogue show that the Z-VAD motif is an even more potent inhibitor of ICE itself (Dolle et al., 1994). The fact that tripeptide inhibitors with the ZVAD motif can progressively inhibit both CPP32 like and ICE proteases suggest that Z-VAD.FMK has the potential to block the proteolytic cascade at different stages. Perhaps this explains why such compound is so effective at blocking apoptosis in many different systems. This may be extremely important in some situations e.g. Fas-mediated apoptosis (Enari et al., 1995a,b;

Enari et al., 1996) where ICE activation is believed to activate the ICE-like protease cascade. The inhibitory effects of Z-VAD.FMK therefore cannot be taken as proof that this inhibitor is acting only on CPP32 like proteases. However in the case of hepatocytes the effect of the YVAD analogues would appear to rule out the involvement of ICE. In agreement, Kwo et al., (1995) have also demonstrated that glycodeoxycholate induced apoptosis in primary hepatocytes does not involve ICE activation as no cleavage activity of the ICE fluorogenic substrate, Ac-YVAD.AMC was detected.

The results with cycloheximide are extremely interesting as it was clearly very effective at blocking apoptosis in hepatocyte cultures but did not inhibit Z-DEVD.AFC cleavage activity in cell lysates. Cycloheximide is a protein synthesis inhibitor and Gant et al. (1992) have shown in hepatocytes that protein synthesis is 80% inhibited at 0.6 μg/ml which is very similar to the concentrations used in these experiments. It is therefore likely that cycloheximide is inhibiting the synthesis of a rapidly turning over protein which is involved in the initial signalling event responsible for activating the first ICE-like protease in the putative proteolytic cascade. The nature of this signalling event is unknown although studies on Fas/Apo1 and TNF/NGF induced apoptosis which are both receptor mediated cell deaths suggest a possible mechanism. The intracellular domain of the Fas/Apo1 receptor interacts with a protein known as MORT1 (or Fas-associated protein with death domain [FADD]) which binds to a protein known as MACH (Mort 1- associated Ced-3 homolog). This protein contains a region with proteolytic activity, sequence homology to ICE (Boldin et al., 1996) and the same protease has been identified independently by Muzio et al. (1996) which they have designated as FLICE. These results suggest that there is an ICE like protease intimately associated with the receptor complex which is activated when the receptor binds its ligand, thereby initiating the proteolytic cascade. It could be envisaged that as TGF-$ß_1$ is also a receptor mediated event and that there are other MACH/FLICE like proteins which can bind and interact with the TGF-$ß_1$ receptor complex. However, the onset of apoptosis after TGF-$ß_1$ addition is relatively slow (8-16h, Fig.6.7) in contrast to the rapid Fas/Apo1 response (Chow et al., 1995). This implies the activation of of a slower acting pathway. In this respect, new studies (Niehrs, 1996) have identified a class of transcriptional factors known as MAD which are phosphorylated and move into the nucleus on activation of the TGF-ß/activin/BMP receptor complex. It is therefore possible that there are specific proteins that are associated with the TGF-$ß_1$ receptor and when phosphorylated, lead to the activation of transcriptional factors and the synthesis of a

protein(s) which then activate the proteolytic cascade. Cycloheximide by blocking this protein synthesis inhibits the activation of the proteolytic cascade. Significantly, cycloheximide did not inhibit staurosporine induced apoptosis in hepatocytes (unpublished results, C. Couet and K. Cain) suggesting that the mechanism of cycloheximide inhibition is specific to the TGF-β_1 mediated apoptosis.

6.4 Summary

This study describes the involvement of the ICE like proteases in TGF-β_1 mediated apoptosis. A variety of ICE like protease inhibitors were shown to block apoptosis, albeit with different potencies and kinetics. Furthermore increased CPP32 like protease activity and cleavage of CPP32 were detected during apoptosis. These activities were both inhibited by Z-VAD.FMK and Z-DEVD.FMK. In addition, these compounds directly inhibited the cleavage activity in lysates prepared from TGF-β_1 treated hepatocytes. In contrast, cycloheximide abrogated the CPP32 like protease activity and apoptosis but was not able to directly inhibit the activity in TGF-β_1 treated hepatocyte lysates. These results suggest that the initial inactivation event requires a protein(s), the synthesis of which when inhibited by cycloheximide also abolishes the apoptotic effects of TGF-β_1.

7. General Discussion

The studies described in this thesis can be divided into two major sections. The first section describes the characterisation of the mechanisms of DNA cleavage during apoptosis and the role of proteases in this process. The second section comprises the follow-up studies performed to characterise TGF-β_1 mediated apoptosis in hepatocytes and the involvement of proteases in this system.

In an attempt to understand the DNA cleavage mechanisms, rat liver nuclei was used as a model system. Several groups have purified endonucleases from rat liver nuclei, although the role of these enzymes in apoptosis have not been determined (Hewish and Burgoyne, 1973; Cordis et al., 1975; Hibino et al., 1988). It is important to note that although rat liver nuclei do not undergo apoptosis, the cationic stimulated DNA cleavage in this model is similar to that observed during apoptosis (Cohen and Duke, 1984).

Studies using rat liver nuclei described in chapters 3 and 4 significantly contribute to the understanding of DNA cleavage processes in apoptosis. As described earlier, it is now evident that during apoptosis, the DNA is initially cleaved into the large fragments (700, 200-300, 30-50 kbp) which in many cases proceeds to internucleosomal degradation (Walker et al., 1991; Brown et al., 1993; Oberhammer et al., 1993b). I confirmed this observation in rat liver nuclei and further characterised the cationic requirements for these cleavage processes. Thus the initial formation of large kbp fragments is a Mg^{2+} dependent process which can be accelerated by Ca^{2+}. The subsequent degradation into oligonucleosomal fragments requires an absolute presence of both Ca^{2+} and Mg^{2+}. In addition, Mn^{2+} depending on the concentration used can substitute for both Mg^{2+} and Ca^{2+}/Mg^{2+} in the DNA cleavage processes.

Evidence that these two processes are distinct comes from the time course studies (chapters 3 and 4). In this respect, incubation of Mg^{2+} alone (or low Mn^{2+}) only induced the large kbp fragments which produced 30-50kbp at 3h and remained unaltered at 4h, with no internucleosomal cleavage activity. These results indicate that although the endonucleolytic activity is maximal, the endonuclease(s) only cleaves at certain sites of the higher order chromatin to release the 30-50kbp loops. This cleavage activity was not observed when rat liver nuclei were incubated in the presence of Ca^{2+} alone, although this cation facilitated the Mg^{2+} dependent process. In contrast, Zhivotovsky et al. (1994) demonstrated that Ca^{2+} (10μM) alone was sufficient to produce DNA fragments of 700 and 300kbp which contradict

the findings in this thesis and others (Walker et al., 1994; Sun and Cohen,1994). This discrepancy could be due to differences in the methods/buffers used in the isolation of liver nuclei or preparation of agarose plugs for FIGE. It is important to note that the nuclei were resuspended in a buffer containing 5mM Mg^{2+} prior to the formation of agarose blocks in Zhivotovsky's studies. It is therefore possible that Mg^{2+} in this case was also responsible for the cleavage of DNA into the large fragments, and this requires further attention.

The internucleosomal cleavage activity in rat liver nuclei requires the presence of both Ca^{2+} and Mg^{2+}. In addition, high concentrations of Mn^{2+} can induce DNA laddering as well. These results suggest that a separate catalytic activity is involved in this cleavage which is distinct from the Mg^{2+} dependent activity. Indeed earlier studies have identified some endonucleases in rat liver (reviewed in Patel and Gores, 1995). The cationic requirements of these endonucleases have also been characterised, for example Mg^{2+} is required for the maximal activity of the endonucleases purified by Cordis et al. (1975) and Hibino et al.(1988). On the other hand, the endonucleases purified by Hewish and Burgoyne (1973), Ishida et al. (1974) and Burgoyne and Hewish (1977) require both Ca^2 and Mg^{2+} for its peak activity. However the role of these enzymes in liver apoptosis has not yet been established.

Although many mammalian endonucleases have been identified to date, there are a few candidates characterised which might be responsible for the DNA cleavage in apoptosis. These are summarised in Table 7.1 (Peitsch et al., 1994)

Table 7.1 Proposed endonucleases involved in apoptosis

DNases (M_r)	optimum pH	cationic dependence	tissue distribution	cellular localisation
NUC-18 (18 kD)	7.5	Ca^{2+} and Mg^{2+}	studied in thymocytes	nuclei
DNase I (32-37 Kd)	7.5 (5.5-9.0)	Ca^{2+} and Mg^{2+}/Mn^{2+}	widely distributed	secreted ER/nuclear envelope
DNase II (29 kD)	5.5 (3.0-7.0)	none	widely distributed	lysosomes, nuclei

This table has been adapted from Peitsch et al. (1994).

It could be envisaged from the cationic studies that DNase I (or its homologues) is the most likely candidate involved in DNA cleavage in rat liver nuclei. The role of DNase I in apoptosis is a new function for an old enzyme, discovered almost half a century ago by Kunitz (1940) from bovine pancreas (reviewed in Mannherz et al., 1995). DNase I has a pH optimum

of 7.5 and requires Ca^{2+} and Mg^{2+}/Mn^{2+} for its optimal enzymatic activity. Its enzymatic activity is blocked by Zn^{2+} and also chelating agents such as EDTA. Similar pattern of inhibition was observed in this study where Zn^{2+} inhibited both the Mg^{2+} dependent process as well as the Ca^{2+}/Mg^{2+} stimulated DNA cleavage. Furthermore, similar results with Zn^{2+} were obtained in Mn^{2+} dependent DNA cleavage. It is notable that Patel et al. (1994) demonstrated the increase of intracellular Mg^{2+} concentration during bile-salt induced hepatocyte apoptosis. This was accompanied with the increased activity of the Mg^{2+}-dependent endonuclease in the nuclear extract. Interestingly, Zn^{2+} inhibited the activity of this endonuclease.

However there are three lines of evidence which do not support for DNAse I as an apoptotic nuclease in the liver. Firstly, the highest levels of DNase I activity were detected in the parotid gland, kidney and small intestine whereas rat liver showed low levels of this activity (Lacks, 1981). Secondly, DNase I has been shown to be present in the perinuclear space (which is part of the endoplasmic reticulum) by histochemical analysis and not in the nucleus (Peitsch et al., 1993). Finally, DNase I was not inhibited by NEM (Hashida et al., 1982) and DCI (Walker et al., 1994) and is not consistent with the inhibitory characteristics described in this study.

Topoisomerase II has been shown to be associated with AT rich region at the bases of the loop domains and therefore it is possible that this enzyme cleaves DNA into the large fragments (Zlatanova and van Holde, 1992). Furthermore, this enzyme requires Mg^{2+} in promoting enzyme-substrate interactions (Osheroff, 1987). The Mg^{2+} ions participates directly in the enzyme-mediated DNA cleavage reactions. In addition, these cations are involved in topoisomerase II mediated ATPase reactions and functions by providing the enzyme with Mg^{2+} -ATP substrate. In addition Mn^{2+} can replace Mg^{2+} in topoisomerase mediated DNA cleavage (Schomburg and Grosse, 1986). However there are two reasons why this enzyme is probably not responsible for the formation of large fragments in this study. The first reason is that the isolated nuclei system used in this study was not provided with ATP, which is essential for topoisomerase II activity. Secondly, and perhaps the most compelling reason comes from the ISEL results described in chapter 3. The formation of the large kbp fragments in rat liver nuclei can be quantified by ISEL which uses the TdT reaction to label the 3'-OH DNA ends. Topoisomerase II covalently binds to the 5'-phosphate group of DNA and conceals the 3'-OH ends. Such concealment of DNA breaks by associated protein hinders the incorporation of the deoxynucleotides, hence no labelling of DNA strand breaks. This is not the case in liver nuclei

as the formation of large fragments produced many 3'-OH DNA ends that were labelled in the TdT reaction.

To determine the involvement of proteases in the multi-step DNA cleavage processes, I have employed a variety of protease inhibitors as described in chapter 4. The results showed that unlike TLCK and TPCK, DCI was a potent inhibitor of DNA cleavage in liver nuclei. Studies in this laboratory using thymocyte nuclei also showed that TLCK did not inhibit DNA fragmentation (Fearnhead et al., 1995). However, Zhivotovsky et al. (1994) demonstrated that chromatin degradation to 50kbp and smaller (oligonucleosome-size) fragments in rat liver nuclei was prevented by TLCK and TPCK. The differences in these findings are still unclear.

Furthermore, the results with DCI are not compatible with the findings by Walker's group (Weaver et al., 1993; Walker et al., 1994). In fact it is interesting to note that this group published contradictory results in these two papers. Weaver et al. (1994) showed that DCI (100μM) did not inhibit the Ca^{2+}/Mg^{2+} dependent endonuclease activity in isolated thymocyte nuclei and therefore suggested that these compounds did not have a direct effect on the nuclease. In contrast the same group demonstrated that autodigestion of liver and thymocytes nuclei in the presence of DCI (100μM) led to the accumulation of 50-300kbp but no internucleosomal DNA cleavage (Walker et al., 1994). However, both these contradictory findings do not agree with the results described in this study. As described in chapter 4, DCI blocked both the Mg^{2+} and Ca^{2+}/Mg^{2+} dependent processes with similar I_{50}s (10-14μM). Similarly, NEM inhibited these processes with I_{50}s of 6-12μM. However, it should be noted that in the nuclei buffers used in Walker's studies, 0.2mM dithiothreitol (DTT) was included and it has been shown that this dithiol inactivates DCI (Djaballah et al., 1992) and in the current study I showed that the inhibitory effect of DCI was blocked when the inhibitor was incubated in the presence of DTT (Cain et al., 1995, see chapter 4).

DCI and NEM were also able to inhibit the Mn^{2+} dependent DNA cleavage at similar concentrations to the Mg^{2+} and Ca^{2+}/Mg^{2+} dependent processes. As DCI and NEM react with thiols (reversible in the presence of DTT), it is proposed that a critical thiol(s) is involved in this multi-step DNA cleavage. The thiol could be located on the endonuclease and these compounds react with the -SH group rendering it inactive. On the other hand, the thiol could be located on the protease that activates the endonuclease or degrades proteins that block the access to the nuclease. It will be interesting to find out if there is an increase in the nuclear

protease activity and if these inhibitors can block it. Both NEM and DCI have I_{50}s in the low micromolar range which make them useful tools to identify the enzyme(s) involved in DNA cleavage. Future studies using biotinylated DCI or radiolabelled NEM will prove useful in identifying the enzymes involved in the multi-step DNA cleavage and for the histochemical localisation of these targets.

Once the multi-step DNA cleavage in rat liver nuclei was characterised, it was important to determine if such cleavage processes could be duplicated in hepatocytes during apoptosis. In this respect, TGF-$ß_1$ was chosen to mediate apoptosis in hepatocytes and treatment with this cytokine did not induce necrosis (chapter 5). Therefore, any DNA cleavage that occurred after treatment with TGF-$ß_1$ was primarily due to apoptosis. It had been reported by Oberhammer et al. (1993a) that TGF-$ß_1$ treated hepatocytes underwent apoptosis without endonuclease activation. However the studies described in chapter 5 disagree with Oberhammer's findings. In an attempt to investigate the mechanisms of DNA cleavage in hepatocyte apoptosis, I applied the ISEL technique used in rat liver nuclei. Indeed, nuclei isolated from TGF-$ß_1$ treated hepatocytes were end-labelled, confirming the occurrence of DNA strand breaks. When these nuclei were subjected to gel electrophoresis, the same pattern of multi-step DNA cleavage was observed. This observation confirmed the cleavage of higher order chromatin structure and endonuclease activation in hepatocyte apoptosis.

In this study, it was not established if the large fragments occurred prior to internucleosomal cleavage. One difficulty in using this model is that the TGF-$ß_1$ treated hepatocytes did not all die in synchrony, i.e. a subpopulation of cells was affected earlier than others. However further insights into the mechanisms of DNA cleavage were achieved by employing inhibitors such as cycloheximide and Zn^{2+}. Cycloheximide is documented as a potent inhibitor of apoptosis in thymocytes treated with glucocorticoids (Cohen and Duke, 1984; Wyllie et al., 1984) and gamma-irradiation (Sellins and Cohen, 1987). The inhibition has been attributed to the loss of the Ca^{2+}/Mg^{2+} dependent endonuclease possibly due to its rapid turnover (McConkey et al., 1990a). In addition formation of the large fragments of DNA has been shown to be dependent on protein synthesis (Cohen et al., 1994). Furthermore, Sun and Cohen (1994) have observed that cycloheximide inhibits both the Mg^{2+} and Ca^{2+}/Mg^{2+} dependent in thymocyte nuclei from cycloheximide treated animals. These results suggests that a decrease in the large fragment activity which ultimately produce the oligosomal fragments is responsible for the loss of the Ca^{2+}/Mg^{2+} internucleosomal cleavage activity. In this study,

cycloheximide blocked apoptosis as assessed by gel electrophoresis and ISEL. Although it is possible that cycloheximide blocked the synthesis of the enzymes involved in DNA cleavage, studies in this thesis have shown that it inhibited upstream of the DNA cleavage processes (see later).

However, Zn^{2+} which inhibited both the Mg^{2+} and Ca^{2+}/Mg^{2+} dependent DNA cleavage processes in rat liver nuclei, did not show the same pattern of inhibition in TGF-$ß_1$ treated hepatocytes. Therefore while Zn^{2+} inhibited apoptosis as assessed by morphology and ISEL, it only prevented the internucleosomal cleavage activity but not the large fragments. Possible explanations for this discrepancy were described in chapter 5 although exactly why this occurred needs further investigation. However there was an interesting observation with Zn^{2+} in that it blocked the condensation of chromatin and formation of apoptotic bodies during apoptosis as assessed by H33258. Recent findings have shown that lamin cleavage is required for packaging of the condensed chromatin into apoptotic bodies (Lazebnik et al., 1995a). The lamin cleavage activity is sensitive to TLCK inhibition. Later studies by the same group have demonstrated that millimolar concentrations of Zn^{2+} inhibits lamin cleavage by Mch2α (Takahashi et al., 1996). It is therefore possible that in addition to blocking endonuclease(s), Zn^{2+} also inhibited lamin cleavage and this is the reason why morphological apoptosis was abrogated in this study. Further support for this also comes from studies by Kwo et al. (1995) who showed that Zn^{2+} inhibited the non-lysosomal proteolysis and nuclear serine-like protease activity which increased in hepatocyte apoptosis. It will be interesting to determine whether lamins are cleaved in TGF-$ß_1$ treated hepatocytes and what effects Zn^{2+} have on this cleavage.

The final work of this thesis was to characterise the role of proteases in TGF-$ß_1$ mediated apoptosis (chapter 6). Three different approaches were taken to establish the involvement of these proteases. Firstly, a range of protease inhibitors were screened for its ability to inhibit apoptosis, especially the serine and ICE-like protease inhibitors. Once the inhibition pattern was established, the proteolytic activities of these proteases were determined using fluorogenic substrates. Finally immunoblotting was performed to ascertain the cleavage of the proteases and substrate during apoptosis.

Earlier observations indicating the involvement of serine proteases came from studies using protease inhibitors (reviewed Kumar and Harvey, 1995). In the current study, the effects of serine protease inhibitors (DCI, TLCK and TPCK) were also studied in TGF-$ß_1$ induced

apoptosis. The results showed that both TLCK and TPCK did not inhibit TGF-β_1 mediated hepatocyte apoptosis. As mentioned earlier, a recent study demonstrated that TLCK inhibits bile salt induced hepatocyte apoptosis (Kwo et al., 1995). However the inhibitory effects of TLCK seemed to diminish with time of culture. For example, DNA fragmentation at 2h and 4h after bile salt treatment was about 51-52% whereas co-incubation with TLCK resulted in 21% and 35% DNA cleavage respectively. Interestingly the levels of DNA cleavage in control cells also increased significantly with time (1% at 2h and 23% at 4h). Therefore TLCK did not fully protect the cells from dying by apoptosis. TGF-β_1 treated hepatocytes normally takes about 16h before a significant increase in apoptosis can be assessed. A possible reason why TLCK did not inhibit TGF-β_1 induced apoptosis is that the TLCK target(s) was short-lived, and replacement of these targets occurred by de novo protein synthesis. In order to overcome this problem, TLCK was added at 4h and 8h after TGF-β_1 treatment, however no inhibition was observed suggesting that trypsin-like serine protease was not involved in TGF-β_1 induced apoptosis.

The results obtained with DCI were rather difficult to interpret as it exhibited both inhibition and augmentation on TGF-β_1 induced apoptosis. Isocoumarins have a limited stability and lifetime in aqueous buffers and plasma and they are hydrolytically destroyed by physiological nucleophiles such as glutathione and albumin (Harper et al., 1985; Powers and Kam, 1994).The chances of DCI inactivation in the culture is high as intracellular concentrations of glutathione in the hepatocytes are known to be in the millimolar range (Bellomo et al., 1992). Furthermore albumin is synthesised by hepatocytes (Telford and Bridgman, 1995). However, if DCI was inactivated by either glutathione or albumin in the hepatocytes, why it augmented apoptosis in other experiments with exactly similar conditions is still not understood. Therefore it is not possible to state unequivocally the involvement of serine proteases in TGF-β_1 mediated hepatocyte apoptosis. At this stage it cannot be ruled out that these proteases may be required in hepatocyte apoptosis induced by other stimuli.

To investigate the involvement of ICE like proteases in hepatocyte apoptosis, a number of site-directed ICE like inhibitors were employed in this study (see chapter 6). In particular, Z-VAD.FMK and Z-DEVD.FMK, potent inhibitors of ICE-like and CPP32-like proteases respectively blocked apoptosis induced by TGF-β_1. These results suggested that ICE/CPP32-like proteases were required for the execution of apoptosis in this system. In order to further characterise this proteolytic activity, fluorogenic substrates Z-DEVD.AFC and Ac-

YVAD.AMC for both CPP32 and ICE-like proteases respectively were used to assay the cleavage activity of lysates prepared from TGF-$ß_1$ treated hepatocytes. Cleavage activity for the ICE fluorogenic substrate was not detected in the activated lysates. In contrast a time dependent increase in cytosolic CPP32-like protease activity was observed. Interestingly, this activity occurred prior to any detectable nuclear morphological changes. These results propose that the involvement of CPP32-like proteases occurs at a much earlier time and upstream in the apoptotic process.

The CPP32-like activity was abolished when the cells were incubated with Z-VAD.FMK and Z-DEVD.FMK. When these inhibitors were incubated directly with the activated lysate, the proteolytic cleavage activity was also abolished. Further studies on the kinetics revealed that the *k* (second order rate for enzyme inactivation) value for Z-DEVD.FMK was higher than for Z-VAD.FMK. Interestingly, Ac-DEVD.CHO which is a potent inhibitor of CPP32 (Nicholson et al., 1995) and Mch3α (Fernandes-Alnemri et al., 1995b) showed the highest *k* value, suggesting that a major component of this proteolytic activity is CPP32/Mch3α like proteases. Furthermore, immunoblotting studies showed that the increased proteolytic activity was accompanied by processing of pro-CPP32 to its active form. This processing was inhibited by Z-VAD.FMK and Z-DEVD.FMK. In addition Mch3α was also cleaved during TGF-$ß_1$ mediated apoptosis (C. Couet, S.H. Inayat-Hussain, X-M. Sun, G.M. Cohen and K. Cain, unpublished results). Taken together, these results imply that during apoptosis in hepatocytes, a number of proteases are activated to execute this cell death programme.

The members of ICE/CED-3 family are synthesised as pro-forms which require processing to their active forms either by other members of the family, granzyme B or by auto-processing (Kumar and Lavin , 1996). In this respect, a CPP32 activating protease (CAP) has been purified and characterised from hamster liver that cleaves and activates CPP32 (Liu et al., 1996). Protein sequencing reveals that CAP is the hamster homologue of Mch2α. Furthermore, Orth et al. (1996b) have confirmed that Mch2α not only activates pro-CPP32 but it is able to process pro-Mch3α as well. Also since recombinant Mch3α cannot cleave pro-CPP32 but CPP32 can cleave pro-Mch3α, it is possible that CPP32 acts as an intermediate between Mch2α and Mch3α. The inhibitor profile of these proteases have been characterised. For example, CAP was resistant to both ICE specific inhibitor, Ac-YVAD.CHO and Ac-

DEAD.CHO, inhibitor of CPP32 up to 1μM. Studies in this laboratory have demonstrated that Z-VAD.FMK inhibits apoptosis by preventing the processing of CPP32 to its active form (Slee et al., 1996). It is tempting to speculate that during TGF-$ß_1$ induced apoptosis, CPP32 was activated by CAP/Mch2α and Z-VAD.FMK blocked this processing. It is apparent from the kinetics data that Z-VAD.FMK which required μM concentrations to abrogate the proteolytic activity of TGF-$ß_1$ treated lysates, had a *k* value of 400 fold slower than Ac-DEVD.CHO. Similar concentrations of Z-VAD.FMK inhibited apoptosis in the cells, and together these results would suggest that Z-VAD.FMK's target(s) are upstream of CPP32/Mch3α.

As Z-VAD.FMK has been shown to inhibit ICE (Dolle et al., 1994), and ICE can cleave pro-CPP32 (Tewari et al., 1995b; Quan et al., 1995) it is necessary to determine the role of ICE in this system. However there are three lines of evidence derived from this study which suggest that ICE is not involved in TGF-$ß_1$ mediated apoptosis. Firstly, the ICE specific inhibitors Ac-YVAD.CMK and Ac-YVAD.CHO were both poor inhibitors of apoptosis. It could be argued that the aldehyde analogue is not permeable (Los et al., 1995) and therefore these results are not truly representative. However another aldehyde, Ac-DEVD.CHO a potent inhibitor of CPP32-like proteases blocked apoptosis significantly from 25μM-100μM. One would expect that this compound is less permeable than Ac-YVAD.CHO as it contains two glutamic acid residues and therefore less permeable than the latter. Secondly, the ICE specific activity could not be detected with the fluorogenic substrate for ICE, Ac-YVAD.AMC. Similar results were obtained in bile-salt induced hepatocyte apoptosis (Kwo et al., 1995). Finally, the K_i of Ac-YVAD.CHO for the proteolytic activity in the activated lysate was 12.63μM, which is more than 10,000 fold higher from the K_i of ICE (0.73nM) (Thornberry et al., 1992). It is worth noting that Enari et al. (1996) have demonstrated that Fas sequentially activates ICE and CPP32-like proteases and that the CPP32 like activity depends on the presence of ICE-like activity. This type of study is difficult to perform in this system because hepatocytes do not respond to TGF-$ß_1$ simultaneously, therefore it is difficult to see any increase in ICE activity.

There is now an increasing wealth of information on the substrates cleaved during apoptosis by ICE-like proteases (reviewed in chapter 1). CPP32, for example has been shown to cleave PARP (Nicholson et al., 1995), D4-GDI (Na et al., 1996), DNA-PK_{cs} (Casciola-Rosen et al., 1996), U1-70kDa (Casciola-Rosen et al., 1996) and SREBPs (Wang et al., 1996b). As the fluorogenic substrate (Z-DEVD.AFC) contains the PARP cleavage site (DEVD), the cleavage of this nuclear protein was investigated using immunoblotting

technique. The results showed that PARP cleavage was not detected in either the whole cells, nuclei or lysates from TGF-$ß_1$ treated hepatocytes. These results are in agreement with previous studies by Armstrong et al. (1994) who showed the absence of PARP cleavage during apoptosis in breast cancer cells. Furthermore PARP knockout mice developed normally indicating that PARP is not an essential target during apoptosis (Wang et al., 1994a). However cleavage of other CPP32 substrates during apoptosis in hepatocytes has not been investigated in this study.

Cycloheximide, a widely used protein inhibitor blocked apoptosis induced by TGF-$ß_1$ in this system. In addition to preventing the nuclear changes, cycloheximide (0.5µg/ml) also abrogated the increase in proteolytic activity during apoptosis. Interestingly, this compound did not directly inhibit the cleavage activity in activated lysates. Although inhibition of protein synthesis by cycloheximide was not assessed in this study, previous studies have demonstrated that cycloheximide (0.6µg/ml) blocks approximately 80% protein synthesis in primary hepatocytes (Gant et al., 1992). Recent studies have also shown that CPT-11 (a topoisomerase II inhibitor) induced apoptosis in human hepatoma cells is blocked by cycloheximide (0.5µg/ml) (Suzuki and Kato, 1996). They propose that apoptosis in human hepatoma cells requires de novo synthesis of an apoptotic initiator. However, in this laboratory, inhibition by cycloheximide was unique to TGF-$ß_1$ treatment as staurosporine induced hepatocyte apoptosis was not affected by cycloheximide (C. Couet, S.H. Inayat-Hussain, K.Cain, unpublished results). Collectively, these results suggest that cycloheximide inhibits the synthesis of the 'death activator' which is required for activation of the proteolytic cascade in TGF-$ß_1$ induced apoptosis. From the studies described in this thesis, a scheme for TGF-$ß_1$ mediated apoptosis is presented as shown in Figure 7.1.

The molecular mechanisms by which TGF-$ß_1$ prime the cells to apoptosis have not been established. Recent studies showed that TGF-$ß_1$ directly suppressed the expression of anti-oxidative enzymes including Mn-SOD, Cu/Zn-SOD, catalase and gluthathione -s-transferase in cultures of rat hepatocytes (Kayanoki et al., 1994). Furthermore they found an increase of peroxides and suggested that TGF-$ß_1$ augmented production of peroxides by suppressing anti-oxidative enzymes which may participate in cellular injury. However this study did not investigate the effects of TGF-$ß_1$ on hepatocyte apoptosis, although the concentration used

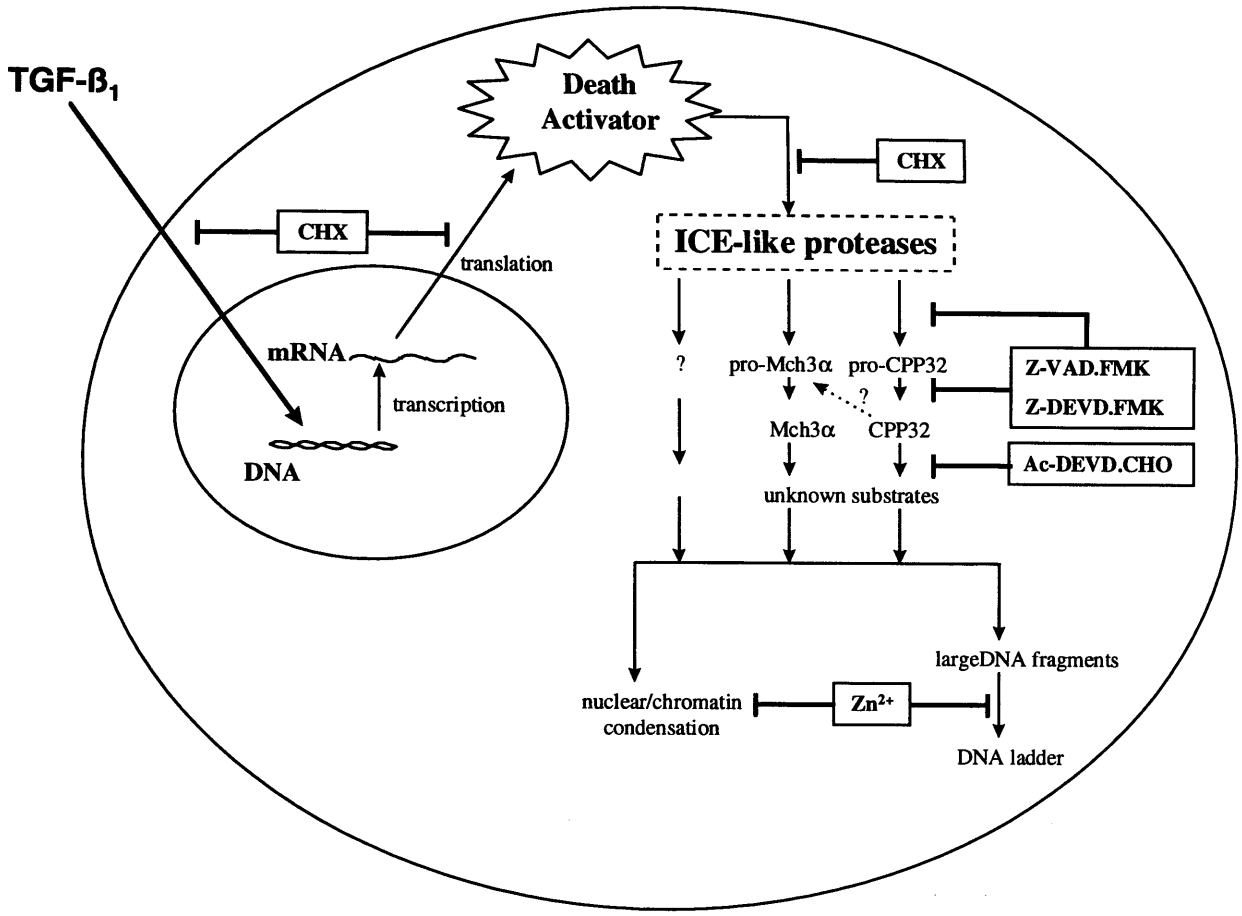

Figure 7.1 Involvement of ICE-like proteases in TGF-ß1 mediated hepatocyte apoptosis

This illustration summarises the effects of the inhibitors used in this study and their possible targets in hepatocytes undergoing apoptosis. In brief, TGF-ß1 mediates its action through a newly synthesised death activator. The death activator triggers off the cascade of ICE-like proteases which precedes the endonuclease activation and nuclear fragmentation.

(10ng/ml) are known to induce apoptosis (Oberhammer et al., 1992; Cain et al., 1996b). To further corroborate this suggestion, Sanchez et al. (1996) demonstrated that TGF-ß1 induced apoptosis in foetal hepatocytes was preceded by an induction of reactive oxygen species production and a decrease in the gluthathione intracellular content. In addition, the mRNA levels of c-fos, a gene whose expression is modulated by redox state was elevated after treatment with high apoptotic concentration of TGF-ß1 (2.5ng/ml).Taken together, these results provide evidence for the involvement of oxidative process in apoptosis. Investigating the effects of cycloheximide and the ICE-like inhibitors on this process will lead to better understanding on the hierarchy and sequence of events during apoptosis.

The studies described in this thesis provide evidence for the activation of ICE-like proteases as an early event during apoptosis. The increased proteolytic activity is perhaps a good marker to identify cells that are committed to die but have not exhibited any

morphological changes. This is particularly relevant in the liver system as the detection of earliest visible stage of apoptosis is somewhat difficult and rare because the appearance is limited to only a few minutes (Goldsworthy et al., 1996). Conversely, apoptotic bodies are normally visible for a few hours in the liver but exist in diverse forms and sizes This complicates the quantification of the incidence in the liver. Therefore new and sensitive method for detecting apoptosis is required and in this respect, ICE-like proteases are good candidates. Moreover, further work will be necessary before a complete understanding of the molecular mechanism of TGF-$ß_1$ mediated apoptosis can be accomplished.

In conclusion, this study has provided a much fuller understanding of the DNA cleavage processes in liver nuclei and provided the first demonstration that TGF-$ß_1$ induced apoptosis occurs through the activation of ICE-like proteases.

References

Alnemri, E.S., Livingston, D.J., Nicholson, D.W., Salvesen, G., Thornberry, N.A. Wong, W.W. and Yuan, J. (1996) Human ICE/CED-3 protease nomenclature. Cell 87, 171.

An, B. and Dou, Q.P. (1996) Cleavage of retinoblastoma protein during apoptosis : an interleukin 1ß-converting enzyme-like protease as candidate. Cancer Res. 56, 438-442.

Anand, R. and Southern, E.M. (1990) Pulsed Field Gel Electrophoresis. *In* Gel Electrophoresis of Nucleic Acids : A Practical Approach 2nd Ed. *Edited by* D. Rickwood and B.D. Hames. IRL Press, Oxford. pp. 101-123.

Ando, K., Moriyama, T., Guidotti, L.G., Wirth, S., Schreiber, R.D., Schlicht, H.J., Huang, S.-N. and Chisari, F.V. (1993) Mechanisms of class I restricted immunopathology. A transgenic mouse model of fulminant hepatitis. J. Exp. Med. 178, 1541-1554.

Arends, M.J., Morris, R.G. and Wyllie, A.H. (1990) Apoptosis: The role of the endonuclease. Am. J. Pathol. 136, 593-608.

Arends, M.J. and Wyllie, A.H. (1991) Apoptosis: Mechanisms and roles in pathology. Int. Rev. Exp. Path. 32, 223-254.

Armstrong, D.E., Kaufmann, S.H., Ottaviano, Y.L., Furuya, Y., Buckley, J.A., Isaacs, J.T. and Davidson, N.E. (1994) Epidermal growth factor-mediated apoptosis of MDA-MB-468 human breast cancer cells. Cancer Res.54, 5280-5283.

Armstrong, R.C., Aja, T., Xiang, J., Gaur, S., Krebs, J.F., Hoang, K., Bai, X., Korsmeyer, S.J., Karanewsky, D.S., Fritz, L.C. and Tomaselli, K.J. (1996) Fas-induced activation of the cell death-related protease CPP32 is inhibited by bcl-2 and by ICE family protease inhibitors. J. Biol. Chem. 271, 28, 16850-16855.

Assoian, R.K. Komoriya, A and Meyers, C.A. (1983) Transforming growth factor-beta in human platelets. Identification of a major storage site, purification, and characterization. J. Biol. Chem., 258, 11, 7155-7160.

Barbieri, B., Troiana, L., Grassilli, E., Agnesini, C., Cristofalo, E.A., Monti, D., Capri, M., Cossarizza, Franceschi, C. (1992) Inhibition of apoptosis by zinc: A reappraisal. Biochem. Biophys. Res. Commun. 187, 1256-1261.

Barres, B. A., Hart, I.K., Coles, H.S.R., Burne, J.F., Voyvodic, J.T. and Richardson, W.D. (1992) Cell death and control of cell survival in the oligodendrocyte lineage. Cell 70, 31-46.

Baxter, G.D., Smith, P.J. and Lavin, M.F. (1989) Molecular changes associated with induction of cell death in human T-cell leukemia : putative nucleases identified as histones. Biochem. Biophys. Res. Commun. 162, 30-37.

Bayly, A.C., Roberts, R.A. and Dive, C. (1994) Suppression of liver cell apoptosis in vitro by the non-genotoxic hepatocarcinogen and peroxisome proliferator nafenopin. J. Cell Biol., 125, 1, 197-203.

Beere, H.M., Chresta, C.M., Alejo-Herberg, A., Skladanowski, A., Dive, C., Larsen, A.K. and Hickman, J.A. (1995) Investigation of the mechanism of higher order chromatin fragmentation observed in drug-induced apoptosis. Mol. Pharmacol. 45, 986-996.

Bellomo, G., Vairetti, M., Stivala, L., Mirabelli, F., Richelmi, P. and Orrenius, S. (1992) Demonstration of nuclear compartmentalisation of glutathione in hepatocytes. Proc. Natl. Acad. Sci. USA. 89, 4412-4416.

Bellomo, G., Perotti, M., Taddei, F., Mirabelli, F., Finardi, G., Nicotera, P. and Orrenius, S. (1992a) Tumour necrosis factor α induces apoptosis in mammary adenocarcinoma cells by an increase in intranuclear free Ca^{2+} concentration and DNA fragmentation. Cancer Res. 52, 1342-1346.

Benedetti, A., Brunelli, E., Risicato, R., Cilluffo, T., Jesequel, A.M. and Orlandi, F. (1988) Subcellular changes and apoptosis induced by ethanol in rat liver. J. Hepatol. 6, 137-143.

Beynon, R.J. and Boyd, J.S. (1994) Proteolytic Enzymes: a practical approach. IRL Press

Bhathal, P and Gall, J.A.M. (1985) Deletion of hyperplastic biliary epithelial cells by apoptosis following removal of the proliferative stimulus. Liver 5, 311-325.

Boe, R., Gjertsen, B.T., Vintermeyr, O.K., Houge, G., Lanotte, M. and Doeskeland, S.O. (1991) The protein phosphatase inhibitor okadaic acid induces morphological changes typical of apoptosis in mammalian cells. Exp. Cell. Res. 195, 237-246.

Boldin, M.P., Goncharov, T.M., Goltsev, Y.V. and Wallach, D. (1996) Involvement of Mach, a novel Mort1/FADD-interacting protease, in Fas/APO-1- and TNF receptor-induced cell death. Cell 85, 803-815.

Bortner, C.D., Oldenburg, N.B.E. and Cidlowski, J.A. (1995) The role of DNA fragmentation in apoptosis. Trends Cell Biol. 5, 21-26.

Boudreau, N., Sympson, C.J., Werb, Z. and Bissell, M.J. (1995) Suppression of ICE and apoptosis in mammary epithelial cells by extracellular matrix. Science 267, 891-893.

Brown, D.G., Sun X-M and Cohen, G.M. (1993) Dexamethasone-induced apoptosis involves cleavage of DNA to large fragments prior to internucleosomal fragmentation. J. Biol. Chem. 268, 3037-3039.

Browne, S. J., Williams, A.C., Hague, A., Butt, A.J. and Paraskeva, C. (1994) Loss of APC protein expresed in human colonic epithelial cells and the appearance of a specific low-molecular-weight form is associated with apoptosis in vitro. Int. J. Cancer 59, 56-64.

Bruno, S., Del Bino, G., Lassota, P., Giaretti, W. and Darzynkiewicz, Z. (1992) Inhibitors of proteases prevent endonucleolysis accompanying apoptotic death of HL-60 leukemic cells and normal thymocytes. Leukemia 6, 1113-1120.

Bump, N.J., Hackett, M., Hugunin, M., Seshagiri, S., Brady, K., Chen, P., Ferenz, C., Franklin,S., Ghayur, T., Li, P., Licari, P., Mankovich, J., Shi, L., Greenberg, A.H., Miller, L.K. and Wong, W.W. (1995) Inhibition of ICE family proteases by baculovirus antiapoptotic protein p35. Science 269, 1885-1888.

Burgoyne, L.A. and Hewish, D.R. (1977) The regular substructure of mammalian nuclei and nuclear Ca-Mg endonuclease. In 'The Cell Nucleus' vol. 6, Chromatin, Part A, Bursch, H. (ed), pp. 48-74.

Bursch ,W., Buesterberg, B.and Schulte-Hermann,R. (1986) Growth, regression and cell death in rat liver as related to tissue levels of the hepatomitogen cyproterone acetate. Arch. Toxicol. 95, 221-227.

Bursch, W., Lauer, B., Timmerman-Trosiener I., Barthel, G., Schuppler, J. and Schulte-Hermann R. (1984) Controlled death (apoptosis) of normal and putative preneoplastic cells in rat liver following withdrawal of tumour promoters. Carcinogenesis 5, 453-458.

Bursch, W., Oberhammer, F., Jirtle, R.L., Askari, M., Sedivy, R., Grasl-Kraupp, B., Purchio, A.F. and Schulte-Hermann, R. (1993) Transforming growth factor-$ß_1$ as signal for induction of cell death by apoptosis. Br. J. Cancer 67, 531-536.

Bursch, W., Paffe, S., Putz, B., Barthel, G. and Schulte-Hermann, R. (1990) Determination of the length of the histological stages of apoptosis in rat liver and altered hepatic foci. Carcinogenesis. 11, 847-853.

Bursch, W., Taper, H.S., Lauer, B. and Schulte-Hermann, R. (1985) Quantitative histological and histochemical studies on the occurrence and stages of controlled cell death (apoptosis) during regression of rat liver hyperplasia. Virchows Arch. (Cell Pathol.) 50, 153-166.

Cain, K., Inayat-Hussain, S.H., Kokileva, L. and Cohen, G.M. (1995) Multi-step DNA cleavage in rat liver nuclei is inhibited by thiol reactive agents. FEBS Lett. 358, 255-261.

Cain, K., Inayat-Hussain, S.H., Wolfe, J.T. and Cohen, G.M. (1994) DNA fragmentation into 200-250 and/or 30-50 kilobase pair fragments in rat liver nuclei is stimulated by Mg^{2+} alone and Ca^{2+}/Mg^{2+} but not by Ca^{2+} alone. FEBS Lett. 349, 385-391.

Cain, K., Inayat-Hussain, S.H., Couet, C. and Cohen, G.M. (1996a) A cleavage-site-directed inhibitor of interleukin-1ß-converting enzyme-like proteases inhibits apoptosis in primary cultures of rat hepatocytes. Biochem. J. 314, 27-32.

Cain, K., Inayat-Hussain, S.H., Couet, C., Qin, H.-M. and Oberhammer, F.A. (1996b) A novel method for detecting apoptosis shows that hepatocytes undergo a time dependent increase in DNA cleavage and chromatin condensation which is augmented after TGF-$ß_1$ treatment. Cytometry 23, 312-321.

Carr, B.I., Hayashi, I., Branum, E.L. and Moses, H.L. (1986) Inhibition of DNA synthesis in rat hepatocytes by platelet-derived type ß transforming growth factor. Cancer Res. 46, 2330-2334.

Carthew, P., Nolan, B.M., Edwards, R.E. and Smith, L.L. (1996) The role of cell death and cell proliferation in the promotion of rat liver tumours by tamoxifen. Cancer Lett. 106, 2, pp.163-169.

Cascales, M., Alvarez, A., Gasco, P., Fernandez-Simon, L., Sanz, N. and Bosca, L. (1994) Cocaine-induced liver injury in mice elicits specific changes in DNA ploidy and induces programmed death of hepatocytes. Hepatology 20, 4, 992-1001.

Casciola-Rosen, L.A., Anhalt, G.J. and Rosen, A. (1995) DNA-dependent protein kinase is one of a subset of autoantigen specifically cleaved early during apoptosis. J. Exp. Med. 182, 1625-1634.

Casciola-Rosen, L.A., Miller, D.K., Anhalt, G.J. and Rosen, A. (1994) Specific cleavage of the 70kDa protein component of the U1 small nuclear ribonucleoprotein is a characteristic biochemical feature of apoptotic cell death. J. Biol. Chem. 269, 30757-30760.

Casciola-Rosen, L., Nicholson, D.W., Chong, T., Rowan, K.R., Thornberry, N., Miller, D.K. and Rosen, A (1996) Apopain/CPP32 cleaves proteins that are essential for cellular repair: a fundamental principle of apoptotic death. J. Exp. Med. 183, 1957-1964.

Cerretti., D.P., Kozlosky, C.J., Mosley, B., Nelson, N., Van Ness, K., Greenstreet, T.A., March, C.J., Kronheim, S.R., Druck, T., Cannizzaro, L.A., Huebner, K. and Black, R.A. (1992) Molecular cloning of the interleukin-1ß converting enzyme. Science 256, 97-100.

Chinnaiyan, A.M. and Dixit, V.M. (1996) The cell death machine. Curr. Biol. 6, 555-562.

Chinnaiyan, A.M., Hanna, W.L., Orth, K., Duan, H., Poirier, G.G., Froelich, C.J. and Dixit, V.M. (1996) Cytotoxic T-cell derived granzyme B activates the apoptotic protease ICE-LAP3. Curr. Biol. 6, 7, 897-899.

Chow, S.C., Weis, M., Kass, G.E.N., Holstrom, T.H., Eriksson, J.E. and Orrenius, S. (1995) Involvement of multiple proteases during Fas-mediated apoptosis in lymphocytes. FEBS Lett. 364, 134-138.

Chuang, L.-Y., Hung, W.-C., Chang, C.-C. and Tsai, J.-H. (1994) Characterization of apoptosis induced by transforming growth factor-$ß_1$ in human hepatoma cells. Anticancer Res. 14, 147-152.

Clawson, G., Norbeck, L., Hatem, C., Rhodes, C., Amiri, P., McKerrow, J., Patierno, S. and Fiskum, G. (1992) Ca^{2+} regulated serine protease associated with the nuclear scaffold. Cell Growth Differ. 3, 827-838.

Clem, R.J. and Miller, L.K. (1994) Control of programmed cell death by the baculovirus genes p35 and iap. Mol. Cell. Biol. 14, 5212-5222.

Cleveland, J.L. and Ihle, J.N. (1995) Contenders in FasL/TNF death signalling. Cell 81, 479-482.

Cohen, G.M., Sun, X.-M., Fearnhead, H., MacFarlane, M., Brown, D.G., Snowden, R.T. and Dinsdale, D. (1994) Formation of large molecular weight fragments is a key committed step of apoptosis in thymocytes. J. Immunol. 153, 507-516.

Cohen, G.M., Sun, X.-M., Snowden, R.T. Dinsdale, D. and Skilleter, D.N. (1992) Key morphological features of apoptosis may occur in the absence of internucleosomal DNA fragmentation. Biochem. J. 286, 331-334.

Cohen, J.J. and Duke, R.C. (1984) Glucocorticoid activation of a calcium-dependent endonuclease in thymocyte nuclei leads to cell death. J. Immunol. 132, 38-42.

Collins, R.J., Harmon, B.V., Gobe, G.C. and Kerr, J.F.R. (1992) Internucleosomal DNA cleavage should not be the sole criterion for identifying apoptosis. Int. J. Radiat. Biol. 61, 4, 451-453.

Columbano, A., Ledda-Columbano, G.M., Coni, P.P., Faa, G., Liguori, C., Santa Cruz, G. and Pani, P. (1985) Occurrence of cell death (apoptosis) during the involution of liver hyperplasia. Lab. Invest. 52, 6, 670-675.

Compton, M.M. (1992) a biochemical hallmark of apoptosis : internucleosomal degradation of the genome. Cancer Metastasis Rev. 11, 105-119.

Cordis, G.A., Goldblatt, P.J. and Deutscher, M. (1975) Purification and characterisation of a major endonuclease from rat liver nuclei. Biochem. 14, 2596-2603.

Darmon, A.J., Nicholson, D.W. and Bleackley, R.C. (1995) Activation of the apoptotic protease CPP32 by cytotoxic T-cell-derived granzyme B. Nature, 377, 446-448.

Darzynkiewicz, Z. (1990) Acid-induced denaturation of DNA in situ as a probe of chromatin structure. Methods Cell Biol. 33, 337-351.

Darzynkiewicz, Z., Traganos, F., Andreeff, M., Sharpless, T.K., Melamed, M.R. (1979) Different sensitivity of chromatin to acid denaturation in quiescent and cycling cells as revealed by flow cytometry. J. Histochem. Cytochem. 27, 1, 478-485.

Darzynkiewicz, Z., Traganos, F., Sharpless, T.K., Melamed, M.R. (1977) Cell cycle related changes in nuclear chromatin of stimulated lymphocytes as measured by flow cytometry. Cancer Res. 37, 4635-4640.

Darzynkiewicz, Z., Williamson, B., Carswell, E.A. and Old, L.J. (1984) Cell cycle - specific effects of tumor necrosis factor. Cancer Res. 44, 83-90.

Datto, M.B., Li, Y., Panus, J.F., Howe, D.J., Xiong, Y. and Wang, X.-F. (1995) Transforming growth factor ß induces the cyclin-dependent kinase inhibitor p21 through a p53-independent mechanism. Proc. Natl. Acad. Sci. USA 92, 5545-5549.

Davie, R.D. (1995) The nuclear matrix and the regulation of chromatin organisation and function. Int. Rev. Cyto. 162A, 191-250.

Davies, R., Cain, K., Edwards, R.E., Snowden, R.T., Legg, R.F. and Neal, G.E. (1990) The preparation of highly enriched fractions of binucleated hepatocytes by centrifugal elutriation and flow cytometry. Anal. Biochem. 190, 266-270.

de Murcia , G. and de Murcia, J.M (1994) Poly (ADP-ribose) polymerase: a molecular nick-sensor. Trends Biochem. Sci. 19, 172-176.

Dennis, P. A., and Rifkins, D.B. (1991) Cellular activation of latent transforming growth factor ß requires binding to the cation -independent mannose 6-phosphate/insulin growth factor-II receptor. Proc. Natl. Acd. Sci. USA, 88, 580-584.

Derynck, R. (1994) TGF-$ß_1$-receptor mediated signalling. Trends in Biochem. Sci., 19, 548-553.

Dinarello, C.A. (1991) Interleukin-1 and interleukin-1 antagonism. Blood 77, 1627-1652.

Djaballah, H., Harness, J.A., Savory, J. and Rivett, A.J. (1992) Use of serine-protease inhibitors as probes for the different proteolytic activities of the rat liver multicatalytic proteinase complex. Eur. J. Biochem. 209, 629-634.

Dolle, R.E., Hoyer, D., Prasad, V.C., Schimdt, S.J., Helaszek, C.T., Miller, R.E. and Ator, M.A. (1994) P_1 aspartate-based peptide α-(2,6-dichlorobenzoyl)oxy)methyl ketones as potent time-dependent inhibitors of interleukin-1ß-converting enzyme. J. Med. Chem. 37, 563-564.

Duan, H., Chinnaiyan, A.M., Hudson, P.L., Wing, J.P., He, W.W. and Dixit, V.M. (1996a) ICE-LAP3, a novel mammalian homolog of the *Caenorhabditis elegans* cell death protein CED-3 is activated during Fas- and Tumour Necrosis Factor-induced apoptosis. J. Biol. Chem. 271, 35013-35035.

Duan, H., Orth, K., Chinnaiyan, A.M., Poirier, G.G., Froelich, C.J., He, W.W. and Dixit, V.M. (1996b) ICE-LAP6, a novel member of the ICE/Ced-3 gene family, is activated by the cytotoxic T cell protease granzyme B. J. Biol. Chem. 271, 16720-16724.

Duke, R.C., Chervenak, R. and Cohen, J.J. (1983) Endogenous endonuclease-induced DNA fragmentation: an early event in cell-mediated cytolysis. Proc. Natl. Acad. Sci. USA 80, 6361-6365.

Duvall, R. and Wyllie, A.H. (1985) Death and the cell. Immunol. Today 7, 115-119.

Earnshaw, W.C. (1995) Apoptosis: lessons from in vitro systems. Trends Cell Biol. 5, 217-220.

Ellis, R.E., Yuan, J. and Horvitz, H.R. (1991) Mechanisms and functions of cell death. Annu. Rev. Cell Biol. 7, 663-698.

Emoto, Y., Manome, Y., Meinhardt, G., Kisaki, H., Kharbanda,S., Robertson, M., Ghayur, T., Wong, W.W, Kamens, R., Weicheselbaum, R. and Kufe, D. (1995) Proteolytic activation of protein kinase C δ by an ICE-like protease in apoptotic cells. EMBO J. 14, 6148-6156.

Enari, M., Hase, A. and Nagata, S. (1995a) Apoptosis by a cytosolic extract from Fas-activated cells. EMBO J. 14, 21, 5201-5208.

Enari, M., Hug, H. and Nagata, S. (1995b) Involvement of an ICE-like protease in Fas-mediated apoptosis. Nature 375, 78-81.

Enari, M., Talanian, R.V., Wong, W.W. and Nagata, S. (1996) Sequential activation of ICE-like and CPP32-like proteases during Fas-mediated apoptosis. Nature 380, 723-726.

Evans, D.L. and Dive, C. (1993) Effects of cisplatin on the inductin of apoptosis in proliferating hepatoma cells and nonproliferating immature thymocytes. Cancer Res. 53, 2133-2139.

Faa, G., Ledda-Columbano, G.M., Ambu, R., Congiu, T., Coni, P., Riva, A. and Columbano, A. (1994) An electron microscopic study of apoptosis induced by cycloheximide in rat liver. Liver 14, 270-278.

Fabregat, I., Sanchez, A., Alvarez, A.M., Nakamura, T. and Benito, M. (1996) Epidermal growth factor, but not hepatocyte growth factor, suppresses the apoptosis induced by transforming growth factor-beta in fetal hepatocytes in primary culture. FEBS Lett. 384, 14-18.

Fan, G., Ma, X., Kren, B.T. and Steer, C.J. (1996) The retinoblastoma gene product inhibits TGF-$ß_1$ induced apoptosis in primary rat hepatocytes and human HuH-7 hepatoma cells. Oncogene 12, 1909-1919.

Faucheu, C., Diu, A., Chan, A.W.E., Blanchet, A-M, Miossec, C., Herve, F., Collard-Dutilleul, V., Gu, Y., Aldape, R.A. , Lippke, J.A., Rocher, C., Su, M.S.-S., Livingston, D.J., Hercend, T. and Lalanne, J.-L. (1995) A novel human protease similar to the interleukin-1ß converting enzyme induces apoptosis in transfected cells. EMBO J. 14, 1914-1922.

Faucheu, C., Blanchet, A-M, Collard-Dutilleul, V., Lalanne, J.-L., Diu-Hercend, T. (1996) Identification of a cysteine protease closely related to interleukin-1ß-coverting enzyme. Eur. J. Biochem. 236, 207-123.

Fearnhead, H.O., Rivett, A.J., Dinsdale,D. and Cohen, G.M. (1995) A pre-existing protease is a common effector of thymocyte apoptosis mediated by diverse stimuli. FEBS Lett. 357, 242-246.

Fernandes-Alnemri, T., Armstrong, R.C., Krebs, J.,Srinivasula, S.M., Wang, L., Bulrich, F., Fritz, L., Trapani, J.A., Tomaselli, K.J., W.C., Litwack, G. and Alnemri, E.S. (1996) In vitro activation of CPP32 and Mch3 by Mch4, a novel human apoptotic cysteine protease containing two FADD-like domains. Proc. Natl. Acad. Sci. USA 93, 7464-7469.

Fernandes-Alnemri, T., Litwack, G. and Alnemri, E.S. (1994) CPP32, a novel human apoptotic protein with homology to *Caenorhabditis elegans* cell death protein Ced-3 and mammalian interleukin-1-ß-converting enzyme. J. Biol. Chem. 269, 343-352.

Fernandes-Alnemri, T., Litwack, G. and Alnemri, E.S. (1995a) *Mch2,* a new member of the apoptotic *Ced-3/Ice* cysteine protease gene family. Cancer Res. 55, 2737-2742.

Fernandes-Alnemri, T., Takahashi, A., Armstrong, R., Krebs, J., Fritz, L., Tomaselli, K.J., Wang, L., Yu, Z., Croc, C.M., Earnshaw, W.C., Litwack, G. and Alnemri, E.S. (1995b) Mch3, a novel human apoptotic cysteine protease highly related to CPP32. Cancer Res. 55, 6045-6052.

Filipski, J., Leblanc, J., Youdale, T., Sikorska, M. and Walker, P.R. (1990) Periodicity of DNA Folding in High Order Chromatin Structures. EMBO J. 9, 1319-1327.

Foreman, J.E., Luu, N.T., Powers, J.D. and Eveleth, D.D. (1993) 3,4-dichlorisocoumarin inhibits the thiol protease calpain. FASEB J. 7, 1183 (Abstr.763).

Fukuda, K., Kojiro, M. Chiu, J-F. (1993) Induction of apoptosis by transforming growth factor-$ß_1$ in the rat hepatoma cell line McA-RH7777 : A possible association with tissue transglutaminase expression. Hepatology 18, 945-953.

Gagliardini, E.L., Miller, D.K., Yamin, T-T., Casciola-Rosen, L and Rosen, A. (1996) Sequential activation of three distinct ICE-like activities in Fas-ligated Jurkat cells. FEBS Lett. 390, 299-303.

Galle, P.R., Hofmann, W.J., Walczak, H., Schaller, H., Otto, G., Stremmel, W., Krammer, P.H. and Runkel, R. (1995) Involvement of the CD95 (APO-1/Fas) receptor and ligand in liver damage. J. Exp. Med. 182, 1223-1230.

Gant, T.W., Silverman, J.E and Thorgeirsson, S.S. (1992) Regulation of P-glycoprotein gene expression in hepatocyte cultures and liver cell lines by a *trans* -acting transcriptional repressor. Nucl. Acids Res. 20, 2841-2846.

Gaziev, A. and Kutsyi, M. (1992) Gamma irradiated DNA activates histone H1-specific proteinase of rat liver nuclei. Int. J. Radiat. Biol. 61, 169-174.

Geng, Y. and Weinberg, R. A. (1993) Transforming growth factor ß effects on expression of G_1 cyclins and cyclin-dependent protein kinases. Proc. Natl. Acad. Sci. USA 90, 10315-13019.

Gold, R., Schmied, G., Rothe, H., Zischler, H., Breitschope, H and Lassman, H. (1993) Detection of DNA fragmentation in apoptosis: application of in situ nick translation to cell culture systems and tissue sections. J. Histochem. Cytochem. 41, 1023-1030.

Goldsworthy, T.L., Fransson-Steen, R.L. and Moser, G.J. (1995) Assessing proliferation and apoptosis inliver tumor development. CIIT Activities 15, 8, 1-10.

Goldsworthy, T.L., Fransson-Steen, R. and Maronpot, R.R. (1996) Importance of and approaches to quantification of hepatocyte apoptosis. Toxicol. Pathol. 24, 1, 24-35.

Gorczyca, W., Bruno, S., Darzynkiewicz, R.j., Gong, J. and Darzynkiewicz, Z. (1992) DNA strand breaks occurring during apoptosis : their early in situ detection by the terminal deoxynucleotidyl transferase and nick translation assays and prevention by serine protease inhibitors. Int. J. Oncol. 1, 493-501.

Grasl-Kraupp, B., Bursch, W., Ruttkay-Nedecky, B., Wagner, A., Lauer, B. and Schulte-Hermann, R. (1994) Food restriction eliminates preneoplastic cells through apoptosis and antagonizes carcinogenesis in rat liver. . Proc. Natl. Acad. Sci. USA 91, 9995-9999.

Greenberg and Litchfield (1994) Granzymes and apoptosis: Targeting the cell cycle. Current Topic In Microbiology and Immunology, 198, 95-119.

Greidinger, E.L., Miller, D.K., Yamin, T.T., Casciola-Rosen, L. and Rosen, A. (1996) Sequential activation of three distinct ICE-like activities in Fas-ligated Jurkat cells. FEBS Lett. 390, 299-303

Gu, Y., Aldape, R.A., Lippke, J.A., Rocher, C., Su, M.S.-S., Livingston, D.J., Hercend, T. and Lalanne, J.-L. (1995a) A novel human protease similar to the interleukin-1ß converting enzyme induces apoptosis in transfected cells. EMBO J. 14, 1914-1922.

Gu, Y., Sarnecki, C., Aldape, R.A., Livingston, D.J. and Su, M.S.-S. (1995b) Cleavage of poly (ADP-ribose) polymerase by interleukin-1ß converting enzyme and its homologs TX and Nedd-2. J. Biol. Chem. 270, 32, 18715-18718.

Gu, Y., Sarnecki, C., Fleming, M.A., Lippke, J.A., Bleackley, R.C. and Su, M.S.-S. (1996) Processing and activation of CMH-1 by granzyme B. J. Biol. Chem. 271, 18, 10816-10820.

Hale, A.J., Smith, C.A., Sutherland, L.C., Stoneman, V.E.A., Longthorne, V.L., Culhane, A.C. and Williams, G.T. (1996) Apoptosis : molecular regulation of cell death. Eur. J. Biochem. 236, 1-26.

Hannon, G.J. and Beach, D. (1994) $p15^{INK4B}$ is a potential effector of TGF-ß-induced cell cycle arrest. Nature 371, 257-261.

Hara , S., Halicka, H.D., Bruno, S., Gong, J., Traganos, F. and Darzynkiewicz, Z. (1996) Effect of protease inhibitors on early events of apoptosis. Exp. Cell. Res. 223, 372-384.

Harper, J.W., Hemmi, K. and Powers, J.C. (1985) Reaction of serine proteases with substituted isocoumarins : discovery of 3,4-dichlorisocoumarin, a new mechanism based serine protease inhibitor. Biochemistry 24, 1831-1841.

Hashida, T., Tanaka, Y., Matsunami, N., Yoshihara, K., Kamiya, T., Tanigawa, Y. and Koide, S.S. (1982) Purification and properties of bull seminal plasma Ca^{2+}, Mg^{2+} dependent endonuclease. J. Biol. Chem. 257, 13114-13119.

Hebert, L., Pandey, S. and Wang, E. (1994) Commitment to cell death is signaled by the appearance of a terminin protein of 30kDa. Exp. Cell. Res. 210, 10-18.

Heby, O. and Persson, L. (1990) Molecular genetics of polyamine synthesis in eukaryotic cells. Trends Biochem. Soc. 15, 153-158.

Helgason, C.D., Atkinson, E.A., Pinskoski, M.J. and Bleackley, R.C. (1995) Proteinases are involved in both DNA fragmentation and membrane damage during CTL-mediated target cell killing. Exp. Cell Res. 218, 50-56.

Hengartner, M.O. and Horvitz, H.R. (1994) C. elegans cell survival gene ced-9 encodes a functional homolog of the mammalian proto-oncogene bcl-2. Cell 76, 665-676.

Henkart, P.A. (1996) ICE family proteases : mediators of all apoptotic cell death? Immunity 4, 195-201.

Hewish, D. R. and Burgoyne, L.A. (1973) The calcium endonuclease activity of isolated nuclear preparations. Relationships between its occurrence and the occurrence of other classes of enzymes found in nuclear preparations. Biochem. Biophys. Res. Commun. 52, 475-481.

Hibino, Y., Yoneda, T. and Sugano, N. (1988) Purification and properties of a magnesium - dependent endodeoxyribonuclease endogenous to rat-liver nuclei. Biochem. Biophys. Acta 950, 313-320.

Higaki, K., Yano, H. and Kojiro, M. (1996) Fas antigen expression and its relationship with apoptosis in human hepatocellular carcinoma and noncancerous tissues. Am. J. Pathol. 149, 2, 429-437.

Hiramatsu, N., Hayashi, N., Katayama, K., Mochizuki, K., Kawanishi, Y., Kasahara, A., Fusamoto, H. and Kamada, T. (1994) Immunohistochemical detection of Fas antigen in liver tissue of patients with chronic hepatitis C. Hepatology 19, 1354-1359.

Hully, J.R., Chang, L., Schwall, R.H., Widmer, H.R., Terrell, T.G. and Gillett, N.A. (1994) Induction of apoptosis in the murine liver with recombinant human activin A. Hepatology 20, 4, 854-862.

Ignotz,R. and Massague, J. (1986) Transforming growth factor beta stimulates the expression of fibronectin and collagen and their incorporation into the extracellular matrix. J. Biol. Chem. 261, 4337-4345.

Ishida, R., Akiyoshi, H. and Takahashi, T. (1974) Isolation and purification of calcium and magnesium dependent endonuclease from rat liver nuclei. Biochem. Biophys. Res. Commun. 56, 3, 703-710.

Jacobson, M.D., Burne, J.F., King, M.P., Miyashita, T., Reed, J.C. and Raff.M.C (1993) Bcl-2 blocks apoptosis in cells lacking mitochondrial DNA. Nature 361, 265-369.

Jacobson, M.D., Burne, J.F. and Raff.M.C (1994) Programmed cell death and bcl-2 protection in the absence of a nucleus. EMBO J 13, 1899-1910.

Jacobson, M.D., Weil, M. and Raff.M.C. (1996) Role of Ced-3/ICE-family proteases in staurosporine-induced programmed cell death. J. Cell Biol. 133, 1041-1051.

James, N.H. and Roberts, R.A. (1996) Species differences in response to peroxisome proliferators correlate in vitro with induction of DNA synthesis rather than suppression of apoptosis. Carcinogenesis 17, 8, 1623-1632.

Jirtle, R.L., Hankins, G.R., Reisenbichler, H. and Boyer, I.J. (1994) Regulation of mannose 6-phosphate/insulin-like growth factor-II receptors and transforming growth factor beta during liver tumor promotion with phenobarbital. Carcinogensis 15, 8, 1473-1478.

Jirtle, R.L. and Meyer, S.A. (1991) Liver tumor promotion : Effect of phenobarbitol on EGF and protein kinase C signal transduction and transforming growth factor-$ß_1$ expression. Digestive Diseases and Sciences 36, 5, 659-668.

Jocelyn, P.C. (1987) Spectrophotometric assay of thiols. Methods Enzymol. 143, 44-67.

Jones, D.P., McConkey, D.J., Nicotera, P. and Orrenius, S. (1989) Calcium-activated DNA fragmentation in rat liver nuclei. J. Biol. Chem. 264, 6398-6403.

Kamens, J.M., Paskind, M., Hugunin, M., Talanian, R.V., Allen, H., Banach, D., Bump, N., Hackett, M., Johnston, C.G., Li, P., Mankovich, J.A., Terranova, M. and Ghayur, T. (1995) Identification and characterisation of ICH-2, a novel member of the interleukin -1ß-converting enzyme family of cysteine proteases. J. Biol. Chem. 270, 15250-15256.

Kaneko, Y. and Tsukamoto, A. (1994) Thapsigargin-induced persistent intracellular calcium pool depletion and apoptosis in human hepatoma cells. Cancer Letts. 97, 147-155.

Kaufmann, S.H. (1989) Induction of endonucleolytic DNA cleavage in human acute myelogenous leukemia cells by etoposide, campthotecin, and other cytotoxic anticancer drugs: a cautionary note. Cancer Res. 49, 5870-5878

Kaufmann, S.H., Desnoyers, S., Ottaviano, Y., Davidson, N.E. and Poirier, G.G. (1993) Specific proteolytic cleavage of poly(ADP-ribose) polymerase: an early marker of chemotherapy-induced apoptosis. Cancer Res. 53, 3976-3985

Kaufmann, S.H. (1996) Proteolytic cleavage during chemotherapy-induced apoptosis. Molecular Medicine Today 2, 298- 303.

Kayalar, C., Ord, T., Testa, M.P., Zhong, L.T. and Bredesen, D.E. (1996) Cleavage of actin by interleukin 1ß-converting enzyme to reverse DNase I inhibition. Proc. Natl. Acad. Sci. USA. 93, 2234-2238.

Kayanoki, Y., Fujii, J., Suzuki, K., Kawata, S., Matsuzawa, Y. and Taniguchi, N. (1994) Suppression of antioxidative enzyme expression by transforming growth factor-$ß_1$ in rat hepatocytes. J. Biol. Chem. 269, 22, 15488-15492.

Kedderis, G.L. (1996) Biochemical basis of hepatocellular injury. Toxicol. Pathol. 24, 1, 77-83.

Kerr, J.F.R. (1969) An electron-microscope study of liver cell necrosis due to heliotrine. J. Path. 97, 557-562.

Kerr, J.F.R. (1970) An electron microscope study of liver cell necrosis due to albitocin. J. Path. 2, 251-259.

Kerr, J.F.R. (1971) Shrinkage necrosis: a distinct mode of cellular death. J. Path. 105,13-20.

Kerr, J.F.R., Searle, J., Halliday, W.J., Roberts, I., Cooksley, W.G.E., Halliday, J.W., Holder, L., Burnett, W. and Powell, L.W. (1979) The nature of piecemeal necrosis in chronic active hepatitis. The Lancet 20, 827-828.

Kerr, J.F.R., Winterford, C.M. and Harmon, B.V. (1994) Apoptosis - its significance in cancer and cancer therapy. Cancer 73, 8, 2013-2026.

Kerr, J.F.R., Wyllie, A.H. and Currie, A.R. (1972) Apoptosis: A basic biological phenomenon with wide ranging implications in tissue kinetics. Br. J. Canc. 26, 239-257.

Koff, A., Ohtsuki, M., Polyak, K., Roberts, J.M. and Massague J. (1993) Negative regulation of G1 in mammalian cells : inhibition of cyclin E-dependent kinase by TGF-ß. Science 260, 536-539.

Kokileva, L. (1981) Initial stages of endogenous DNA degradation in rat liver nuclei isolated and incubated in the presence of Mg^{2+} or polyamines. Int. J. Biochem. 13, 483-488.

Kosower, N.S. and Kosower, E.M. (1987) Formation of disulfides with diamide. Methods Enzymol. 143, 264-270.

Krams, S.M., Egawa, H., Quinn, M.B. and Martinez, O.M. (1995a) Apoptosis as a mechanism of cell death in a rat model of liver allograft rejection. Transplantation Proceedings 27, 1, 466-467.

Krams, S.M., Egawa, H., Quinn, M.B., Villanueva, J.C., Garcia-Kennedy, R. and Martinez, O.M. (1995b) Apoptosis as a mechanism of cell death in liver allograft rejection. Transplantation 59, 4, 621-625.

Kuida, K., Lippke, J.A., Ku, G., Harding, M.W., Livingston, D.J., Su, M.S.-S. and Flavell, R.A. (1995) Altered cytokine export and apoptosis in mice deficient in interleukin-1ß converting enzyme. Science 267, 2000-2003.

Kumar, S. (1995) ICE-like proteases in apoptosis. Trends Biochem. Sci. 20, 198-202.

Kumar, S. and Harvey, N. L. (1995) Role of multiple cellular proteases in the execution of programmed cell death. FEBS Lett. 375, 169-173.

Kumar, S., Kinoshita, M., Noda, M., Copeland, N.G. and Jenkins, N.A. (1994) Induction of apoptosis by the mouse Nedd2 gene, which encodes a protein similar to the product of the *Caenorhabditis elegans* cell death gene ced-3 and the mammalian IL-1ß-converting enzyme. Genes Dev. 8, 1613-1626.

Kumar, S. and Lavin, M.F. (1996) The ICE family of cysteine proteases as effectors of cell death. Cell Death Diff. 3, 255-267.

Kumar, S., Tomooka, Y. and Noda, M. (1992) Identification of a set of genes with developmentally down regulated expression in the mouse brain. Biochem. Biophys. Res. Commun. 185, 1155-1161.

Kwo, P., Patel, T., Bronk, S.F. and Gores, G.J. (1995) Nuclear serine protease activitity contributes to bile acid -induced apoptosis in hepatocytes. Am. J. Physiol. 268, G613-G621.

Kyprianou, N and Isaacs, J.T. (1989) Expression of transforming growth factor in the rat ventral prostate during castration induced programmed cell death. Mol. Endocrinol. 3, 1515-1522.

Kyprianou, N., English, H.F. and Isaacs, J.Y. (1990) Programmed cell death during regression of PC-82 human prostate cancer following androgen ablation. Cancer Res. 50, 3748-3753.

Kyriakis, J.M., Banerjee, P., Nikolakaki, E., Dai, T., Rubie, E.A., Ahmad, M.F., Avruch, J. and Woodgett, J.R. (1994) The stress-activated protein kinase subfamily of c-Jun kinases. Nature 369, 156-160.

Lacks, S.A. (1981) Deoxyribonuclease I in mammalian tissues. Specificity of inhibition by actin. J. Biol. Chem. 256, 2644-2648.

Lacronique, V., Mignon, A., Fabre, M., Violett, B., Rouquet, N., Molina, T., Porteu, A., Henrion, A., Bouscary, D., Varlet, P., Joulin, V. and Kahn, A. (1996) Bcl-2 protects from lethal hepatic apoptosis induced by an anti-Fas antibody in mice. Nature Medicine 2, 1, 80-86.

Laiho, M., DeCaprio, J.A., Ludlow, J.W., Livingston, D.M. and Massague, J. (1990) Growth inhibition by TGF-ß linked to suppression of retinoblastoma protein phosphorylation. Cell 62, 175-185.

Lazebnik, Y.A., Cole, S., Cooke, C.A., Nelson, W.G. and Earnshaw, W. C. (1993) Nuclear events of apoptosis *in vitro* in cell free extracts: a model system for analysis of the active phase of apoptosis. J. Cell Biol. 123, 7-22.

Lazebnik, Y.A., Kaufmann, S.H., Desnoyers, S., Poirer, G.G. and Earnshaw, W. C. (1994) Cleavage of Poly (ADP-ribose) polymerase by a proteinase with properties like ICE. Nature 371, 346-347.

Lazebnik, Y.A., Takahashi, A., Moir, R.D., Goldman, R.D., Poirer, G.G., Kaufmann, S.H., and Earnshaw, W. C. (1995a) Studies of the lamin proteinase reveal multiple parallel biochemical pathways during apoptotic execution. Proc. Natl. Acad. Sci. USA 92, 9042-9046.

Lazebnik, Y.A., Takahashi, A., Poirer, G.G., Kaufmann, S.H., and Earnshaw, W. C. (1995) Characterization of the execution phase of apoptosis in vitro using extracts from condemned-phase cells. J. Cell Sci. Supp. 19, 41-49.

Ledda-Columbano, G.M., Coni, P., Curto, M., Giacomini, L., Faa, G., Oliverio, S., Piacentini, M., Columbano, A. (1991) Induction of two different modes of cell death, apoptosis and necrosis, in rat liver and after a single dose of thioacetamide. Am. J. Pathol. 139, 1099-1109.

Ledda-Columbano, G.M., Coni, P., Faa, G., Manenti, G. and Columbano, A. (1992) Rapid induction of apoptosis in rat liver by cycloheximide. Am. J. Pathol. 140, 545-549.

Leist, M., Gantner, F., bohlinger, I., Germann, P.G., Tiegs, G.and Wendel, A. (1994) Murine hepatocyte apoptosis induced in vitro and in vivo by TNF-α requires transcriptional arrest. J. Immunol. 153, 1778-1788.

Li, P., Allen, H., Banerjee, S., Franklin, S., Herzog, L., Johnston, C., McDowell, J., Paskind, M., Rodman, L., Salfield, J., Towne, E., Tracey, D., Wardwell, S., Wei, F.-Y., Wong, W., Kamen, R. and Seshadri, T. (1995) Mice deficient in IL-1ß converting enzyme are defective in production of mature IL-1ß and resistant to endotoxic shock. Cell 80, 401-411.

Lin, J-K. and Chou, C.-K. (1992) In vitro apoptosis in the human hepatoma cell line induced by transforming growth factor $ß_1$. Cancer Res. 52, 385-388.

Lippke, J.A., Gu, Y., Sarnecki, C., Caron, P.R. and Su, M.S.-S. (1996) Identification and characterization of CPP32/Mch2 homolog 1, a novel cysteine protease similar to CPP32. J. Biol. Chem. 271, 4, 1825-1828.

Liu, X., Kim, C.N., Pohl, J and Wang, X. (1996) Purification and characterization of an interleukin-1ß-converting enzyme family protease that activates cysteine protease P32 (CPP32). J. Biol. Chem. 271, 23, 13371-13376.

Lohmann, R.D. and Beyersmann, D. (1993) Cadmium and zinc mediated changes of the Ca^{2+}-dependent endonuclease in apoptosis. Biochem. Biophys. Res. Commun. 190, 1097-1103.

Lopez, A.R., Cook, J., Deininger, P.L. and Derynck, R. (1992) Dominant negative mutants of transforming growth factor-beta1 inhibit the secretion of different transforming growth factor-beta isoforms Mol. Cell Biol. 12, 4, 1674-1679.

Los, M., Van De Craen, M., Penning, L.C., Schenk, H., Westendorp, M., Baeuerle, P.A., Droge, W., Krammer, P.H., Fiers, W. and Schulze-Osthoff, K. (1995) Requirement of an ICE/CED-3 protease for Fas/APO-1-mediated apoptosis. Nature 375, 81-83.

Mackintosh, C. and Mackintosh, R.W. (1994) Inhibitors of protein kinases and phosphatases. Trends Biochem. Sci. 19, 444-448.

Maeda, S., Lin, K.H., Inagaki, H. and Saito, T. (1996) Induction of apoptosis in primary culture of rat hepatocytes by protease inhibitors. Biochem. Mol. Biol. Int. 39, 3, 447-453.

Mannherz, H.G., Peitsch, M.C., Zanotti, S., Paddenberg, R. and Polzar, B. (1995) A new function for an old enzyme: Curr. Topics Microbiol. Immunol. 198, 161-174.

Markowitz, S.D. and Roberts, A.B. (1996) Tumor suppressor activity of the TGF-ß pathway in human cancers. Cytokine and Growth Factor Reviews 7, 1, 93-102.

Martin, S.J. and Cotter, T. G.(1994) Apoptosis of human leukemia: Induction, morphology and molecular mechanisms. In Tomei, L.D. and Cope, F.O. (eds): Apoptosis II: The Molecular Basis of Apoptosis in Disease. Cold Spring Harbor Lab. Press. pp 185-229.

Martin, S.J. and Green, D.R. (1995) Protease activation during apoptosis: death by a thousand cuts? Cell 82, 349-352.

Mashima, T., Naito, M., Kataoka, S., Kawai, H. and Tsuruo, T. (1995) Aspartate-based inhibitor of interleukin-1ß-converting enzyme prevents antitumour agent -induced apoptosis in human myeloid leukemia U937 cells. Biochem. Biophys. Res. Commun. 209, 907-915.

Massague, J. (1990) The transforming growth factor-ß family. Annu. Rev. Cell Biol. 6, 597-641.

Massague, J. (1996) TGF-ß signalling : Receptors, transducers, and mad proteins. Cell 85, 947-950.

Massague, J. and Polyak, K. (1995) Mammalian antiproliferative signals and their targets. Current Opinion in Genetics and Development 5, 91-96.

McCabe Jr, M.J., Jiang, S.A. and Orrenius, S. (1993) Chelation of intracellular zinc triggers apoptosis in mature thymocytes. Lab. Invest. 69, 101-110.

McConkey, D.J., Hartzell, P., Nicotera, P., Wyllie, A.H. and Orrenius, S.(1988) Stimulation of endogenous nuclease activity in hepatocytes exposed to oxidative stress. Toxicol. Lett. 42, 123-130.

McConkey, D.J., Chow, S.C., Orrenius, S. and Jondal, M. (1990) NK cell-induced cytotoxicity is dependent on a Ca^{2+} increase in the target. FASEB J. 4, 9, 2661-2664

McConkey, D.J., Hartzell, P., Nicotera, P. and Orrenius, S (1990a) Rapid turnover of endogenous endonuclease activity: effects of inhibitors macromolecular synthesis. Arch. Biochem. Biophys. 278, 284-287.

McConkey, D.J., Nicotera, P., Hartzell, P., Bellomo, G., Wyllie, A.H. and Orrenius, S. (1989) Glucocorticoids activate a suicide process in thymocytes through an elevation of cytosolic Ca^{2+} concentration. Arch. Biochem. Biophys. 269, 365-370

McConkey, D.J., Zhivotovsky, B. and Orrenius, S. (1996) Apoptosis - molecular mechanisms and biomedical implications. Mol. Aspects Med. 17, 1, 1-110.

Mellgren, R.L., Song, K. and Mericle, M.T. (1993) m-calpain requires DNA for activity on nuclear proteins at low calcium concentrations. J. Biol. Chem. 268, 653-657.

Mills, J.J., Chari, R.S., Boyer,I.V., Gould, M.N. and Jirtle, R.L. (1995) Induction of apoptosis in liver tumours by the monoterpene periyll alcohol. Cancer Res. 55, 979-983.

Miller, B.E., Krasney, P.A., Gauvin, D.M., Holbrook, K.B., Koonz, D.J., Abruzzese, R.V., Miller, R.E., Pagani, K.A., Dolle, R.E., Ator, M.A. and Gilman, S.C. (1995) Inhibition of mature IL-1ß production in murine macrophages and a murine model of inflammation by WIN 67694, an inhibitor of IL-1ß converting enzyme. J. Immunol. 154, 1331-1338.

Mita ,E., Hayashi, N., Iio, S., Takehara, T., Hijioka, T., Kasahara, A., Fusamoto, H. and Kamada, T. (1994) Role of Fas ligand in apoptosis induced by hepatitis C virus infection. Biochem. Biophys. Res. Commun. 204, 468-474.

Miura, M., Friedlander, R.M. and Yuan, J. (1995) Tumour necrosis factor-induced apoptosis is mediated by a CrmA-sensitive cell death pathway. Proc. Natl. Acad. Sci. USA 92, 8318-8322

Miura, M., Zhu, H., Rotello, R., Hartwieg, E.A. and Yuan, J. (1993) Induction of apoptosis in fibroblast by IL-1ß-converting enzyme, a mammalian homolog of the *C. elegans* cell death gene ced-3. Cell 75, 653-660.

Morrison, J.F. (1982) The slow binding and slow tight-binding inhibition of enzyme catalysed reactions. Trends Biochem. Sci. 7, 102-105.

Moses, H.L., Branum, E.L., Proper, J.A. and Robinson, R.A. (1981) Transforming growth factor production by chemically transformed cells. Cancer Res., 1.41, 7,2842-2848.

Moslen, M.T. (1995) Toxic responses of the liver. Cassarett and Doull's Toxicology. Basic Science of Poisons. (5th ed).McGraw-Hill publisher

Motizuki, M., Tsurugi, K. and Ogata, K. (1984) Purification and properties of a thiol protease from rat liver nuclei. Eur. J. Biochem. 138, 39-43.

Moulton, B.C. (1994) Transforming growth factor-ß stimulates endometrial stromal apoptosis in vitro. Endocrinology 134, 3, 1055-1060.

Mullauer, L., Grasl-Kraupp, B, Bursch, W. and Schulte-Hermann, R. (1996) Transforming growth factor $ß_1$-induced cell death in preneoplastic foci of rat liver and sensitization by the antiestrogen tamoxifen. Hepatology 23, 4, 840-847.

Munday, N.A., Vaillancourt, J.P., Ali, A., Casano, F.J., Miller, D.K., , Molineaux, S.M., Yamin, T.T., Yu, V.L. and Nicholson, D.W. (1995) Molecular cloning and pro-apoptotic activity of $ICE_{rel}II$ and $ICE_{rel}III$ members of the ICE/CED-3 family of cysteine proteases. J. Biol. Chem. 270, 15870-15876.

Muzio, M., Chinnaiyan, A.M., Kischkel, F.C., O'Rourke, K., Shevchenko, A., Ni, J, Scaffidi, C., Bretz, J.D., Zhang, M., Gentz, R., Mann, M., Krammer, P.H., Peter, M.E. and Dixit, V.M. (1996) FLICE, a novel FADD-homologous ICE/CED-1-like protease, is recruited to the CD95 (Fas/APO-1) death-inducing signalling complex.. Cell 85, 817-827.

Na, S., Chuang, T.H., Cunningham, A., Turi, T.G., Hanke, J.H., Bokoch, G.M. and Danley, D.E. (1996) D4-GDI, a substrate of CPP32, is proteolysed during Fas-induced apoptosis. J Biol. Chem. 271, 49, 11209-11213.

Nagata, S. and Golstein, P. (1995) The Fas death factor. Science 267, 1449-1456.

Nakamura, T., Tomita, Y., Hirai, R., Yamaoka, K., Kaji, K. and Ichihara, A. (1985) Inhibitory effect of transforming growth factor -ß on DNA synthesis of adult rat hepatocytes in primary culture. Biochem. Biophys. Res. Commun. 133, 1042-1050.

Neamati, N., Fernandez, A., Wright,S., Kiefer, J. and McConkey, D.J. (1995) Degradation of lamin B_1 precedes oligonucleosomal DNA fragmentation in apoptotic thymocytes and isolated thymocyte nuclei. J. Immunol. 154, 3788-3795.

Ni, R., Tomita, Y., Matsuda, K., Ichihara, A., Ishimura, A., Ogasawara, J. and Nagata, S. (1994) Fas-mediated apoptosis in primary cultured mouse hepatocytes. Exp. Cell Res. 215, 332-337.

Nicholson, D.W. (1996) ICE/CED3-like proteases as therapeutic targets for the control of inappropriate apoptosis. Nature Biotech. 14, 297-301.

Nicholson, D.W., Ali, A., Thornberry, N.A., Vaillancourt, J.P., Ding, C.K., Gallant, M., Gareau, Y., Griffin, P.R., Labelle, M., Lazebnik, Y.A., Munday, N.A., Raju, S.M., Smulson, M.E., Yamin, T.-T., Yu, V.L. and Miller, D.K. (1995) Identification and inhibition of the ICE/Ced-3 protease necessary for mammalian apoptosis. Nature 376, 37-43.

Nicotera, P., McConkey, D.J., Jones, D.P. and Orrenius, S. (1989) ATP stimulates Ca^{2+} uptake and increases the free Ca^{2+} concentration in isolated rat liver nuclei. Proc. Natl. Acad. Sci. USA 86, 453-457.

Niehrs, C. (1996) Mad connection to the nucleus. Nature 381, 561-562.

Nikonova, L.V., Beletsky, I.P. and Umansky, S.R. (1993) Properties of some nuclear nucleases of rat thymocytes and their changes in radiation-induced apoptosis. Eur. J. Biochem. 215, 893-901.

Oberhammer, F., Bursch, W., Tiefenbacher, R., Froschl, G., Pavelka, M., Purchio, T., Schulte-Hermann, R. (1993) Apoptosis is induced by transforming growth factor-$ß_1$ with 5 hours in regressing liver without significant fragmentation of the DNA. Hepatology 18, 1238-1246.

Oberhammer, F.A., Fristch, G., Schmeid, M., Pavelka, M., Prints, D., Purchio, T., Lassmann, H. and Schulte-Hermann, R. (1993a) Condensation of the chromatin at the membrane of an apoptotic nucleus is not associated with activation of an endonuclease. J. Cell Sci. 104, 317-326.

Oberhammer, F.A., Froschl, G., Tiefenbacher, R, Inayat-Hussain, S.H., Cain, K. and Stopper, H. (1996) Hepatocyte death following transforming growth factor-beta1 addition. Microscopy Res.Tech. 34, 3, 247-25.

Oberhammer, F.A., Hochegger, K., Froschl, G., Tiefenbacher, R. and Pavelka, M. (1994) Chromatin condensation during apoptosis is accompanied by degradation of lamin A + B, without enhanced activation of cdc2 kinase. J. Cell Biol. 126, 827-837.

Oberhammer, F.A., Pavelka, M., Sharma, S., Tiefenbacher, R., Purchio, A.F., Bursch, W. and Schulte-Hermann, R. (1992) Induction of apoptosis in cultured hepatocytes and in regressing liver by transforming growth factor $ß_1$. Proc. Natl. Acad. Sci. 89, 5408-5412.

Oberhammer, F.A. and Qin, H.-M. (1995) Effect of three tumour promoters on the stability of hepatocyte cultures and apoptosis after transforming growth factor-$ß_1$. Carcinogenesis 16, 6, 1363-1371.

Oberhammer, F.A. and Roberts, R.A. (1994) Apoptosis : A widespread process involved in liver adaptation and carcinogenesis. In The Liver : Biology and Pathobiology, Third Edition. Edited by I.M. Arias, J.L. Boyer, N. Fausto, W.B. Jakoby, D.A. Schachter and D.A. Shafritz. Raven Press Ltd, New York. Pp 1547-1555.

Oberhammer, F.A., Wilson, J.W., Dive, C., Morris, I.D., Hickman, J.A., Wakeling, A.E., Walker, P.R. and Sikorska, M. (1993b) Apoptotic death in epithelial cells: cleavage of DNA to 300 and/or 50 kb fragments prior to or in the absence of internucleosomal fragmentation. EMBO J. 12, 3679-3684.

Ogasawara, J., Watanabe-Fukunaga, R., Adachi, M., Matsuzawa, A., Kasugai, T., Kitamura, Y., Itoh, N., Suda, T., and Nagata,S. (1993) Lethal effect of the anti-Fas antibody in mice. Nature 364, 806-809.

Orrenius, S. (1995) Apoptosis : molecular mechanisms and implications for human disease. J. Int. Med. 237, 529-536.

Orrenius, S, McConkey, D.J. and Nicotera, P. (1989) The role of calcium in cytotoxicity. Basic Science in Toxicology (Taylor and Francis ed) pp 629-635.

Orth, K., Chinnaiyan, A.M., Garg, M. Froelich, C.J. and Dixit,V.M. (1996a) The CED-3/ICE-like protease Mch2 is activated during apoptosis and cleaves the death substrate lamin A. J. Biol. Chem. 271, 28, 16443-16446.

Orth, K., O'Rourke, K., Salvesen, G.S. and Dixit, V.M. (1996b) Molecular ordering of apoptotic mammalian CED-3/ICE-like proteases. J. Biol. Chem. 271, 35, 20977-20980.

Osheroff, N. (1987) Role of divalent cations in topoisomerase II mediated reactions. Biochemistry 26, 6402-6406.

Otto, F. (1990) DAPI staining of fixed cells for high resolution flow cytometry of nuclear DNA. Methods. Cell Biol. 33, 105-111.

Ozaki, T, Saijo, M, Murakami, K., Enomoto, H., Taya, Y. and Sakiyama, S. (1994) Complex formation between lamin A and the retinoblastoma gene product: Identification of the domain on lamin A required for its interaction. Oncogene 9, 9, 2649-2653.

Pai, J.T., Brown, M.S. and Goldstein, J.L. (1996) Purification and cDNA cloning of a second apoptosis-related cysteine protease that cleaves and activates sterol regulatory element binding proteins. Proc. Natl. Acad. Sci. USA 93, 5437-5442

Park, K., Kim, S.-J., Bang, Y.-J., Park, J.-G., Kim, N.K., Roberts, A.B. and Sporn, M.B. (1994) Genetic changes in the transforming growth factor ß (TGF-ß) type II receptor gene in human gastric cancer cells : Correlation with sensitivity to growth inhibition by TGF-ß. Proc. Natl. Acad. Sci. USA 91, 8772-8776.

Patel, T., Bronk, S.F. and Gores, G.J. (1994) Increases of intracellular magnesium promote glycodeoxycholate-induced apoptosis in rat hepatocytes. J. Clin. Invest. 94, 2183-2192.

Patel, T and Gores, G.J.(1995) Apoptosis and hepatobiliary disease. Hepatology 21, 6, 1725-1741.

Peitsch, M.G., Mannherz, H.G. and Tschopp, J. (1994) The apoptosis endonucleases; cleaning up after cell death. Trends Biochem. Sci. 4, 37-41.

Peitsch, M.C., Polzar, B., Stephen, H., Crompton, T., MacDonald, H.R., Mannherz, H.G. and Tschopp, J. (1993) Characterisation of the endogenous deoxyribonuclease involved in nuclear DNA degradation during apoptosis (programmed cell death). EMBO J. 12, 371-377.

Perry, R.R., Kang, Y. and Greaves, B.R. (1995) Relationship between tamoxifen-induced transforming growth factor $ß_1$ expression, cytostasis and apoptosis in human breast cancer cells. Br. J. Cancer 72, 1441-1446.

Polyak, K., Kato, J.-Y., Solomon. M.J., Massague, J., Roberts, J.M. and Koff, A. (1994) p27Kip1, a cyclin-Cdk inhibitor, links transforming growth factor-ß and contact inhibition to cell cycle arrest. Genes Dev. 8, 9-22.

Powers, J.C. and Harper, J.W. (1986) Inhibitors of serine proteases. *In* Proteinase inhibitors. *Edited by* A.J. Barrett and G.S. Salvesen. Elsevier Science Publisher BV (Biomedical Division). pp 55-151.

Powers, J.C. and Kam, C.-H. (1994) Isocoumarin inhibitors of serine peptidases. Methods Enzymol. 244, 442-457.

Pritchard, D.J. and Butler, W.H. (1989) Apoptosis - the mechanism of cell death in dimethylnitrosamine-induced hepatotoxicity. J. Pathol. 158, 253-260.

Pronk, G.J., Ramer, K., Amiri, P. and Williams, L.T. (1996) Requirement of an ICE-like protease for induction of apoptosis and ceramide generation by REAPER. Science 271, 808-810.

Purchio, A.F., Cooper, J.A., Brunner, A.M., Lioubin, M.N., Gentry, L.E., Kovacina, K.S., Roth, R.A. and Marquardt, H. (1988) Identification of mannose-6-phosphate in two asparagine-linked sugar chains of recombinant transforming growth factor-beta-1 precursor. J. Biol. Chem. 263, 14211-14215.

Quan, L.T., Muneesh, T., O'Rourke, K., Dixit, V.M., Snipas, S.J., Poirier, G.G., Ray, C., Pickup, D.J. and Salvesen, G.S. (1996) Proteolytic activation of the cell death protease Yama/CPP32 by granzyme B. Proc. Natl. Acad. Sci. USA 93, 1972-1976.

Rabizadeh, S., LaCount, D.J., Friesen, P.D. and Bredesen, D.E. (1993) Expression of the baculovirus p35 gene inhibits mammalian neural cell death. J. Neurochem. 61, 2318-2321.

Ray, C., Black, R.A., Kronheim, S.R., Greenstreet, T.A., Sleath, P.R., Salvesen, G.S. and Pickup, D.J. (1992) Viral inhibition of inflammation: cowpox virus encodes an inhibitor of the interleukin-1ß converting enzyme. Cell 69, 597-604.

Reynolds, E.S., Kanz, M.F., Chieco, P. and Moslen, M.T. (1984) 1,1-Dichloroethylene : An apoptotic hepatotoxin? Environ. Health Persp. 57, 313-320.

Ribeiro, J.M. and Carson, D.A. (1993) Ca^{2+}/Mg^{2+}-dependent endonuclease from human spleen: purification, properties, and role in apoptosis. Biochemistry 32, 9129-9136.

Riordan, J.F. and Vallee, B.L. (1972) Reactions with *N*-ethyl-maleimide and *p*-mercuribenzoate. Methods Enzymol. 25, 449-456.

Ritter, M.A. and Crispe, I.N. (1992) The Thymus. IRL Press.

Roberts, A.B., Anzano, M.A. and Lamb, L.C. (1981) New class of transforming growth factors potentiated by epidermal growth factor: Isolation from non-neoplastic tissues. Proc. Natl. Acad. Sci., 78, 5339-5343.

Roberts, R.A., Soames, A.R., Gill, J.H., James, N.H. and Wheeldon, E.B. (1995) Non-genotoxic hepatocarcinogens stimulate DNA synthesis and their withdrawal induces apoptosis, but in different hepatocyte populations. Carcinogenesis 16, 1693-1698.

Robey, P.G., Young, M. F., Flanders, K.C., Roche, N.S., Kondiah, P., Reddi, A.H., Termine, J.D., Sporn, M.B. and Roberts, A.B (1987) Osteoblasts synthesize and respond to TGF-β_1 in vitro. J. Cell Biol., 105, 457-463.

Rorke, E.A. and Jacobberger, J.W. (1995) Transforming growth factor-B1 (TGF-β_1) enhances apoptosis in human papillomavirus type 16-immortalized human ectocervical epithelial cells. Exp. Cell Res. 216, 65-72.

Rotello, R.J., Leibermann, R.C., Purchio, A., Gerschenson, L.E. (1991) Coordinated regulation of apoptosis and cell proliferation by transforming growth factor β_1 in cultured uterine epithelial cells. Proc. Natl. acad. Sci. USA 88, 3412-3415.

Rouquet, N., Pages, J.C., Molina, T., Briand, P. and Joulin, V. (1996) ICE inhibitor YVAD.CMK is a potent therapeutic agent against in-vivo liver apoptosis. Curr. Biol. 6, 9, 1192-1195.

Rusnak, J.M., Calmels, T.P.G., Hoyt, D.G., Kondo, Y., Yalowich, J.C. and Lazo, J.S. (1996) Genesis of discrete higher order DNA fragments in apoptotic human prostatic carcinoma cells. Mol. Pharm. 49, 244-252.

Sanchez, A., Alvarez, A.M., Benito, M. and Fabregat, I. (1996) Apoptosis induced by transforming growth factor-ß in fetal hepatocyte primary cultures. J. Biol. Chem. 271, 13, 7416-7422.

Sanchez, V., Lucas, M., Sanz, A. and Gobernam R. (1992) Decreased protein kinase C activity is associated with programmed cell death (apoptosis) in freshly isolated hepatocytes. Biosci. Rep. 12, 199-206.

Schwall, R.H., Robbins, K., Jardieu, P., Chang, L., Lai, C. and Terrell, T.G. (1993) Activin induces cell death in hepatocytes in vivo and in vitro. Hepatology 18 No. 2, 347-356.

Sanderson, N., Factor, V., Nagy, P., Kopp, J., Kondaiah, P., Wakefield, L., Roberts, A.B., Sporn, M.B. and Thorgeirsson, S.S. (1995) Hepatic expression of mature transforming growth factor-$ß_1$ in transgenic mice results in multiple tissue lesions. Proc. Natl. Acad. Sci. USA 92, 2572-2576.

Schomburg, U.and Grosse, F. (1986) Purification and characterisation of DNA topoisomerase II from calf thymus associated with polypeptides of 175 and 150kDa. Eur. J. Biochem. 160, 451-457.

Schulte-Hermann, R., Bursch, W. and Grasl-Kraupp, B. (1995) Active cell death (apoptosis) in liver biology and disease. Prog. Liver Dis. 13, 1-35.

Schulze-Osthoff, K., Walczak, H., Droge, W. and Krammer, P.H. (1994) Cell nucleus and DNA fragmentation are not required for apoptosis. J Cell Biol. 127, 1, 15-20.

Schwall, R.H., Robbins, K., Jardieu, P., Chang, L., Lai, C. and Terrell, T.G. (1993) Activin induces cell death in hepatocytes in vivo and in vitro. Hepatology 18, 2, 347-356.

Schwartzman, R.A. and Cidlowski, J.A. (1993) Apoptosis: The biochemistry and molecular biology of programmed cell death. Endocrine Rev. 14, 133-151.

Searle, J., Harmon, B.V., Bishop, C.J., Kerr, J.F.R. (1987) The significance of cell death by apoptosis in hepatobilliary disease. J. Gastroent. Hepatol. 2, 77-96.

Searle, J., Kerr, J.F.R. and Battersby, C. (1977) An electron microscope study of the mode of donor cell death in unmodified rejection of pig liver allografts. Aust. J. Exp. Biol. Med. Sci., 55, 401-406.

Seglen, P.O. (1973) Preparation of rat liver cells. III. Enzymic requirements for tissue dispersion. Exp. Cell Res. 82, 391-398.

Sellins, K.S. and Cohen, J.J. (1987) Gene induction by γ-irradiation leads to DNA fragmentation in lymphocytes. J. Immunol. 139, 3199-3206

Shen, W., Kamendulis, L.M., Ray, S.D. and Corcoran, G.B. (1991) Acetaminophen-induced cytotoxicity in cultured mouse hepatocytes: Correlation of nuclear Ca^{2+} accumulation and early DNA fragmentation with cell death. Toxicol. Appl. Pharmacol. 111, 242-254.

Sherr, C.J. and Roberts, J.M. (1995) Inhibitors of mammalian G_1 cyclin-dependent kinases. Genes Dev. 9, 1149-1163.

Shinagawa, T., Yoshioka, K., Kakuma, S., Wakita, T., Ishikawa, T., Itoh, Y. and Takayanagi, M. (1991) Apoptosis in cultured hepatocytes : the effects of tumor necrosis factor α and interferon γ. Pathol. 165, 247-253.

Shirai, Y., Kawata, S, Tamura, S., Ito, N., Tsushima, H., Takaishi, K., Kiso, S. and Matsuzawa, Y. (1994) Plasma Transforming Growth Factor-$ß_1$ in patients with hepatocellular carcinoma. Comparison with chronic liver diseases. Cancer 73, 9, 2275-2279.

Skalka, M., Matyasova, J. and Cejkova, M. (1976) DNA in chromatin of irradiated lymphoid tissues degrades in vivo into regular fragments. FEBS Lett. 72, 271-275.

Skilleter, D.N. and Cain, K. (1981) Effects of thiol agents on the accumulation of cadmium by rat liver parenchymal and kupffer cells. Chem. Bio. Interact. 37, 289-298.

Slee, E.A., Zhu, H., Chow, S.C., MacFarlane, M., Nicholson, D.W. and Cohen, G.M. (1996) Benzyloxycarbonyl-Val-Ala-Asp (OMe) fluoromethylketone (Z-VAD.FMK) inhibits apoptosis by blocking the processing of CPP32. Biochem. J. 315, 21-24.

Smith, C.L. and Cantor, C.R. (1987) Purification, Specific fragmentation and separation of large DNA molecules. Meths. Enzmol. 155, 449-465.

Snover, D.C., Sibley, R.K., Freese, D.K., Sharp, H.L., Bloomer, J.R., Najarian, J.S. and Ascher, N.L (1984) Orthotopic liver transplantation: a pathological study of 63 serial liver biopsies from 17 patients with special reference to the diagnostic features and natural history of rejection. Hepatology 4, 6, 1212-1222.

Sorenson, C.M., Barry, M.A. and Eastman, A. (1990) Analysis of events associated with cell cycle at G_0 phase and cell death induced by cisplatin. J. Natl. Cancer Inst. 82, 749-755.

Sporn, M.B., Roberts, A.B., Wakefield, L.M. and De Crombrugghe, B.(1987) Some recent advances in the chemistry and biology of transforming growth factor-beta. J.Cell. Biol. 105, 3, 1039-1045.

Squier, M.K.T., Miller, A.C.K., Malkinson, A.M. and Cohen, J.J. (1994) Calpain activation in apoptosis. J. Cell Physiol. 159, 229-237.

Stinchcombe,S., Buchmann, A., Bock, K.W. and Schwarz, M. (1995) Inhibition of apoptosis during 2,3,7,8-tetrachlorodibenzo-*p*-dioxin mediated tumour promotion in rat liver. Carcinogenesis 16, 1271-1275.

Strain, A.J., Frazer, A., Hill, D.J. and Milner, R.D.G. (1987) Transforming growth factor ß inhibits DNA synthesis in hepatocytes isolated from normal and regenerating rat liver. Biochem. Biophys. Res. Comm. 145, 1, 436-442.

Strange, R., Li, F., Saurer, S., Burkhardt, A. and Friis, R.R. (1992) Apoptotic cell death and tissue remodelling during mouse mammary gland involution. Development 115, 49-58.

Sun, X.-M. and Cohen, G.M. (1994) Mg^{2+}-dependent cleavage of DNA into kilobase pair fragments is responsible for the initial degradation of DNA in apoptosis. J. Biol. Chem. 269, 14857-14860.

Suzuki, A. and Kato, M. (1996) Chemotherapeutic agent CPT-11 induces the new expression of the apoptosis initiator to the cytoplasm. Exp. Cell Res. 227, 154-159.

Szabo, G. Jr., Boldog, F. and Wikonkal, N. (1990) Disassembly of chromatin into ≅50 kb units by detergent. Biochem. Biophys. Res. Commun. 169, 2, 706-712.

Takahashi, A., Alnemri, E.S., Lazebnik, Y.A., Fernandes-Alnemri, T., Litwack, G., Moir, R.D., Goldman, R.D., Poirier, G.G., Kaufmann, S.H. and Earnshaw, W.C. (1996) Cleavage of lamin A by Mch2α but not CPP32 : Multiple interleukin 1ß-converting enzyme-related proteases with distinct substrate recognition properties are active in apoptosis. Proc. Natl. Acad. Sci. USA (In press).

Takahashi, A., Earnshaw, W.C. (1996) ICE-related proteases in apoptosis. Curr. Opin. Gen. Dev. 5, 50-55.

Takatani, M., Yamada, G., Tsugeno, H., Kishi, F., Doi, T., Yonehara, S. and Tsuji, T. (1996) Immunohistochemical observation of Fas in the human liver: Light and electron microscopic observation by immuno-peroxidase method. Int. Hep. Comm. 1996, 4, 6, 334-342.

Takiya, S., Tagaya, T., Takahashi, K., Hawashima, H., Kamiya, M., Fukuzawa, Y., Kobayashi, S., Fukatsu, A., Katoh, K. and Kakumu, S. (1995) Role of transforming growth factor-$ß_1$ on hepatic regeneration and apoptosis in liver diseases. J. Clin. Pathol. 48, 1093-1097.

Tanaka, Y., Yoshihara, K. and Itaya, A. (1984) Mechanism of the inhibition of Ca^{2+}, Mg^{2+}-dependent endonuclease of bull seminal plasma induced by ADP-ribosylation. J. Biol. Chem. 259, 10, 6579-6585.

Telford, I.R. and Bridgman, C.F. (1995) Introduction to functional histology (2^{nd} Ed) Harper Collins College Publishers.

Teraoka, H., Yumoto, Y., Watanabe, F., Tsukada, K., Suwa, A., Enari, M. and Nagata, S. (1996) CPP32/Yama/apopain cleaves the catalytic component of DNA-dependent protein kinase in the holoenzyme. FEBS Lett. 396, 1-6

Terrell, T.G., Woking, P.K., Chow, C.P., Green, J.D. (1993) Pathology of recombinant human transforming growth factor-$ß_1$ in rats and rabbits. Int. Rev. Exp. Pathol. 34, 43-67.

Tewari, M., Beidler, D.R. and Dixit, V.M. (1995a) Crm-A inhibitable cleavage of the 70-kDa protein component of the U1 small ribonucleoprotein during Fas- and Tumour Necrosis Factor-induced apoptosis. J. Biol. Chem. 270, 18738-18741

Tewari, M and Dixit, V.M. (1995) Fas- and tumour necrosis factor -induced apoptosis is inhibited by the poxvirus *crmA* gene product. J. Biol. Chem. 270, 3255-3260.

Tewari, M., Quan, L.T., O'Rourke, K., Desnoyers, S., Zeng, Z., Beidler, D.R.,.Poirier, G.G., Salvesen, G.S. and Dixit, V.M. (1995b) Yama/CPP32ß, a mammalian homolog of CED-3, is a CrmA-inhibitable protease that cleaves the death substrate poly(ADP-ribose) polymerase. Cell 81, 801-809.

Thompson, C.B. (1995) Apoptosis in pathogenesis and treatment of disease. Science 267, 1456-1462.

Thornberry, N.A. (1994) Interleukin -1ß converting enzyme. Methods Enzymol. 244, 615-631.

Thornberry, N.A., Bull, H.G., Calaycay, J.R., Chapman, K.T., Howard, A.D., Kostura, M.J., Miller, D.K., Molineaux, S.M., Weidner, J.R., Aunins, J., Elliston, K.O., Ayla, J.M., Casano, F.J., Chin, J., Ding, G.J.-F., Egger, L.A., Gaffney, E.P., Limjuco, G., Palyha, O.C., Raju, S.M., Rolando, A.M., Salley, J.P., Yamin, T.-T., Lee, T.D., Shively, J.E., MacCross, M., Mumford, R.A., Schmidt, J.A. and Tocci, M.J. (1992) A novel heterodimeric cysteine protease is required for interleukin-1ß processing in monocytes . Nature 356, 768-774.

Thornberry, N.A., Miller, D.K. and Nicholson, D.W. (1995) Interleukin-1ß-converting enzyme and related proteases as potential targets in inflammation and apoptosis. Persp. Drug Disc. Des. 2, 389-399.

Thornberry, N.A. and Molineaux, S.M. (1995) Interleukin-1ß converting enzyme: A novel cysteine protease required for IL-1ß production and implicated in programmed cell death. Prot. Sci. 4, 3-12.

Thornberry, N.A., Peterson, E.P., Zhao, J.T., Howard, A.D., Griffin, P.R. and Chapman, K.T. (1994) Inactivation of interleukin-1ß converting enzyme by peptide (acyloxy) methyl ketones. Biochem. 33, 3934-3940.

Tian, Q., Streuli, M., Saito, M., Schlossman, S.F. and Anderson, P. (1991) A polyadenylate binding protein localised to the granules of cytolytic lymphocytes induces DNA fragmentation. Cell 67, 629-639.

Trump, B.F. , Berezesky, I.K., Sato, T, Laiho, K.U., Phelps, P.C. and DeClaris, N. (1984) Cell calcium, cell injury and cell death. Environ. Health Perspect. 57, 281-287.

Tsukidate , K., Yamamoto, K., Snyder, J.W. and Farber, J.L. (1993) Microtubule antagonists activate programmed cell death (apoptosis) in cultured rat hepatocytes. Am. J. Pathol. 143, 918-925.

Tucker, R.F., Volkenant, M.E., Branum, E.L. and Moses, H.L. (1983) Comparison of intra and extracellular transforming growth factors from nontransformed and chemically transformed mouse embryo cells. Cancer Res. 43, 1581-1586

Ucker, D.S., Obermiller, P.S., Eckhart, W., Apgar, J.R., Berger, N.A. and Meyers, J. (1992) Genome digestion is a dispensable consequence of physiological cell death mediated by cytotoxic T lymphocytes. Mol. Cell Biol. 12, 3060-3069.

Vallee, B.L. and Ulmer, D.D. (1972) The biochemical effects of cadmium, mercury and lead. Annu. Rev. Biochem. 41, 91-128.

Van Antwerp, D.J., Martin, S.J., Kafri, T., Green, D.R. and Verma, I.M. (1996) Supression of TNF-α-induced apoptosis by NF-κB. Science, 274, 787-789.

Wahl,S.M., Hunt, D.A., Wakefield, L.M., McCartney-Francis, N., Wahl, L.M., Roberts, A.B. and Sporn, M.B. (1987) Transforming growth factor type beta induces monocyte chemotaxis and growth factor production. Proc. Natl. Acad. Sci. USA 84,16, 5788-5792.

Walker, P.R., Pandey, S. and Sikorska, M. (1995) Degradation of chromatin. Cell Death Diff. 2, 97-104.

Walker, P.R., Smith, C., Youdale, T., Leblanc, J., Whitfield, J.F. and Sikorska, M. (1991) Topoisomerase II-reactive chemotherapeutic drugs induce apoptosis in thymocytes. Cancer Res. 51, 1078-1085.

Walker, P.R., Weaver, V.M., Lach, B., LeBlanc, J. and Sikorska, M. (1994) Endonuclease activities associated with high molecular weight and internucleosomal DNA fragmentation in apoptosis. Exp. Cell Res. 213, 100-106.

Wang, Z.-Q., Auer, B., Sting, L., Berghammer, H., Haidacher, D., Schweiger, M. and Wagner, E.F. (1995a) Mice lacking ADRT and poly(ADP-ribosyl)ation develop normally but are susceptible to skin disease. Genes Dev. 9, 509-520.

Wang, L., Miura, M., Bergeron, L., Zhu., H. and Yuan, J. (1994) *Ich-1* an *Ice/ced-3*-related gene encodes both positive and negative regulators of programmed cell death. Cell 78, 739-750.

Wang, X., Pai, J.T, Wiedenfeld, E.A., Medina, J.C., Slaughter, C.A., Goldstein, J.L. And Brown, M.S. (1995b) Purification of an interleukin-1ß converting enzyme-related cysteine protease that cleaves sterol regulatory element-binding proteins between the leucine zipper and transmembrane domains. J. Biol. Chem. 270, 18044-18050

Wang, X., Zelenski, N.G., Yang, J., Sakai, J., Brown, M.S. and Goldstein, J.L. (1996) Cleavage of sterol regulatory element binding proteins (SREBPs) by CPP32 during apoptosis. EMBO. J 15,1012-1020

Weaver, V.M., Lach, B., Walker, P.R. and Sikorska, M. (1993) Role of proteolysis in apoptosis : involvement of serine proteases in internucleosomal DNA fragmentation in immature thymocytes. Biochem. Cell Biol. 71, 488-450.

Weinberg, R.A. (1995) The retinoblastoma protein and cell cycle control. Cell 81, 323-330.

Weller, M., Frei, B., Groscurth, P., Krammer, P.H., Yonekawa, Y. and Fontana, A. (1994) Anti-Fas/APO-1 antibody-mediated apoptosis in cultured human glioma cells. Induction and modulation of sensitivity by cytokines. J. Clin. Invest. 94, 954-964

Whitson, R.H. and Itakura, K. (1992) TGF-$ß_1$ inhibits DNA synthesis and phosphorylation of the retinoblastoma gene product in a rat liver epithelial cell line. J. Cell. Biochem. 48, 305-315.

Williams, M. and Henkart, P. (1994) Apoptotic cell death induced by intracellular proteolysis. J. Immunol. 153, 4247-4255.

Wrana, J.L., Attisano, L., Wieser, R., Ventura, F. and Massague, J. (1994) Mechanism of activation of the TGF-ß. Nature 370, 341-347.

Wright, S.C., Wei, Q.S., Zhong, J., Zheng, H., Kinder, D.H. and Larrick, J.W. (1994) Purification of a 24-kD protease from apoptotic tumor cells that activates DNA fragmentation. J.Exp. med. 180, 2113-2123.

Wyllie, A.H. (1980) Glucocorticoid-induced apoptosis is associated with endogenous endonuclease activation. Nature 284, 555-556.

Wyllie, A.H. (1992) Apoptosis and the regulation of cell number in normal and neoplastic tissues. Cancer Metastasis Rev. 11, 95-103.

Wyllie, A.H., Arends, M.J., Morris, R.G., Walker, S.W. and Evans, G. (1992) The apoptosis endonuclease and its regulation. Seminars in Immunol. 4, 389-397.

Wyllie, A.H. and Duvall, E. (1995) In Oxford Textbook Of Pathology, Eds., J.O.D. Mcgee, O.G. Isaacson and N.A. Wright, Vol 1, 141-1157.

Wyllie, A.H., Morris, R.G., Smith, A.L. and Dunlop, D. (1984) Chromatin cleavage in apoptosis : Association with condensed chromatin morphology and dependence on macromolecular synthesis. J. Pathol. 142, 67-77.

Xue, D and Horvitz, H.R. (1995) Inhibition of the *Caenorhabditis elegans* cell-death protease CED-3 by a CED-3 cleavage site in a baculovirus p35 protein. Nature 377, 248-251

Yasuda, H., Mine, T., Shibata, H., Eto, Y., Hasegawa, Y, Takeuchi, T., Asano, S.and Kojima, I. (1993) Activin A : an autocrine inhibitor of initiation of DNA synthesis in rat hepatocytes. J. Clin. Invest. 92, 1491-1496.

Yokoyama, I., Hayakawa, A., Hayashi, S., Kobayashi, T., Negita, M., Katayama, A., Nagasaka, R., Namii, Y., Kojima, T., Koike, C., Uchida, K. and Takagi, H. (1996) Fas antigen expression and apoptosis induction of in vitro cultured hepatocytes with high concentrations of cyclosporine A. Transplantation Proc. 28, 3, 1383-1384.

Yuan, J and Horvitz, H.R. (1990) Genetic mosaic analyses of ced-3 and ced-4, two genes that control programmed cell death in the nematode *C. elegans*. Dev. Biol. 138, 33-41.

Yuan, J., Shaham, S., Ledoux, S., Ellis, H.M. and Horvitz, H.R. (1993) The *C. elegans* cell death gene *ced-3* encodes a protein similar to mammalian interleukin 1-ß converting enzyme. Cell 75, 641-652.

Zalewski and Forbes (1993) Intracellular zinc and the regulation of apoptosis. in Programmed cell death. The cellular and molecular biology of apoptosis. Lavin, M. and Watters, D. (eds) harwood academic publishers.

Zhang, J., Dawson, V.L., Dawson, T.M. and Synder, S.H. (1994) Nitric oxide activation of poly(ADP-ribose) synthetase in neurotoxicity. Science 263, 687-689.

Zhivotovsky, B., Wade, D., Grahm, A., Orrenius, S. and Nicotera, P. (1994) Formation of 50 kbp chromatin fragments in isolated liver nuclei is mediated by protease and endonuclease activation. FEBS Lett. 351, 150-154.

Zhu, H., Fearnhead, H.O. and Cohen, G.M. (1995) An ICE-like protease is a common mediator of apoptosis induced by diverse stimuli in human monocytic THP.1 cells. FEBS Lett. 374, 303-308.

Zlatanova, J. and van Holde, K. (1992) Chromatin loops and transcriptional regulation. Crit. Rev. Euk. Gene. Exp. 2, 211-224.